Uplink Radio Resource Management for QoS Provisioning in Long Term Evolution

with Emphasis on Admission Control and Handover

Anas, Mohmmad

Publication date:
2009

Document Version
Publisher's PDF, also known as Version of record

Uplink Radio Resource Management for QoS Provisioning in Long Term Evolution

With Emphasis on Admission Control and Handover

PhD Thesis

by

Mohmmad Anas

A dissertation submitted to
the Faculty of Engineering, Science and Medicine of Aalborg University
in partial fulfillment for the degree of
Doctor of Philosophy.
Aalborg, Denmark
January 2009

Supervisor:
Preben Elgaard Mogensen, PhD,
Professor, Aalborg University, Denmark.

Co-supervisor:
Klaus Ingemann Pedersen, PhD,
Senior Wireless Network Specialist, Nokia Siemens Networks, Aalborg, Denmark.

Assessment Committee:
Laurent Schumacher, PhD,
Associate Professor, University of Namur, Belgium.
Carsten Ball, PhD,
R&D Manager, Nokia Siemens Networks, Munich, Germany.
Tatiana Kozlova Madsen, PhD,
Associate Professor, Aalborg University, Denmark.

Defence Moderator:
Flemming B. Frederiksen,
Associate Professor, Aalborg University, Denmark.

ISSN 0908-1224
ISBN 978-87-92328-03-8

To my parents – Mr. Hasnain Alam and Late Mrs. Shaheena Begum.

Abstract

Long Term Evolution (LTE) is a beyond 3G wireless system based on a decentralized architecture which shall support end-to-end Quality of Service (QoS). The radio resource management functionalities in the LTE uplink is based on a dynamically shared channel with fast Link Adaptation (LA) including Adaptive Modulation and Coding (AMC) and Fractional Power Control (FPC), Hybrid Automatic Repeat reQuest (HARQ), Packet Scheduler (PS), Admission Control (AC) and handover. To provide efficient QoS control, it is necessary that both AC and PS are QoS aware. The AC maintains the QoS of in-progress bearers in a cell by admitting a new bearer only if all the existing and new bearers can be guaranteed their QoS requirements. Additionally, LTE will provide seamless access to voice and multimedia services which is achieved by supporting handover. The problem of providing seamless access becomes even more important in LTE since it uses hard handover (break-before-make type). This PhD study mainly focuses on AC and handover issues for QoS provisioning in LTE uplink.

In the first part, a novel AC algorithm is proposed for LTE uplink to fulfill the required QoS of new radio bearer and in-progress bearers. In this study Guaranteed Bit Rate (GBR) is considered as the main QoS parameter. The proposed AC algorithm estimates the required resources for the new and existing bearers to fulfill their required GBR taking into account users respective channel conditions. The proposed AC algorithm is based on a closed-form estimator derived utilizing the FPC scheme standardized in 3GPP. To evaluate the performance of FPC based AC, a reference AC which does not take channel conditions into account is proposed. Furthermore, a QoS aware PS is proposed and is combined with the AC algorithm for effective QoS provisioning. The performance is evaluated using a full-blown multi-cell, multi-user, semi-static system level simulator following the 3GPP LTE standard. The results show that the FPC based AC, unlike reference AC, is robust and automatically adjusts to the traffic mixes, cell load, and user channel conditions. Additionally, the proposed AC and PS framework guarantees the respective GBR requirements of different user classes in a best-effort traffic scenario with mixed GBR settings. Further, this framework is shown to guarantee the QoS of users with a realistic Constant Bit Rate (CBR) streaming traffic and an ON/OFF traffic source using CBR traffic to model the ON periods.

In the second part, performance of an intra-LTE hard handover algorithm is evaluated at user speeds of 3 kmph to 120 kmph. Handover algorithm based on Received Signal Strength (RSS) and Carrier to Interference Ratio (CIR) measurements on downlink reference symbols (pilots) is studied. Additionally, Layer 3 (L3) filtering in linear and logarithmic domain is evaluated. A realistic estimate of measurement imperfections due to the limited number of reference symbols is modeled and added to the handover measurements before L3 filtering. RSS on reference symbols is known as Reference Signal Re-

ceived Power (RSRP) and is standardized as one of the measurements for intra-frequency handover in LTE. This study is evaluated using a detailed multi-cell, multi-user, dynamic system-level simulator i.e., a simulator suitable for mobility studies, following 3GPP LTE recommended assumptions. The results show that the downlink measurement bandwidth of 1.25 MHz will lead to best tradeoff between average number of handovers and average uplink Signal-to-Interference-plus-Noise Ratio (SINR). Moreover, it is shown that for an adaptive choice of L3 filtering period, depending on the user speed, the gain for using larger measurement bandwidth can be made negligible for a small penalty on signal quality.

Dansk Resumé [1]

Long Term Evolution (LTE) er den nyeste 3GPP standard, som er baseret på en distribueret arkitektur med slutbruger QoS (Quality of service). Radio resource management (RRM) funktionerne i uplink (UL) er baseret på en fælles dynamisk kanal med hurtig link adaption (LA) med variabel kodning og modulation, power kontrol, samt Hybrid ARQ (automatic repeat request). Dynamisk pakketransmission og adgangs kontrol er også en del af konceptet for at sikre QoS. Adgangskontrollen har til opgave kun at tillade nye kald, hvis disse kan accepteres uden at kvaliteten af eksisterende kald bliver for lav, samt at QoS af det nye kald kan opfyldes. LTE har også en optimeret handover funktion, som bl.a. sikrer, at brugere kan skifte celle, uden at dette medfører kvalitets forringelse.

I første del af dette studium analyseres adgangskontrol algoritmen til LTE. En ny algoritme foreslås, hvor eneste QoS parameter er guaranteed bit rate (GBR). Algoritmen er baseret på et estimat af, hvor mange transmissions- resurser den nye bruger kræver, samt antal resurser krævet af de eksisterende brugere for at opfylde deres minimum QoS. Der udledes et matematisk udtryk for dette, baseret på antagelserne i LTE UL mht. til power kontrol og dynamisk LA. En simpel reference adgangskontrol algoritme testes også. Adgangskontrol algoritmen evalueres med en detaljeret quasi-statisk netværks simulator, med multiple celler, terminaler, osv., i overensstemmelser med LTE systemspecifikationerne. Resultaterne fra disse simuleringer viser, at den nye adgangskontrol algoritme er robust og virker efter hensigten, så nye brugere kun gives adgang hvis dette er muligt uden at kompromittere QoS. Den nye algoritme er klart bedre end den testede reference adgangskontrol algoritme. Den nye adgangskontrol algoritme er også blevet evalueret sammen med en avanceret QoS pakketransmissions algoritme med minimum GBR krav. Også i dette tilfælde viste det sig, at den foreslåede adgangskontrol algoritme viste gode resultater. Kombinationen af avanceret QoS adgangskontrol og pakketransmission er også blevet studeret for data trafik med ikke konstant pakkeaktivitet.

I anden del at rapporten studeres handover, med fokus på intra-frequency handover. En handover algoritme baseret på terminalmålinger af signalstyrke og signal-til-interference blev undersøgt. Forskellige filtre af disse målinger blev undersøgt for at finde det bedste kriterium til handovers. En realistisk modellering af diverse målefejl ved terminalen var en vigtig del af disse studier, bl.a. som funktion af måle-båndbredden, antal af reference symboler, osv. De forskellige handover algoritmer blev evalueret i en dynamisk netværkssimulator, som blev specielt udviklet til dette formål. Resultaterne viste, at en måle-båndbredde på 1.25 MHz var nok til at opnå gode resultater, hvis signal-til-interference målinger benyttes til handovers. Filterlængden af disse målinger kan optimeres afhængigt af hastigheden af terminalerne.

[1] Translation by Klaus I. Pedersen and Jytte Larsen, Nokia Siemens Networks, Aalborg, Denmark.

Preface and Acknowledgments

This thesis is the result of three years of PhD fellowship grant in the area of radio resource management, mobility, and system performance analysis for B3G/4G systems. This project is co-financed by the Aalborg University and Nokia Siemens Networks, Aalborg, Denmark. The research is carried out at the Radio Access Technology section, Institute of Electronic Systems, Aalborg University under the supervision of Professor Preben E. Mogensen (Aalborg University) and Dr. Klaus I. Pedersen (Nokia Siemens Networks). This thesis investigates the uplink radio resource management issues to provide QoS support in 3GPP LTE systems.

The presented work would not have been possible without being part of an inspiring network of colleagues, enabling interesting discussions and collaboration. First of all, I would like to thank my PhD supervisors for their guidance, co-operation, and patience. Their input has been vital, especially our technical discussions were instrumental in improving my understanding of the subject, and enabled me to overcome the technical challenges. I would also like to thank Per-Erik Östling who was my first contact with the Aalborg University and who has also been a good collaborator for the handover studies. Further, I would like to thank the members of the assessment committee who through their detailed reading and constructive feedback have assisted me in the correction and clarification of the text throughout this dissertation.

I would also like to point out the good collaboration with Francesco Calabrese and Claudio Rosa which has also led to common publications. Further, I would like to thank Jeroen Wigard, Jens Steiner, Daniela Laselva, Per-Henrik Michaelsen, and Troels B. Sørensen for their valuable inputs. The constant friendly support, assistance with administrative tasks, and the proofreading provided by our section secretaries Lisbeth Schiønning Larsen and Jytte Larsen is highly appreciated. There are of course many more names, too many to distinguish individually. So I would like to thank all the past and present colleagues at Radio Access Technology section, Aalborg University and Nokia Siemens Networks for their friendly support.

Special thanks to Francesco Calabrese and Guillaume Monghal, cherished friends, who have also made up a major part of my daily life, with whom I shared the entire journey towards our PhD work. Further, I am grateful to my sister Amina Kaosar and the extremely helpful bunch of friends, Oumer Teyeb, Danish Khan, Akhilesh Pokhariyal, Sanjay Kumar, Doa Idris, Basuki Priyanto, Muhammad Imadur Rehman, and Shashi Kant for making my stay in Denamrk enjoyable.

Finally, I would like to thank my family, whose love, support and encouragement have accompanied throughout my life. They supported me in every possible way and they were always beside me although they were so many thousand miles away. Words alone can never express my gratitude.

Abbreviations

16QAM	16 Quadrature Amplitude Modulation
3G	Third Generation
3GPP	Third Generation Partnership Project
64QAM	64 Quadrature Amplitude Modulation
AC	Admission Control
aGW	Access Gateway
AMBR	Aggregate Maximum Bit Rate
AMC	Adaptive Modulation and Coding
APG	Average Path Gain
ARP	Allocation Retention Priority
ATB	Adaptive Transmission Bandwidth
AVI	Actual Value Interface
B3G	Beyond 3G
BCH	Broadcast Channel
BE	Best Effort
BLEP	BLock Error Probability
BLER	BLock Error Rate
CAZAC	Constant Amplitude Zero Auto-Correlation
CBR	Constant Bit Rate
CC	Chase Combining
CIR	Carrier to Interference Ratio
CPICH	Common Pilot Channel
CQI	Channel Quality Information
CSI	Channel State Information

dB	Decibel
DCH	Dedicated Channel
DFT	Discrete Fourier Transform
DL-SCH	Downlink Shared Channel
DRX	Discontinuous Reception
DSCH	Downlink Shared Channel
E-DCH	Enhanced Dedicated Channel
ELIISE	Efficient Layer II Simulator for E-UTRAN
eNode-B	Evolved Node B
EPC	Evolved Packet Core
EPS	Evolved Packet System
E-UTRAN	Evolved Universal Terrestrial Radio Access Network
FD	Frequency-Domain
FDPS	Frequency-Domain Packet Scheduling
FPC	Fractional Power Control
FTP	File Transfer Protocol
GBR	Guaranteed Bit Rate
GPRS	General Packet Radio Service
GPS	Generalized Process Sharing
GSM	Global System for Mobile Communication
HARQ	Hybrid Automatic Repeat reQuest
HSDPA	High Speed Downlink Packet Access
HS-DSCH	High Speed Downlink Shared Channel
HSPA	High Speed Packet Access
HSUPA	High Speed Uplink Packet Access
IIR	Infinite Impulse Response
IR	Incremental Redundancy
KPIs	Key Performance Indicators
L1	Layer 1 (physical layer)
L3	Layer 3 (network layer)

LA	Link Adaptation
LTE	Long Term Evolution
MAC	Medium Access Control
MBMS	Multimedia Broadcast Multicast Service
MCH	Multicast Channel
MCS	Modulation and Coding Scheme
MIMO	Multiple Input Multiple Output
MRC	Maximal Ratio Combining
NRT	Non-Real Time
OFDM	Orthogonal Frequency Division Multiplexing
OFDMA	Orthogonal Frequency Division Multiple Access
OLLA	Outer Loop Link Adaptation
PAPR	Peak-To-Average Power Ratio
PBCH	Physical Broadcast Channel
PBR	Prioritized Bit Rate
PCH	Paging Channel
PDCCH	Physical Downlink Control Channel
PDSCH	Physical Downlink Shared Channel
PDN	Packet Data Network
PF	Proportional Fair
PMCH	Physical Multicast Channel
PRACH	Physical Random Access Channel
PRBs	Physical Resource Blocks
PS	Packet Scheduler
PSD	Power Spectral Density
PUCCH	Physical Uplink Control Channel
PUSCH	Physical Uplink Shared Channel
QCI	Quality Class Identifier
QoS	Quality of Service
QPSK	Quadrature Phase Shift Keying

RACH	Random Access Channel
RAD	Required Activity Detection
RLC	Radio Link Control
RNC	Radio Network Controller
RRC	Radio Resource Control
RRM	Radio Resource Management
RSCP	Received Signal Code Power
RSRP	Reference Signal Received Power
RSS	Received Signal Strength
RSSI	Received Signal Strength Indicator
RT	Real Time
SAE	System Architecture Evolution
SC-FDMA	Single-Carrier Frequency Division Multiple Access
SCH	Synchronization Channel
SINR	Signal-to-Interference-plus-Noise Ratio
SNR	Signal-to-Noise Ratio
SRS	Sounding Reference Signal
TD	Time-Domain
TDPS	Time-Domain Packet Scheduling
TTI	Transmission Time Interval
TTT	Time-to-Trigger
TU	Typical Urban
UE	User Equipment
UL-SCH	Uplink Shared Channel
UMTS	Universal Mobile Telecommunications System
VoIP	Voice over Internet Protocol
WFQ	Weighted Fair Queueing
WCDMA	Wideband Code Division Multiple Access

Contents

Chapter 1

Introduction

The growth in the number of mobile subscribers all around the world and the interest in data services has suggested network operators to introduce mobile Internet packet based services. The introduction of new and demanding services such as audio/video streaming, interactive gaming with rapid response patterns has drawn attention toward possible limitation of the capacity and Quality of Service (QoS). The Third Generation (3G) mobile systems based on Wideband Code Division Multiple Access (WCDMA) radio access technology are being deployed to meet the growing requirement of higher data rates and QoS differentiation. The 3G mobile system evolution in Third Generation Partnership Project (3GPP) standardization and commercial operation is shown in Figure 1.1 [1]. The first step in the evolution of WCDMA has been the introduction of High Speed Downlink Packet Access (HSDPA) and High Speed Uplink Packet Access (HSUPA) providing higher data rates and improved spectral efficiency [2]. This WCDMA evolution is denoted as High Speed Packet Access (HSPA), and it is usually classified as 3.5G. This technology will remain highly competitive for several years to come. However, to ensure 3GPP competitiveness in even longer time frame, i.e. for the next 10 years and beyond, the Long Term Evolution (LTE)[1] of the radio access technology and network architecture are decided within the 3GPP framework. This PhD study is done within the framework of LTE, also referred to as 3.9G.

The rest of the chapter is organized as follows: In Section 1.1 the 3GPP technology road map and important evolutions are presented. The LTE targets and the radio interface along with system architecture evolution is described in Section 1.2. Section 1.3 formulates the scope and objectives of this study. The scientific methodology used is outlined in Section 1.4. The novelty and contributions of the thesis along with the list of articles published during the PhD study period is detailed in Section 1.5. Finally, Section 1.6 presents the organization of the thesis.

[1]LTE is also known as Evolved Universal Terrestrial Radio Access Network (E-UTRAN).

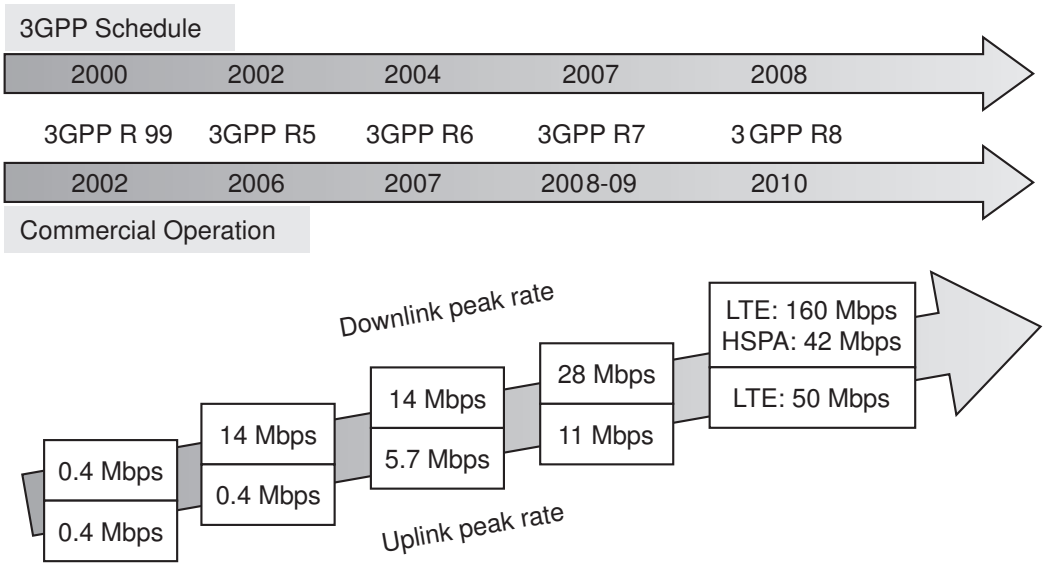

Figure 1.1: Peak data rate for 3G and LTE along with the standardization and commercial operation schedule [1].

1.1 Preliminaries

The first release of WCDMA (Release 99) in theory enabled 2 Mbps in downlink, but in practice gave 384 kbps both in downlink and uplink [1]. WCDMA employs Link Adaptation (LA) techniques such as variable spreading factor and closed-loop power control [3]. The aim of these features is to enable provision of multiple data rates with different reliability requirements. The 3GPP Release 99 supports both circuit switched transmission for voice traffic and packet switched transmission for data. Specifically for circuit switched transmission a Dedicated Channel (DCH) is established between base station (Node-B) and UE, for example to deliver delay stringent voice services to the user. The Packet Scheduler (PS) entity was introduced in WCDMA to support packet switching. The PS is located in the Radio Network Controller (RNC), and as a result its decisions are updated at a slow rate, e.g. in the order of 100 ms to 1 s [3]. For packet switched data, for example the download of a webpage, high peak data rates with low duty cycles are required. To accommodate these needs a Downlink Shared Channel (DSCH) has been defined in addition to the DCH. Therefore, users requiring high data rates for a short time can share the DSCH in a time division multiple access manner.

The HSDPA (Release 5) peak data rate is 14 Mbps, while the HSUPA (Release 6) peak data rate is in the order of 5.7 Mbps [1]. The LA functionality has been evolved to support advanced features such as Adaptive Modulation and Coding (AMC) and physical layer Hybrid Automatic Repeat reQuest (HARQ). The PS entity has a significant role in HSPA, and it is located close to the radio channel, in the Node-B. Thus, it can operate at a faster rate, e.g. in HSDPA the scheduling decisions can be updated every 2 ms. To use the radio frequency resources efficiently and take into account the bursty packet data a new transport channel, High Speed Downlink Shared Channel (HS-DSCH), is introduced in

HSDPA [4]. Similarly, Enhanced Dedicated Channel (E-DCH) is introduced in HSUPA. These evolutions lead to the full support of packet switched transmission both in downlink and uplink.

The HSPA evolution (Release 7), also know as HSPA+, further improves the peak data rates to 28 Mbps and 11 Mbps in downlink and uplink respectively. The increase in data rate is due to the use of Multiple Input Multiple Output (MIMO) by deploying 2 antennas both at the Node-B and User Equipment (UE) [1]. Further evolution steps can be to use dual carrier HSPA i.e. using a second HSPA carrier to create an opportunity for network resource pooling as a way to enhance the user experience, in particular when the radio conditions are such that existing techniques (e.g. MIMO) can not be used [5].

The LTE (Release 8) is described to maintain 3GPP competitiveness in the long-term future as well as to meet the increasing user demands. The related Study Item (SI) titled "Evolved UTRA and UTRAN" was started in December 2004 [6]. The aim of this SI was to propose technical solutions which can provide additional substantial leaps in terms of service provisioning and cost reduction over HSPA [7][8]. 3GPP has concluded on a set of targets and requirements for the LTE, which are enumerated in [9]. The LTE specifications are expected to be ready in 2009, and its trial and commercial deployment are expected as early as in year 2009/2010.

In terms of the radio transmission, communication systems have moved away from circuit switched towards the packet switched paradigm. Further, modern wireless systems are primarily designed to support both high data rate multimedia applications and Voice over Internet Protocol (VoIP). The next generation mobile systems are expected to support end-to-end QoS to a wide range of high data rate multimedia applications, with varying delay and reliability requirements.

1.2 Long Term Evolution

The important targets for LTE radio-interface and radio-access network architecture are as follows [9]:

- Peak data rates exceeding 100 Mbps in the downlink and 50 Mbps in the uplink using a system bandwidth of 20 MHz.
- Significantly higher capacity compared to the Release 6 reference case i.e. increase in spectral efficiency by a factor of three to four times in downlink and two to three times in uplink [1].
- Significantly reduced control plane latency as well as user plane latency (10 ms round-trip time with 5 MHz or higher spectrum allocation [10]).
- Scalable bandwidth operation up to 20 MHz, i.e., 1.4, 3, 5, 10, 15 and 20 MHz [11][12].

- Support for packet switched domain only.
- Enhanced support for end-to-end QoS.
- Optimized performance for user speed of less than 15 kmph, and high performance for speeds up to 120 kmph. The connection should be maintained with speeds even up to 350 kmph [13].
- Reduced cost for operator and end user.

One of the important requirements of LTE is spectrum flexibility, enabling deployment in many different spectrum allocations. Support for wide transmission bandwidth of up to 20 MHz is envisaged in order to support the high data rates. At the same time support for much lower transmission bandwidths, less than 5 MHz, is also possible. Additionally, the focus of LTE is on the enhancement of packet based services. The overall goal is to develop an optimized packet based access system with high data rate and low latency. Examples of intended services include High Definition TeleVision (HDTV) broadcast, movies on demand, interactive gaming, and VoIP [10].

The objective of LTE is to develop a framework for the evolution of the 3GPP radio access technology and network architecture towards a high data rate, low latency, and packet optimized cellular network. In order to achieve this, an evolution of the radio interface as well as the radio network architecture is set forth, which are described in the following sections.

1.2.1 Radio Interface Evolution

Orthogonal Frequency Division Multiple Access (OFDMA) has been chosen as the multiple access technique to achieve higher spectral efficiency for downlink transmission in LTE. The big advantage of using OFDMA is its robustness in the presence of multipath fading, which comes at the cost of high Peak-To-Average Power Ratio (PAPR). Due to the fact that high PAPR is an issue in uplink due to the power limitations of the mobile handset, a Discrete Fourier Transform (DFT) spread OFDMA also known as Single-Carrier Frequency Division Multiple Access (SC-FDMA) has been proposed for uplink transmission in LTE [14]. While retaining most of the advantages of OFDMA, SC-FDMA exhibits significantly lower PAPR resulting in reduced power consumption and improved coverage [15]. The benefit in lower PAPR comes at the cost of single-carrier constraint i.e. it requires the subcarriers and therefore the Physical Resource Blocks (PRBs)[2] allocated to a single user to be adjacent.

The OFDMA and SC-FDMA technologies are based on Orthogonal Frequency Division Multiplexing (OFDM), which is regarded as the key technology for higher spectral

[2]The basic time-frequency resource available for data transmission consisting of 12 adjacent OFDM subcarriers equally spaced at 15 kHz and 14 OFDM symbols in time. Its size is equal to 180 kHz in frequency domain and 1 ms in time domain.

efficiency and scalable bandwidth because of its ability to cope with severe channel conditions for example frequency selective fading due to multipath without complex equalization filters. This technology allows the possibility of flexible bandwidth allocation by varying the number of subcarriers used for transmission, while keeping the subcarrier spacing unchanged. In this way LTE supports the operation in spectrum allocations of 1.4, 3, 5, 10, 15, and 20 MHz [11][12].

1.2.2 System Architecture Evolution

To meet the requirements of reduced latency and cost, LTE has a flat system architecture that contains a reduced number of network nodes along the data path. A reduction of the number of nodes makes it possible for example to reduce the call setup times, as fewer nodes will be involved in the call setup procedure. Figure 1.2 illustrates the architecture evolution of LTE over Release 6 architecture [16].

In Release 6, part of the the Radio Resource Management (RRM) functionalities e.g., PS, are located in the Node-B. While, the RNC handles RRM functionalities e.g., Admission Control (AC), mobility management (locally), etc. and transport network optimization. It further acts as a termination point for the radio protocols. The Serving GPRS Support Node (SGSN) and Gateway GPRS Support Node (GGSN) act as an anchor node and visiting node in the visiting network and home network respectively. Further, SGSN handles both mobility management and session management.

In the LTE architecture, the Access Gateway (aGW) terminates the user plane for the UE, and handles the core network functions provided by the GGSN and SGSN as in Release 6. As shown in Figure 1.3, the RRM functionalities e.g., AC, mobility con-

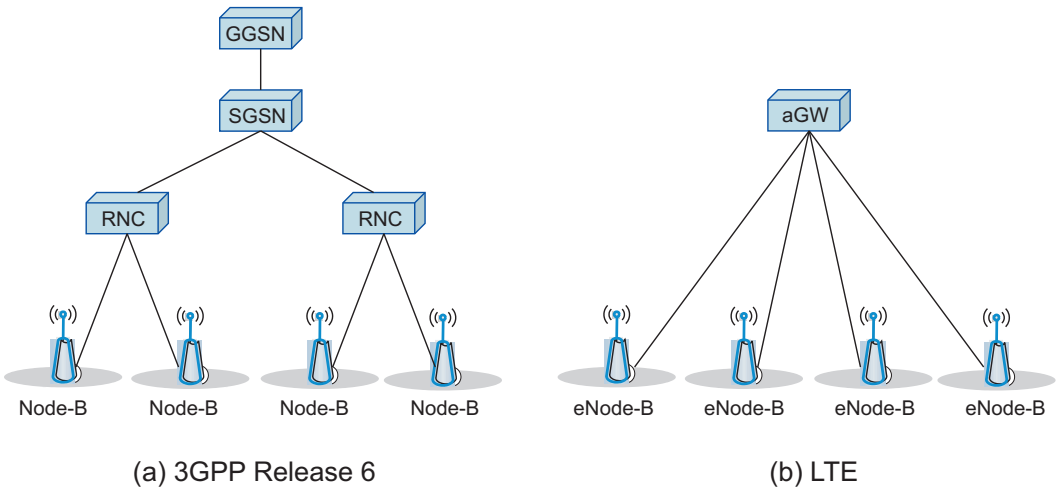

Figure 1.2: The 3GPP Release 6 architecture and evolved system architecture for LTE reducing the number of nodes along the data path from 4 to 2 [16].

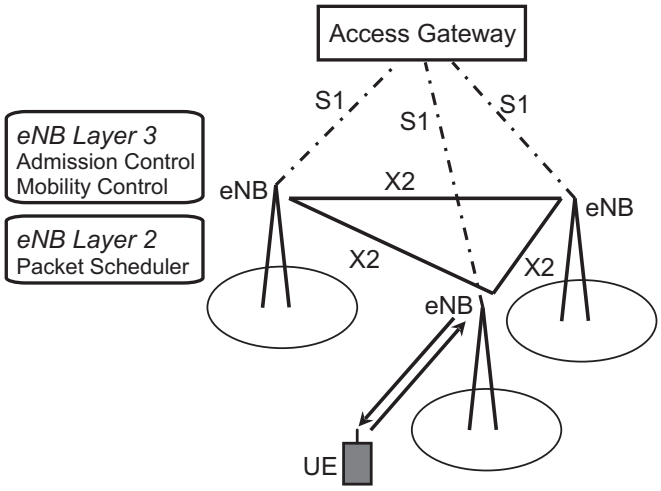

Figure 1.3: UTRAN LTE system architecture

trol including handover, PS etc., are located in Evolved Node B (eNode-B)[3] instead of RNC as in Release 6. The System Architecture Evolution (SAE) focuses on enhancement of packet switched technology i.e. higher data rates, lower latency (both in user plane and control plane), packet optimized system, and support of multiple radio access technologies. These goals will be achieved using fully IP based network, simplified network architecture, and distributed control. The interface between eNode-Bs (X2) of the same aGW supports tunneling of the end user packets between the eNode-Bs. This provides the means to minimize the packet loss during handover. The eNode-Bs are also connected by means of the S1 interface to the aGW which is connected to the Internet. The aGW provides the user plane protocol termination towards the UE. The standardization of hard handover facilitates the decentralized network architecture without a centralized RNC as in Release 6. The absence of inter eNode-B soft handover (macrodiversity) does not preclude the support of softer handover for intra eNode-B case. Therefore, the SAE represents a flat RNC-less radio network architecture, in which most radio access related control functionalities and protocol termination on the network side is located in eNode-B.

1.3 Thesis Scope and Objectives

The evolution of radio interface and network architecture in LTE provides new opportunities and challenges to enhance spectral efficiency and QoS provisioning. The RRM functionalities in uplink are based on a dynamically shared channel with fast LA including AMC and Fractional Power Control (FPC), HARQ, PS, AC, and handover as illustrated in Figure 1.4. These functionalities are located at the eNode-B and hence they can interact and make faster decisions. For example to provide efficient QoS control, it is necessary that both AC and PS are QoS aware. Similarly, spectral efficiency is maximized if the PS interacts with LA during the processing of the scheduling algorithm. Out of these, the

[3]eNode-B and eNB are used alternatively with the same meaning.

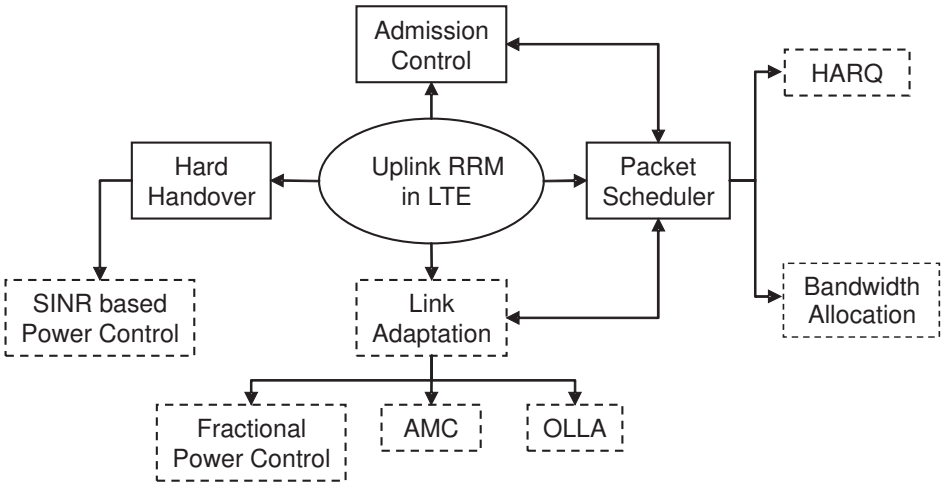

Figure 1.4: The interaction between uplink RRM functionalities in LTE. The functionalities in solid boxes indicate specific focus of the thesis taking into account the interaction with the functionalities contained in dashed boxes.

focus of this research project is on the AC, PS, and handover functionalities taking into account their interaction with other RRM entities. Novel algorithms are derived and the proposed algorithms are investigated at system-level. In order to make the study realistic the LTE framework and design guidelines are employed in the analysis [14].

The AC in LTE is located in the eNode-B, which utilizes the local cell load information to make the admission decision. To maintain the QoS of in-progress bearers in a cell it is important to admit a new radio bearer only if all the existing and the new bearers can be guaranteed QoS according to their requirements [17]. Hence the objective of the first part of the study is to analytically derive a QoS aware uplink AC algorithm taking into account the FPC algorithm standardized in 3GPP. Further, to effectively differentiate between user classes with different QoS requirements a QoS aware PS is proposed. To benchmark the performance of the derived AC algorithm for both Best Effort (BE) traffic with a Guaranteed Bit Rate (GBR) and a realistic Constant Bit Rate (CBR) streaming traffic model a reference AC is proposed. The Key Performance Indicators (KPIs) used for performance evaluation are blocking and outage probabilities, average user throughput, call duration etc. This part of the study is done together with realistic LA including AMC, FPC, fixed or Adaptive Transmission Bandwidth (ATB) allocation, and HARQ modeling using a full-blown semi-static system-level simulation analysis.

Handover is another important functionality which tries to keep a user connected to the best base station such that QoS of the ongoing session is met. One of the goals of LTE is to provide seamless access to voice and multimedia services with strict delay requirements which is achieved by supporting handover. The problem of providing seamless access becomes even more important in LTE since it uses hard handover (break-before-make type). The focus of the second part of the study is on the intra-LTE, intra-frequency, hard handover functionality which is located in eNode-B. Handover in LTE is user assisted and network controlled, and it is usually based on the downlink and/or uplink channel measurements and its processing by the user. The scope of this part is to study the handover

measurements in downlink and evaluate the performance of handover based on the LTE standardized Reference Signal Received Power (RSRP) measurement [18]. The handover negotiation and signaling between serving and target cells is out of the scope of this thesis. This part of the study is done using dynamic system-level simulation analysis.

1.4 Scientific Methods Employed

Analytical evaluation at the system-level is usually mathematically intractable as the system performance is dependent on a large number of parameters whose behavior can not always be known a priori. Consequently closed form analytical expressions characterizing system performance are seldom possible. Therefore, the results presented in this thesis have been obtained through extensive computer simulations using the system model developed during the course of the project. Furthermore, analytical formulation and modeling have been carried out for the algorithm development. The performance of the proposed algorithms is studied using the system-level simulations based on a complex system model and taking into account the 3GPP recommended modeling assumptions for LTE [14].

The first part of the thesis starts with the development of a QoS aware uplink AC algorithm using analytical method. Further, the developed AC algorithm is coupled with the PS to model a framework for QoS provisioning. The performance of the proposed combined AC and PS framework is evaluated using a multi-cell, multi-user, semi-static system simulator. The cellular deployment as well as the modeling assumptions are based on the latest 3GPP recommendations [14][19]. The system model includes detailed implementation of LA based on real AMC and FPC, explicit scheduling of HARQ processes including retransmissions, link-to-system mapping technique suitable for SC-FDMA and dynamic other-cell interference. Further, it includes the Poisson user arrival process along with finite buffer (as BE traffic) and CBR streaming traffic model. This system simulator was developed in co-operation with Nokia Siemens Networks and Radio Access Technology Section at Aalborg University. The aim is to evaluate the performance of the proposed framework for QoS provisioning at the system-level and to recommend the algorithms for practical implementation.

The second part of the thesis on the handover is evaluated using a multi-cell, multi-user, dynamic system simulator. This simulator is mainly developed for mobility studies and hence include relatively simplified model for AMC, power control based on target Signal-to-Interference-plus-Noise Ratio (SINR), HARQ, PS and link-to-system mapping technique suitable for SC-FDMA. The modeling assumptions are mostly based on the 3GPP recommendations [14]. A realistic estimate of the downlink measurement imperfection due to the limited number of reference symbols in LTE is modeled to analyze the affect of realistic handover measurements on the system performance.

1.5 Novelty and Contributions

The main contributions of this study are the design and analysis of an uplink QoS aware framework combining AC and scheduling. Unlike most previous studies this study takes into account the complex interaction of AC, PS, ATB, HARQ, LA including power control and AMC. Additionally, hard handover algorithm is studied and handover parameters are evaluated and recommended for LTE. Moreover, substantial simulator development is carried out during the PhD study to evaluate the proposed algorithms. This include both mathematical modeling considerations as well as software design, implementation and testing.

The first topic of research is the design of uplink AC for LTE to provide QoS support. A novel closed-loop form solution of AC for QoS provisioning is derived utilizing the FPC formula agreed in 3GPP [20]. In this study GBR is considered as the main QoS parameter. It is shown that the proposed AC algorithm effectively admits the users only if their GBR can be fulfilled taking into account the channel conditions and user transmit power limitation. Moreover, a combined AC and a decoupled Time-Domain (TD) and Frequency-Domain (FD) PS framework is used to guarantee the respective QoS requirements of different user classes in a mixed GBR scenario. Furthermore, it is shown that the proposed combined AC and PS is effective for the real CBR streaming traffic. The proposed AC is further modified and analyzed for an ON/OFF traffic taking into account the source activity factor. The results of this study have been partly published in the following articles:

- M. Anas, C. Rosa, F. D. Calabrese, P. H. Michaelsen, K. I. Pedersen, and P. E. Mogensen, "QoS-Aware Single Cell Admission Control for UTRAN LTE Uplink," in *Proceedings of the 67th IEEE Vehicular Technology Conference (VTC)*, Singapore, May, 2008.
- M. Anas, C. Rosa, F. D. Calabrese, K. I. Pedersen, and P. E. Mogensen, "Combined Admission Control and Scheduling for QoS Differentiation in LTE Uplink," in *Proceedings of the 68th IEEE Vehicular Technology Conference (VTC)*, Calgary, Canada, September, 2008.

The second topic of research is the handover parameter design for LTE. The intra-LTE handover based on downlink Received Signal Strength (RSS) and Carrier to Interference Ratio (CIR) measurement at reference symbols are compared. A realistic estimate of measurement imperfection due to the limited number of reference symbols is modeled and added to the handover measurements before the processing. Further, the effect of handover parameters on different KPIs in a realistic LTE scenario is presented. The downlink RSS measurement at the reference symbols is known as RSRP, which is standardized as a handover measurement for LTE. Therefore, a handover algorithm based on RSRP measurement is analyzed, which is further improved by including the Time-to-Trigger (TTT) window to reduce the number of ping-pong handovers. The results of this study have been published in the following articles:

- M. Anas, F. D. Calabrese, P. E. Östling, K. I. Pedersen, and P. E. Mogensen, "Performance Analysis of Handover Measurements and Layer 3 Filtering for UTRAN LTE," in *Proceedings of the IEEE International Symposium on Personal, Indoor and Mobile Radio Communications (PIMRC)*, Athens, Greece, September, 2007.

- M. Anas, F. D. Calabrese, P. E. Mogensen, C. Rosa, and K. I. Pedersen, "Performance Evaluation of Received Signal Strength based Hard Handover for UTRAN LTE," in *Proceedings of the 65th IEEE Vehicular Technology Conference (VTC)*, Dublin, Ireland, April, 2007.

The mobility studies are done using a dynamic system-level simulator – Efficient Layer II Simulator for E-UTRAN (ELIISE). It is jointly developed with Francesco D. Calabrese (PhD student in Radio Access Technology Section at Aalborg University) during September 2005 – October 2006 using the Standard Template Library (STL) in C++ programming language [21]. The contributions include the mathematical modeling and implementation of network layout, mobility, channel, SINR, HARQ and power control in uplink taking into account the LTE assumptions.

In addition, the collaborative work on resource allocation and PS design for LTE uplink has resulted in the following published articles:

- F. D. Calabrese, M. Anas, C. Rosa, K. I. Pedersen, and P. E. Mogensen, "Performance of a Radio Resource Allocation Algorithm for UTRAN LTE Uplink," in *Proceedings of the 65th IEEE Vehicular Technology Conference (VTC)*, Dublin, Ireland, April, 2007.

- F. D. Calabrese, P. H. Michaelsen, C. Rosa, M. Anas, C. U. Castellanos, D. L. Villa, K. I. Pedersen, and P. E. Mogensen, "Search-Tree based Uplink Channel Aware Packet Scheduling for UTRAN LTE," in *Proceedings of the 67th IEEE Vehicular Technology Conference (VTC)*, Singapore, May, 2008.

- F. D. Calabrese, C. Rosa, M. Anas, P. H. Michaelsen, K. I. Pedersen, and P. E. Mogensen, "Adaptive Transmission Bandwidth Based Packet Scheduling for LTE Uplink," in *Proceedings of the 68th IEEE Vehicular Technology Conference (VTC)*, Calgary, Canada, September, 2008.

1.6 Thesis Outline

The PhD thesis is organized as follows:

- Chapter 2: *Overview of Uplink Radio Resource Management in LTE* – This chapter presents the overview of the system architecture and general description of the uplink RRM functionalities in LTE. Further, a description of PS and its interaction with LA including power control and AMC is detailed.

- Chapter 3: *QoS-Aware Uplink Admission Control* – This chapter describes a novel uplink AC algorithm proposed for LTE. Furthermore, the performance enhancement of the proposed AC algorithm over a reference AC is assessed using simulation results with finite buffer traffic model in a single GBR case. The PS is assumed to allocate fixed bandwidth to each user, which is studied by PhD student Francesco D. Calabrese and the related published article is reprinted in Annex I.

- Chapter 4: *Combined Admission Control and Scheduling for QoS Provisioning* – This chapter presents a combined AC and packet scheduling framework to provide the QoS support and service provisioning. The proposed framework is analyzed using the simulation results with finite buffer traffic model in a mixed GBR case. The proposed framework is shown to effectively admit and differentiate between users with different GBR. The PS is assumed to allocate adaptive bandwidth to a user, which is studied by PhD student Francesco D. Calabrese and the related published article is reprinted in Annex II.

- Chapter 5: *Performance of CBR Streaming Services* – This chapter analyzes the performance of CBR streaming traffic. The AC algorithm derived in Chapter 3, is modified for an ON/OFF traffic source taking into account the source activity factor. Further, the performance of the proposed AC and scheduling framework for a realistic CBR streaming is evaluated with single and mixed GBR settings. The performance of an ON/OFF traffic with ON periods modeled as CBR is evaluated. Additionally, an AC framework to differentiate between GBR and Non-GBR bearers is presented.

- Chapter 6: *Handover Measurements and Filtering* – This chapter compares different handover measurements, and Layer 1 (physical layer) (L1) and Layer 3 (network layer) (L3) filtering of handover measurements. Moreover, a realistic estimate of measurement imperfection is modeled and added in the handover measurements. A multi-cell dynamic system-level simulator developed to study the mobility issues is further described in this chapter. Performance of downlink RSS and CIR, and L3 filtering is analyzed for measurement bandwidth, handover margin, and L3 filtering period.

- Chapter 7: *Evaluation of Hard Handover Based on RSRP Measurement* – This chapter evaluates the performance of an intra-LTE, intra-frequency, hard handover based on RSRP measurement for different handover parameters e.g. measurement bandwidth, measurement time interval, handover margin etc. for different user speeds. Additionally, RSRP measurement based handover is modified with TTT window to improve the performance by reducing the number of handovers for a small penalty on signal quality.

- Chapter 8: *Overall Conclusions and Recommendations* – This chapter provides a summary of the overall study and discusses future research issues.

The following appendices are presented to support the work outlined in the main part of the thesis:

- Appendix A: *Semi-Static System Level Simulator Description* – This appendix provides the detailed description of the semi-static multi-cell system level model including network layout, channel model, traffic model, link-to-system level mapping, and definition of important KPIs.
- Appendix B: *Statistical Significance Assessment* – This appendix presents the analysis of statistical significance of KPIs for representative simulation scenarios taken from the study.

Chapter 2

Overview of Uplink Radio Resource Management in LTE

2.1 Introduction

This chapter presents an overview of different uplink Radio Resource Management (RRM) functionalities and their interaction in Long Term Evolution (LTE). Section 2.2 introduces the standardized Quality of Service (QoS) parameter settings. Section 2.3 presents the general description of Admission Control (AC) and it's requirements to support QoS. Section 2.4 discusses the connection mobility control and the challenges due to decentralized architecture. Section 2.5 describes the load balancing mechanism and its interaction with AC and handover. Section 2.6 presents the decoupled time and frequency domain scheduling framework proposed for LTE. Section 2.7 describes the Link Adaptation (LA) functionality which include power control, Adaptive Modulation and Coding (AMC), and Outer Loop Link Adaptation (OLLA). Section 2.8 describes the Hybrid Automatic Repeat reQuest (HARQ) modeling. Section 2.9 presents the transport and physical channels standardized for data and control transmission in LTE. Finally the chapter is summarized in Section 2.10.

2.2 QoS Parameter Settings

The QoS parameters are described in [22]. An Evolved Packet System (EPS) bearer is the level of granularity for bearer level QoS control in the Evolved Packet Core (EPC)/E-UTRAN. One EPS bearer is established when the User Equipment (UE) connects to a Packet Data Network (PDN), and that remains established throughout the lifetime of the PDN connection (i.e. IP address) to provide the UE with always-on IP connectivity to that PDN. That bearer is referred to as the default bearer. Any additional EPS bearer that is established to the same PDN is referred to as a dedicated bearer. The initial bearer level QoS parameter values of the default bearer are assigned by the network, based on

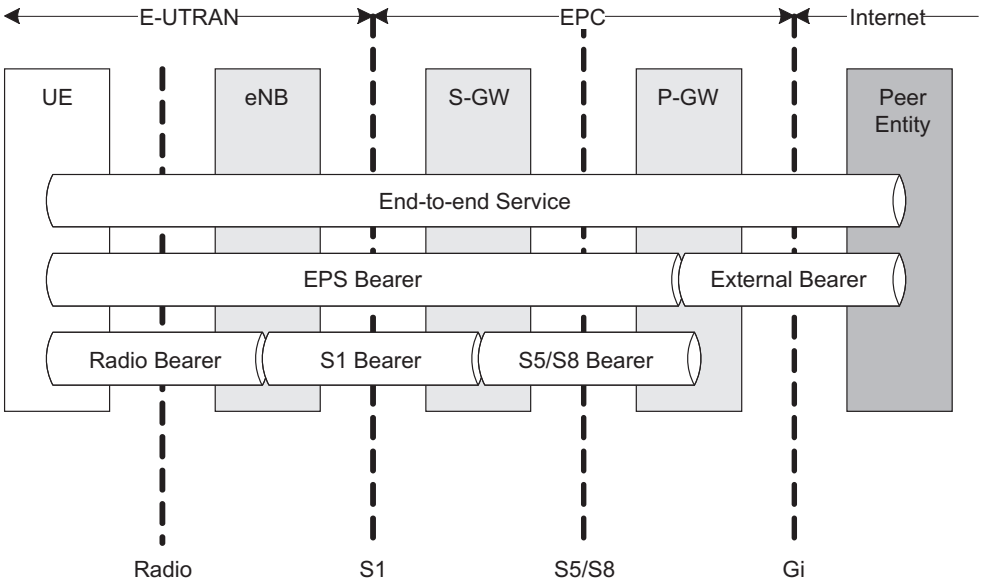

Figure 2.1: EPS bearer service architecture [17]

subscription data. The decision to establish or modify a dedicated bearer can only be taken by the EPC, and the bearer level QoS parameter values are always assigned by the EPC [17].

An EPS bearer is referred to as a GBR bearer if dedicated network resources related to a Guaranteed Bit Rate (GBR) value that is associated with the EPS bearer are permanently allocated (e.g. by an AC function in the eNode-B) at bearer establishment/modification. Otherwise, an EPS bearer is referred to as a Non-GBR bearer. A dedicated bearer can either be a GBR or a Non-GBR bearer while a default bearer shall be a Non-GBR bearer. The EPS bearer service layered architecture is depicted in Figure 2.1.

Each EPS bearer (GBR and non-GBR bearers) is associated with the following bearer level QoS parameter:

- Quality Class Identifier (QCI);
- Allocation Retention Priority (ARP).

These QoS parameters, among others like Aggregate Maximum Bit Rate (AMBR) and GBR, are signaled from the Access Gateway (aGW) to the Evolved Node B (eNode-B) for the bearers as shown in Figure 2.2. The QCI is a scalar identifier which does a mapping to a service type based on bearer priority, packet delay budget, and packet loss rate. A one-to-one mapping of standardized QCI values to standardized characteristics is given in [22]. The primary purpose of ARP is to decide whether a bearer establishment/modification request can be accepted or needs to be rejected in case of resource limitations (typically available radio capacity in case of GBR bearers). In addition, the ARP can be used by the eNode-B to decide which bearer(s) to drop during exceptional resource limitations for

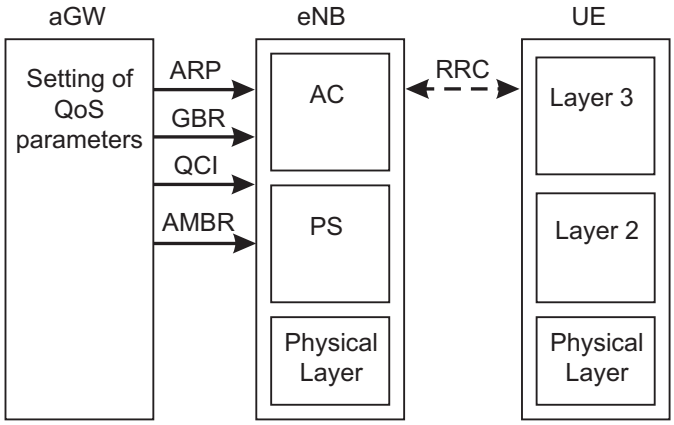

Figure 2.2: QoS parameter settings in LTE

example at handover. Additionally, there is Prioritized Bit Rate (PBR), which is set from the eNode-B in uplink for both GBR and non-GBR bearers in order to avoid starvation of low priority flows [17]. It should be noted that PBR is only relevant for users with multiple bearers.

Each GBR bearer is as well associated with the Guaranteed Bit Rate (GBR), which is the bit rate that can be expected to be provided to a GBR bearer. Additionally, each PDN connection is associated with AMBR. Multiple EPS bearers of the same PDN can share the same AMBR. The AMBR limits the aggregate bit rate that can be expected to be provided by the EPS bearers sharing the AMBR. It is important to note that AMBR only includes the non-GBR bearers while GBR bearers are outside the scope of AMBR.

2.3 Admission Control

The task of AC is to admit or reject the establishment requests for new radio bearers. In order to do this, AC takes into account the overall resource situation, the QoS requirements, the priority levels and the provided QoS of in-progress sessions and the QoS requirement of the new radio bearer request. The goal of AC is to ensure high radio resource utilization (by accepting radio bearer requests as long as radio resources available) and at the same time to ensure proper QoS for in-progress sessions (by rejecting radio bearer requests when they cannot be accommodated) [17]. AC is located at Layer 3 (network layer) (L3) in the eNode-B, and is used both for setup of a new bearer and for handover candidates.

Hence a QoS aware AC is a requirement for GBR bearers in LTE. The AC for non-GBR bearers is optional. The QoS aware AC determines whether a new UE should be granted or denied access based on if QoS of the new UE will be fulfilled while guaranteeing the QoS of the existing UEs [23]. Further, due to the fact that AC is located in L3 in the eNode-B, it will utilize the local cell load information to make an admission/rejection decision. The eNode-B could also interact on X2 interface sharing load information in neighboring cells and make AC decision based on the multi-cell information.

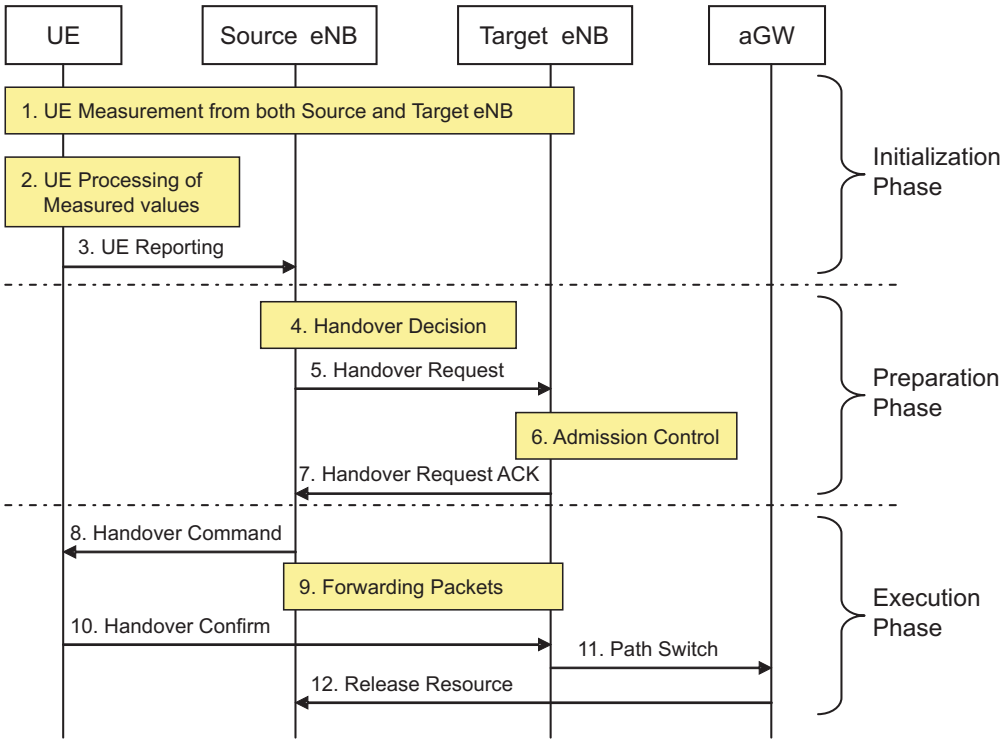

Figure 2.3: Intra-LTE handover procedure [17].

2.4 Connection Mobility Control

Connection mobility control is concerned with the management of radio resources in connection with idle (RRC_IDLE) or connected (RRC_CONNECTED) mode mobility. In idle mode, the cell reselection algorithms are controlled by setting of parameters (thresholds and hysteresis values) that define the best cell and/or determine when the UE should select a new cell. Further, LTE broadcasts parameters that configure the UE measurement and reporting procedures. In connected mode, the mobility of radio connections has to be supported. Handover decisions may be based on UE and eNode-B measurements. In addition, handover decisions may take other inputs, such as neighbor cell load, traffic distribution, transport and hardware resources, and operator defined policies into account [17]. Connection mobility control is located at L3 in the eNode-B.

2.4.1 Handover

The intra-LTE handover in RRC_CONNECTED state is UE assisted and network controlled. One of the goals of LTE is to provide seamless access to voice and multimedia services with strict delay requirements which is achieved by supporting handover from one cell i.e., source cell, to another i.e. target cell. The problem of providing seamless access becomes even more important in LTE since it uses hard handover (break-before-make type).

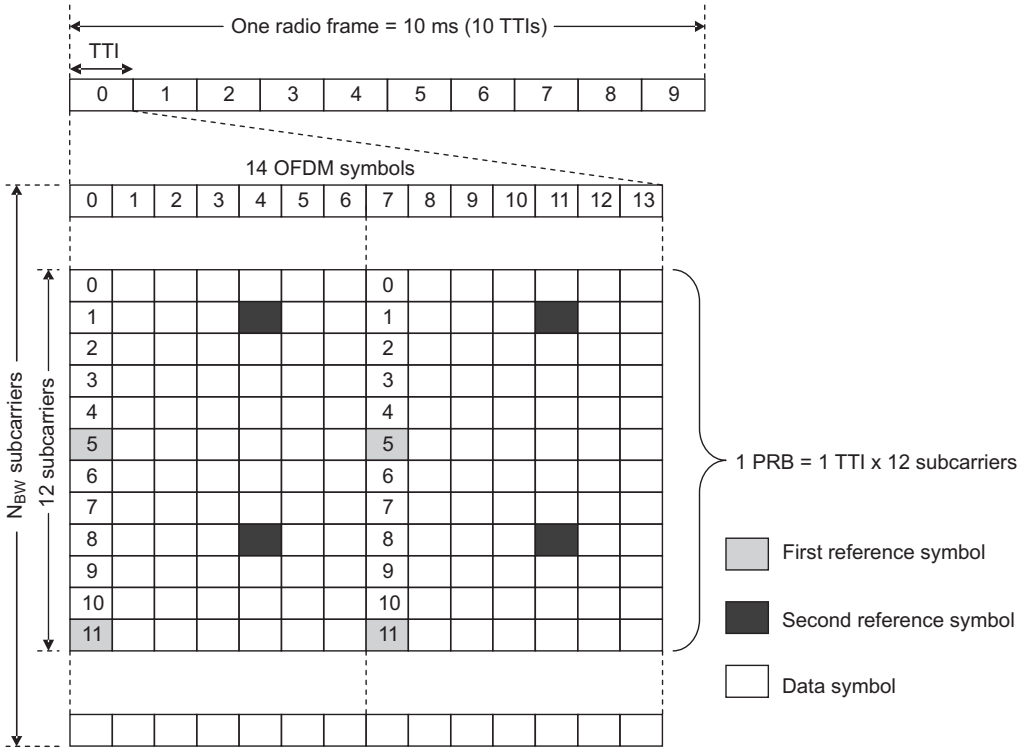

Figure 2.4: Frame structure of E-UTRA FDD containing 14 OFDM symbols per TTI including downlink subcarrier structure with reference signal (pilot) structure for one eNode-B transmit antenna port [14].

The handover procedure in LTE can be divided into three phases: Initialization, Preparation, and Execution as shown in Figure 2.3. In the initialization phase UE does the channel measurements from both source and target eNode-B, followed by the processing and reporting of the measured value to the source eNode-B. The channel measurements for handover are done at the downlink and/or uplink reference symbols (pilots). The downlink reference symbols structure in an E-UTRA FDD frame is illustrated in Figure 2.4. In the preparation phase the source eNode-B makes a handover decision, and it requests handover with target eNode-B. Further, the AC unit in target eNode-B makes the decision to admit or reject the user, which is sent to the source eNode-B using handover request ACK or NACK. Finally, in the execution phase source eNode-B generates the handover command towards UE, followed by which the source eNode-B forwards the packet to the target eNode-B. After this UE performs synchronization to the target eNode-B and accesses the target cell via Random Access Channel (RACH). When UE has successfully accessed the target cell, the UE sends the handover confirm message along with an uplink buffer status report when required to the target eNode-B to indicate that handover procedure is complete. Further, target eNode-B sends a path switch message to the aGW to inform that UE has changed the cell, followed by a release resource message the source eNode-B is informed of the success of handover. After receiving the release resource message the source eNode-B releases radio as well as user-plane and control-plane related resources associated to the UE context [17].

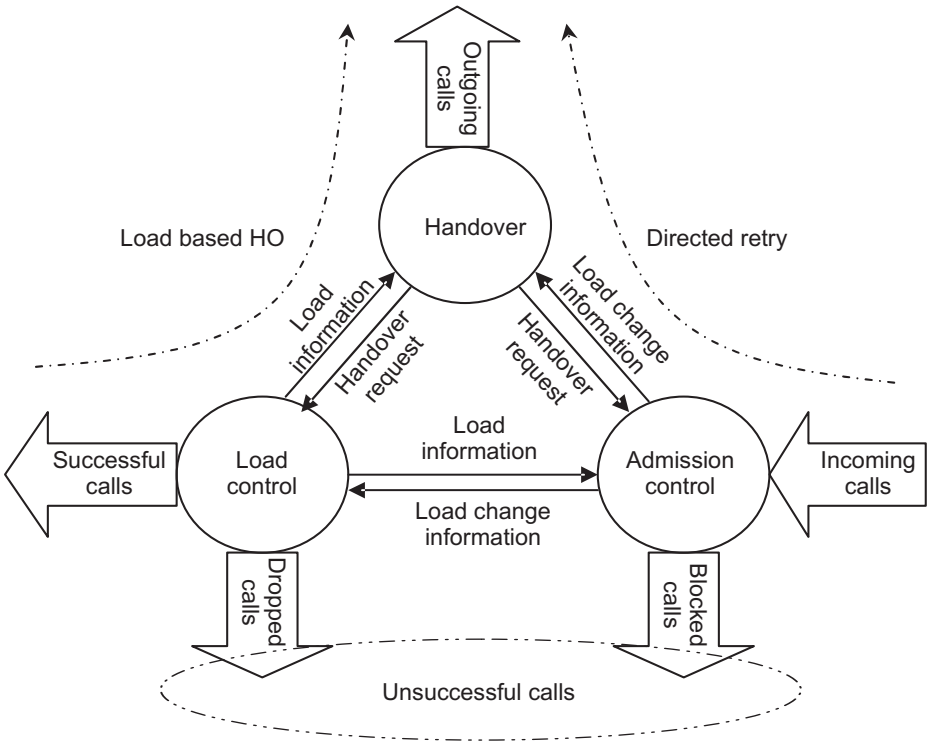

Figure 2.5: Interaction between admission control, handover, and load control.

2.5 Load Balancing

Load balancing (or load control) has the task to handle uneven distribution of the traffic load over multiple cells. The purpose of load balancing is thus to influence the load distribution in such a manner that radio resources remain highly utilized and the QoS of in-progress sessions are maintained to the extent possible and call dropping probabilities are kept sufficiently small. Load balancing algorithms may result in the handover or cell reselection decisions with the purpose of redistributing traffic from highly loaded cells to underutilized cells. Load balancing functionality is located in the eNode-B.

Figure 2.5 shows that the AC, handover, and load control are closely coupled RRM functionalities. Handover is made when an active user in the source cell could be best served in the target cell. AC with the feedback from the load control functionality decides whether an incoming call (new or handover call) should be accepted or blocked. AC then informs the load control about the change in load conditions due to admission of a new or handover call. If an incoming call cannot be served in the originating cell, and if the call can be served by an adjacent cell, the call is immediately handed over to the adjacent cell. This is called directed retry which is a well known concept used in Global System for Mobile Communication (GSM) [24], and could potentially be used for LTE as well. Load control keeps track of the load condition in a cell and in case of overloaded situation it drops a Best Effort (BE) call to maintain the QoS of the active calls in the cell. One way to decrease the call dropping probability is to make a handover to an adjacent cell if this call could be served in the adjacent cell with the required QoS. This is called

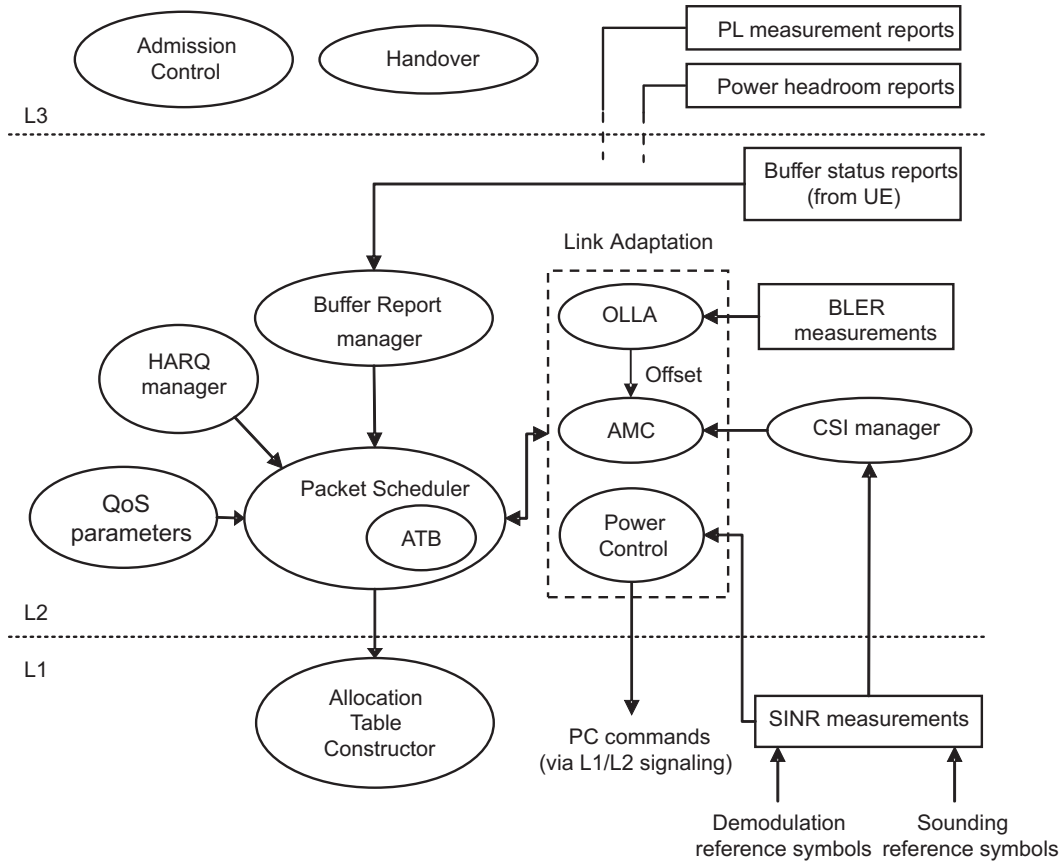

Figure 2.6: Interaction between layer 2 functional entities involved in scheduling and LA and their location in protocol stack.

load based handover. Beside call dropping or handover of lower priority calls the QoS of lower priority calls can be degraded to free resources. This is especially useful in situation where no appropriate adjacent cell is available and therefore call drops can be avoided at the expense of degraded quality of lower priority calls.

2.6 Packet Scheduling

Packet scheduling plays a fundamental role of multiplexing users in time and frequency domain based on some optimization criterion. If the system is affected by time and frequency selective fading the Packet Scheduler (PS) can exploit the multi-user diversity by assigning each user to the resources which exhibit favorable conditions for that user. The optimal solution to the resource allocation problem for orthogonal multiple access system requires joint optimization over all the available domains i.e., exhaustive search over all possible combinations of transmit parameters (for example subcarrier or transmit power) and users. An optimal solution to maximize the system capacity for OFDMA system is proposed in [25]. The optimal multi-user resource allocation at the subcarrier level granularity is not a feasible solution, for complexity reasons [26], i.e. state of the art hardware

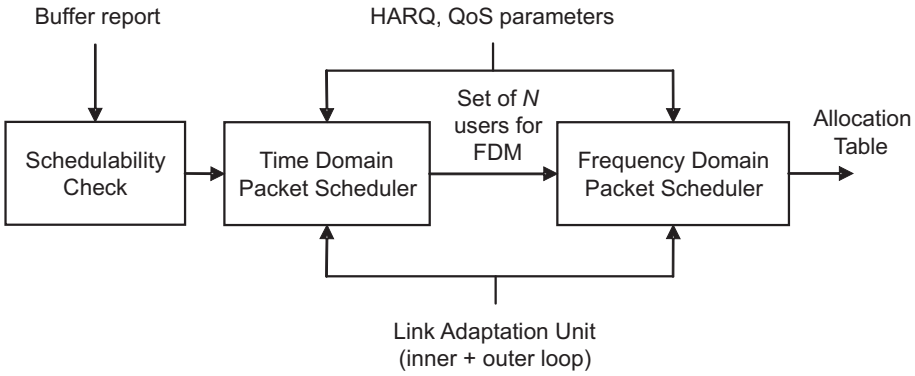

Figure 2.7: Packet scheduler framework illustrating the split between Time-Domain scheduling and Frequency-Domain scheduling parts [30][31].

and software are not able to calculate the optimal solution within one TTI.

Single-Carrier Frequency Division Multiple Access (SC-FDMA) also known as Discrete Fourier Transform (DFT) spread OFDMA has been selected for LTE uplink [27]. SC-FDMA requires the subcarriers, and therefore Physical Resource Blocks (PRBs) allocated to a user, to be adjacent which is an additional constraint to design a PS algorithm. Further, the state of the art optimal solutions does not include the QoS aspect and control channel constraint, which are important in a practical scenario. Similarly, the theoretical approach does not include the HARQ constraints. Previous works on the uplink PS design have limited the problem complexity by either removing the constraint on the contiguity of PRBs and assuming perfect channel knowledge at the eNode-B [28], or by assuming a different and less reliable mechanism than Channel State Information (CSI) [29]. In practice the entities which interact with PS to allocate resources in LTE are QoS parameters, HARQ manager, buffer report manager, Adaptive Transmission Bandwidth (ATB), and LA as shown in Figure 2.6. These entities are further introduced in the chapter.

The practical scheduler design approach used in several studies for LTE is a decoupled Time-Domain (TD) scheduler followed by a Frequency-Domain (FD) scheduler, as illustrated in Figure 2.7 [30]. The packet scheduling is done as a two step algorithm, first TD scheduler selects a subset of N users from the available users in the cell, which are frequency multiplexed by the FD scheduler as shown in Figure 2.7 [32]. This framework is attractive from complexity point of view, since FD scheduler has to consider only frequency multiplexing of maximum N users per TTI. The value of N is set according to the potential channel constraints as well as the available number of PRBs. Assuming the number of users in the cell, D, is larger than N (i.e. $D > N$), the TD scheduler provides the primary mechanism for controlling the QoS, while the FD scheduler mostly tries to optimize the spectral efficiency per TTI. For the case when $D < N$, the FD scheduler should be able to fulfill the required QoS of users along with optimizing the spectral efficiency per TTI. Note that the overall scheduler performance will be sub-optimal due to the limited user diversity at the FD scheduler. Although the scheduling framework consists of two successive steps, there is in many cases a dependency between the TD and the FD schedulers. This is especially the case for those TD schedulers which depends on the average delivered throughput to users in the past (i.e. dependent on the FD scheduler

decisions). Note that due to user transmit power constraints, the uplink allocation might consist only of few PRBs. Hence to maintain a reasonable spectral efficiency the number N should be sufficiently high.

The HARQ manager provides the set of users that have to undergo a fast Layer 1 (physical layer) (L1) retransmission of the data packet. The buffer report manager gives an estimate of the buffer occupancy at the UE [33]. The uplink buffer status report determines the schedulable user set (i.e. the users that have data packets to be transmitted in the next TTI) by using the schedulability check prior to the TD scheduler. Schedulability check additionally based on the information from HARQ manager identifies the scheduling candidate set. The FD scheduler performs the most computationally intense operations by trying to determine the best allocation table based on a scheduling metric. Assuming that a metric value is available for each user and each PRB, the goal can be defined so as to maximize, under the single-carrier constraint, the utility function:

$$M_{sum} = \sum M_{i,j} A_{i,j} \text{ with } i \in \Omega_i,\ j \in \Omega_j \tag{2.1}$$

where $M_{i,j}$ is the metric for user i and PRB j, Ω_i is the set of users, Ω_j is the set of PRBs, and $A_{i,j} = \{0, 1\}$ with 1 for user i allocated to PRB j, and 0 otherwise. This problem can be solved using an exhaustive search-tree based algorithm for fixed number of PRBs allocated to each user per TTI [34], or flexible number of PRBs allocated to each user per TTI also known as ATB [35].

2.6.1 Adaptive Transmission Bandwidth

The multiplexing of users in FD depending on the scheduling metric is a way to exploit the multi-user diversity and to satisfy the QoS [36]. The Adaptive Transmission Bandwidth (ATB) provides a flexible PRB allocation algorithm depending on the scheduling metric representing the channel quality and the requirement to guarantee the QoS which can accommodate for different traffic types e.g., Voice over Internet Protocol (VoIP), which requires a limited bandwidth. The ATB algorithm allocate users with high path loss (cell edge users) lower number of PRBs, while allocating higher number of PRBs to the low path loss users (cell center users). Information on the user Power Spectral Density (PSD) is important in order to correctly allocate the transmission bandwidth (PRBs) and the Modulation and Coding Scheme (MCS). Inaccurate knowledge of the PSD could e.g. cause the allocation of a too high transmission bandwidth (given the maximum UE power capabilities), thus resulting in a low SINR. Therefore, information on the UE transmission power is conveyed from the UE to the eNode-B using power headroom reports [33]. Hence, the advantage of ATB algorithm is that it has the capability to cope with varying traffic loads as well as power limitations [35].

2.7 Link Adaptation

Link Adaptation (LA) is a technique that adapts bandwidth, modulation, coding, transmit power, and/or other signal transmission parameters to the instantaneous channel conditions, aiming to increase the spectrum efficiency and reliability of wireless systems [37]. LA includes power control and AMC as shown in Figure 2.6 [17]. In LTE uplink intra-cell interference is ideally non-existent because of the use of an orthogonal multiple access scheme, i.e. SC-FDMA. The power control is primarily used to compensate for the slow variations of the channel and interference conditions. The slow power control opens for the possibility to perform fast link adaptation based on AMC. These mechanisms are discussed in detail in the following sections.

2.7.1 Power Control

It has been agreed in 3GPP that a UE set its total transmission power (P) using the following Fractional Power Control (FPC) formula [20]:

$$P = \min\{P_{\max}, P_0 + 10\log_{10} N + \alpha L + \Delta_{MCS} + f(\Delta_i)\} \text{ [dBm]} \qquad (2.2)$$

In (2.2), P_{max} is the maximum user transmission power, N is the number of assigned PRBs in a TTI, P_0 and α are power control parameters (α is cell-specific, while P_0 can either be cell- or user- specific), L is the downlink path loss measured at the UE, Δ_{MCS} is a cell specific parameter given by Radio Resource Control (RRC), Δ_i is a user specific aperiodic closed loop correction included in the uplink grant. The selected FPC concept for LTE uplink is based on a mixed open loop and closed loop power control scheme. The main scope of the compensation factor (α) in FPC is to operate different UEs at different target SINR levels depending on their path loss to the serving base station, thus reducing the generated inter-cell interference. The FPC is studied, and the power control parameters (P_0, α) are optimized in [38].

2.7.2 Adaptive Modulation and Coding

It is well known that Adaptive Modulation and Coding (AMC) can significantly improve the spectral efficiency of a wireless system [39]. Therefore this feature is included in several wireless standards e.g., GPRS/EDGE, HSPA [2], WiMAX [40], LTE [14]. In LTE uplink the supported data-modulation schemes are Quadrature Phase Shift Keying (QPSK), 16 Quadrature Amplitude Modulation (16QAM), and 64 Quadrature Amplitude Modulation (64QAM) [11].

The basic functioning of AMC is to select the most suitable MCS for transmission on a TTI basis to adapt to the changing channel conditions. Figure 2.8 illustrates an example of the spectral efficiency versus average SNR for different MCS. It should be noticed that at

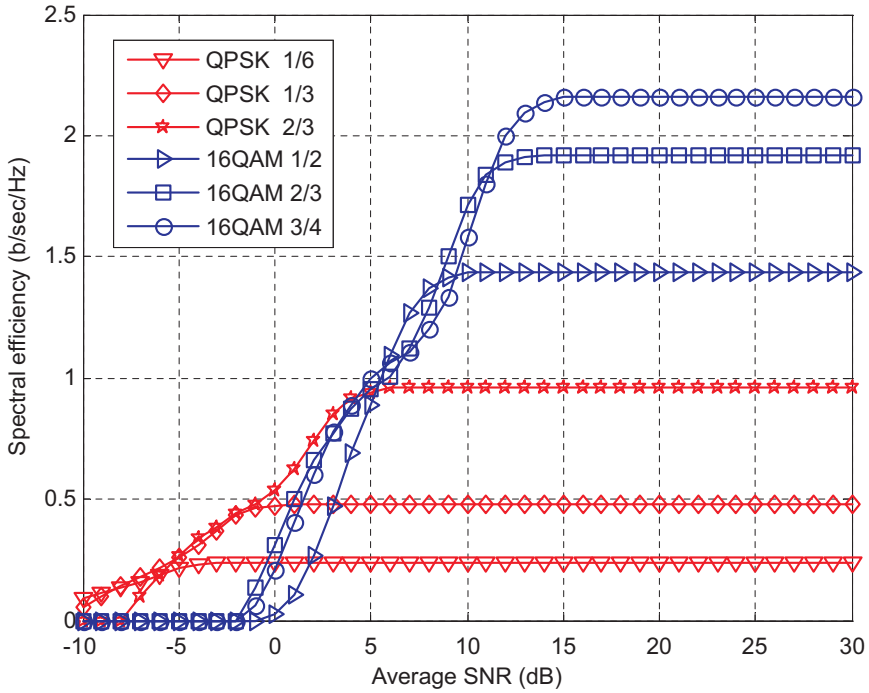

Figure 2.8: Spectral efficiency vs. average SNR for different MCS including LTE specific overhead [42].

higher average SNR (i.e. better channel quality), higher order MCS can be supported giving higher spectral efficiency. The MCS selection depends on the estimate of SINR with a given accuracy that a user will experience in correspondence of the scheduled bandwidth and at scheduled time instant. The AMC can be done on a fast basis for example on per TTI basis, or on a slow basis for example every power control command which is sent every certain number of TTIs. In [41], it is shown that the fast AMC is significantly better compared to slow AMC in terms of average cell throughput. The gain in using fast AMC is coming from the fact that high instantaneous SINR conditions that occur sometimes (due to power control only compensating for slow channel and interference variations) are better exploited by the allocation of high order MCSs compared to slow AMC that selects MCS only based on average channel and interference conditions. The AMC for LTE uplink is studied in detail in [41].

2.7.2.1 Channel State Information

The SINR estimate used by AMC is also referred to as the Channel State Information (CSI). The Channel State Information (CSI) is estimated using the channel sounding concept as well as uplink reception on Physical Uplink Shared Channel (PUSCH) [14]. In channel sounding the UE transmits a Sounding Reference Signal (SRS) in the uplink covering the entire or a part of bandwidth eligible for allocation. The SRS is used at the eNode-B to extract the near-instantaneous frequency selective CSI. Taking advantage of uplink synchronous transmission and of the orthogonality provided by Constant Amplitude Zero Auto-Correlation (CAZAC) sequences users in the same sector can transmit

sounding pilots over the same frequency band without interfering with each other [43]. In reality there exists a constraint on the number of users in one cell that can simultaneously sound the same bandwidth without interfering with each other. This particularly depends on the method used to multiplex SRSs from different users. Moreover, the user transmit power capabilities typically impose a limit on the sounding bandwidth, or alternatively to the level of accuracy of the corresponding SINR measurements. The CSI model used in this study is presented in Section A.2.

2.7.3 Outer Loop Link Adaptation

The LA mechanism is implicitly error prone. Typical errors are due to SINR measurement, link adaptation delay, interference variability, etc. These errors cause the experienced BLock Error Rate (BLER) at first transmission to deviate from the predefined target (in the order of 10–30% [41]). Hence an OLLA algorithm is required to compensate for such errors [44]. OLLA is not standardized for LTE and is vendor specific.

In the scenario where CSI errors cannot be totally avoided, the OLLA algorithm is usually employed to stabilize the overall LA performance on a slow time basis. The OLLA algorithm monitors success of past transmissions to each user, based on Ack/Nack's received, which are used to calculate an offset parameter as input to the AMC as shown in Figure 2.6. Further, the CSI is modified according to the OLLA offset before using them for AMC. The OLLA model used in this study is presented in Section A.3.

2.8 HARQ

The HARQ ensures that in case a data packet is not correctly decodable, then the transmitter (UE) performs fast L1 retransmission of that data packet, thus receiver (eNode-B) can achieve SNR gain by combining soft information for all transmissions. The LTE in uplink supports the HARQ functionality to ensure the packet delivery between peer entities at L1 [45]. HARQ provides robustness against LA errors caused by the uncertainties in CSI estimation and reporting. Further, if the service can tolerate additional delay, HARQ can improve the spectral efficiency by allowing LA to be more aggressive [3]. The HARQ within the Medium Access Control (MAC) sublayer has the following characteristics [45]:

- N-process Stop-And-Wait (SAW) protocol based HARQ is used between a UE and eNode-B. The transmitter persists with the transmission of each packet for a given number of transmission attempts, before discarding the packet. The HARQ processes are transmitted over N parallel time channels in order to ensure continuous transmission to a single UE. The choice of the parameter N depends on the feedback delays and QoS delay constraints. Increasing N leads to extra buffering requirement at the receiver and transmitter, longer delay per HARQ process, and increased signaling load. In LTE eight HARQ processes are standardized.

- The HARQ is based on Ack/Nack's. The data packets are acknowledged after each transmission. A Nack implies that a retransmission is requested either for additional redundancy (Incremental Redundancy (IR)) or a combining gain (Chase Combining (CC)), to enable error free packet delivery to the higher protocol layers. The basic idea of CC scheme is to transmit an identical version of erroneously detected data packet, while with the IR scheme additional redundant information is incrementally transmitted.

- Synchronous retransmissions with both adaptive and non-adaptive transmission parameters are supported in the uplink. Synchronous HARQ implies that retransmissions for a certain HARQ process occur at certain known time instants. Adaptive HARQ operation in the frequency-domain implies that the retransmission can be scheduled on different PRBs in comparison to the first transmission, while non-adaptive HARQ implies that the retransmission are scheduled on the same PRBs as that of the first transmission.

If the HARQ retransmissions fail or exceed the maximum number of retransmissions allowed, the Radio Link Control (RLC) layer handles further ARQ retransmissions if needed. For example the ARQ retransmissions are not required for the VoIP traffic because of the short delay budget. The HARQ gain comes at the cost of increased memory requirement at the UE, required to buffer the soft values at the output of the Turbo decoder. Further, HARQ combining also increases the packet delay.

2.9 Transport and Physical Channels

In LTE the data generated at higher layers is carried using transport channels, which are mapped in the physical layer to different physical channels to be sent over air interface [17].

In uplink, two types of transport channels exist: Uplink Shared Channel (UL-SCH) and Random Access Channel (RACH). The UL-SCH is used to support dynamic LA, HARQ, and dynamic and semi-static resource allocation. The RACH is used for limited control information and for collision avoidance. These transport channels are mapped to

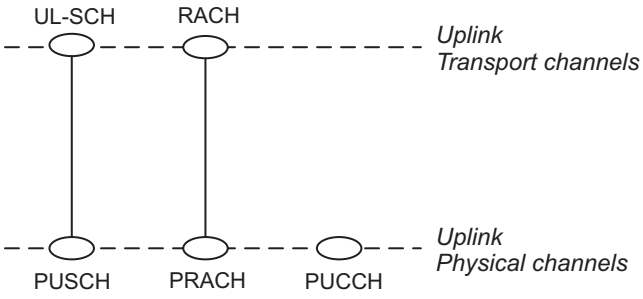

Figure 2.9: Mapping between uplink transport channels and uplink physical channels [17].

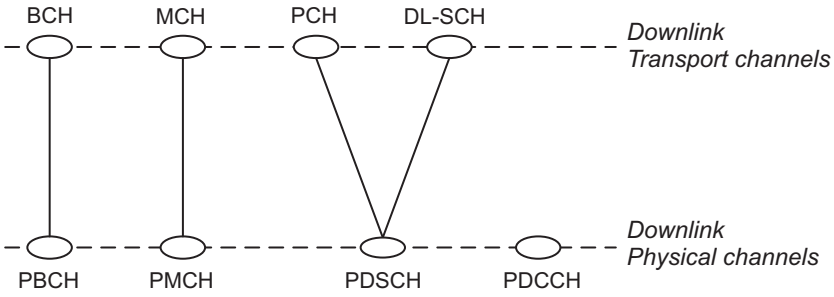

Figure 2.10: Mapping between downlink transport channels and downlink physical channels [17].

the physical channels as shown in Figure 2.9. There are three types of physical channels: Physical Uplink Shared Channel (PUSCH), Physical Uplink Control Channel (PUCCH), and Physical Random Access Channel (PRACH). The PUSCH carries the UL-SCH, PUCCH carries HARQ Ack/Nack's in response to downlink transmission, scheduling requests, and Channel Quality Information (CQI) reports.

In downlink, four types of transport channels exist: Broadcast Channel (BCH), Multicast Channel (MCH), Paging Channel (PCH), and Downlink Shared Channel (DL-SCH). The DL-SCH is used to support dynamic LA, HARQ, dynamic and semi-static resource allocation, and to support Discontinuous Reception (DRX) to enable UE power saving. The BCH is characterized by a fixed, pre-defined transport format, and is required to be broadcasted in the entire coverage area of the cell. The PCH is used to support DRX (DRX cycle is indicated by the network to the UE), and is also required to be broadcasted in the entire coverage area of the cell. The MCH is used to support Multimedia Broadcast Multicast Service (MBMS) transmission on multiple cells. These transport channels are mapped to the physical channels as shown in Figure 2.10. There are four types of physical channels: Physical Downlink Shared Channel (PDSCH), Physical Downlink Control Channel (PDCCH), Physical Broadcast Channel (PBCH), and Physical Multicast Channel (PMCH). The PDSCH carries the DL-SCH and PCH, and PMCH carries the MCH. The PDCCH informs the UE about the resource allocation of PCH and DL-SCH, and HARQ information related to DL-SCH. The PBCH is a coded BCH transport block mapped to four sub-frames within a 40 ms interval, and each sub-frame is assumed to be self-decodable assuming a sufficiently good channel conditions.

2.10 Summary

This overview chapter has provided the concept of uplink RRM in 3GPP LTE Release 8. The uplink RRM functionalities in LTE are located in Layer 2 and Layer 3 at the eNode-B. The QoS parameters setting, LA algorithms including FPC and AMC, and physical and transport channels are described in detail. Additionally, PS is described along with its interaction with ATB and HARQ. In uplink the data is scheduled on the PUSCH based on the uplink grants sent using PDCCH. Further, the concept of AC and handover are introduced, which are studied thoroughly in this thesis.

Chapter 3

QoS-Aware Uplink Admission Control

3.1 Introduction

The Quality of Service (QoS) aware Admission Control (AC) determines whether a new radio bearer should be granted or denied access based on if required QoS of the new radio bearer will be fulfilled while guaranteeing the required QoS of the in-progress sessions [17]. The AC for LTE uplink is located in the Evolved Node B (eNode-B) at Layer 3, which will utilize the local cell load information to make the AC decision. Hence, the focus of this study is on the single cell AC.

This chapter proposes a QoS-aware AC algorithm for Long Term Evolution (LTE) uplink utilizing the user radio channel condition to make an admission decision. This algorithm uses the Fractional Power Control (FPC) formula agreed in Third Generation Partnership Project (3GPP) [20] and hence it is referred to as the FPC based AC. A reference AC algorithm is also developed to compare the performance of the FPC based AC algorithm. The performance is evaluated in terms of blocking probability, outage probability, and unsatisfied user probability.

This chapter is organized as follows: In Section 3.2, the state of the art of AC is presented. The reference AC and FPC based AC algorithms are proposed in Section 3.3. The FPC based AC algorithm is compared with the reference AC algorithm using a detailed semi-static system simulator with the modeling assumptions described in Section 3.4. In Section 3.5, simulation results are presented illustrating the comparison of the proposed AC algorithms, and Section 3.6 contains the conclusions.

3.2 State of the Art

Several studies have been done on the AC for Wideband Code Division Multiple Access (WCDMA) and Orthogonal Frequency Division Multiple Access (OFDMA) based sys-

tems. The uplink AC algorithms for WCDMA system are based on estimating and maintaining the increase in intra-cell interference for admitting a new user [46][47]. As opposed to WCDMA, in LTE uplink intra-cell interference is in principle non-existent because of the use of orthogonal multiple access scheme. Furthermore, in LTE uplink users are scheduled on the dynamically shared channel with fast Link Adaptation (LA) based on Adaptive Modulation and Coding (AMC), FPC, Hybrid Automatic Repeat reQuest (HARQ) and Transmission Time Interval (TTI) of 1 ms. Therefore, the AC algorithms for WCDMA system will not be suitable for LTE. The AC algorithms for OFDMA are studied in [48][49][50][51].

In [48] an adaptive capacity threshold based AC for delay-sensitive Real Time (RT) and delay-tolerable Non-Real Time (NRT) traffic is presented for the downlink IEEE 802.16e system (WiMAX). The proposed AC scheme estimates the downlink cell capacity to cope with the time-varying characteristic of capacity. The capacity threshold used for RT traffic is the ratio of the capacity that can be occupied by the RT traffic. The ratio of the capacity allocated to the RT traffic is estimated by guaranteeing certain packet drop rate for RT traffic. This AC algorithm cannot directly be used in uplink LTE because the affect of user transmit power which is different for all the users and it varies with time due to power control is not present in downlink. Therefore to use this scheme in uplink the cell-capacity estimation need to be extended to include the affect of power control.

In [49] a theoretical framework for an uplink queue-aware AC is presented in which a user is admitted with a certain acceptance probability based on the number of packets in the queue. A two dimensional discrete time Markov Chain capturing the dynamics in terms of number of connections and queue status is used to simulate the system performance. The queue-aware AC is shown to be able to adapt to the traffic load, but it relies on subcarrier and rate allocation for QoS differentiation among the service classes. A simple event-driven simulation considering single transmitter and single service class is used to validate the analytical framework.

In [50] a simple Carrier to Interference Ratio (CIR) threshold based AC for IEEE 802.16 system is presented. This study shows that the blocking performance can be improved at the expense of throughput degradation for different CIR thresholds. This AC is a simple threshold based scheme and does not take into account the radio bearer's QoS requirements. Another AC for WiMAX to optimize the operator revenues and a utility-constrained optimal revenue policy is presented in [51]. Moreover, a cooperative cross-layer resource management scheme is proposed to combine the radio resource management and bandwidth resource management. A simple one-dimensional Markov Chain model is used to evaluate the performance of the AC.

Another important QoS issue is how to control the admission of handover calls. The dropping of handover calls are considered to be more detrimental to the network performance than the blocking of new calls. Several strategies for bandwidth reservation for handover calls [52], and to prioritize the handover calls over new calls are studied [53]. In [53] an AC algorithm is proposed to adaptively control the admission threshold in each cell in order to keep the dropping probability due to handover below a predefined level.

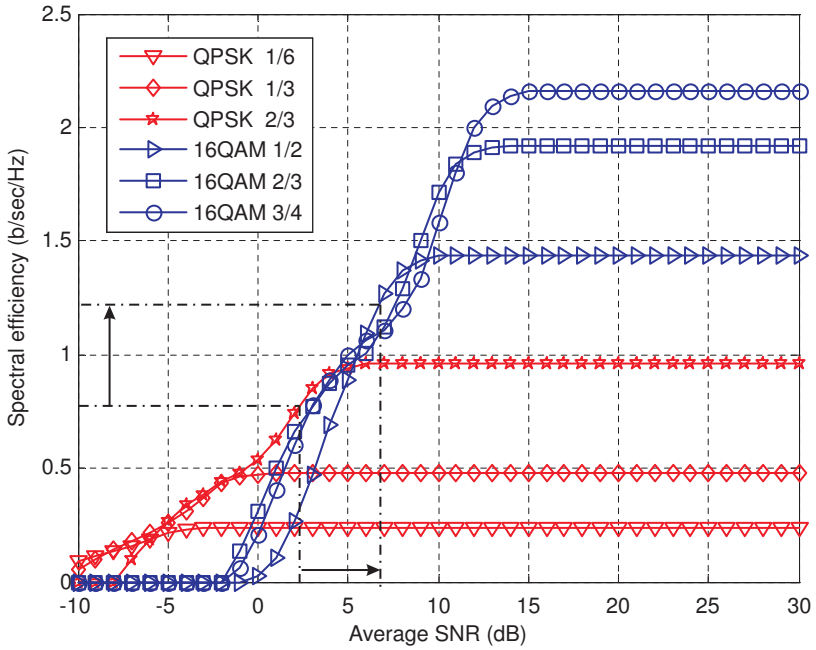

Figure 3.1: Spectral efficiency vs. SINR curve for different MCS. GBR can be maintained using lesser number of PRBs at higher MCS i.e., higher spectral efficiency, and hence higher SINR using higher PSD limited by the maximum user transmit power.

In this thesis AC algorithms are presented considering Guaranteed Bit Rate (GBR) as the main QoS criterion, and each user is assumed to have a single bearer. The handover and new calls are not differentiated in this study.

3.3 Uplink Admission Control

3.3.1 Reference Admission Control Algorithm

The reference AC algorithm decides to admit a new user if the sum of the required GBR of the new and the existing users is less than or equal to the predefined average uplink cell throughput ($R_{\max}$) as expressed in (3.1).

$$\sum_{i=1}^{K} GBR_i + GBR_{new} \leq R_{\max}, \tag{3.1}$$

where K is the number of existing users in the cell. The users in a cell require different amount of resources to fulfill their required GBR as it depends on their radio channel quality. A drawback of the reference AC algorithm is that it does not differentiate the users based on their channel quality. Furthermore, R_{max} is a tunable parameter and does not represent the actual average uplink cell throughput, which is time-variant as it depends on the resources allocated to the users and their experienced channel quality [54]. For

$R_{max} \rightarrow \infty$ this algorithm will admit all the users requesting admission and is equivalent to the case of no AC.

3.3.2 Fractional Power Control based Admission Control Algorithm

To fulfill the GBR a user can either be allocated larger bandwidth and transmit at lower Power Spectral Density (PSD) i.e., lower Modulation and Coding Scheme (MCS), and hence lower Signal-to-Interference-plus-Noise Ratio (SINR). Otherwise, a user can be allocated smaller bandwidth and is required to transmit at higher PSD i.e., higher MCS and hence higher SINR, to achieve the required GBR. This is intuitive from the link-level curves shown in Figure 3.1. Moreover, for a delay tolerable traffic the user can either be allocated more number of Physical Resource Blocks (PRBs) with lower scheduling activity, or lower number of PRBs with higher scheduling activity.

The proposed AC algorithm decides if the current resource allocation can be modified so as to admit the new user and satisfy the GBR requirements of all the active users and the new user. Hence, the admission criterion for the new user is that the sum of the average required number of PRBs per TTI by a new user (N_{new}) requesting admission and existing users (N_i) is less than or equal to the total number of PRBs in the system bandwidth (N_{tot}) e.g. 50 PRBs in 10 MHz [14]. The proposed AC depends on the long term average of required number of PRBs to fulfill the GBR. For example, the GBR of a user can either be fulfilled by allocating N_i PRBs every TTI, or $2 \cdot N_i$ PRBs every second TTI, which corresponds to the same number of average resources on long term, therefore the required number of PRBs are specified in terms of PRBs per TTI. The proposed AC criterion can be expressed as

$$\sum_{i=1}^{K} N_i + N_{new} \leq N_{tot} - \Delta N, \tag{3.2}$$

where ΔN is the load safety margin parameter, which also compensates for signaling overhead. Hence, the problem of AC is to estimate the required number of PRBs per TTI of a user while satisfying its GBR requirement and transmit power constraint.

3.3.2.1 Estimation of N_i and N_{new}

The N_i of the existing users can be measured at the eNode-B by using the average number of PRBs allocated to these users by the PS, while the N_{new} needs to be estimated using the path loss (PL) and required GBR information.

In this section we estimate the N_i and N_{new} assuming that the required GBR and path loss of the existing users and new user requesting admission is known to the AC unit at the eNode-B. The modified Shannon formula [55] in (3.3) is used to estimate the required average number of PRBs per TTI (N_i) for a known GBR_i and PL_i for user i.

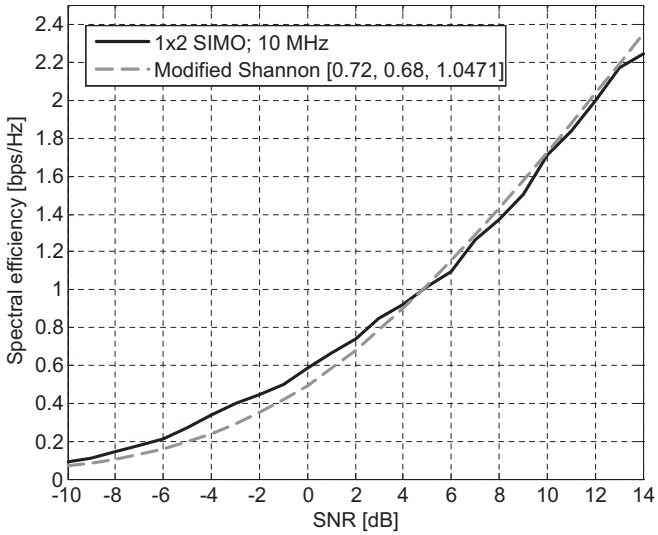

Figure 3.2: Modified Shannon fit curve using the link-level results in [42].

$$S[\text{bits/s/Hz}] = BW_{eff} \cdot \eta \cdot \log_2\left(1 + \frac{SNR}{SNR_{eff}}\right) \tag{3.3}$$

where BW_{eff} is the system bandwidth efficiency, SNR_{eff} adjusts for the Signal-to-Noise Ratio (SNR) implementation efficiency, and $\eta \in [0, 1]$ is the correction factor. As shown in Figure 3.2, $[BW_{eff}, \eta, SNR_{eff}] = [0.72, 0.68, 1.0471]$ for 1x2 antenna deployment, gives a good curve fit to the LTE uplink link-level results in [42]. Actual spectral efficiency versus SINR mapping curves obtained from the field trials and network deployment can be used for improved accuracy instead of simulated link-level results. The required spectral efficiency (S_i) for GBR_i and N_i PRBs is,

$$S_i = \frac{GBR_i}{N_i \cdot BW_{PRB}} \tag{3.4}$$

where BW_{PRB} = 180 kHz. The SINR of user i with transmit PSD (δ_i) in mWatts per PRB is,

$$SINR_i = \frac{\delta_i}{PL_i \cdot IoT \cdot N_0 \cdot NF \cdot BW_{PRB}} \tag{3.5}$$

where IoT is the total uplink received interference plus thermal noise power over the thermal noise power, N_0 is the thermal noise power density per antenna, and NF is the noise figure at the eNode-B.

It has been concluded within 3GPP that the power control for the Physical Uplink Shared Channel (PUSCH) will be FPC consisting of open loop power control along with aperiodic closed-loop adjustments as [20][56][57]

$$P_i = \min\left\{P_{\max}, P_0 + 10\log_{10} N_i + \alpha L_i + \Delta_{MCS} + f(\Delta_i)\right\} \tag{3.6}$$

where P_i is total user power in dBm, P_0 can be a cell or user specific parameter, N_i is the number of assigned PRBs to user i, α is the path loss compensation factor, L_i is the path

loss in dB ($L_i = 10\log_{10} PL_i$), Δ_{MCS} is signaled by the Radio Resource Control (RRC) and Δ_i is a user specific correction value depending on $f()$.

Assuming user is operating within the transmit power dynamic range, the PSD (δ_i) in mWatts per PRB of user i using FPC formula in (3.6) is,

$$10\log_{10}\delta_i = P_i - 10\log_{10} N_i = P_0 + \alpha L_i + \Delta_{MCS} + f(\Delta_i) \tag{3.7}$$

Replacing the δ_i in (3.5) gives the SINR, which gives the closed form solution for N_i using (3.3) and (3.4) as,

$$N_i = \frac{GBR_i}{BW_{PRB}\cdot S_i} = \frac{GBR_i}{BW_{PRB}\cdot BW_{eff}\cdot \eta \cdot \log_2\left(1+\frac{SINR_i}{SNR_{eff}}\right)} \tag{3.8}$$

N_i and N_{new} in (3.2) are estimated using (3.8) to make the AC decision. Additionally, if $\delta_{new}\cdot N_{new} > P_{max}$ the new user is denied admission since it is power limited. In this study Δ_{MCS} and $f(\Delta_i)$ terms are set to zero.

3.3.2.2 Measurement of Input Parameters

In this study the number of PRBs per TTI for existing users are estimated using the method in Section 3.3.2.1. In reality the N_i for existing users in (3.8) can be measured by the Packet Scheduler (PS) at the eNode-B as,

$$N_i = \frac{GBR_i}{\mathbf{R}_{sch,PRB,i}} \tag{3.9}$$

where $\mathbf{R}_{sch,PRB,i}$ is the average scheduled throughput per PRB which is past average of the scheduled throughput ($\mathbf{R}_{sch,i}$) over the number of PRBs allocated to user i. Where $\mathbf{R}_{sch,i}$ is an estimate of user throughput if user i was scheduled every TTI is calculated as [58],

$$\mathbf{R}_{sch,i}[n] = (1-\{B_i[n]>0\}\cdot\beta)\mathbf{R}_{sch,i}[n-1] + \beta\hat{\mathbf{d}}_i[n,k] \tag{3.10}$$

where $\{B_i[n]>0\}$ is a boolean expression which is either 1 or 0 depending on whether the user i is multiplexed in frequency domain or not respectively, β is the forgetting factor, and $\hat{\mathbf{d}}_i[n,k]$ is the estimated achievable throughput for user i on TTI n and PRB k.

The N_{new} is estimated using the estimated path loss by using (3.8). The path loss of a user can be estimated at the eNode-B by using the downlink Reference Signal Received Power (RSRP) measurement signaled over the RRC in uplink [59].

The total number of PRBs (N_{tot}) available for data transmission is the total number of PRBs minus the number of PRBs used for control transmission and signaling overhead. The PRBs used for control transmission by Random Access Channel (RACH) and Physical Uplink Control Channel (PUCCH) are time variable, and this should be taken into account when setting N_{tot}. In this study a constant number of PRBs are assumed for control and data transmission.

Table 3.1: Simulation Parameters and Assumptions

Parameter	**Assumptions**
Inter site distance	500 m (Macro case 1) 1732 m (Macro case 3)
System bandwidth	10 MHz (50 PRBs)
TTI	1 ms
Number of PRBs for data transmission	48
Number of PRBs for control transmission	2
Users multiplexed per TTI	8
PRBs per user per TTI	6 (ATB = OFF)
TD scheduling	GBR-aware
FD scheduling	Proportional Fair scheduled
Forgetting factor (β) for scheduling	0.01
Initial $\mathbf{R}_i$ value	GBR_i [60]
Initial $\mathbf{R}_{sch,i}$ value	GBR_i [60]
HARQ	Synchronous, Adaptive
BLER Target	20%
Power control	Fractional power control
P_o, α	Macro Case 1: -59 dBm, 0.6 Macro Case 3: -64 dBm, 0.6
User arrival	Poisson process
User arrival rate	1, 2, 3, 4, 5, 6, 7, 8, 10 users/cell/s
Traffic model	Finite buffer model
Initial buffer size	1 Mbit
GBR requirement	256 kbps
Number of admitted calls simulated	10000

3.4 Modeling Assumptions

The performance evaluation is done using a detailed multi-cell system level simulator described in Appendix A, which follows the guidelines in [14]. The default simulator parameters and assumptions are listed in Table A.1.

The users in the system are created according to a Poisson call arrival process. If the AC decision criterion proposed in Section 3.3 is fulfilled the user is admitted, otherwise the user is blocked. A finite buffer traffic model is used, where each user uploads a 1 Mbit packet call. All the users in the network are assumed to have the same GBR requirements. The scheduler does not limit the users by their GBR but allows for higher throughput if possible. The session is terminated as soon as the upload is completed.

The packet scheduling is done as a two step algorithm, first Time-Domain (TD) scheduling is used to select the users which will then be multiplexed using Frequency-Domain (FD) scheduling as explained in Section 2.6 [31]. In this chapter a GBR-aware PS is used

in TD, which prioritizes the users which have the average throughput below their GBR requirement based on the metric in (4.1). The users with average throughput above the required GBR are given to FD PS in a uniform random way with equal probability.

$$\mathbf{M}_{\text{TD},i}[n] = \begin{cases} \frac{GBR_i}{\mathbf{R}_i[n]} & \mathbf{R}_i[n] < GBR_i \\ 1.0 & \mathbf{R}_i[n] \geq GBR_i \end{cases}, \tag{3.11}$$

where $\mathbf{R}_i$ is the past average throughput of user i is calculated using exponential average filtering as [60]

$$\mathbf{R}_i[n] = (1-\beta)\mathbf{R}_i[n-1] + \beta\hat{\mathbf{d}}_i[n,k]. \tag{3.12}$$

The FD scheduler allocates the fixed number of PRBs to the users selected by the TD scheduler according to proportional fair scheduled metric defined as [31]

$$\mathbf{M}_{\text{FD},i}[n,k] = \frac{\hat{\mathbf{d}}_i[n,k]}{\mathbf{R}_{sch,i}[n]}. \tag{3.13}$$

The allocated bandwidth per user is assumed to be fixed and the same for all the scheduled users [34]. The collaborative work in [34] is reprinted in Annex I. In this chapter, 8 users are multiplexed per TTI, giving 6 PRBs per user per TTI. The total number of PRBs used for data transmission is 48 PRBs while 2 PRBs are reserved for control transmission. Since the fixed number of PRBs are allocated to the users, the good channel condition users will be scheduled less often compared to poor channel condition users by TD scheduler to fulfill the same GBR.

The power control is done according to the FPC formula standardized in [20]. The optimal FPC parameters for finite and infinite buffer traffic model will be different because of the different path loss distributions in the two cases. In this study, the FPC parameters optimized for infinite buffer traffic model in [38] are used. The simulation parameters specific to this chapter are given in Table 3.1.

3.5 Performance Evaluation

The performance of the proposed AC algorithms is evaluated using the blocking probability, outage probability, and unsatisfied user probability, which are defined in Section A.7. Blocking probability (P_b) is defined as the ratio of the number of blocked users to the total number of new users requesting admission. Outage probability (P_o) is calculated as the ratio of the number of users not fulfilling their GBR requirement, to the total number of admitted users. The unsatisfied user probability (P_u) is calculated as,

$$P_u = 1 - (1-P_b)(1-P_o) \tag{3.14}$$

3.5.1 Macro Case 1 Scenario

This section presents the results in Macro Case 1 scenario, which is represented by the inter-site-distance of 500 m.

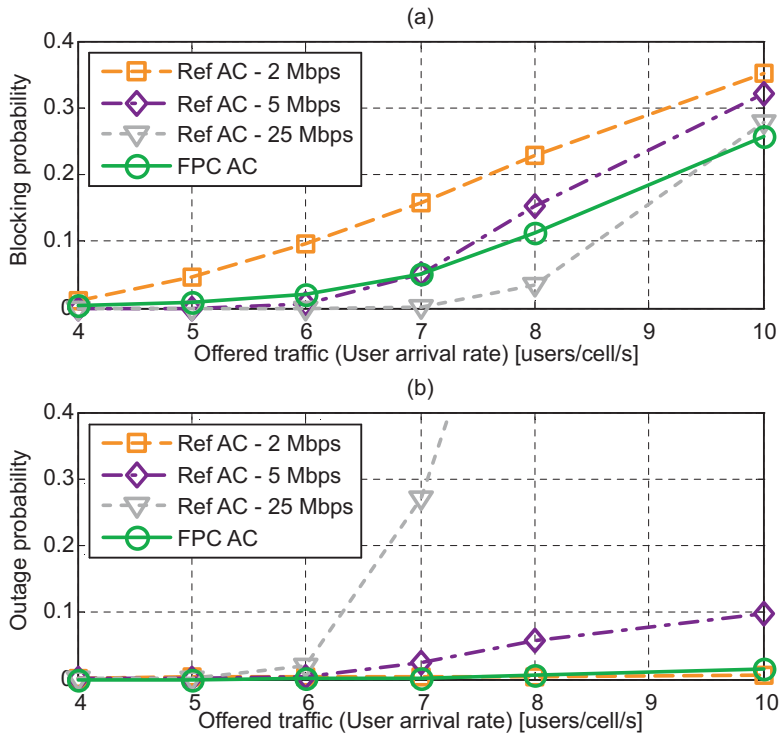

Figure 3.3: (a) Blocking probability vs. offered traffic, (b) outage probability vs. offered traffic for FPC based AC and reference AC algorithms.

Figure 3.3 shows the blocking and outage probabilities vs. offered traffic (user arrival rate) for FPC based AC and reference AC with R_{max} setting of 2, 5, 25 Mbps. In Figure 3.3 (a) we notice that the blocking probability increases with the increasing offered traffic. Even at very low offered traffic FPC based AC denies admission to the users whose QoS cannot be fulfilled. Furthermore, the reference AC makes admission decision without taking into account the average channel condition of users requesting admission. The R_{max} parameter for the reference AC is set as [2, 5, 25] Mbps. For the reference AC algorithm, the blocking probability decreases while the outage probability increases for the increasing value of R_{max} as shown in Figure 3.3 (b). The FPC based AC is shown to be better in terms of the blocking probability while maintaining the outage probability within 1.5%.

For the increasing R_{max}, reference AC block lesser number of users at low and moderate offered traffic but their blocking probability tend to converge for high offered traffic as seen in Figure 3.3 (a). This is because at high offered traffic the users tend to concentrate on the cell edge. Moreover, at higher offered traffic (10 users/cell/s) the blocking probability is lower for the FPC based AC, because the users are admitted such that their average call length is limited by a certain maximum, to fulfill the GBR requirement.

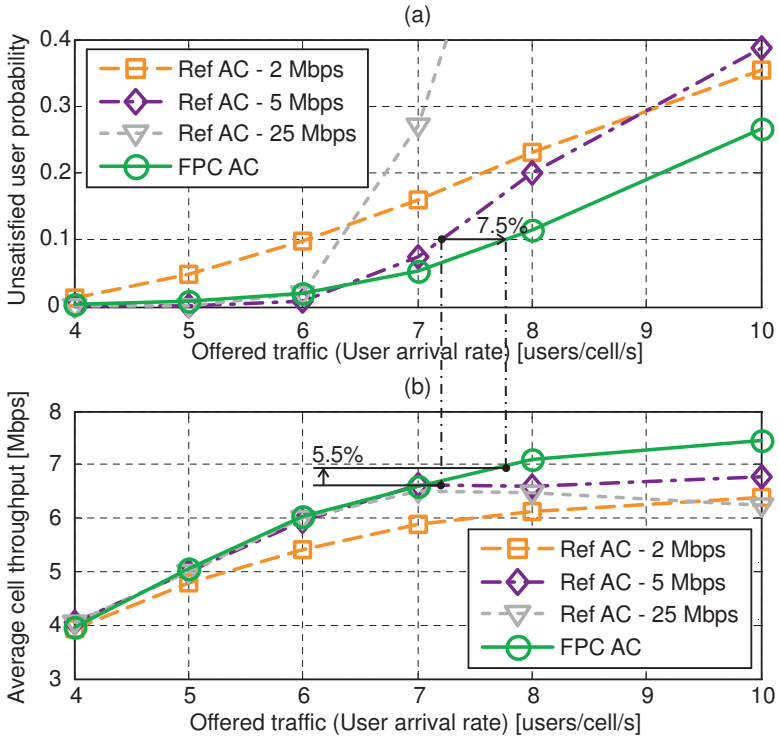

Figure 3.4: (a) Unsatisfied user probability vs. offered traffic, (b) average cell throughput vs. offered traffic for FPC based AC and reference AC algorithms.

Figure 3.4 shows the unsatisfied user probability and average cell throughput (carried traffic) for different AC algorithms. The unsatisfied user probability is derived from Figure 3.3 as in (3.14). We notice that the proposed FPC based AC is the best among the studied AC algorithms in terms of low unsatisfied user probability and high carried traffic, and the performance of reference AC - 5 Mbps is closest to the FPC based AC. At 10% of the unsatisfied user probability, the FPC based AC can support 5.5% more carried traffic, and 7.5% more offered traffic over the reference AC - 5 Mbps as shown in Figure 3.4. It is important to note that the R_{max} for the reference AC is a tunable parameter and is not the actual average cell throughput.

At 10% of the unsatisfied user probability for different AC algorithms the carried traffic will be limited between the range of 90% and 100% offered traffic as in (3.15). For the FPC AC, at 10% unsatisfied user probability the offered traffic is around 7.75 Mbps and the carried traffic is 6.96 Mbps which lies within the range in (3.15). This range as well holds true for the reference AC - 5 Mbps which has the offered traffic of 7.2 Mbps and the carried traffic of 6.6 Mbps at 10% unsatisfied user probability.

$$0.9 \cdot \text{offered traffic} \leq \text{carried traffic} \leq \text{offered traffic} \tag{3.15}$$

Figure 3.5 shows the number of users per cell for different AC algorithms. It is shown that for reference AC - 25 Mbps the number of users grow rapidly for arrival rates 7 users/cell/s and higher. This is because for very high R_{max} the reference AC tend to behave like system with no AC.

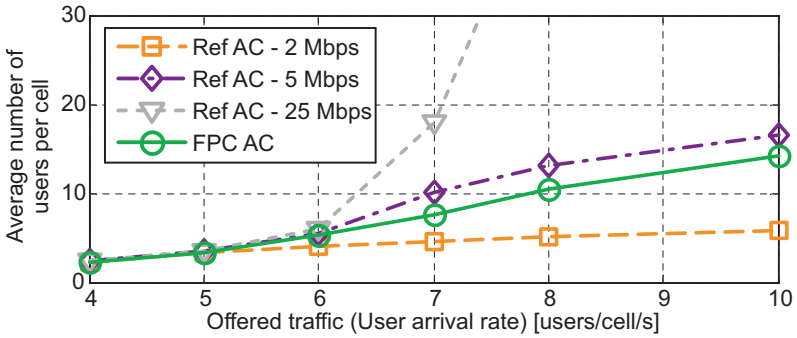

Figure 3.5: Average number of users per cell vs. offered traffic for FPC based AC and reference AC algorithms.

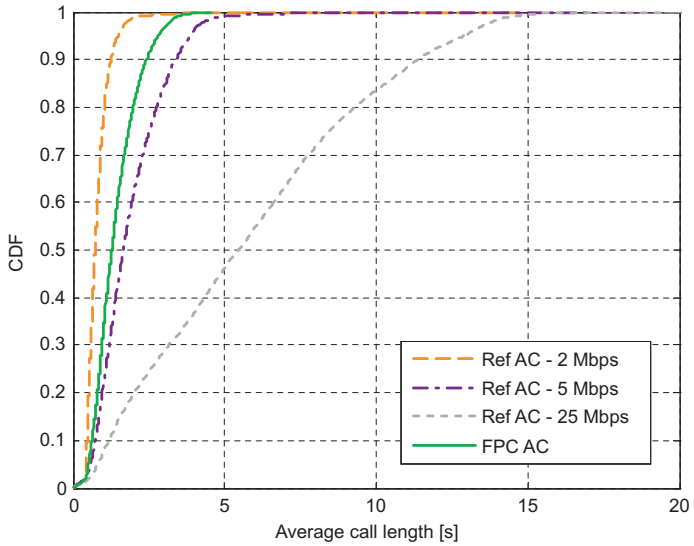

Figure 3.6: CDF of average call length for FPC based AC and reference AC algorithms. User arrival rate = 8 users/cell/s.

Figure 3.6 shows the average call length for different AC algorithms. The average call length of reference AC increases with increasing R_{max}. It is due to the fact that higher average number of users are active for higher R_{max}. For FPC based AC the average call length is limited by a certain maximum equivalent to the maximum time to complete the call with a certain GBR.

Figure 3.7 shows the CDF of path gain (including distance dependent path gain, shadowing, and antenna gain) of admitted users for FPC based AC and reference AC algorithms. It should be noticed that for the FPC based AC the path gain distribution of users in the cell is modified for the cell edge users (low path gain users). This is because the FPC based AC denies admission to a user with a certain GBR requirement at the cell edge with higher probability compared to the user located at the cell center. Moreover, we notice that the path gain distribution of the users is same for the reference AC algorithm because this algorithm treat all the users requesting admission equally regardless of their channel conditions.

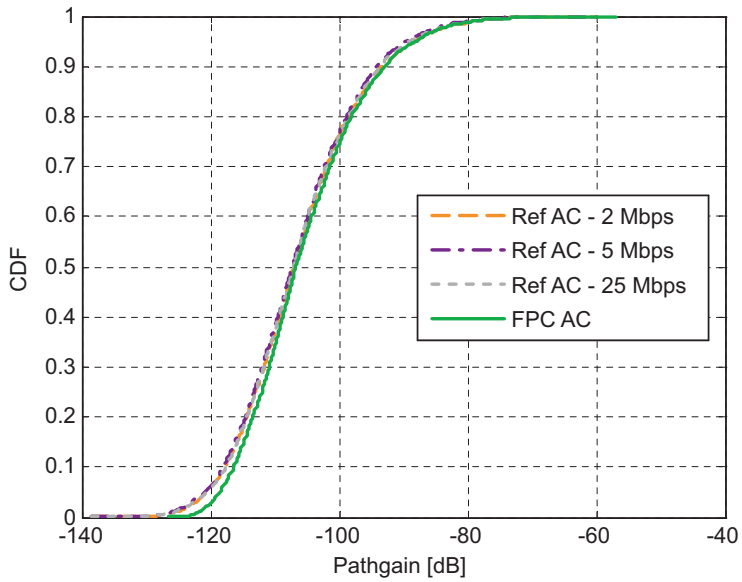

Figure 3.7: CDF of path gain of admitted users for FPC based AC and reference AC algorithms. User arrival rate = 8 users/cell/s.

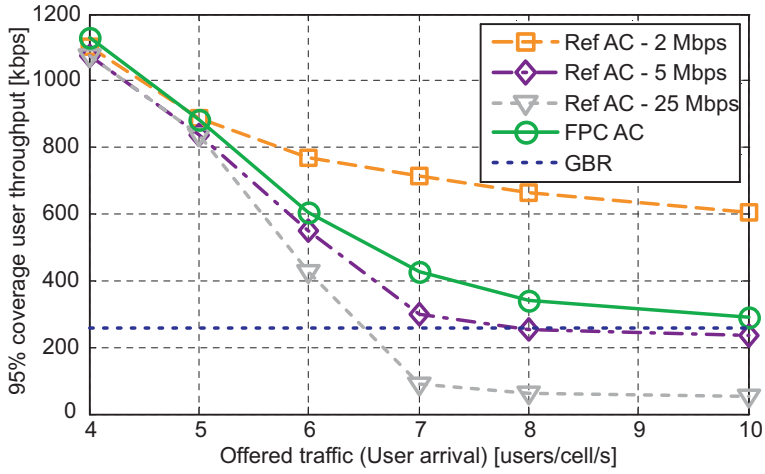

Figure 3.8: 95% coverage user throughput vs. offered traffic for FPC based AC and reference AC algorithms.

Figure 3.8 compares the 95% coverage user throughput for different AC algorithms. We notice that the FPC based AC and reference AC - 2 Mbps are the only evaluated algorithms for which the 95% coverage user throughput is always higher than the GBR. But the unsatisfied user probability is much lower and the carried traffic is significantly higher for using the FPC based AC over the reference AC - 2 Mbps.

Figure 3.9 shows the CDF of the average user throughput and scheduling activity (frequency of user being multiplexed in frequency-domain). For increasing R_{max} the average user throughput as well as scheduling activity decreases. This is due to higher number of active users in the system for higher R_{max} as shown in Figure 3.5.

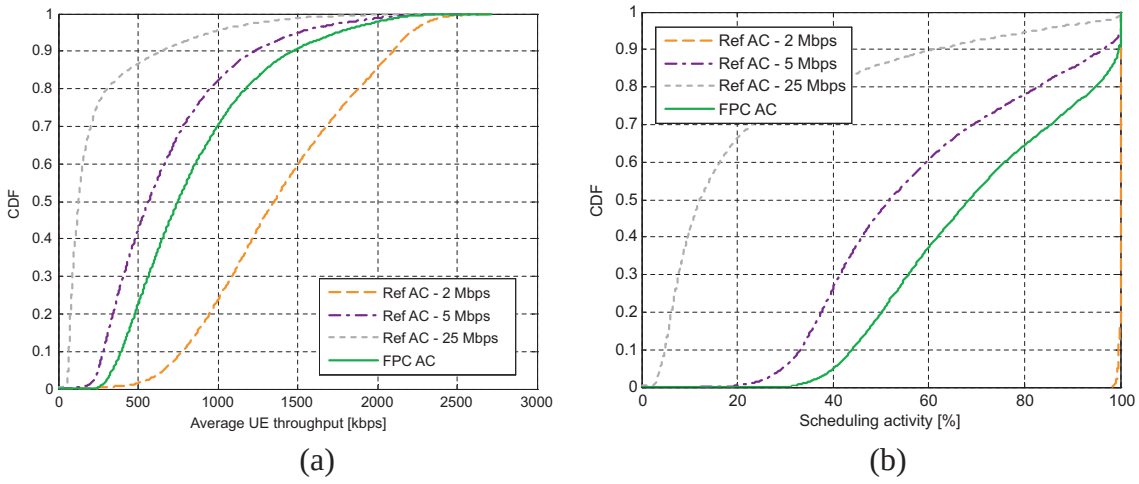

Figure 3.9: (a) Average user throughput, and (b) Scheduling activity for FPC based AC and reference AC algorithms. User arrival rate = 8 users/cell/s.

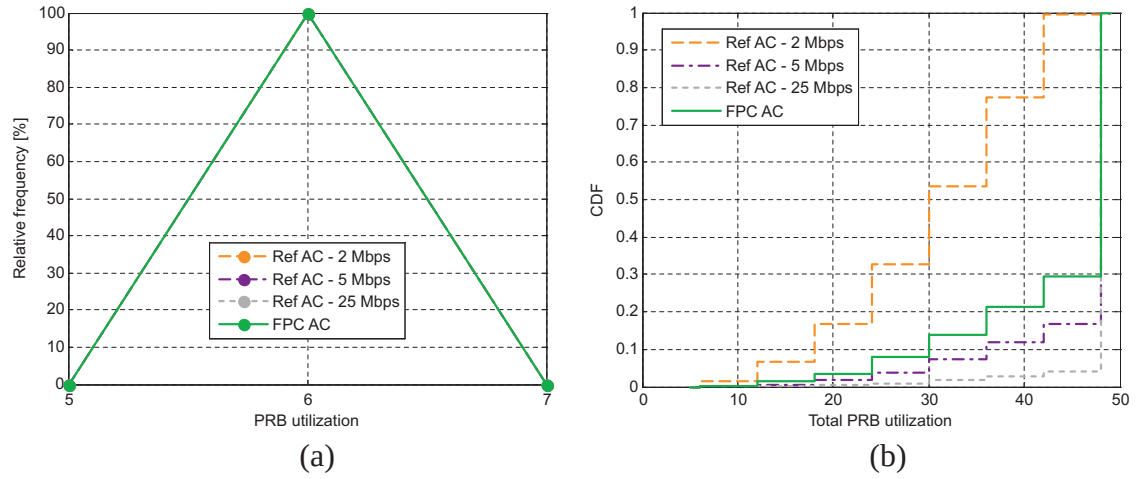

Figure 3.10: (a) PRB utilization per user, and (b) Total PRB utilization for FPC based AC and reference AC algorithms. User arrival rate = 8 users/cell/s.

Figure 3.10 shows the PRB utilization per user (number of PRBs allocated to a user per TTI) and CDF of the total PRB utilization (total number of PRBs allocated to all the active users per cell per TTI). Figure 3.10 (a) shows that for the different AC algorithms each user is allocated 6 PRBs per TTI. This is because the PS is set to allocate fixed transmit bandwidth to the users according to the FDPS metric priority. In Figure 3.10 (b) the reference AC - 2 Mbps almost never utilizes the full system bandwidth (48 PRBs), this is because of the fewer average number of users per cell than that can be multiplexed in frequency domain. For FPC based AC the total PRB utilization is not full for about 30% time. The PRB utilization can be improved by multiplexing the users in the frequency domain using Adaptive Transmission Bandwidth (ATB) based PS [35].

Figure 3.11 shows the CDF of average scheduled SINR and instantaneous IoT for different AC algorithms. Figure 3.11 (a) shows that the SINR distribution is fairer for FPC based AC compared to the reference AC algorithm for the studied R_{max} values. This is

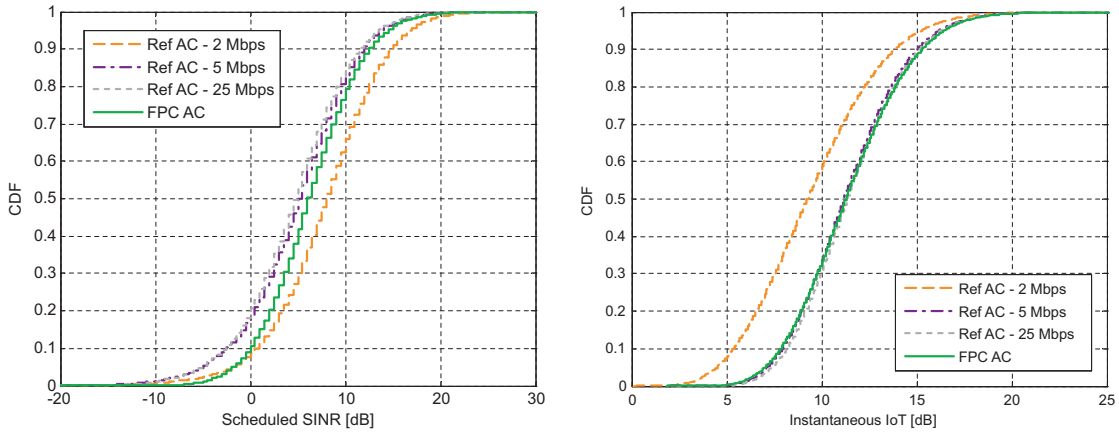

(a) (b)

Figure 3.11: (a) Scheduled SINR, and (b) Instantaneous IoT for FPC based AC and reference AC algorithms. User arrival rate = 8 users/cell/s.

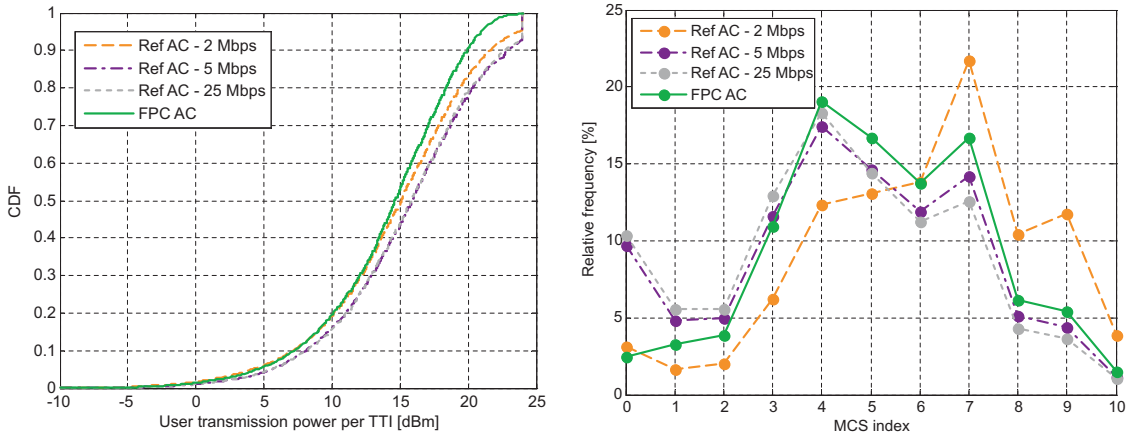

(a) (b)

Figure 3.12: (a) User transmit power, and (b) Relative frequency of MCS index used for FPC based AC and reference AC algorithms. User arrival rate = 8 users/cell/s.

because FPC based AC denies admission to a user with a certain GBR requirement at cell edge with higher probability compared to a user near cell center. Hence the improvement in the SINR at the lower edge of scheduled SINR distribution. The gain in average scheduled SINR for the reference AC - 2 Mbps is due to the lower average IoT as shown in Figure 3.11 (b). This is due to the fractional PRB utilization as shown in Figure 3.10 (b). The average IoT for FPC based AC and reference AC with R_{max} value of 5 Mbps and 25 Mbps are similar. This is due to the fact that each user is transmitting at the fixed transmit power based on the average path gain utilizing the FPC formula.

Figure 3.12 shows the CDF of user transmit power and relative frequency of MCS index[1] used for different AC algorithms. It is seen that for FPC based AC none of the users

[1]The MCS index represents the MCS used in increasing MCS order i.e. MSC index 0 is for QPSK 1/10 and 10 is for 16QAM 5/6. The MCS used in this study are listed in Table A.1.

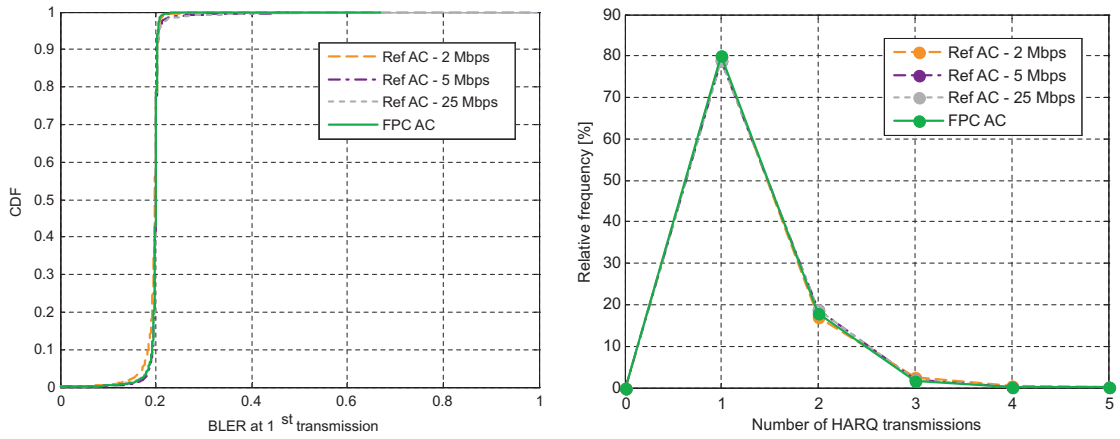

(a) (b)

Figure 3.13: (a) BLER target at 1st transmission, and (b) Number of HARQ transmissions for FPC based AC and reference AC algorithms. User arrival rate = 8 users/cell/s.

are power limited. This is because for FPC based AC a user is rejected if it cannot fulfill the required GBR due to the transmit power constraint of 24 dBm. It should be noticed that up to 8% of users are power limited in the case of reference AC algorithm. This is because the reference AC algorithm does not take into account the channel conditions and the user transmit power limitations to make an admission decision. In Macro case 1 scenario (inter-site-distance is 500 m) few users will be power limited, and hence the blocked users due to the transmit power constraint will be negligible. Admission denials due to the transmit power constraint will be higher in the Macro case 3 scenario (inter-site-distance is 1732 m). The lower MCS is used with higher frequency for reference AC, this is because higher number of users are power limited in this case.

Figure 3.13 shows the CDF of average BLER per user at the 1st transmission and the number of HARQ transmissions for different AC algorithms. The average BLER at the 1st transmission is seen to match well with the BLER target for all of the studied AC algorithms. The maximum number of HARQ transmission attempts per code-block is equal to 4. Figure 3.13 (b) shows that the first HARQ transmission is unsuccessful for 20% which is equal to BLER target. This also verifies that Outer Loop Link Adaptation (OLLA) is able to match the selected BLER target.

3.5.2 Macro Case 3 Scenario

This section presents the results in Macro Case 3 scenario, which is represented by the inter-site-distance of 1732 m. The higher inter-site-distance compared to Macro Case 1 increases the performance limitation due to the user transmit power constraint.

Figure 3.14 shows the blocking and outage probabilities vs. offered traffic (user arrival rate) for different AC algorithms. In Figure 3.14 (a) we notice that the blocking probability increases with the increasing offered traffic. Even at very low offered traffic FPC based AC denies admission to the users whose GBR cannot be fulfilled. Furthermore, the

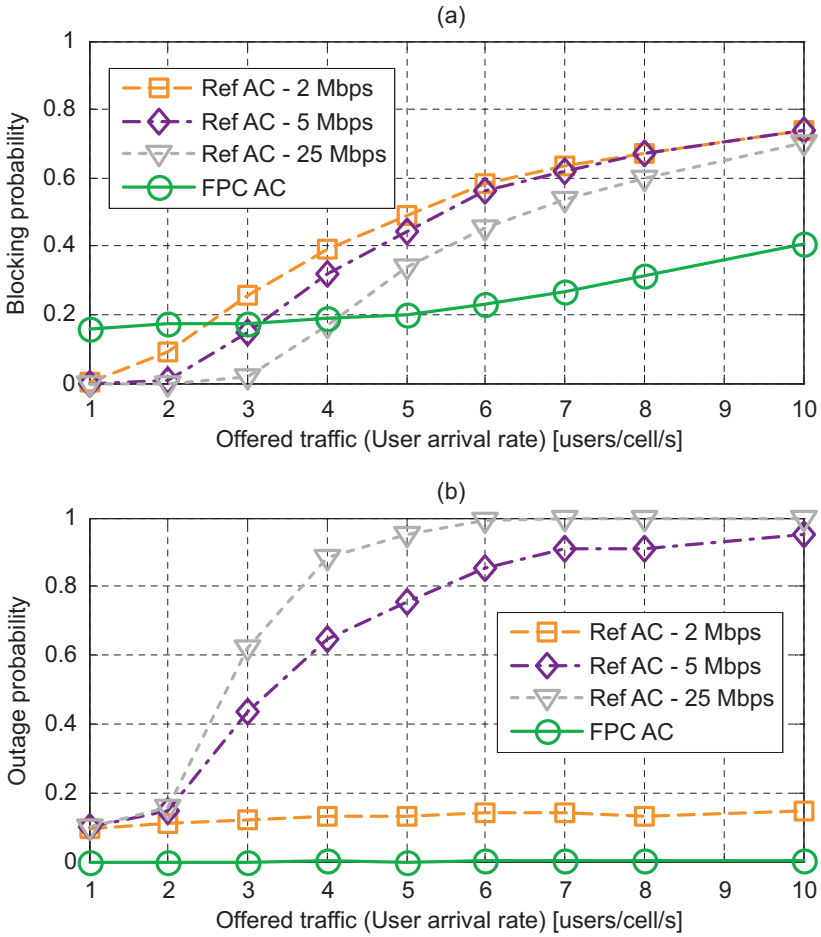

Figure 3.14: (a) Blocking probability vs. offered traffic, (b) outage probability vs. offered traffic for FPC based AC and reference AC algorithms.

reference AC makes admission decision without taking into account the average channel condition of users requesting admission. For the reference AC algorithm, the blocking probability decreases while the outage probability increases for the increasing value of R_{max} as shown in Figure 3.14 (b). We notice that the blocking and outage probabilities are on average higher for Macro case 3 compared to the Macro case 1. This is due to the fact that the users are transmit power limited in Macro case 3, and it leads to higher outage probability for the reference AC. The FPC based AC is shown to be best in terms of negligible outage probability.

Figure 3.15 shows the unsatisfied user probability and average cell throughput (carried traffic) for different AC algorithms. We notice that the proposed FPC based AC is the best among the studied AC algorithms in terms of low unsatisfied user probability and high carried traffic. The carried traffic gain in the Macro case 3 by using FPC based AC is higher because it effectively rejects the user which are unable to fulfill the GBR requirement due to the transmit power limitation.

Figure 3.16 shows the number of users per cell for different AC algorithms. For reference AC the number of users per cell increases with increase in R_{max}. It should be

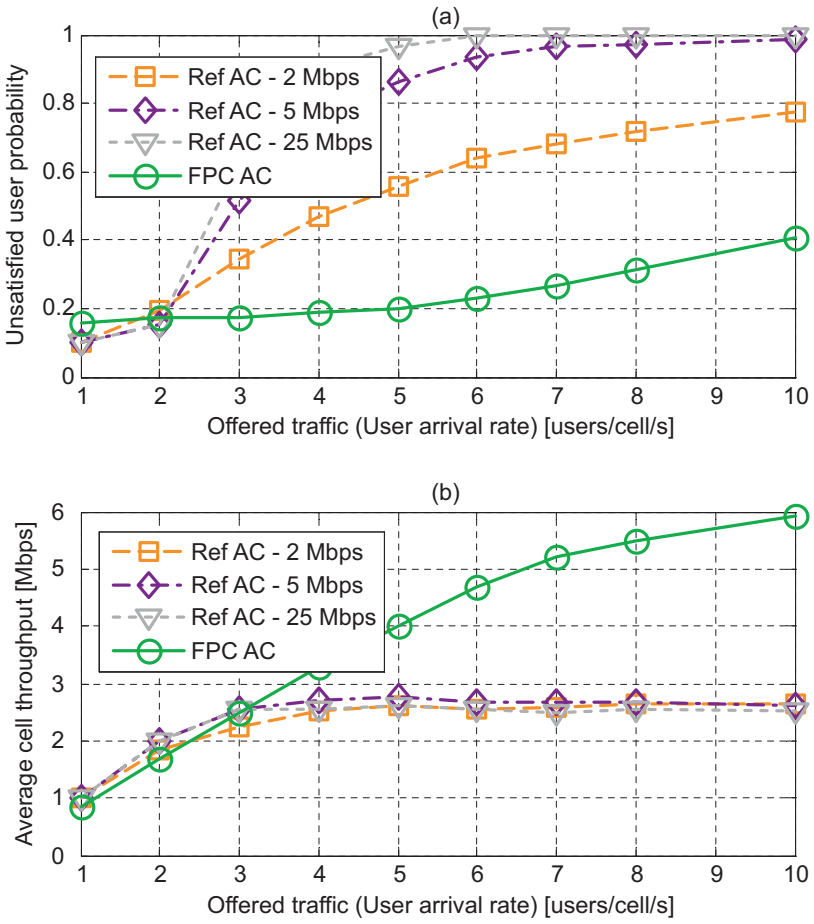

Figure 3.15: (a) Unsatisfied user probability vs. offered traffic, (b) average cell throughput vs. offered traffic for FPC based AC and reference AC algorithms.

noticed that the average number of users per cell in this case is close for FPC based AC and reference AC - 2 Mbps. Instead, in the Macro case 1, the average number of users per cell for FPC based AC is close to reference AC - 5 Mbps as shown in Figure 3.5. This shows that R_{max} of reference AC is dependent on the deployment scenario and need to be tuned, while FPC based AC tunes itself inherently.

Figure 3.17 shows the CDF of the average user throughput and scheduling activity (frequency of user being multiplexed in frequency-domain). The outage user throughput performance for reference AC is much lower compared to the FPC based AC is because it rejects the user at the cell edge if its GBR cannot be fulfilled. For reference AC with increasing R_{max} the average user throughput as well as scheduling activity decreases. This is due to higher number of active users in the system for higher R_{max} as shown in Figure 3.16.

Figure 3.18 shows the CDF of path gain of blocked and admitted users for proposed AC algorithms. It should be noticed that for FPC based AC the path gain distribution of blocked and hence admitted users is modified for the cell edge users (low path gain users). The FPC based AC denies admission to a user with a certain GBR requirement at the cell

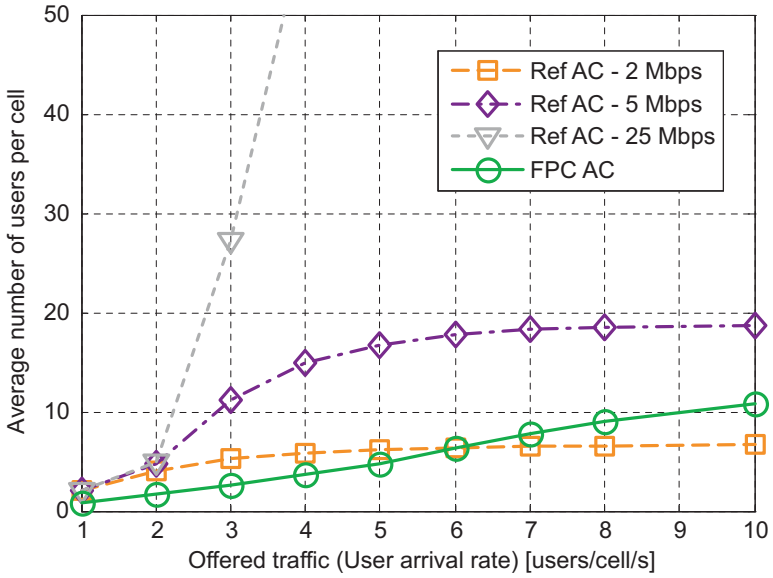

Figure 3.16: Average number of users per cell vs. offered traffic for FPC based AC and reference AC algorithms.

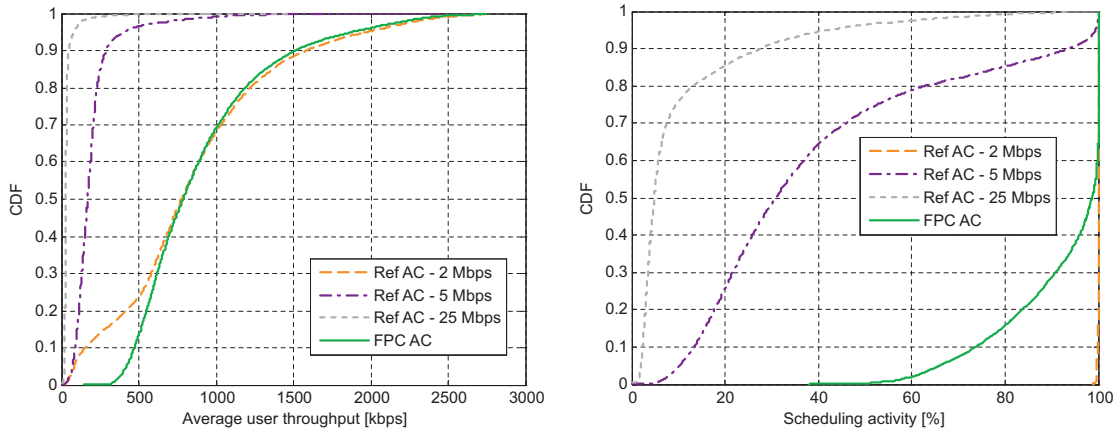

Figure 3.17: (a) Average user throughput, and (b) Scheduling activity for FPC based AC and reference AC algorithms. User arrival rate = 6 users/cell/s.

edge with higher probability compared to the user located at the cell center. This is due to the fact that in Macro case 3 higher number of users are power limited compared to Macro case 3 because of larger inter-site-distance. Moreover, we notice that the path gain distribution of the users is same for the reference AC algorithm because this algorithm makes admission decision independent of their channel conditions.

Figure 3.19 shows the CDF of user transmit power and relative frequency of MCS used for different AC algorithms. It is seen that for FPC based AC none of the users are power limited. This is because for FPC based AC a user is rejected if it cannot fulfill the required GBR due to the transmit power constraint of 24 dBm. In Macro case 3 we notice that for reference AC more than 60% of users are transmit power limited. This is

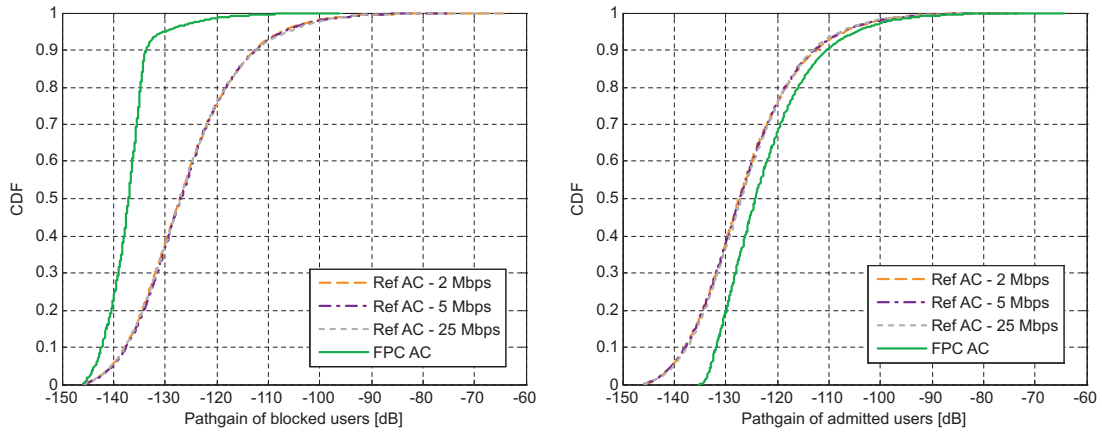

Figure 3.18: (a) CDF of path gain of blocked users, and (b) CDF of path gain of admitted users for FPC based AC and reference AC algorithms. User arrival rate = 6 users/cell/s.

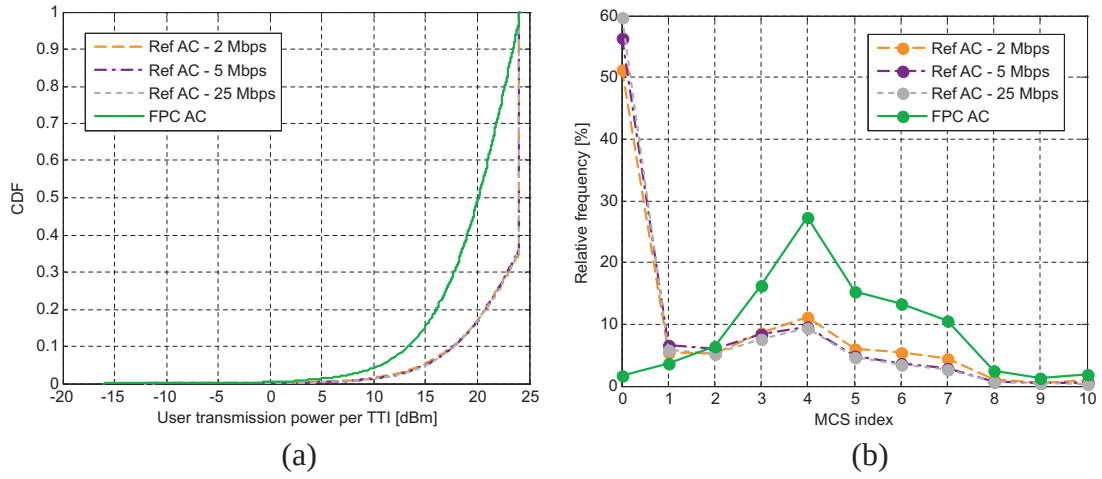

Figure 3.19: (a) CDF of user transmit power, and (b) Relative frequency of MCS used for FPC based AC and reference AC algorithms. User arrival rate = 6 users/cell/s.

because the reference AC algorithm does not take into account the channel conditions and the user transmit power limitations. In Macro case 3 the admission denials by using FPC based AC due to the user transmit power limitation are significantly higher compared to Macro case 1. Due to the fact that higher number of users are power limited in reference AC, it tends to use lower order MCS with comparatively higher frequency compared to FPC based AC as shown in Figure 3.19 (b). Hence it is important to use an AC scheme which takes into account the channel conditions as well as user transmit power constraint to fulfill the required GBR to make an admission decision.

3.6 Conclusions

An AC algorithm for LTE uplink, utilizing the FPC formula agreed in 3GPP, is proposed along with a reference AC algorithm. The FPC based AC determines if a user requesting admission can be accepted based on the average path gain so as to fulfill the QoS of the new and existing users. The results show that FPC based AC performs best in terms of blocking probability, outage probability, and hence unsatisfied user probability. It has been shown that the outage probability is negligible for FPC based AC. The performance of the proposed algorithm is evaluated for both Macro case 1 and case 3. It is shown that for reference AC, in Macro case 1 with average cell throughput of 6–7 Mbps, R_{max} has to be set to around 5 Mbps, whereas for Macro case 3 with average cell throughput of 2–3 Mbps, R_{max} of around 2 Mbps is more suitable. Hence, the R_{max} value for reference AC is sensitive to the deployment scenario and therefore need to be tuned.

The FPC based AC is based on a novel closed form solution. The FPC based AC algorithm is shown to be robust and it tunes itself inherently to the load conditions, unlike R_{max} tuning in reference AC. Hence, the FPC based AC is a good QoS-aware AC algorithm for LTE uplink. Similar AC design approach could also be used for other Beyond 3G (B3G) standards which uses orthogonal multiple access techniques in uplink. The findings of this study have been partially published in [61].

In this chapter, each user is allocated fixed number of PRBs in the frequency domain which lead to the fractional bandwidth utilization. Hence, it is important to study the performance gain with full bandwidth utilization by allocating flexible bandwidth (or ATB) to the users as studied in [35]. Rest of the study is done using ATB based scheduling. Furthermore, the closed loop adjustments of FPC which are included in the derivation of FPC based AC are not taken into account in the performance assessment in this study. In real situation the closed loop adjustments of FPC should be taken into account. Additionally, the offered and carried traffic gains in using FPC based AC for a mixed GBR users case and realistic traffic model need to be investigated. The next chapter studies the QoS differentiation for mixed GBR users case.

Chapter 4

Combined Admission Control and Scheduling for QoS Differentiation

4.1 Introduction

LTE is targeted to efficiently guarantee the Quality of Service (QoS) of services. To provide QoS control, it is necessary that Admission Control (AC) and Packet Scheduler (PS) are QoS aware [54][23]. This chapter studies the performance of combined AC and PS for QoS support and service differentiation. Therefore, a QoS aware PS is proposed and it is combined with the AC algorithm designed in Chapter 3. In this chapter users are allocated PRBs using an Adaptive Transmission Bandwidth (ATB) based scheduling unlike the previous chapter where each user is allocated a fixed number of PRBs. This study considers Guaranteed Bit Rate (GBR) as the main QoS parameter for a bearer, and each user is assumed to have a single bearer. A mixed Best Effort (BE) traffic scenario with different GBR settings are simulated to show that the proposed framework of combined AC and PS is suitable for the QoS differentiation. In practice BE users are non-GBR bearers, but in this study GBR is used as the target bit rate for BE users to verify the proposed algorithms.

This chapter is organized as follows: In Section 4.2, the state of the art of combined AC and PS for mixed traffic types is presented. In Section 4.3, the QoS aware PS for differentiating between user classes is designed. In Section 4.4, the modeling assumptions are described. In Section 4.5, simulation results are presented, and Section 4.6 contains the conclusions.

4.2 State of the Art

Scheduling is one of the major components to provide QoS differentiation in a mixed traffic scenario. Several studies on combined AC and scheduling are done for systems

providing data services e.g., GPRS, HSDPA, and IEEE 802.16, [62] [63] [64] [65] [66] [67].

In [62] a scheduling and AC framework to differentiate between QoS-sensitive and BE flows is presented for broadband wireless systems such as IEEE 802.16. A simple threshold based AC is used to limit the number of connections of the QoS-sensitive queue, while no AC is used for the BE users. The two user classes are differentiated using the Weighted Fair Queueing (WFQ) based on Generalized Process Sharing (GPS) by allocating resources depending on scheduler weights for the QoS-sensitive and BE queues. The proposed method is evaluated numerically using a queueing analytical framework.

In [63] a scheduling problem for a mixed Constant Bit Rate (CBR) and BE with a minimum throughput guarantee is formulated as a utility maximization problem. The proposed scheduling utility function is combined with an AC in order for the proposed QoS scheduler to work as desired. The studied framework assumes single-cell downlink scenario with only one user being served at a time, and the achievable data rate is given by the Shannon bound. Although it had been shown that the proposed combination works under the single-cell downlink scenario, it is not studied if this analytical framework could be extended to a realistic multi-cell scenario with mixed GBR-bearers.

In [64] scheduling policies to guarantee the QoS for High Speed Downlink Packet Access (HSDPA) network are proposed. The proposed scheduling algorithm tries to find a balance between throughput maximization by using opportunistic scheduling, and satisfying QoS constraints. In this study higher priority class users are assumed to have higher GBR. Similar scheduling policies can also be used for LTE in Time-Domain (TD) and/or Frequency-Domain (FD) PS to provide QoS differentiation.

In [65] an Adaptive Cross-Layer (ACL) scheduling algorithm is proposed and it is shown to outperform WFQ schedulers with respect to average normalized packet delay, average effective user throughput, user blocking, and user dropping for data services in downlink. The name is derived from the fact that the proposed algorithm adapts to the packet delay deadlines on link layer and channel qualities on the physical layer. The performance of the ACL algorithm is evaluated using a simple AC algorithm which limits the number of active queues to grow beyond a specified threshold.

In [66] a combined AC and PS is proposed to study the performance of a mixed Real Time (RT) and BE services for IEEE 802.16 downlink. The proposed scheduler does not assign higher priority to RT packets over BE packets unconditionally. Instead, only the RT packets which are close to the delay deadline are given higher priority. This improves the performance of BE services at the cost of RT services. The scheduling policy used to allocate the resources are best-channel first i.e., sorted in order of the downlink channel quality, and Proportional Fair (PF). In this study AC is used as a congestion controller and it is applied to all the bearers irrespective of its traffic type. The proposed AC compares the buffer status of the RT services with a predetermined value to decide whether the network is congested. This AC might be difficult to adopt for LTE uplink because the buffer status of the radio bearers are not instantaneously available at the base station.

In [67] a set of schedulers are studied modifying the PF with QoS scaling weights

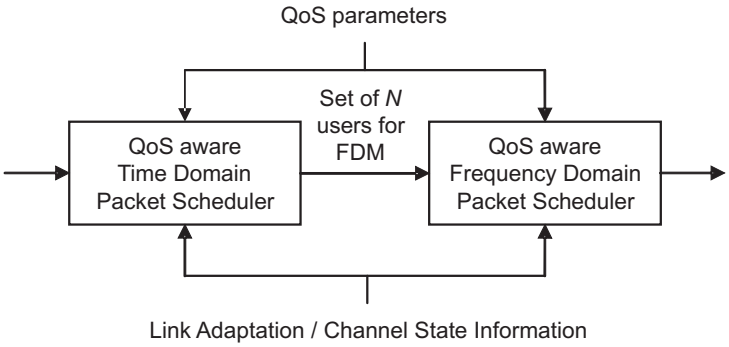

Figure 4.1: QoS-aware packet scheduler design

for HSDPA. It has been shown that the PF with Required Activity Detection (RAD) is insensitive and robust to support a general traffic mix of RT (streaming) and Non-Real Time (NRT) (web browsing) type of users. The PF with RAD scheduler uses GBR as the only QoS parameter and could be extended for LTE uplink to be useful as TD and/or FD PS.

4.3 QoS Aware Packet Scheduling

The packet scheduling is done as a two step algorithm, first TD scheduler selects a subset of N users from the available users in the cell, which are frequency multiplexed by the FD scheduler as shown in Figure 4.1 [32]. This framework is attractive from complexity point of view, since FD scheduler has to consider only frequency multiplexing of maximum N users per TTI. The value of N is set according to the potential channel constraints as well as the available number of PRBs. Note that the overall scheduler performance will be sub-optimum due to the limited user diversity at the FD scheduler. The scheduling metrics used in TD and FD to fulfill the GBR are studied in the following section.

4.3.1 Time-Domain Packet Scheduling

4.3.1.1 GBR-aware TD Metric

In this study a GBR-aware Time-Domain Packet Scheduling (TDPS) is used, which prioritize the users according to the metric in (4.1) giving highest priority to the user which is farthest below its GBR requirement. $\mathbf{R}_i$ is the past average throughput of user i calculated using exponential average filtering as in (3.12) [60].

$$\mathbf{M}_{\mathrm{TD},i}[n] = \frac{GBR_i}{\mathbf{R}_i[n]} \tag{4.1}$$

4.3.2 Frequency-Domain Packet Scheduling

The users selected by the TDPS are allocated PRBs based on the FD metric. In this chapter flexible number of PRBs are allocated per user by using an ATB based scheduling to maximize the sum of the FD metric [35][36]. The proposed FD scheduling metrics are described in the following section.

4.3.2.1 Proportional Fair Scheduled FD Metric (PFsch)

The Frequency-Domain Packet Scheduling (FDPS) allocates the PRBs to the users selected by the TDPS according to the PF-scheduled metric [31]. This metric is expressed as

$$\mathbf{M}_{\text{FD},i}[k,n] = \frac{\hat{\mathbf{d}}_i[k,n]}{\mathbf{R}_{sch,i}[n]}, \tag{4.2}$$

where $\hat{\mathbf{d}}_i[k]$ is the estimated achievable throughput for user i on PRB k, and $\mathbf{R}_{sch,i}$ is an average of scheduled user throughput, i.e. the scheduled throughput is averaged over the TTIs where user i is multiplexed in frequency domain as in (3.10) [60].

The reason for using the PF-scheduled metric instead of the typical PF metric is that in the case of mixed GBR scenario the PF metric tends to bias the higher GBR users by giving them lower priority in FD. However, in the special case of single GBR bearers in the system the PF and PF-scheduled metric will behave similarly.

4.3.3 QoS Control in Frequency Domain

The TDPS metric in (4.1) provides a QoS control mechanism. However, when all the bearers are multiplexed in frequency domain by the TD scheduler, the FD metric should be able to differentiate between the GBR bearers. Hence to provide QoS control in frequency domain a weight $(\mathbf{W}[\mathbf{n}])$ is applied to the FD metric of the users in (4.2) as,

$$\mathbf{M}_{\text{FD},i}[k,n] = \frac{\hat{\mathbf{d}}_i[k,n]}{\mathbf{R}_{sch,i}[n]} \cdot \mathbf{W}[\mathbf{n}] \tag{4.3}$$

4.3.3.1 MAX weighted FD Metric (MAXwt)

A FD metric in (4.4) is proposed which modifies the metric in (4.2) so as to give higher priority to the bearers with average throughput below the required GBR, and to serve the bearers with average throughput above the required GBR with the PF-scheduled metric [31]. The MAX weighted FDPS trades off the GBR differentiation and the frequency diversity gain.

$$\mathbf{M}_{\text{FD},i}[k,n] = \frac{\hat{\mathbf{d}}_i[k,n]}{\mathbf{R}_{sch,i}[n]} \cdot \max\left(1.0, \frac{GBR_i}{\mathbf{R}_i[n]}\right) \tag{4.4}$$

Table 4.1: Simulation Parameters and Assumptions

Parameter	**Assumptions**
Inter site distance	500 m (Macro case 1) [14]
System bandwidth	10 MHz
TTI	1 ms
Number of PRBs for data transmission	48
Number of PRBs for control transmission	2
Users multiplexed per TTI	8
PRBs per user per TTI	1 – 48 (ATB = ON)
TD scheduling	GBR-aware
FD scheduling	PFsch, MAXwt, GBRwt
Forgetting factor (β) for scheduling	0.01
Initial $\mathbf{R}_i$ value	GBR_i
Initial $\mathbf{R}_{sch,i}$ value	GBR_i
HARQ	Synchronous, Adaptive
BLER Target	30%
Power control	Fractional power control
P_o, α	-58 dBm, 0.6
User arrival	Poisson process
User arrival rates	4, 5, 6, 7, 8, 10 users/cell/s
Traffic model	Finite buffer model
Initial buffer size	1 Mbit
Number of admitted calls simulated	10000

4.3.3.2 GBR weighted FD Metric (GBRwt)

In a mixed GBR scenario when the required GBR of the bearers are far apart e.g., bearers with GBR of 64 kbps and 1000 kbps, the MAX weighted FDPS may not be able to differentiate the two types of users because of the dominant PF-scheduled term in (4.4) for lower GBR bearers. To overcome this issue the FD metric is modified to differentiate between users in both the cases when the average throughput is above or below the required GBR. Hence, a FD metric in (4.5) is proposed so as to prioritize the bearers based on both PF-scheduled and GBR-aware metric. This metric tends to give higher priority to a user which is far below its GBR requirement.

$$\mathbf{M}_{\text{FD},i}[k,n] = \frac{\hat{\mathbf{d}}_i[k,n]}{\mathbf{R}_{sch,i}[n]} \cdot \frac{GBR_i}{\mathbf{R}_i[n]} \tag{4.5}$$

4.4 Modeling Assumptions

The performance evaluation is done using a detailed multi-cell system level simulator described in Appendix A. The default simulator parameters and assumptions are listed in Table A.1.

The users in the system are created in the system according to a Poisson call arrival process. If the AC decision criterion proposed in Chapter 3 is fulfilled, the user is admitted, otherwise the user is blocked. A finite buffer traffic model is used with a GBR requirement, where each user uploads a 1 Mbit packet call. The session is terminated as soon as the upload is completed. This represents a File Transfer Protocol (FTP) type of traffic with a GBR requirement.

The allocated bandwidth per user is assumed to be adaptive between 1 – 48 PRBs for all the scheduled users using ATB based scheduling [35]. The collaborative work in [35] is reprinted in Annex II. In this chapter, 8 users are multiplexed per TTI in frequency domain. The total number of PRBs used for data transmission is 48 PRBs while 2 PRBs are reserved for control transmission. The PS uses GBR-aware TD metric to select the users to be forwarded to FDPS, and one of the proposed FD metrics to allocate the PRBs to the forwarded users.

The main simulation parameters listed in Table 4.1 are according to the assumptions in [14].

4.5 Performance Evaluation

The performance of proposed FDPS metrics are compared for the reference AC (R_{max} = 5 Mbps) and FPC based AC. The evaluation is done for three cases of mixed GBR user classes as listed in Table 4.2. For example Case I considers two types of users, 50% with 64 kbps and 50% with 256 kbps GBR requirements.

Figure 4.2 shows the CDF of user throughput of different user classes in Case I for combined FPC based AC and proposed FDPS metrics. We notice that GBR weighted FDPS (GBRwt) has fairer throughput distribution compared to PF-scheduled FDPS (PF-

Table 4.2: User Class Probability Distribution

User class	Case I	Case II	Case III
QoS user GBR – 64 kbps	50%	50%	25%
QoS user GBR – 128 kbps	0%	0%	50%
QoS user GBR – 256 kbps	50%	0%	25%
QoS user GBR – 1000 kbps	0%	50%	0%

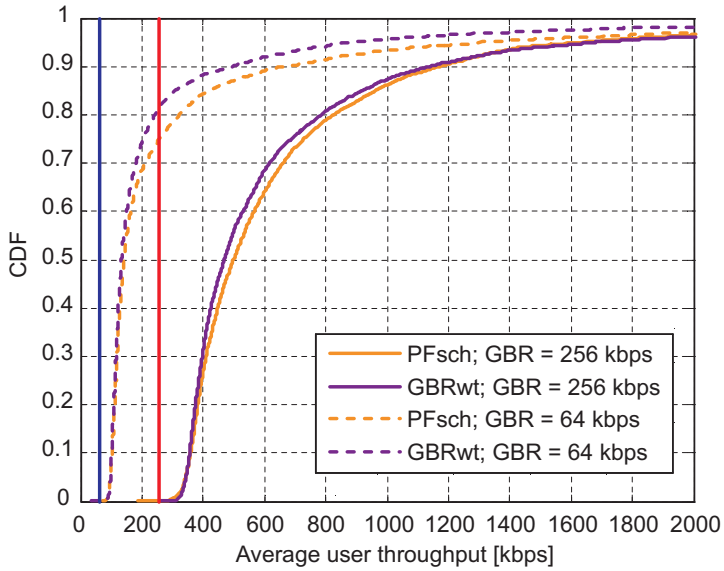

Figure 4.2: CDF of individual user throughput for a mixed GBR of [64, 256] kbps as in Case I. FPC based AC, user arrival rate = 8 users/cell/s.

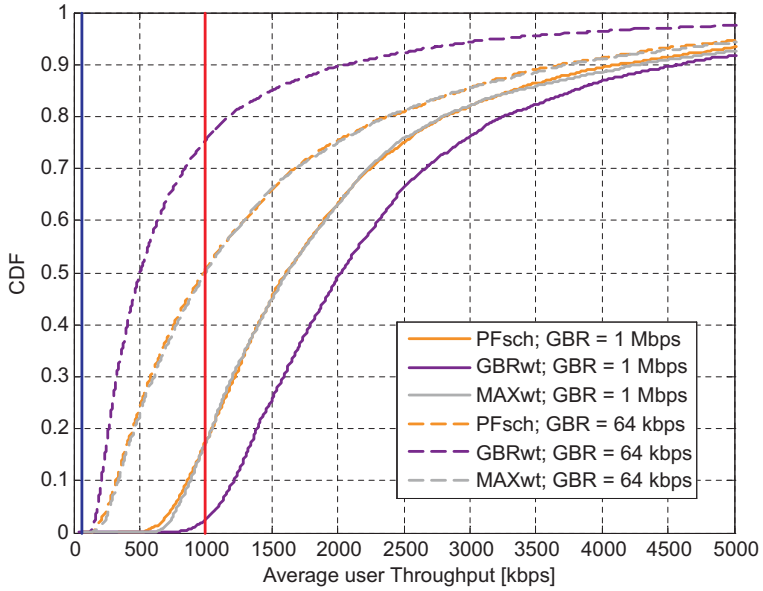

Figure 4.3: CDF of individual user throughput for a mixed GBR of [64, 1000] kbps as in Case II. FPC based AC, user arrival rate = 8 users/cell/s.

sch), but the gain in 95% coverage throughput performance is negligible. This is because the two user classes in Case I have relatively low GBR requirements, and therefore more than the maximum number of users scheduled per TTI (8 users) in frequency domain are active in the cell. Hence GBR-aware TDPS is sufficient to differentiate between the users and GBR-aware FDPS becomes redundant.

Figure 4.3 shows the CDF of user throughput of different user classes in Case II for combined FPC based AC and proposed FDPS metrics. We notice that there is a negli-

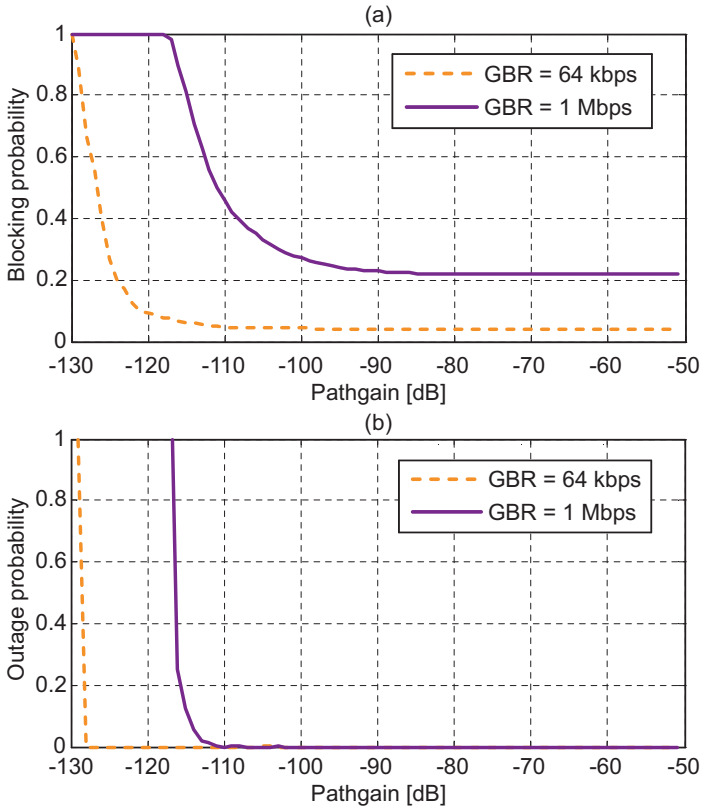

Figure 4.4: (a) Blocking probability vs. path gain, (b) Outage probability vs. path gain for individual user classes in Case II. FPC based AC, GBR weighted FDPS, user arrival rate = 8 users/cell/s.

gible improvement in the 95% coverage throughput performance of 1000 kbps users for using MAX weighted FDPS (MAXwt) over PF-scheduled FDPS. This is because the PF-scheduled term in MAX weighted FD metric overrides the effect of MAX weight, and the MAX weighted FDPS does not effectively differentiate between non-identical GBR user classes. Furthermore, we observe that GBR weighted FDPS improves the coverage throughput performance of 1000 kbps GBR user class significantly. In this case on average there are less number of users per cell compared to the maximum number of users scheduled per TTI (8 users) in frequency domain. Therefore, if the relative difference between the GBR requirements is high in a mixed traffic scenario proposed GBR weighted FDPS metric is necessary to differentiate between users.

Figure 4.4 (a) shows the blocking probability versus path gain (including distance dependent path gain, shadowing, and antenna gain) for different user classes in Case II. As expected from the design of FPC based AC, the blocking probability is dependent on GBR requirements and path gain, and it increases rapidly below certain path gain value. For low path gain users (cell-edge users) the FPC based AC blocks 1000 kbps users with higher probability compared to 64 kbps users. The blocking at the cell-center for 64 kbps and 1000 kbps PBR users is non-zero because of the cell loading conditions. This shows that FPC based AC effectively differentiates between users based on their GBR

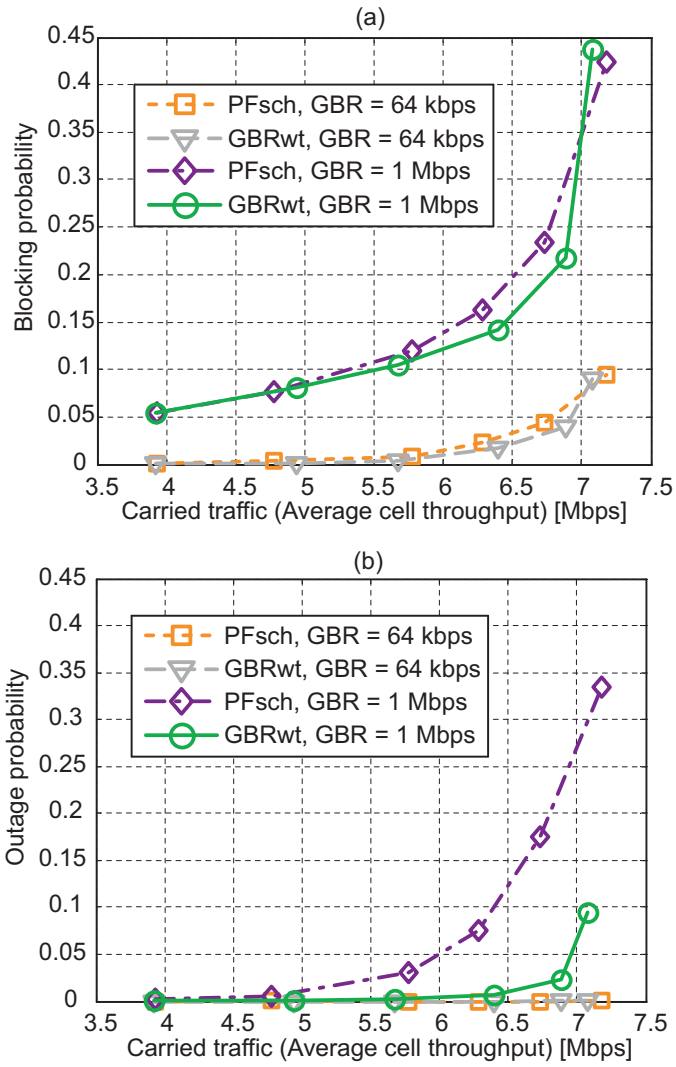

Figure 4.5: (a) Blocking probability vs. carried traffic, (b) Outage probability vs. carried traffic for individual user classes in Case II.

requirement and path gain.

Figure 4.4 (b) shows the outage probability versus path gain in Case II. It shows that FPC based AC effectively blocks the user if its QoS cannot be satisfied. This means that if the user is blocked it is because the user's GBR can not be fulfilled due to the poor channel conditions (low path gain). Moreover, it means a very high GBR requirement (e.g. 1000 kbps) may not be supported at the cell border due to coverage limitation leading to cell shrinkage. At the same time users with lower GBR requirement can even be supported at the cell border. Therefore, the blocking and outage probabilities are dependent on the GBR requirement of user class since FPC based AC takes both path gain and cell load conditions into account to make an AC decision.

Figure 4.5 shows the blocking and outage probabilities versus carried traffic (average cell throughput) for different user classes in Case II using FPC based AC. The blocking probability for 1000 kbps user class is higher than 64 kbps user class, this is due to the

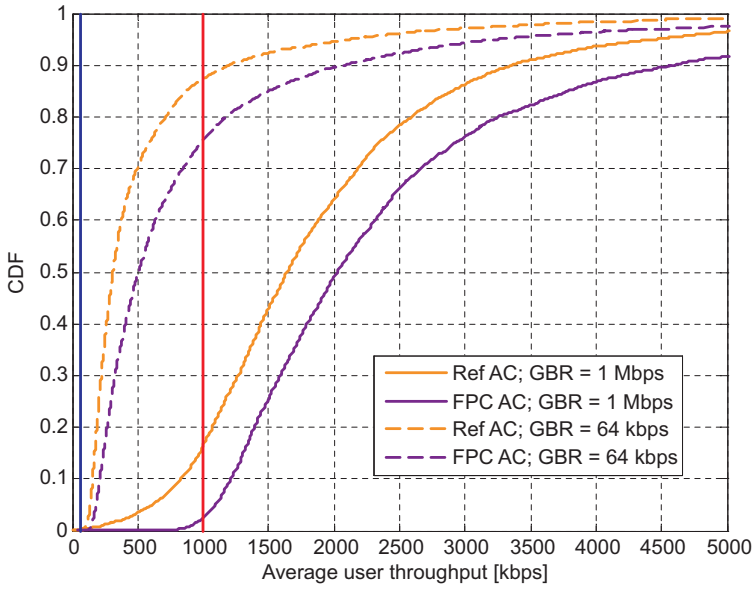

Figure 4.6: CDF of individual user throughput for a mixed GBR of [64, 1000] kbps as in Case II. GBR weighted FDPS, user arrival rate = 8 users/cell/s.

fact that more resources are required by 1000 kbps user class, as well as the blocking depends on the load conditions in the cell. This means that although the percentage share of users arriving of each class is 50%, due to higher blocking probability of 1000 kbps user class there will be more than 50% active users of 64 kbps user class. Additionally, we observe that the outage probability is best for the GBR weighted FDPS for both 64 kbps and 1000 kbps user class.

Figure 4.6 shows the CDF of user throughput of different user classes in Case II for FPC based AC and reference AC combined with the GBR weighted FDPS. We observe that the FPC based AC improves the average and 95% coverage throughput performances of both 64 kbps and 1000 kbps user classes significantly. This is because FPC based AC admits a user only if the required GBR of the user can be fulfilled, and hence its coverage throughput performance is better.

Figure 4.7 shows the blocking and outage probabilities versus carried traffic for Case II. It should be noticed that FPC based AC blocks the users at low carried traffic if the GBR cannot be fulfilled. Hence the outage probability is lowest for the combination of FPC based AC and GBR weighted FDPS among the studied AC and PS combinations. Furthermore, for the same outage probability the combined FPC based AC and GBR weighted FDPS have a higher carried throughput. This result shows that both AC and PS need to be QoS aware for the effective QoS control.

Figure 4.8 shows the CDF of number of users per cell and average number of scheduled PRBs for different combination of FPC based AC and reference AC, and the proposed FDPS metrics for Case II. Figure 4.8 (a) shows that the average number of users per cell is lower for FPC based AC for either of the FDPS metrics. This is because FPC based AC tends to admit a user only if there are sufficient number of PRBs available to fulfill

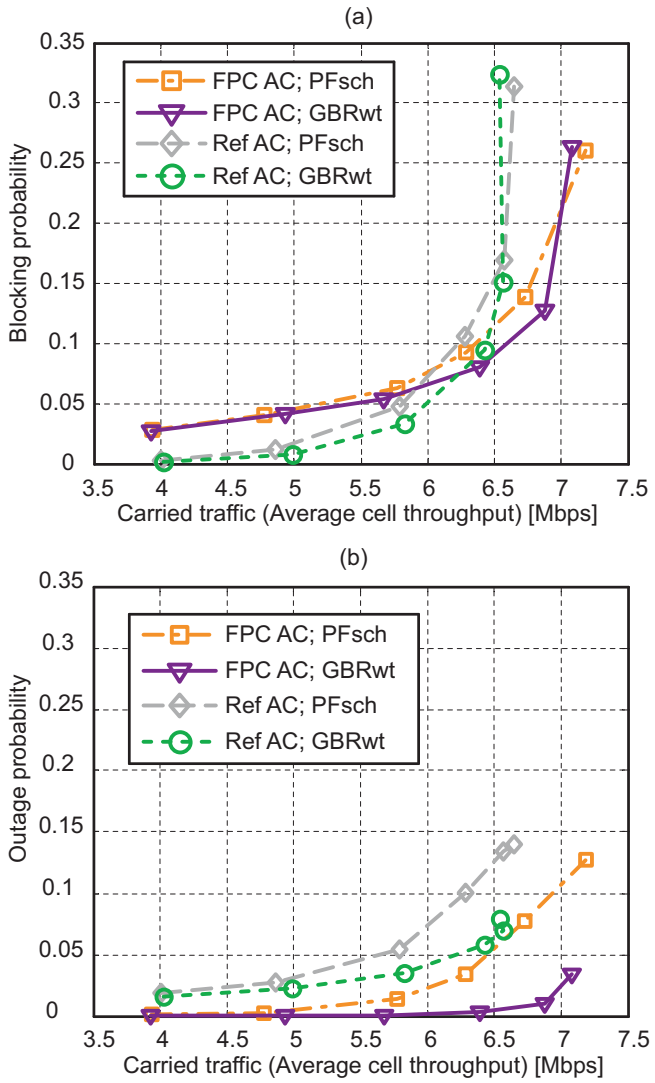

Figure 4.7: (a) Blocking probability vs. carried traffic, (b) Outage probability vs. carried traffic for Case II. FPC based AC.

its GBR. Similarly, the average number of users per cell is higher for the GBR weighted FDPS for either of the AC algorithms. This is because the GBR weighted FDPS is able to guarantee the respective GBR requirement of different user classes in a mixed traffic scenario, while PF scheduled FDPS does not differentiate between user classes especially if the average number of users is in the order of TD scheduler limit of 8 users. Due to the fact that 64 kbps users are delayed to fulfill the QoS of 1000 kbps users in GBR weighted FDPS, leads to higher average number of users for GBR weighted FDPS for either of the AC algorithms. In Figure 4.8 (b) it is shown that the average number of scheduled PRBs is 6, which is around the same for all the cases. This is because maximum of 8 users are forwarded by the TDPS to FDPS which on average share the total number of PRBs (i.e. 48 PRBs) equally.

Figure 4.9 shows the CDF of scheduling activity, and the CDF of average call length for different combination of FPC based AC and reference AC, and the proposed FDPS

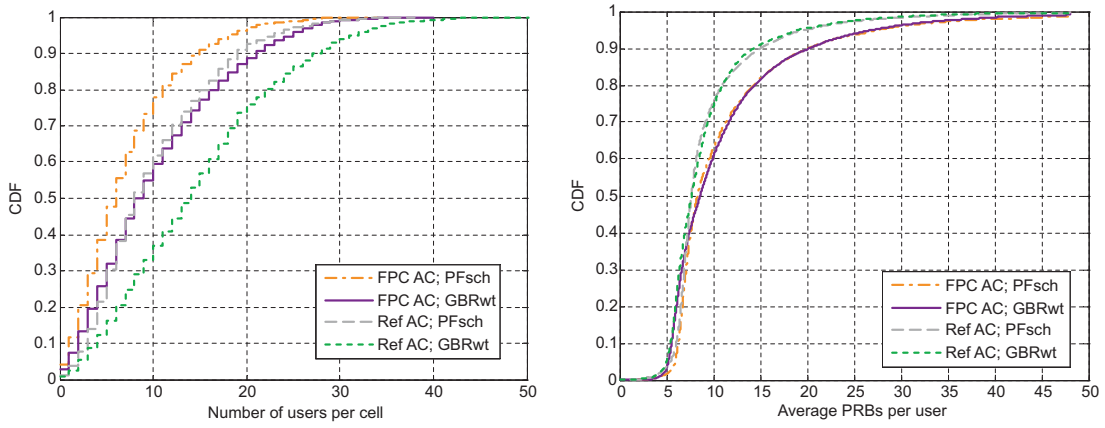

Figure 4.8: (a) CDF of number of users per cell, (b) CDF of average number of scheduled PRBs per user for Case II. User arrival rate = 8 users/cell/s.

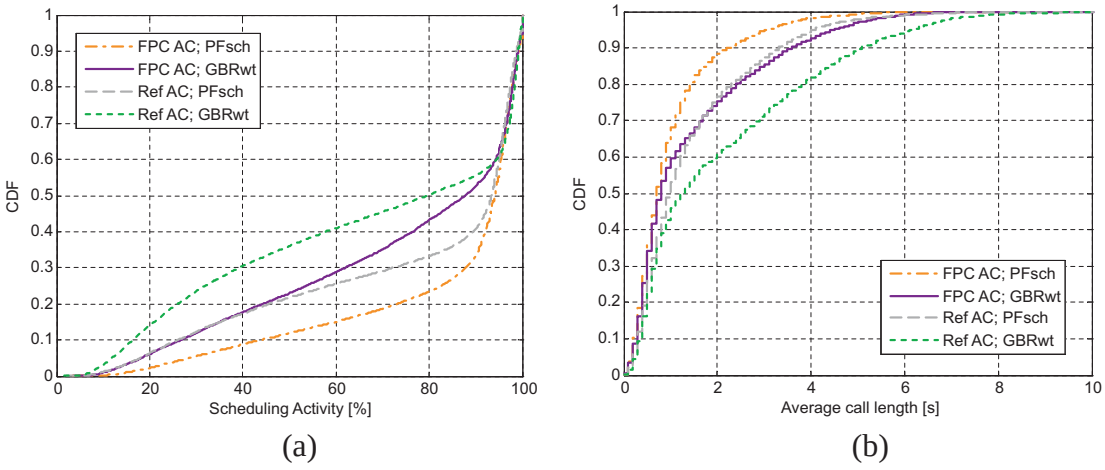

Figure 4.9: (a) CDF of scheduling activity, (b) CDF of average call length for Case II. User arrival rate = 8 users/cell/s.

metrics for Case II. The scheduling activity is shown to be inversely proportional to the average number of users per cell. In other terms, for the increase in number of users per cell the frequency of users being multiplexed in frequency domain is reduced. In Figure 4.9 (b) it is shown that the GBR weighted FDPS has longer call duration, this is because it reduces the average throughput and hence prolongs the call duration of the 64 kbps users to fulfill the GBR of the 1000 kbps users. It should be noticed that independently *QoS aware AC* or *QoS aware PS* are unable to fulfill the QoS requirements, hence a combination of both is required for the effective QoS control especially in a mixed GBR scenario.

Figure 4.10 shows the PRB utilization per user and the CDF of total PRB utilization for different combination of FPC based AC and reference AC, and the proposed FDPS metrics for Case II. Figure 4.10 (a) shows that the adaptive number of PRBs between 1 to 48 are allocated to each user. It is seen that even number of PRBs are allocated

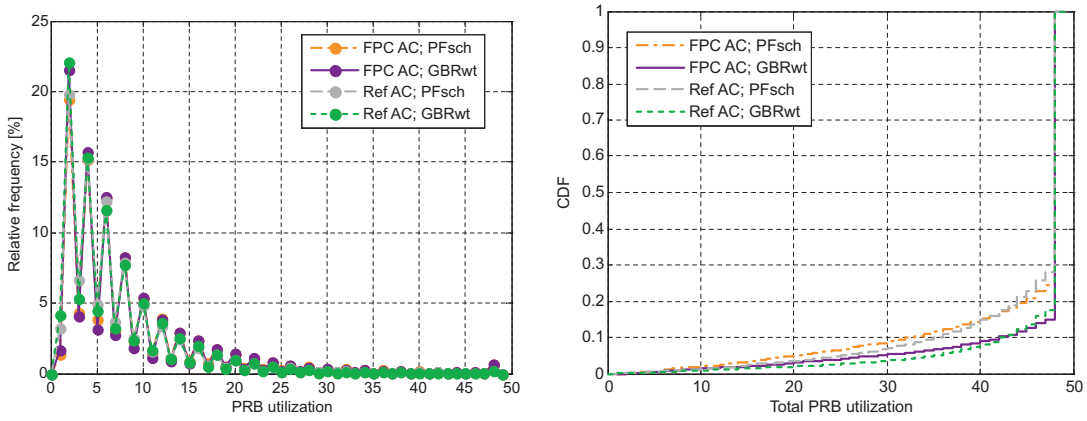

(a) (b)

Figure 4.10: (a) PRB utilization per user, (b) CDF of total PRB utilization for Case II. User arrival rate = 8 users/cell/s.

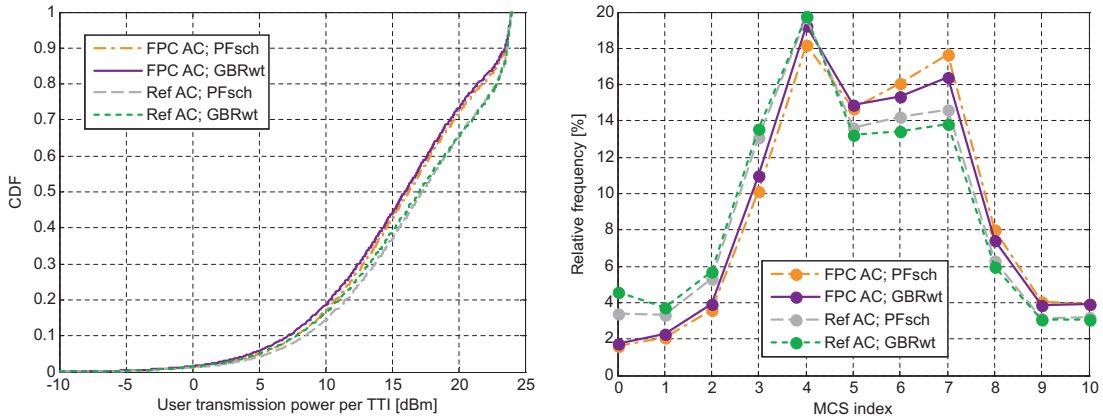

(a) (b)

Figure 4.11: (a) CDF of user transmission power, (b) MCS distribution for Case II. User arrival rate = 8 users/cell/s.

with higher probability, which is because Channel State Information (CSI) granularity is 2 PRBs. Odd number of PRBs are allocated only when the user is transmit power limited. Figure 4.10 (b) shows that the total PRB utilization is higher for GBR weighted FDPS because of the higher number of users per cell for both FPC based AC and reference AC algorithms.

Figure 4.11 shows the CDF of user transmission power and the MCS distribution for different combination of FPC based AC and reference AC, and the proposed FDPS metrics for Case II. In this case we notice that the FPC based AC has a larger power headroom[1] compared to the reference AC. This is because FPC based AC admits a user only if its GBR can be fulfilled while meeting the user transmit power constraint. In this case none of the users are power limited because ATB adaptively selects the transmission

[1]Power headroom (in dB scale) is defined as the difference between user's maximum transmit power and the actual transmit power level.

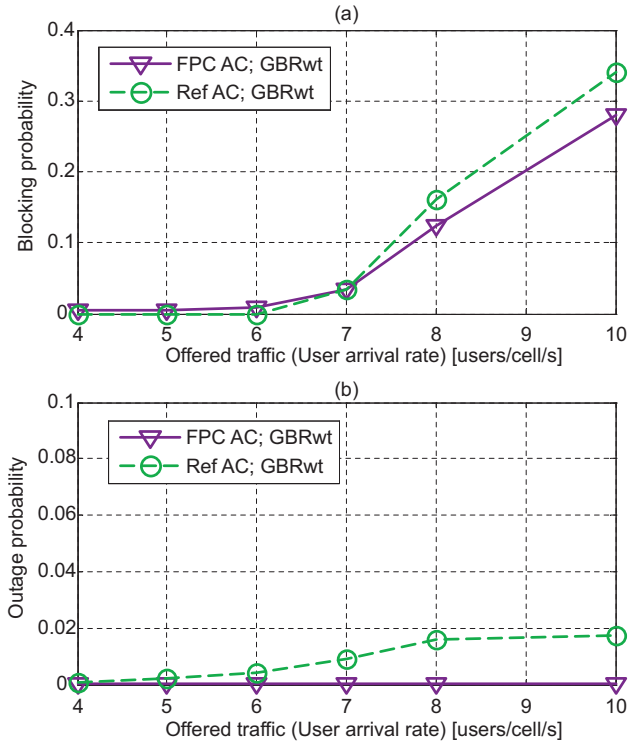

Figure 4.12: (a) Blocking probability vs. offered traffic, (b) Outage probability vs. offered traffic for Case III.

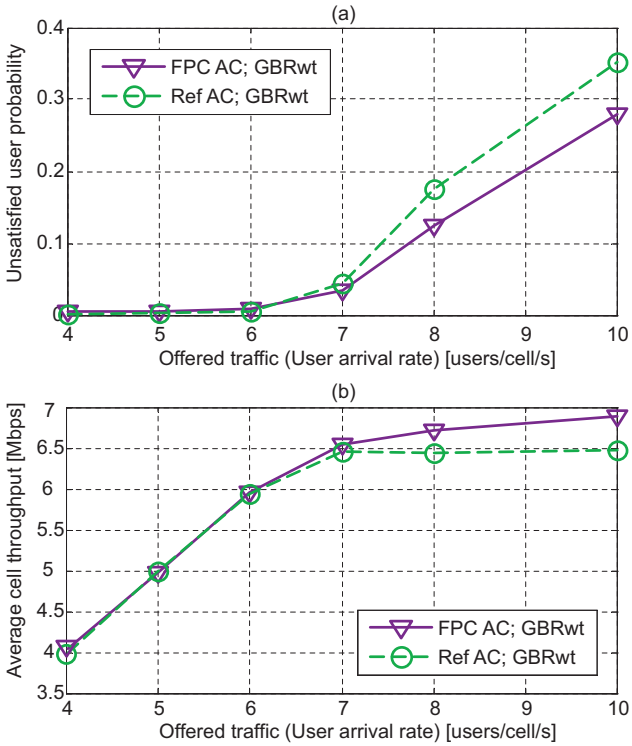

Figure 4.13: (a) Unsatisfied user probability vs. offered traffic, (b) Average cell throughput vs. offered traffic for Case III.

bandwidth such that the user is transmitting below the maximum user transmit power. In Figure 4.11 (b) it is noticed that the FPC based AC selects the lower MCS order with less probability because of lesser number of users in cell edge since it denies admission to the user at cell edge with higher probability compared to reference AC.

Figure 4.12 shows the blocking probability and outage probability versus offered traffic for Case III with three non-identical GBR user classes. It is shown that the FPC based AC admit users with lower blocking probability as well as lower outage probability especially at higher offered traffic conditions.

Figure 4.13 shows the unsatisfied user probability and carried traffic versus offered traffic for Case III. FPC based AC in combination with GBR weighted FDPS is shown to perform best among the studied algorithms both in terms of unsatisfied user probability and carried traffic. It should be noticed that a GBR user would perceive an outage as more annoying compared to the blocking if the user's required GBR is not fulfilled.

4.6 Conclusions

In this chapter a combined AC and PS framework for QoS provisioning in LTE uplink is proposed. The GBR aware TDPS and FDPS metrics are proposed to fulfill the GBR of the admitted users. The PRBs per user are allocated based on the ATB based scheduling to maximize the sum of the FDPS metric. The combined FPC based AC and GBR weighted FDPS is shown to be able to fulfill the respective QoS requirements of different user classes in a mixed traffic scenario. Furthermore, GBR weighted FDPS is shown to improve the outage performance compared to the PF-scheduled FDPS and MAX weighted FDPS in the case of a mixed traffic scenario with relatively high difference in the GBR requirements for example in a mixed GBR scenario of 64 kbps and 1000 kbps. The FPC based AC blocks the bearer with a very low path gain, and fulfill the required GBR of admitted bearers with a very low outage probability. The reference AC, unlike FPC based AC, admits a bearer irrespective of its channel condition and very low path gain bearers are eventually served with a significantly higher outage probability. It is shown that FPC based AC automatically adjusts to the traffic mixes, cell load, and user channel conditions. The findings of this study have been published in [68].

The next chapter generalizes the proposed AC algorithms in Chapter 3 for a realistic ON/OFF traffic source by taking into account the source activity factor. Additionally, the proposed framework is evaluated for the realistic CBR streaming services.

Chapter 5

Performance of CBR Streaming Services

5.1 Introduction

This chapter evaluates the performance of a Constant Bit Rate (CBR) streaming traffic for the proposed combined Admission Control (AC) and Packet Scheduler (PS) framework to provide QoS support and differentiation. A CBR traffic is modeled as only one ON period of an ON/OFF traffic source. An ON/OFF traffic source e.g., Voice over Internet Protocol (VoIP), is characterized by the ON periods where the data packets are generated at a certain inter packet arrival time followed by the OFF periods at a certain interval as illustrated in Figure 5.1. The source activity factor is defined as sum of ON periods over the call duration (i.e. sum of ON and OFF periods). Therefore, to make an AC decision for an ON/OFF traffic source it is important to take the source activity factor into account.

This chapter is organized as follows: In Section 5.2, the two AC algorithms derived in Chapter 3 are modified to take into account the activity factor of an ON/OFF traffic source. In Section 5.3, the modeling assumptions are presented. In Section 5.4, the performance of a realistic CBR streaming traffic with single and mixed GBR settings is evaluated. Further, the performance of an ON/OFF traffic source using CBR traffic to model the ON periods is analyzed. In Section 5.5, the proposed AC framework is extended for a mixed GBR and Non-GBR bearers, and Section 5.6 contains the concluding remarks.

5.2 Admission Control for an ON/OFF Traffic Source

The ON/OFF traffic source is characterized by the source activity factor. Hence, the proposed AC algorithms in Section 3.3 should be modified to include the activity factor term. The source activity factor of a bearer is assumed to be known at the AC unit. For example, source activity factor can be set in the Quality Class Identifier (QCI) table based

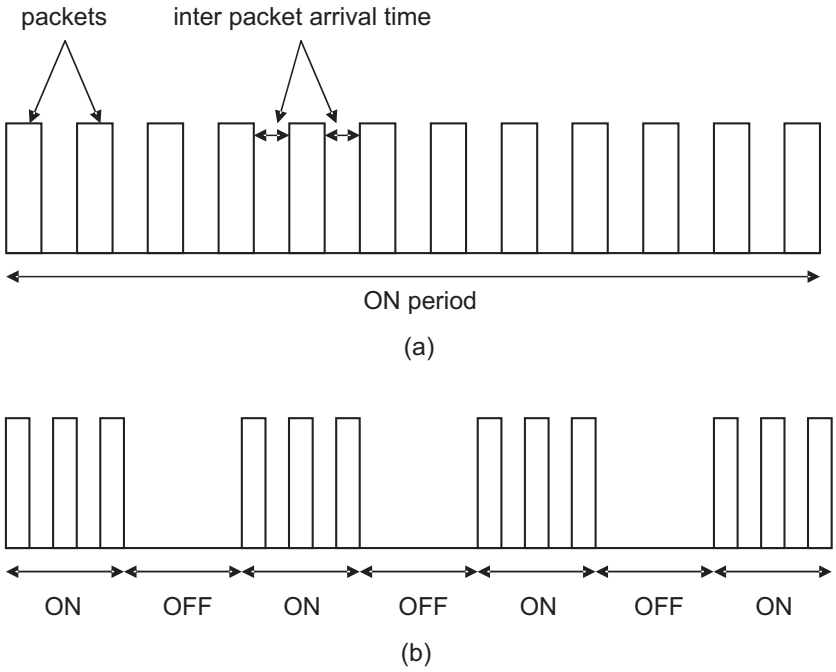

Figure 5.1: (a) CBR streaming traffic with only ON spurt, (b) ON/OFF traffic model.

on a service type [22]. The realistic estimate of source activity factor for the existing users can be measured at the eNode-B, but it is not studied in this thesis.

It is important to note that the probability of number of users being in their ON state depends on the number of existing users in the cell [69]. The probability of k number of users being in their ON state out of the total n number of existing users in the cell (assuming the ON and OFF states of existing users are independent of each other) is defined using the binomial probability law[1], which is analytically expressed as [70]:

$$p_n(k) = \frac{n!}{n!(n-k)!}\lambda^k(1-\lambda)^{(n-k)}, \tag{5.1}$$

where, $n!$ is called n factorial and is defined by $n! = n(n-1)...(2)(1)$, and λ is the probability of user being in ON state (i.e. source activity factor).

Figure 5.2 shows the CDF of the fraction of number of users in ON state for different number of users in the cell for λ = 0.5. The distribution becomes fairer for increasing number of users. For lower number of users, the higher variance in the distribution leads to a higher probability of more than 50% of users being in ON state at a time. Furthermore, increasing the number of users in a cell the probability of users being in ON state tends toward 50%. Therefore based on the number of users in a cell certain resources may need to be reserved in case more than expected number of users are in ON state at the same time. Moreover, reserving the resources would also lead to the waste of capacity in the cases when less than expected number of users are in the ON state. Hence, the AC can

[1]If k be the number of successes in n independent Bernoulli trials, then the probabilities of k are given by the binomial probability law, where λ is the probability of success of a single Bernoulli trial.

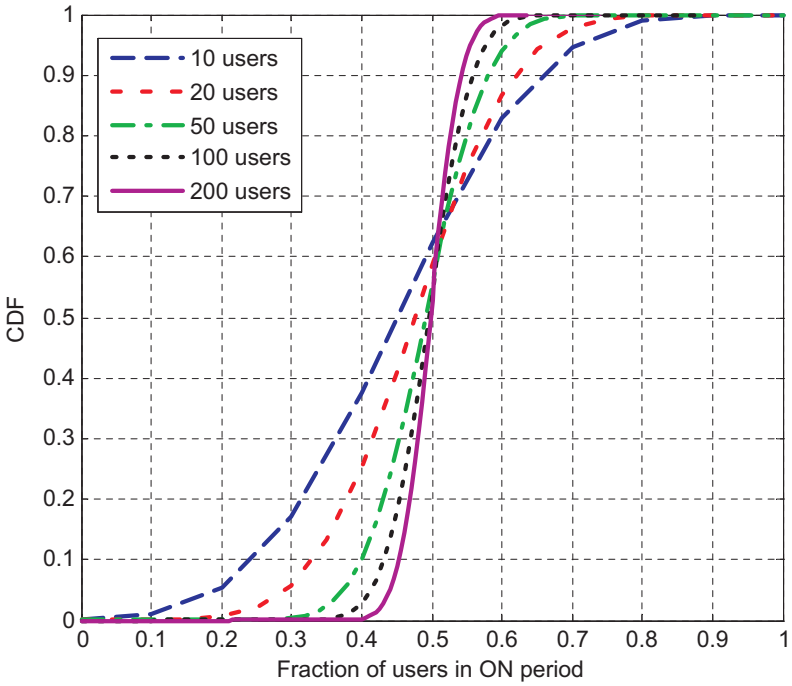

Figure 5.2: Fraction of users in ON state for different number of users with source activity factor of 0.5.

also probabilistically overbook the resources such that the outage probability is below a given probability threshold [71].

5.2.1 Reference Admission Control

The reference AC algorithm in (3.1) is generalized for an ON/OFF traffic by taking into account the activity factor of user i (λ_i) as

$$\sum_{i=1}^{K} GBR_i \cdot \lambda_i + GBR_{new} \cdot \lambda_{new} \leq R_{\max}, \tag{5.2}$$

where K is the number of existing users in the cell and $R_{\max}$ is the predefined average uplink cell throughput. The $GBR_i \cdot \lambda_i$ represents the required capacity over a long term including several ON and OFF periods, where GBR_i is the required bit rate during the ON periods. It should be noted that the AC algorithm in (5.2) assumes that the existing users in ON state are in proportion to the activity factor at a certain moment of time, but depending on the number of existing users it is probable that more than expected number of users are in ON state as shown in Figure 5.2. To take into account the effect of this situation R_{max} is tuned accordingly depending on the number of existing users in the cell. The equation in (3.1) is a special case of the algorithm in (5.2) with λ_i and λ_{new} equal to unity i.e. traffic source only with an ON spurt.

5.2.2 Fractional Power Control based Admission Control

Similarly, the FPC based AC algorithm in (3.2) is modified as

$$\sum_{i=1}^{K} N_i \cdot \lambda_i + N_{new} \cdot \lambda_{new} \leq N_{tot} - \Delta N, \tag{5.3}$$

where N_i is the required number of PRBs by user i to fulfill the GBR during the ON periods, N_{tot} is the total number of PRBs in the system bandwidth, and ΔN is the load safety parameter. The load safety parameter can be used to reserve some PRBs to counter the effect of more than expected number of users being in ON state at a time. The required number of PRBs for existing and new users will be estimated using the method derived in Section 3.3.2.1. The equation in (3.2) is a special case of the algorithm in (5.3) with λ_i and λ_{new} equal to unity.

Table 5.1: Simulation Parameters and Assumptions

Parameter	**Assumptions**
Inter site distance	500 m (Macro case 1) [14]
System bandwidth	10 MHz
TTI	1 ms
Number of PRBs for data transmission	48
Number of PRBs for control transmission	2
Users multiplexed per TTI	8
PRBs per user per TTI	1 – 48 (ATB = ON)
TD scheduling	GBR-aware
FD scheduling	PFsch, GBRwt
Forgetting factor (β) for scheduling	0.01
Initial $\mathbf{R}_i$ value	GBR_i
Initial $\mathbf{R}_{sch,i}$ value	GBR_i
HARQ	Synchronous, Adaptive
BLER Target	30%
Power control	Fractional power control
P_o, α	-58 dBm, 0.6
R_{max} for Reference AC	5 Mbps
User arrival	Poisson process
User arrival rates	1, 2, 3, 4, 5, 6, 7, 8 users/cell/s
Number of admitted calls simulated	10000

Table 5.2: CBR Streaming Traffic with only ON spurt

Parameter	Settings
CBR – 512 kbps	
GBR	512 kbps
Packet size	4096 bits
Inter packet arrival time	8 ms
Call length	3.9 s
Initial buffer size	∼2 Mbits
CBR – 256 kbps	
GBR	256 kbps
Packet size	2048 bits
Inter packet arrival time	8 ms
Call length	7.8 s
Initial buffer size	∼2 Mbits

Table 5.3: ON/OFF Traffic with CBR during ON periods

Parameter	Settings
CBR – 512 kbps	
GBR	512 kbps
Packet size	4096 bits
Inter packet arrival time	8 ms
ON period	1.0 s
OFF period	1.0 s
Number of ON spurts	4

5.3 Modeling Assumptions

The performance evaluation is done using a detailed multi-cell semi-static system level simulator described in Appendix A. The default simulator parameters and assumptions are listed in Table A.1. The simulation parameters specific to this chapter are given in Table 5.1.

A special case of ON/OFF traffic with only ON spurt is used to study the CBR streaming traffic model as shown in Figure 5.1 (a). The constant size data packets are generated at a constant inter packet arrival time. This is the case of a realistic traffic model with activity factor equals unity. The parameters of CBR streaming traffic model used in simulations are given in Table 5.2. The parameters are chosen such that an initial buffer size of around 2 Mbps is serviced depending on the GBR and call length.

Additionally, an ON/OFF traffic source with CBR during ON period is studied. Sev-

eral short ON spurts with interleaved OFF periods are modeled as illustrated in Figure 5.1 (b). The ON/OFF traffic parameters used in simulations are listed in Table 5.3. These are chosen so as to model a 512 kbps CBR streaming during ON periods, source activity factor of 0.5, and purely deterministic ON and OFF durations.

The PS is modeled to check the buffer status report before forwarding the user to be considered by the Time-Domain (TD) PS as shown in Figure 2.7. In this study, PS is assumed to have minimal buffer knowledge (i.e. if an active user has data in the buffer or not, while actual buffer size is unknown). Hence, the Adaptive Transmission Bandwidth (ATB) based scheduling used in Frequency-Domain (FD) allocates Physical Resource Blocks (PRBs) to a user without the constraint due to the actual buffer size. Unlike finite buffer traffic model, which always has data in the buffer to transmit, in a CBR traffic the data packet arrives at a certain interval. Therefore, an active CBR user may not necessarily have data in the buffer to transmit.

5.4 Performance Evaluation

This section present results for following three cases:

- Case I – CBR traffic with single GBR of 512 kbps
- Case II – CBR traffic with mixed GBR of 512 kbps and 256 kbps
- Case III – An ON/OFF traffic with ON periods modeled as CBR with GBR of 512 kbps and activity factor 0.5

It should be noted that for audio streaming and video streaming a packet loss of 1% and 2% respectively is acceptable [72]. In this study, the CBR streaming users in outage are the users with throughput of less than 98% of GBR during the ON periods.

5.4.1 CBR Traffic with Single GBR Case

In this section the performance of the proposed combined AC and PS framework for CBR users with GBR of 512 kbps is analyzed.

Figure 5.3 shows the average user throughput for the case of reference AC and FPC based AC with GBR weighted FDPS (GBRwt) defined in Section 4.3.3.2. We notice that for FPC based AC algorithm the average user throughput is very close to 98% of 512 kbps for all the admitted users. This is due to the fact that FPC based AC denies admission to the users whose GBR cannot be fulfilled based on the channel (i.e. user transmit power limitation) and cell load conditions.

Figure 5.4 shows the blocking probability vs. path gain for the case of reference AC and FPC based AC. The blocking probability of reference AC is uniformly distributed

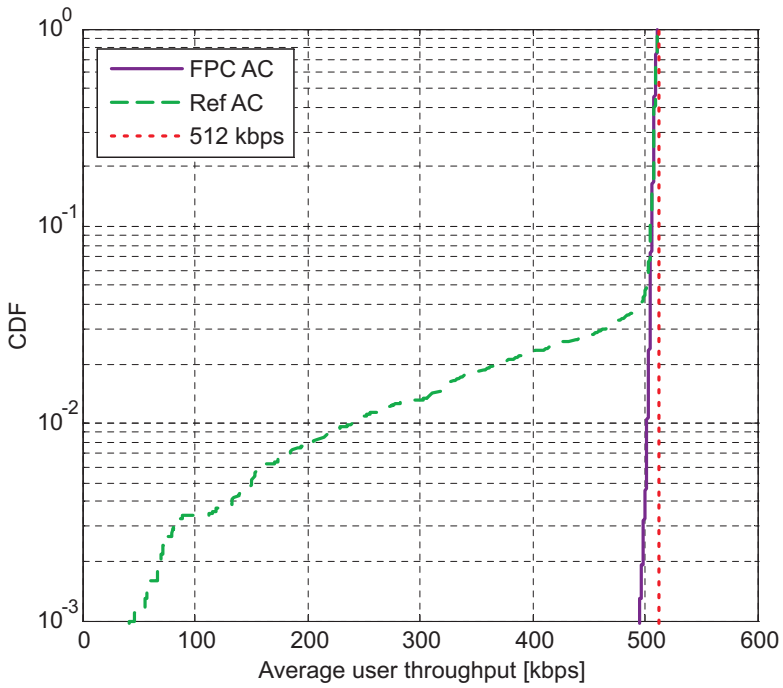

Figure 5.3: CDF of average user throughput for Case I with FPC based AC and reference AC algorithms. GBR weighted FDPS, user arrival rate = 6 users/cell/s.

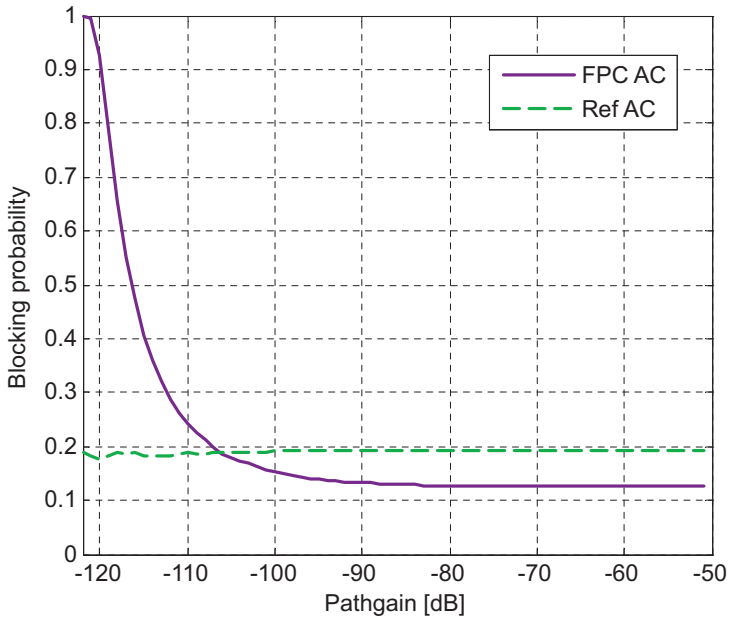

Figure 5.4: Blocking probability vs. path gain for Case I with FPC based AC and reference AC algorithms. GBR weighted FDPS, user arrival rate = 2 users/cell/s.

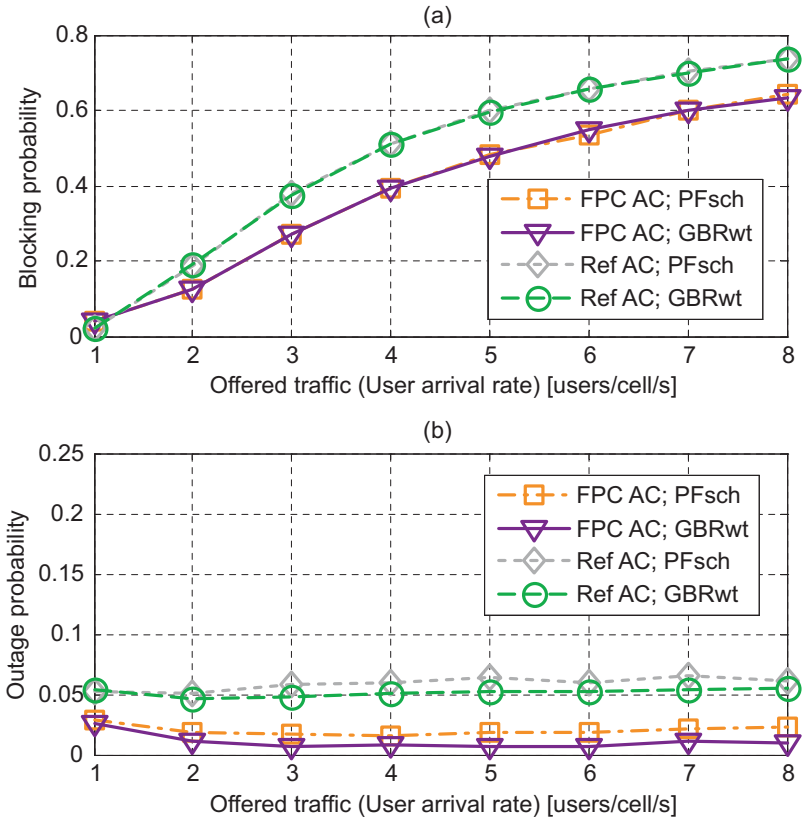

Figure 5.5: (a) Blocking probability vs. offered traffic, (b) outage probability vs. offered traffic for Case I with FPC based AC and reference AC algorithms.

with respect to path gain, while the blocking probability of FPC based AC is dependent on the path gain. The FPC based AC reject users with low path gain (cell edge users) with higher probability because the required GBR of these users can not be fulfilled due to the user transmit power limitation. Further, the finite blocking at different path gain values for both AC algorithms is due to the cell load condition i.e. all the PRBs are occupied by the active users.

Figure 5.5 shows the blocking and outage probabilities vs. offered traffic for different AC algorithms and FDPS algorithms. It is observed that the blocking probability is growing while the outage probability performance is similar with increasing offered traffic for different combinations of AC and PS. Additionally, both the blocking probability as well as outage probability for FPC based AC is better than reference AC. Moreover, the outage probability performance of GBR weighted FDPS is better than PF scheduled FDPS (PF-sch). This is due to the fact that GBR weighted FDPS is more effective in fulfilling the GBR as discussed in Section 4.3. It should be noticed that a GBR bearer would perceive an outage as more annoying compared to the blocking. The outage probability performance for the combination of FPC based AC and GBR weighted FDPS is best and is within 1%. Hence, in rest of the chapter results using GBR weighted FDPS are presented.

Figure 5.6 shows the unsatisfied user probability and number of users per cell vs. offered traffic for different AC algorithms and FDPS algorithms. It is observed that FPC

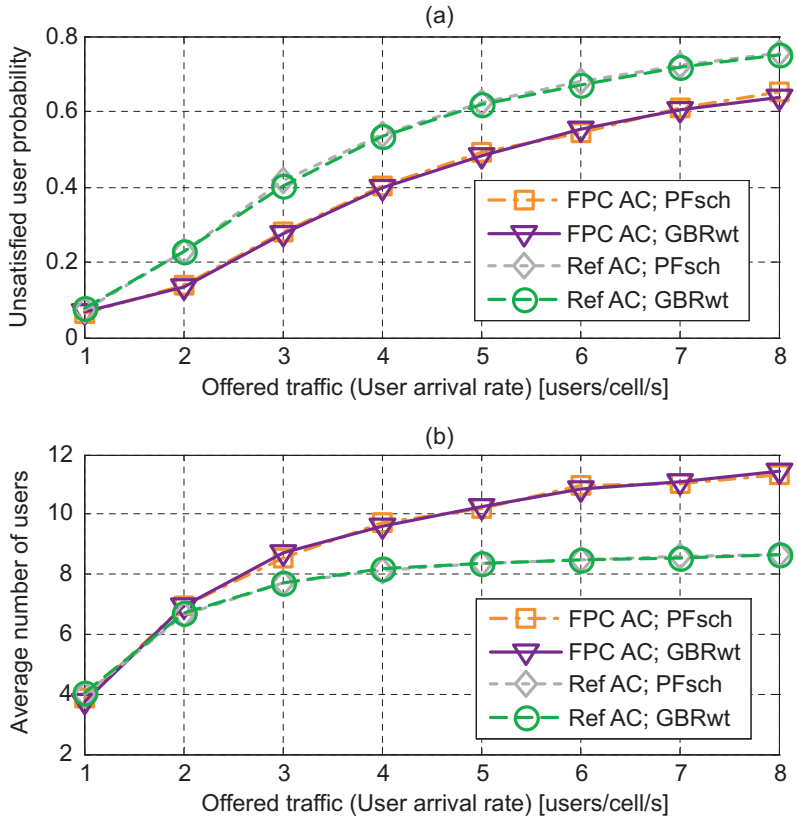

Figure 5.6: (a) Unsatisfied user probability vs. offered traffic, (b) average number of users per cell vs. offered traffic for Case I with FPC based AC and reference AC algorithms.

based AC performs best in terms of unsatisfied user probability at all offered traffics. The average number of users per cell is representative of carried traffic, since most of the users are transmitting data at constant bit rate as seen in Figure 5.3. The FPC based AC supports significantly higher carried traffic, due to the fact that it denies admission to the users at the cell edge with higher probability. Hence, more number of users with better channel conditions can be scheduled compared to the users with on average poor channel conditions to fulfill the GBR.

Figure 5.7 shows the CDF of packet delay and the CDF of average call delay for different AC algorithms. It is noticed that for reference AC around 4% of packets are not received correctly or are infinitely delayed. For FPC based AC the average call length for all of the users is 3.9 s which is same as the call length parameter for 512 kbps CBR users in Table 5.2. At the upper end of the distribution we notice that with reference AC around 3–4% of users are unable to complete call within 3.9 s, which means that these users are in outage.

Figure 5.8 shows the CDF of number of users per cell and the CDF of number of scheduled PRBs per user. It is seen that higher average number of users are served using the FPC based AC. This is because for FPC based AC the average channel condition of a user is better and hence GBR is fulfilled using lower number of PRBs as seen in

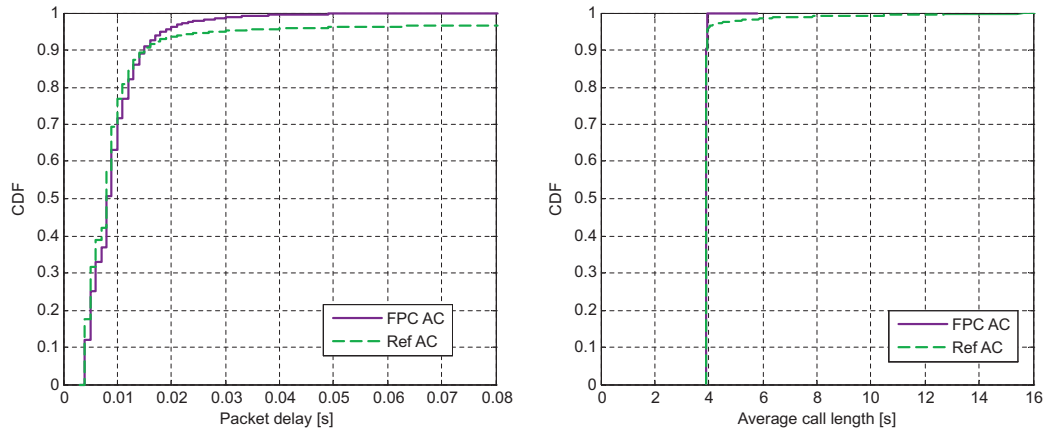

(a) (b)

Figure 5.7: (a) CDF of packet delay, and (b) CDF of average call length for Case I with FPC based AC and reference AC algorithms. User arrival rate = 6 users/cell/s.

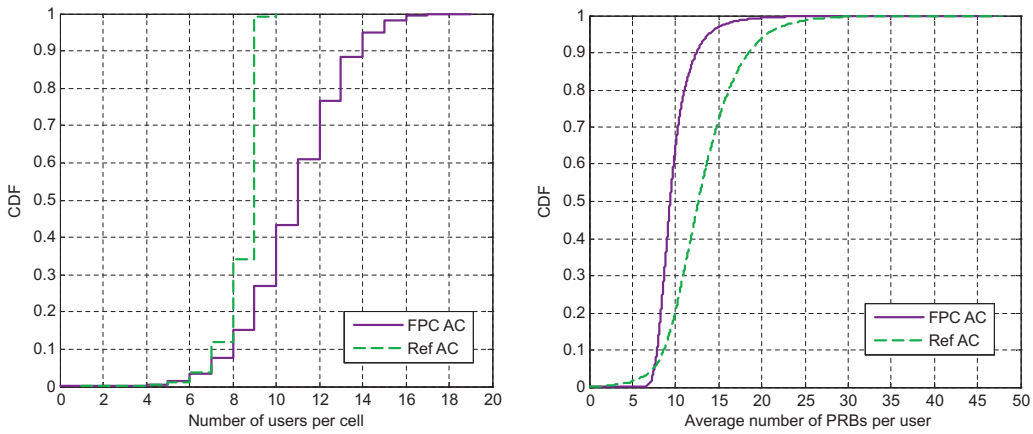

(a) (b)

Figure 5.8: (a) CDF of number of users per cell, and (b) CDF of number of PRBs per user for Case I with FPC based AC and reference AC algorithms. User arrival rate = 6 users/cell/s.

Figure 5.8 (b).

Figure 5.9 shows the PRB utilization per user and CDF of the total PRB utilization. It shows that each user is allocated adaptive number of PRBs between 1–48, and the frequency of use of smaller number of PRBs is higher for FPC based AC. This is due to the fact that FPC based AC admits on average better channel condition users whose GBR can be fulfilled using fewer number of PRBs. This fact leads to higher average number of users per cell as seen in Figure 5.8 (a) and hence the total PRB utilization is higher for the FPC based AC.

Figure 5.10 shows the CDF of path gain of blocked and admitted users. It should be noticed that on average FPC based AC denies admission to users with lower path gain value. As shown in Figure 5.4, the FPC based AC rejects user at the cell edge with higher probability as their GBR can not be fulfilled due to user transmit power limitations. The

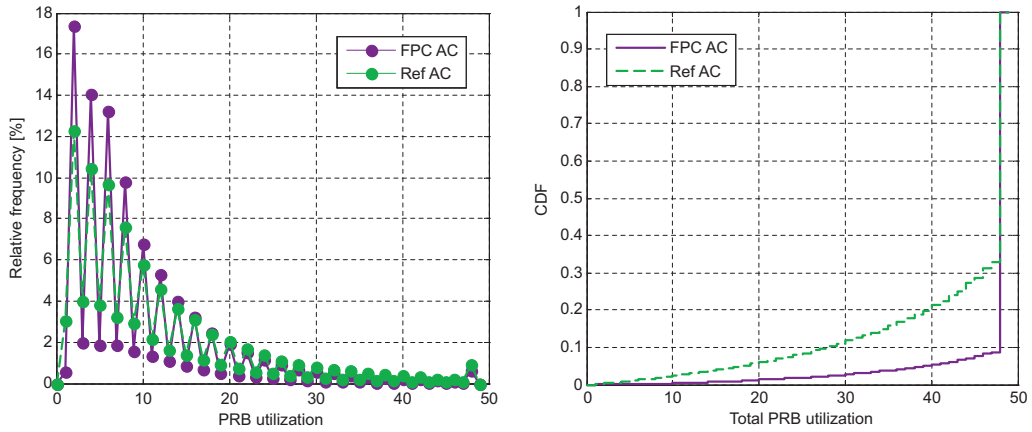

Figure 5.9: (a) PRB utilization per user, and (b) CDF of total PRB utilization for Case I with FPC based AC and reference AC algorithms. User arrival rate = 6 users/cell/s.

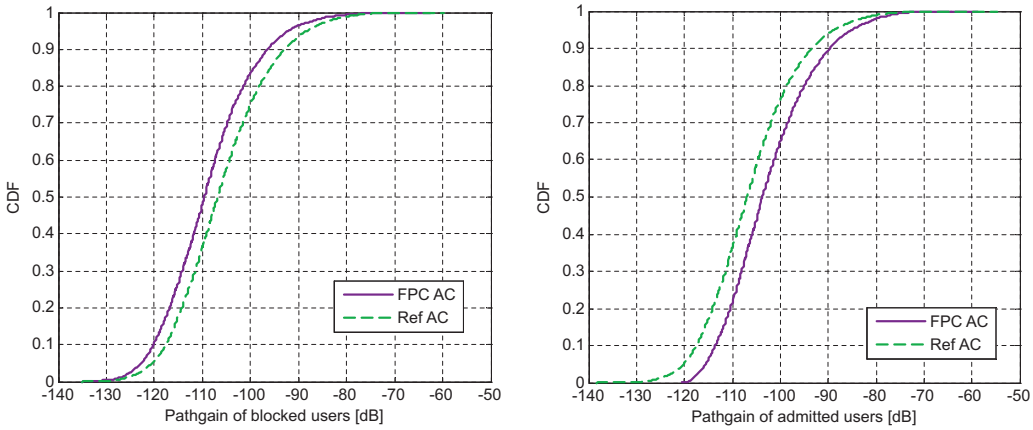

Figure 5.10: (a) CDF of path gain of blocked users, and (b) CDF of path gain of admitted users for Case I with FPC based AC and reference AC algorithms. User arrival rate = 6 users/cell/s.

alteration in the distribution of path gain of blocked users lead to the improvement of path gain distribution for the admitted users.

Figure 5.11 shows the CDF of average scheduled SINR and instantaneous IoT for different AC algorithms. The scheduled SINR distribution is shown to be higher for the FPC based AC. The FPC based AC denies admission to a user with a certain GBR requirement at cell edge with higher probability compared to a user near cell center as shown in Figure 5.10 (b). Hence the improvement in the SINR at the lower edge and average in the scheduled SINR distribution. The average IoT is negligibly lower for reference AC because of the lower number of active users per cell and hence fractional PRB utilization as shown in Figure 5.9 (b).

Figure 5.12 shows the CDF of user transmit power and relative frequency of MCS used for different AC algorithms. In this case we notice that the FPC based AC has a larger

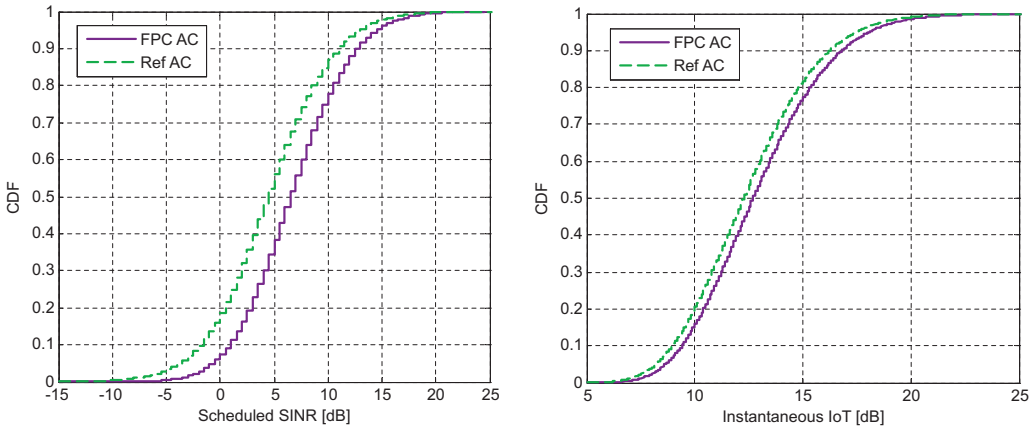

(a) (b)

Figure 5.11: (a) CDF of scheduled SINR, and (b) CDF of instantaneous IoT for Case I with FPC based AC and reference AC algorithms. User arrival rate = 6 users/cell/s.

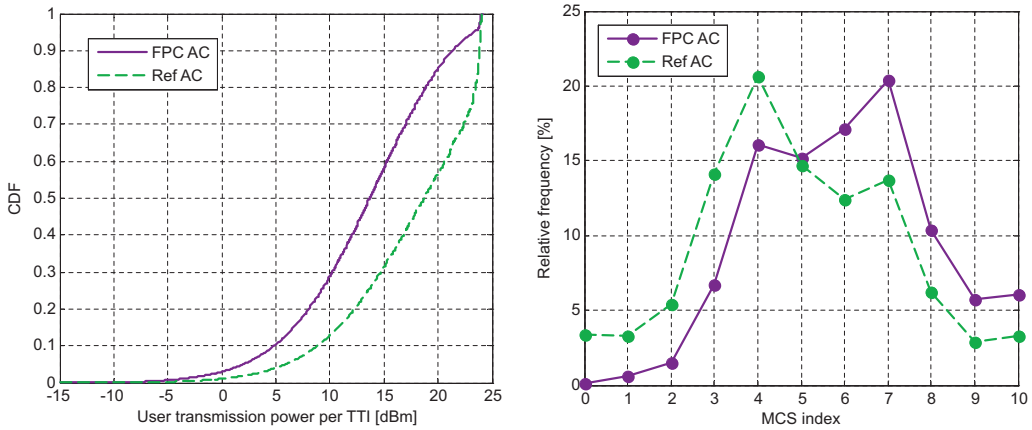

(a) (b)

Figure 5.12: (a) CDF of user transmit power, and (b) CDF of MCS used for Case I with FPC based AC and reference AC algorithms. User arrival rate = 6 users/cell/s.

power headroom compared to the reference AC. This is because FPC based AC admits a user only if its GBR can be fulfilled while meeting the user transmit power constraint. In this case none of the users are power limited because ATB based scheduling adaptively selects the transmission bandwidth such that the user is transmitting below the maximum user transmit power. It is also shown that the FPC based AC selects the lower MCS order with less probability because of lesser number of users at cell edge since it denies admission to the user at cell edge with higher probability compared to the reference AC.

5.4.2 CBR Traffic with Mixed GBR Case

In this section the performance of combined AC and PS framework for mixed CBR traffic with non-identical GBR of 256 kbps and 512 kbps with 50% probability each in terms of

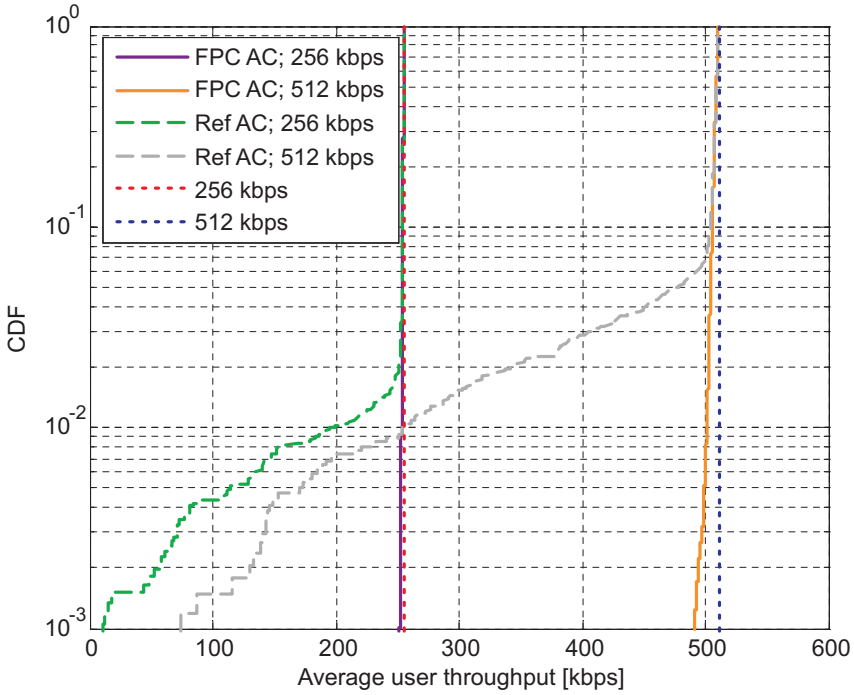

Figure 5.13: CDF of individual user throughput for the mixed GBR of [256, 512] kbps as in Case II with FPC based AC and Reference AC algorithms. GBR weighted FDPS, user arrival rate = 6 users/cell/s.

offered traffic is analyzed.

Figure 5.13 shows the individual user throughput for the user classes [256, 512] kbps for reference AC (R_{max} = 5 Mbps) and FPC based AC. We notice that the proposed QoS aware framework for AC and PS effectively fulfills the individual GBR requirements of 256 kbps and 512 kbps user class. It is observed that for the FPC based AC individual average user throughput of different user classes is close to their required GBR. This is due to the fact that FPC based AC denies admission to the users whose GBR cannot be fulfilled based on channel condition (i.e. user transmit power limitation) and cell load condition.

Figure 5.14 shows the CDF of packet delay and the CDF of average call delay for different AC algorithms. It is noticed that for reference AC around 3% of packets are not received correctly or are infinitely delayed. The average call length for most of the CBR users of each class is equal to the call length parameter as in Table 5.2 (i.e. 3.9 s for 512 kbps, and 7.8 s for 256 kbps). We notice that with reference AC arond 7–8% of 512 kbps users are unable to finish call within the call length parameter, which is because of the high packet loss due to the poor channel conditions. For reference AC, fewer number of 256 kbps users are unable to finish call within the call length parameter compared to 512 kbps, which is due to the higher resource requirement for 512 kbps. For FPC based AC, almost all 256 kbps and 512 kbps users are able to finish call within the defined call length parameter.

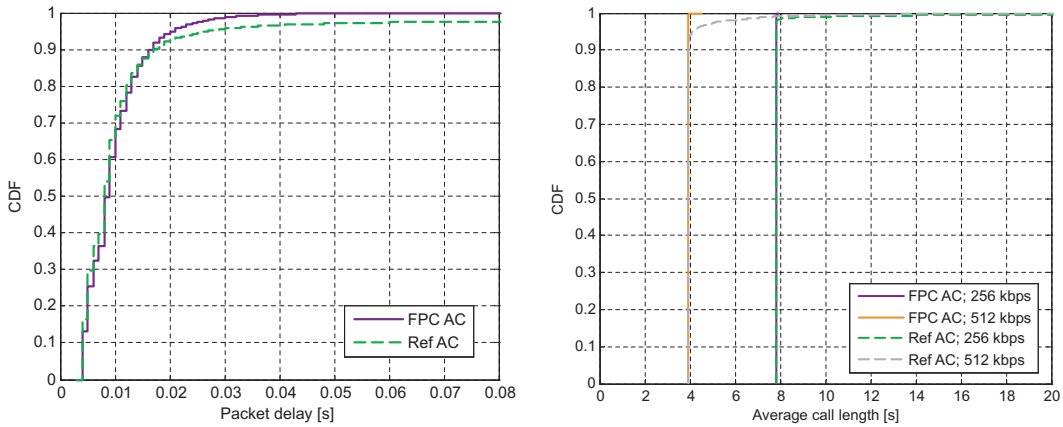

(a) (b)

Figure 5.14: (a) CDF of packet delay, and (b) CDF of average call length for Case II with FPC based AC and reference AC algorithms. User arrival rate = 6 users/cell/s.

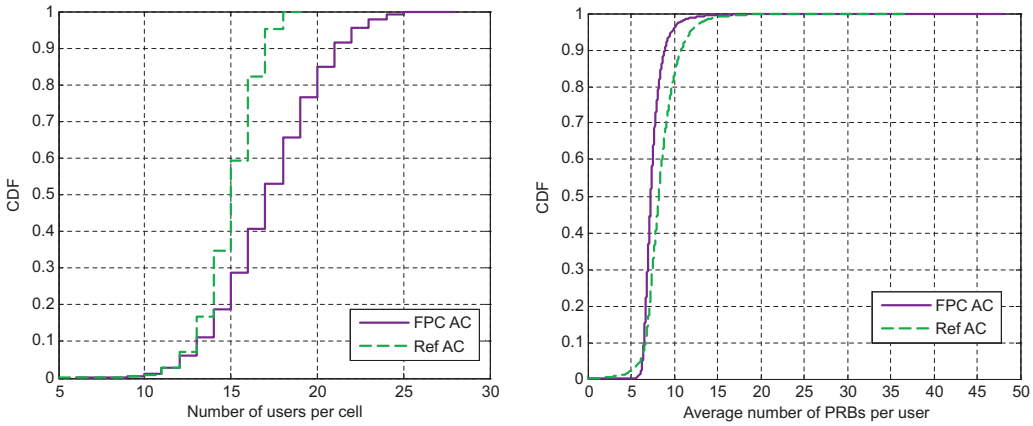

(a) (b)

Figure 5.15: (a) CDF of number of users per cell, and (b) CDF of number of PRBs per user for Case II with FPC based AC and reference AC algorithms. User arrival rate = 6 users/cell/s.

Figure 5.15 shows the CDF of number of users per cell and the CDF of number of PRBs per user. It is seen that higher average number of users are served using the FPC based AC. This is because for FPC based AC the average channel condition of a user is better and hence GBR is fulfilled using lower number of PRBs.

Figure 5.16 shows the blocking and outage probabilities vs. offered traffic for different AC algorithms for individual user classes. The blocking and outage probabilities are lower for relatively smaller GBR, which shows the dependence of proposed AC algorithms on the GBR requirement. The blocking probability is higher for 512 kbps user class, which requires more resources, compared to the 256 kbps user class due to the cell load conditions. It is seen that FPC based AC performs best with the outage probability limited within 2% for both the user classes.

These results show that the proposed combined AC and PS framework is able to effec-

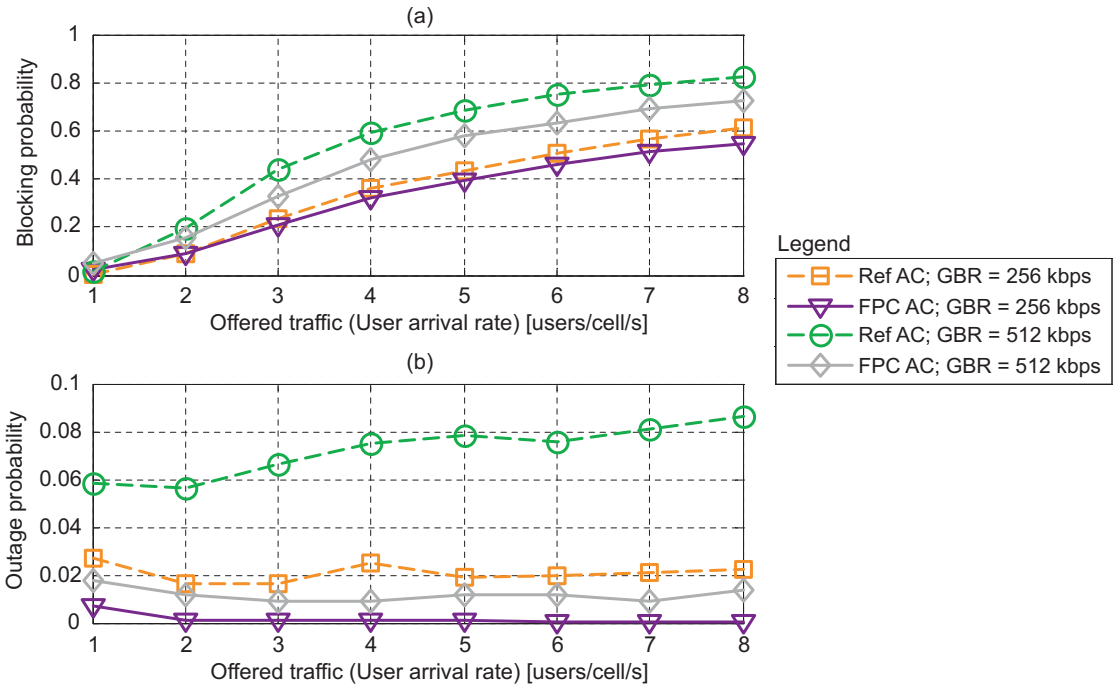

Figure 5.16: (a) Blocking probability vs. offered traffic, (b) outage probability vs. offered traffic for individual user classes in Case II with FPC based AC and reference AC algorithms.

tively differentiates between CBR streaming user classes for a negligible outage probability, reduced blocking probability, and hence improved unsatisfied user probability performance.

5.4.3 ON/OFF Traffic with Single GBR Case

In this section we study the performance of an ON/OFF traffic with CBR during ON period of GBR equals 512 kbps and source activity factor of 0.5 for the traffic modeling assumptions given in Table 5.3.

Figure 5.17 shows the CDF of average user throughput for ON/OFF traffic source with 512 kbps CBR and source activity factor of 0.5. The average user throughput is calculated as the total correctly received bits over the call duration including both the ON and OFF periods. It is noticed that the average cell throughput for both the AC algorithms converges around 256 kbps which is the product of 512 kbps GBR and source activity factor of 0.5. The users with average user throughput less than GBR for reference AC is higher because users in this case are admitted without channel considerations hence users admitted close to the cell edge are unable to fulfill the GBR with higher probability due to the transmit power limitations. Hence the proposed AC algorithms for ON/OFF traffic in Section 5.2 is shown to effectively take into account the source activity factor.

Figure 5.18 shows the CDF of packet delay and average call length for ON/OFF traffic source for FPC based AC and reference AC algorithms. It should be noticed that for

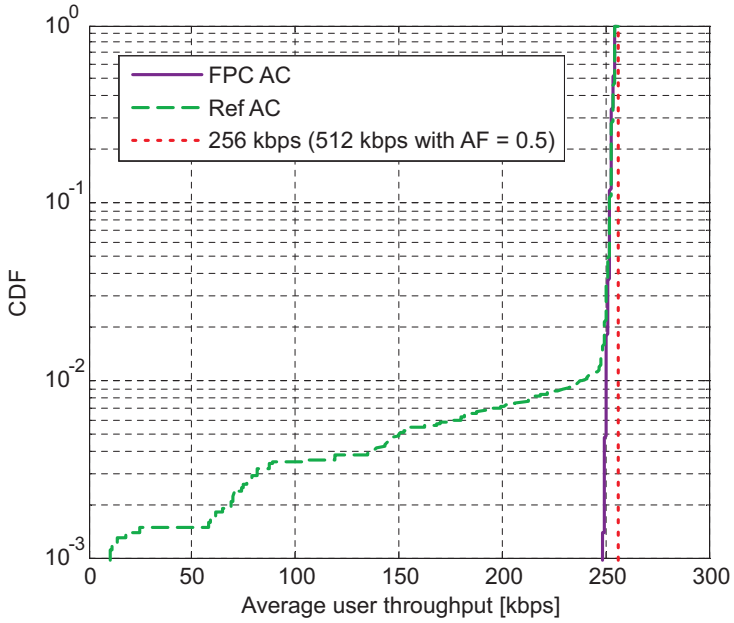

Figure 5.17: CDF of average user throughput for the 512 kbps CBR streaming with activity factor of 0.5 as in Case III, FPC based AC and Reference AC algorithms. GBR weighted FDPS, user arrival rate = 6 users/cell/s.

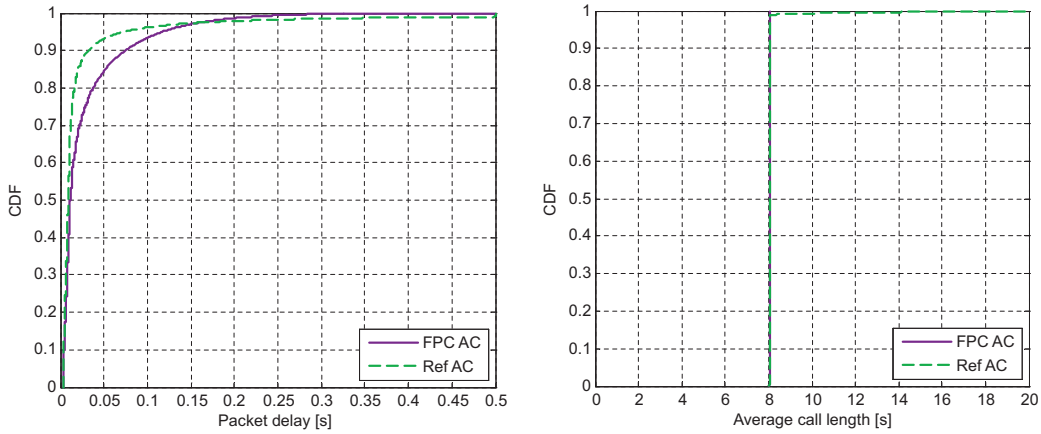

Figure 5.18: (a) CDF of packet delay, and (b) CDF of average call length for Case III with FPC based AC and reference AC algorithms. User arrival rate = 6 users/cell/s.

reference AC there are some packets which are infinitely delayed, while for FPC based AC the packet delay is limited by 0.25 s. The average call length of the finished calls for FPC based AC is limited by the call duration of 8.0 s which is equivalent to 4 ON spurts of 1 s ON period and interleaved 1 s OFF period.

Figure 5.19 shows the blocking and outage probabilities for FPC based AC and reference AC, and ON/OFF traffic. It should be noticed that FPC based AC blocks the users even at very low offered traffic if their GBR can not be fulfilled due to poor channel conditions. The outage probability is similar while blocking probability increases for increasing

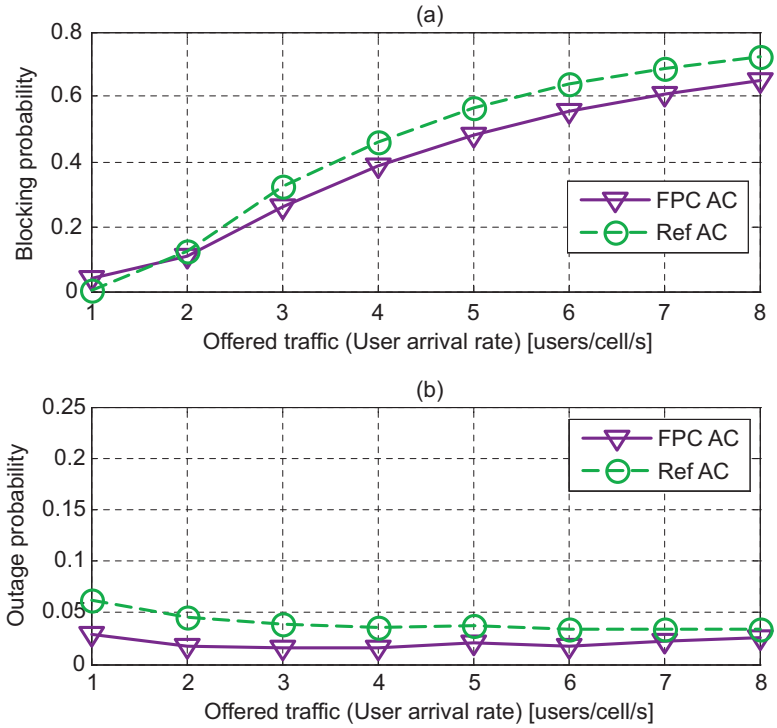

Figure 5.19: (a) Blocking probability vs. offered traffic, (b) outage probability vs. offered traffic for Case III with FPC based AC and reference AC algorithms.

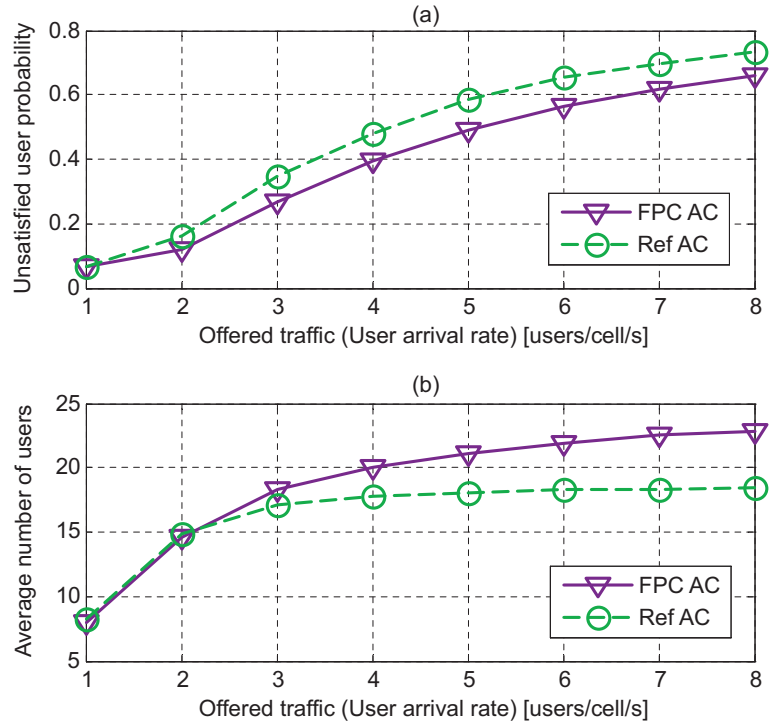

Figure 5.20: (a) Unsatisfied user probability vs. offered traffic, (b) average number of users per cell vs. offered traffic for Case III with FPC based AC and reference AC algorithms.

offered traffic for both the AC algorithms. The FPC based AC is shown to perform best both in terms of blocking and outage probabilities.

Figure 5.20 shows the unsatisfied user probability and average number of users for FPC based AC and reference AC, and ON/OFF traffic. The FPC based AC is shown to perform best in terms of unsatisfied user probability at all offered traffics. The FPC based AC supports significantly higher carried traffic (average number of users per cell), due to the fact that it denies admission to the users at the cell edge with higher probability. Hence, more number of users with better channel conditions can be allocated compared to the users with poor channel conditions to fulfill the GBR.

5.5 Mixed GBR and Non-GBR bearers consideration

In a real wireless network several types of traffics co-exist which are classified in LTE as GBR and Non-GBR bearers [17]. The GBR bearers are admitted based on an AC algorithm for example FPC based AC taking into account the GBR and channel condition of the user. The Non-GBR bearer should always be admitted unless the admission of a user makes the system unstable for example number of users in the system grows infinitely. Hence, a simple AC based on the max number of users (MAX_NUM_USERS) is used to set the limit on the sum of GBR and Non-GBR bearers, while the proposed AC is used to decide the admission of a GBR bearer. This algorithm which takes into consideration both

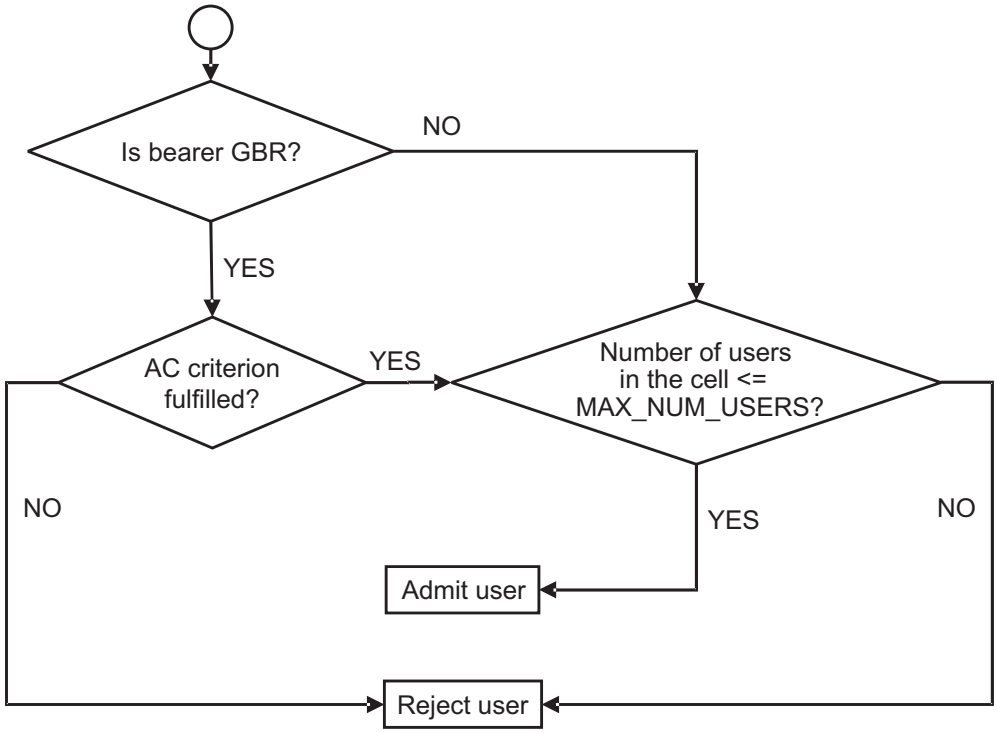

Figure 5.21: Flowchart for AC algorithm to differentiate GBR and Non-GBR bearers.

GBR and Non-GBR bearers is illustrated in Figure 5.21. This framework is an extension of AC algorithm studied for QoS support. To provide QoS control it is important that PS is also able to effectively differentiate and share resources between GBR and Non-GBR bearers. One way to allocate resources is to prioritize GBR bearers over Non-GBR bearers, so that GBR bearers get sufficient resources to fulfill their QoS while the Non-GBR bearers share the remaining resources.

5.6 Conclusions

The AC algorithms taking into account the source activity factor for an ON/OFF traffic are proposed. The proposed combined AC and PS framework is analyzed for CBR streaming traffic for single and mixed GBR cases, as well as for an ON/OFF traffic source with CBR during ON periods. The combined FPC based AC and GBR weighted FDPS is shown to perform best in terms of blocking, outage, and unsatisfied user probabilities as well as carried traffic in terms of average number of users per cell. Additionally, an AC framework to differentiate between mixed GBR and Non-GBR bearers is presented. It suggests to admit a Non-GBR bearer if the total number of bearers are below a certain maximum parameter, and FPC based AC is used for GBR bearers. Hence, the proposed framework can effectively be used in a mixed GBR and Non-GBR bearer scenario.

This study is done for delay tolerable data traffic, and the proposed AC can further be studied for delay sensitive ON/OFF traffic for example VoIP. In order to compensate for the delay budget requirement for the delay sensitive traffic some capacity (or bandwidth) need to be reserved. This is to accommodate for the situation when more than the average number of ON periods become active at the same time. In the case of FPC based AC the load safety parameter (ΔN) can be used to control the number of unsatisfied delay sensitive users. This is especially the case when there is a very high percentage of delay sensitive traffic in the system. In the case when there is a mix of delay sensitive GBR bearers and Non-GBR bearers, Non-GBR bearers can be delayed (or even dropped) to meet the QoS requirements of delay sensitive GBR bearers without the need of load safety parameter.

Chapter 6

Handover Measurements and Filtering

6.1 Introduction

One of the goals of LTE is to provide seamless access to voice and multimedia services, which is achieved by supporting handover from one cell i.e., serving cell, to another i.e., target cell. Hence, handover is an important functionality for QoS provisioning particularly for delay-sensitive services. The decentralized system architecture of LTE facilitates the use of hard handover. Hard handover (break-before-make type) is standardized for LTE while soft handover (make-before-break type) is not included [13], which makes the problem of providing seamless access even more critical. Handover in LTE is user assisted and network controlled, and it is usually based on the downlink channel measurements and its processing (filtering) by the user. The focus of this study is on the downlink handover measurements and filtering for intra-LTE, intra-frequency, hard handover.

This chapter is organized as follows: In Section 6.2, the state of the art of the handover measurement and filtering is presented. In Section 6.3, the handover procedure including the measurements and filtering to process the handover measurements is studied. Further, a realistic handover measurement error model and the handover decision criterion is modeled. Additionally, the linear- and logarithmic- domain filtering for handover based on downlink Received Signal Strength (RSS) and Carrier to Interference Ratio (CIR) measurements for LTE is evaluated and compared using the dynamic system level simulation methodology, which is described in Section 6.4. In Section 6.5, performance comparison in terms of number of handovers and downlink CIR for different user speeds are presented. Section 6.6 contains the concluding remarks.

6.2 State of the Art

Several studies have been done on handover for systems like Global System for Mobile Communication (GSM) and Wideband Code Division Multiple Access (WCDMA)

[73][74][75][76][77][78]. Overview of the handover issues and the importance of handover design algorithms are presented in [73]. In [74] an in-depth study of the soft handover effects on the downlink is presented, while [75][76] present the gains for using soft handover (inter-Node B macrodiversity) in uplink for WCDMA system. In [77] an analytical model for handover measurement based on relative signal strength is presented to determine the averaging interval and hysteresis level that achieve the optimum trade off between the number of unnecessary handovers and the delay in making handover. The numerical results are evaluated considering only two cells. In [78] an adaptive handover algorithm based on the estimated user speed from the signal strength measurement is presented. The idea is to base handover decision and control the handover parameters adaptively based on the user speed.

In GSM, handover is based on Received Signal Strength Indicator (RSSI) measurement, while in Universal Mobile Telecommunications System (UMTS) it is either based on Received Signal Code Power (RSCP) or E_c/N_0 at Common Pilot Channel (CPICH) [79]. RSCP is the absolute power level of the CPICH as received by the User Equipment (UE), while E_c/N_0 is the signal energy per chip over noise power spectral density. These measurements represent absolute and relative pilot signal strength received at the UE. In [80] it is shown that interference has a strong influence on the signal quality and hence it should also be used when making handover decision. This motivates the study and comparison of the RSS and CIR measurements for handover in LTE.

The Layer 3 (network layer) (L3) filtering of RSSI in GSM, and RSCP and E_c/N_0 in UMTS is standardized to be done in Decibel (dB) domain [81]. The performance gain using L3 dB domain filtering is shown in terms of reduced soft handover region in [82], while it is mentioned in [83] that dB domain filtering introduces some extra delay. These studies have been done for UMTS which supports soft handover, and the same conclusions may not hold true for LTE which supports hard handover [13][84]. Hence, linear and dB domain filtering is studied in this chapter.

6.3 Hard Handover

A handover process can typically be divided into three phases: 1) initialization phase including handover measurement, processing, and reporting, 2) preparation phase including handover decision in the target cell, and 3) execution phase as shown in Figure 6.1. The detailed intra-LTE handover timing diagram is shown in Figure 2.3. Handover measurements are done in downlink from the serving and the neighboring cells and are processed in the UE. Processing is done to filter out the effect of fast-fading and Layer 1 (physical layer) (L1) measurement/estimation errors using a L3 filter. A handover event based on the processed measurements is reported back to the serving Evolved Node B (eNode-B) in a periodic or event based manner in uplink using Radio Resource Control (RRC) signaling. Hence a handover is initiated based on the uplink event reporting if certain decision criteria are met. Handover is then executed by transferring the UE control to the target cell performing the network procedures with the assistance of the UE [73].

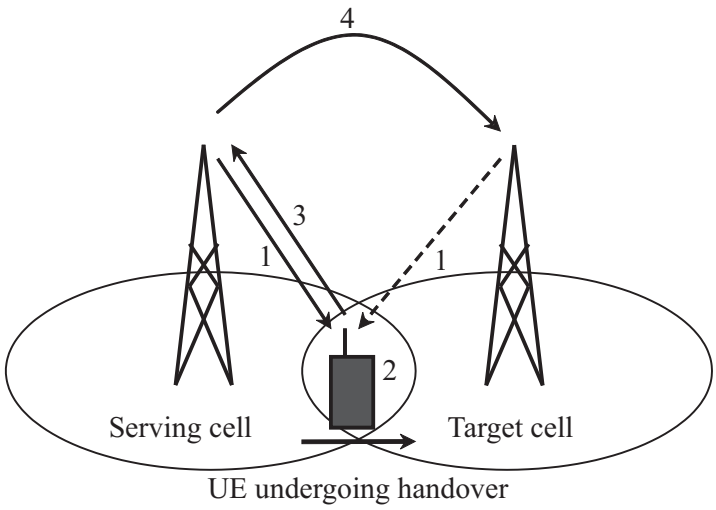

Figure 6.1: The different phases of a handover process. 1) Downlink handover measurements, 2) processing of downlink measurements, 3) uplink reporting, 4) handover decision and execution.

6.3.1 Handover Measurements and Frequency-Domain Averaging

The LTE uses scalable bandwidth up to 20 MHz (1.4, 3, 5, 10, 15, 20 MHz) based on the number of used subcarriers [11]. The frequency selective multi-path fading will have an impact on handover depending on the measurement bandwidth. For wideband signal (e.g. 10 MHz) the frequency selective multi-path fading will not have an impact on the total received power of the reference signal because of the averaging in frequency domain. However, for narrowband signal the multi-path fading can cause the power of the signal to drop rapidly below the low local mean path loss. Consequently the measurements must be updated at a rate corresponding to changes in the local mean path loss and not necessarily react to changes in multipath fading.

Handover decisions are usually based on the downlink channel measurements which consist of RSS or CIR [80]. These handover measurements in LTE are done at the downlink reference symbols in the frame structure as shown in Figure 6.2. The handover decision can also be based on the uplink measurements [85], but the focus of this study is on downlink handover measurements.

The UE measures the RSS which includes path loss, antenna gain, log-normal shadowing and fast fading averaged over all the reference symbols within the measurement bandwidth BW_m. The averaging of fast fading over all the reference symbols is done at L1 and hence is called L1 filtering. The use of scalable bandwidth in LTE allows to do the handover measurement on different bandwidths. Hence, measurement bandwidth is a parameter of L1 filtering and should be optimized for different environments e.g. user speeds.

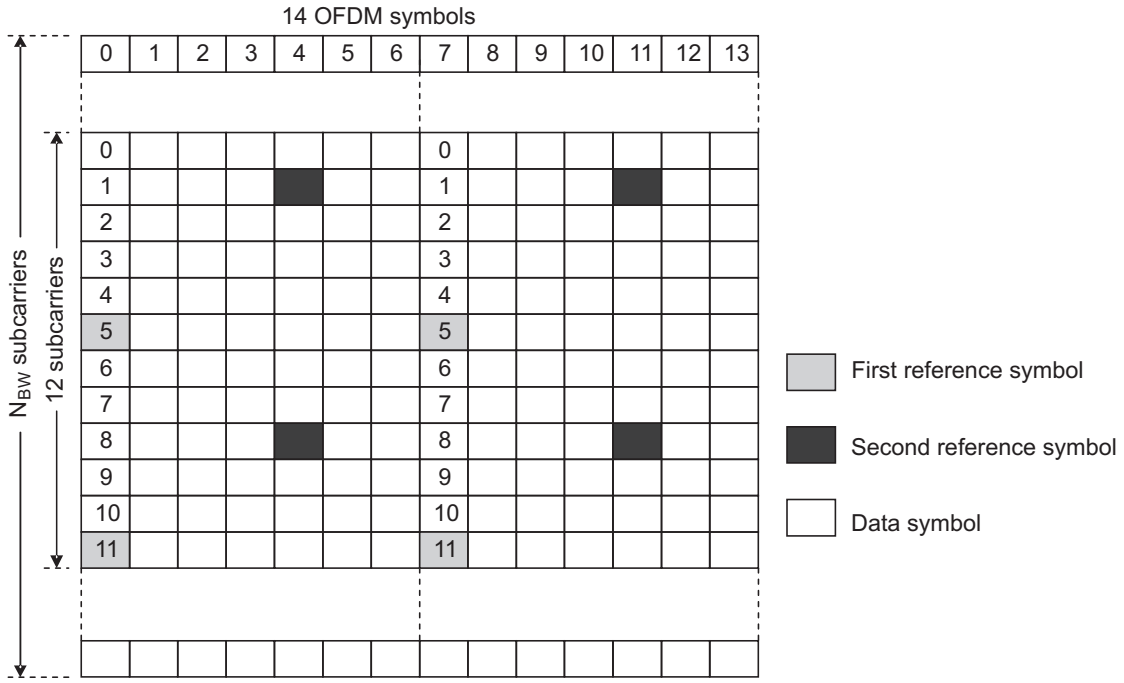

Figure 6.2: Downlink reference signal structure for LTE PRB with one antenna port and short cyclic prefix [14][27]

The downlink RSS[1] from k^{th} cell, RSS_k, is defined as,

$$RSS_k = P \sum_{j \in \text{all reference symbols in } BW_m} G_{kj} \tag{6.1}$$

where P is the transmit power of each reference symbol, and G_{kj} is channel gain of j^{th} reference symbol from k^{th} cell.

The downlink received CIR from the k^{th} cell, CIR_k, is defined as,

$$CIR_k = \frac{RSS_k}{I_k + N_0} \tag{6.2}$$

where $I_k = \sum_{i \neq k} RSS_i$ i.e., the total received power from all the cells except the serving cell, and N_0 is thermal noise.

A single handover observation is defined as the mean measured RSS or CIR observed over the reference symbols within measurement bandwidth and Transmission Time Interval (TTI) of 1 ms with 14 OFDM symbols as shown in Figure 6.2.

6.3.2 Time-Domain Averaging (Layer 3 Filtering)

The frequency averaged handover measurements (Q) i.e., RSS or CIR, are filtered at the UE by using a first order Infinite Impulse Response (IIR) filter as defined in (6.3). Further,

[1]Reference signal RSS is known as Reference Signal Received Power (RSRP) in LTE.

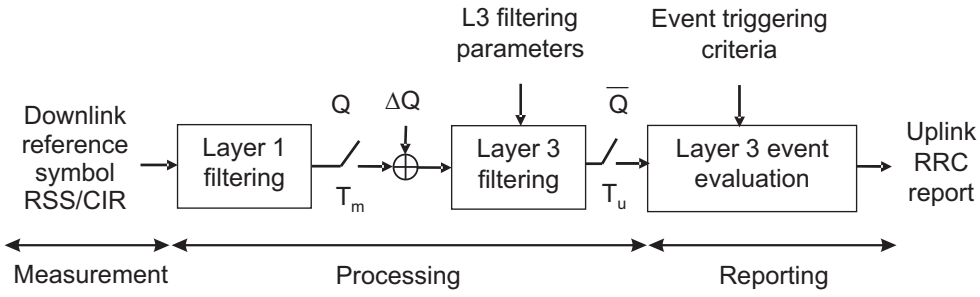

Figure 6.3: Handover initialization phase including handover measurement, filtering and reporting in the UE [79].

the filtered measurement is reported to the eNode-B, which makes the handover decision based on a decision criteria. The frequency averaged measurements could also be reported periodically to the eNode-B and can be processed at the eNode-B. However, in this study the processing is assumed to be done at the UE, which saves uplink capacity due to reduced uplink reporting overhead.

The filtered handover measurement ($\overline{Q}$) is updated every handover measurement period (T_m) at the UE as the output of a first order IIR filter in (6.3). The relative influence on $\overline{Q}$ of the recent measurement and older measurements is controlled by the forgetting factor β, which in this study is chosen depending on the handover decision update period (T_u) and T_m as $\beta = T_m/T_u$, where T_u is an integer multiple of T_m. T_u is also known as L3 filtering period (or time-domain averaging window).

$$\overline{Q}[n] = \beta Q[n] + (1-\beta)\overline{Q}[n-1] \tag{6.3}$$

The L1 and L3 filtering is used to average out the effect of multipath fading, and to determine the local mean path loss i.e. including log-normal shadowing, distance dependent path loss, and antenna gain. Since the successive log-normal shadowing samples are spatially correlated the filtering period is influenced by the degree of correlation present in the signal [86]. The filtering period can be adaptively chosen depending on this degree of correlation present in the log-normal shadowing samples. At high speed, for example, the log-normal shadowing samples are not highly correlated, therefore it would be more accurate to have a shorter filtering period than for slow speed users in order to follow the log-normal shadowing.

The L3 filtering is said to be "linear filtering" when Q and $\overline{Q}$ in (6.3) are expressed in linear units, while it is said to be "logarithmic filtering", when they are expressed in logarithmic units (e.g. dB). The linear- and dB- domain L3 filtering is evaluated for different T_u and user speeds in this study.

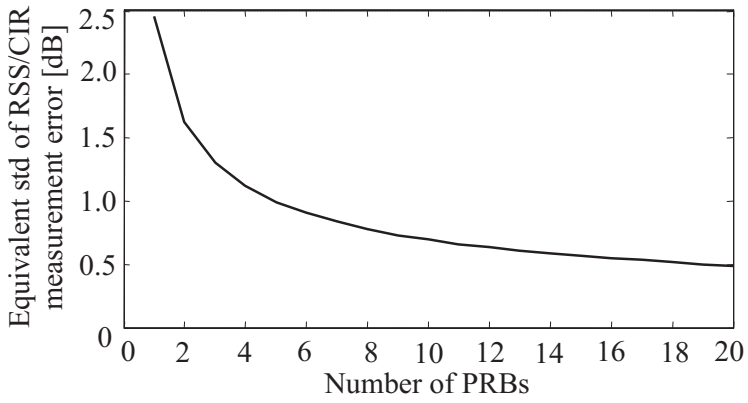

Figure 6.4: Impact of frequency domain averaging (L1 filtering) on RSS estimation error per TTI [87][88].

6.3.3 Handover Measurement Accuracy

The handover measurement is done on the reference symbols of measurement bandwidth. Each PRB at an antenna port has 8 reference symbols as shown in Figure 6.2. The limited number of reference symbols available in handover measurement bandwidth for RSS and CIR measurements introduces measurement error. This error is modeled as uncorrelated and normally distributed in dB (log-normally distributed in linear domain) with zero mean and σ dB standard deviation as defined in (6.4) [89].

$$\Delta Q \sim N(0, \sigma^2) \text{ [dB]} \tag{6.4}$$

If Q is measured in dB the measurement error in (6.4) is added to it before the L3 filtering. If Q is measured in linear domain the measurement error in linear domain ($\sim \ 10^{\Delta Q/10}$) is multiplied to it. For smaller measurement bandwidth (i.e. lower number of reference symbols) larger error level are expected as compared to the larger measurement bandwidth (i.e. higher number of reference symbols) as shown in Table 6.1 which is estimated using Figure 6.4. In this study, downlink measurement bandwidths of 1.25, 2.5, 5, and 10 MHz are analyzed as the scalable bandwidth values used in 3GPP LTE [14]. For example, 1.25 MHz of the measurement bandwidth is equivalent to 6 Physical Resource Blocks (PRBs) and the corresponding σ = 0.8 dB. The PRB size in LTE is determined as 12 subcarriers with fixed 15 kHz spacing which is equivalent to 180 kHz.

6.3.4 Handover Reporting and Decision

The handover reporting event is based on the processed measurement, $\overline{Q}$, and the handover event is triggered if the condition in (6.5) is satisfied, where H_m is handover margin. Handover event in (6.5) is checked and reported every T_u as shown in Figure 6.5. The target

Table 6.1: Standard deviation of measurement error

Measurement bandwidth [MHz]	Number of PRBs	σ [dB]
1.25	6	0.8
2.5	12	0.6
5	25	0.45
10	50	0.35

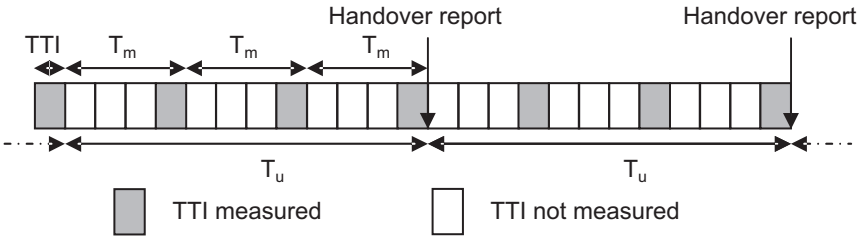

Figure 6.5: Handover measurement period (T_m) and decision update period (T_u)

cell (TC) is defined as the cell[2] from which the UE experiences maximum $\overline{Q}$, excluding the serving cell (SC).

$$\overline{Q}(n)_{\text{TC}} \geq \overline{Q}(n)_{\text{SC}} + H_m \text{ [dB]} \tag{6.5}$$

A user at the cell edge undergoing handover to a target cell which returns to the serving cell after a short time is said to make a ping pong handover [78]. The ping-pong handover is an unnecessary handover that can be reduced by using a timer called handover avoidance timer. Handover avoidance timer limits the time between two consecutive handover by a user. In this study, the handover decision is assumed to be based on (6.5) and it is executed only if the handover avoidance timer is expired. Details about handover execution including negotiation and signaling between serving and target cells are out of the scope of this study.

6.4 Dynamic System Level Simulation Methodology

This part of the study is done using a multi-cell, multi-user, dynamic system level simulator called Efficient Layer II Simulator for E-UTRAN (ELIISE) which was developed to study Radio Resource Management (RRM) in uplink. The functionalities which are implemented include channel model, mobility, handover, power control and packet scheduling. Both the bandwidth fair and channel aware resource allocation schemes are implemented [29].

The simulated network layout is shown in Figure 6.6. The network scenario con-

[2]Terms cell and sector are used interchangeably with the same meaning.

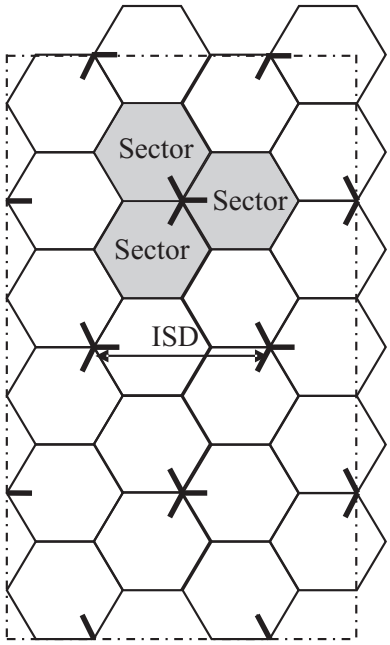

Figure 6.6: The hexagonal network layout used in ELIISE [90].

sidered assumes a hexagonal grid with eight cell sites each consisting of three sectors (or cells) per site with a corner-excited structure [90]. The users are uniformly distributed over the network area. Each user is given a uniform random direction in the range $[0°, 360°)$ and it moves in the same direction at a constant speed during the whole simulation time. In order to avoid the drawback of a limited network area also known as boundary effect the wrap-around technique is deployed [91]. Wrap around technique ensures that each user experiences interference as if it was in the center of a hexagonal grid which includes the first tier of interference. Single transmit and dual receive antennas are used both in uplink and downlink with Maximal Ratio Combining (MRC). The network layout used in this part is different from the layout used in the semi-static system level simulator as shown in Figure A.1. The semi-static simulator used in first part of the study takes into account the interferers from two tiers, while for handover studies interference from only one tier is modeled. The additional degree of freedom in the ELIISE is that the users are mobile which was not the case in the semi-static simulator.

The channel model consists of three components, namely, path loss, shadow fading (shadowing), and multipath fast fading. The path loss component is determined primarily by the distance between the eNode-B and user. In the absence of the fading, this causes the signal strength to decrease gradually with distance. The shadow fading give rise to a random fluctuation about its mean value determined by the path loss component. The statistics of shadow fading component conform to log-normal distribution with its standard deviation representing the degree of shadowing present. Shadow fading is assumed to be fully correlated between cells of the same site, while it is completely uncorrelated between sites. The component due to multipath which give rise to rapid fluctuations in the received signal over short distances, is averaged out by L1 and L3 filtering at normal

Table 6.2: Simulation Parameters and Assumptions

Parameter	Assumptions
Cellular layout	Hexagonal grid, 8 cell sites, 3 cells per site
Inter Site Distance (ISD)	500 m (Macro case 1) [14]
Path loss	$128.1 + 37.6 \log_{10}(\text{distance in km})$ dB
Log-normal shadowing	standard deviation = 8 dB correlation distance = 50 m correlation between cells = 1.0 correlation between cell sites = 0.0
Fast fading	TU3 (20 taps) [92]
Antenna gain	UE: 0 dBi, eNodeB: 14 dBi
Antenna pattern	$A(\theta) = -\min\left[12\left(\frac{\theta}{\theta_{3\text{dB}}}\right)^2, A_m\right]$ $\theta_{3\text{dB}} = 70°$, $A_m = 20$ dB
System bandwidth	10 MHz
Number of PRBs	50 PRBs (180 kHz per PRB)
TTI	1 ms
Total eNode-B Tx power	46 dBm
eNode-B noise figure	5 dB
UE power class	24 dBm (250 mW)
UE noise figure	9 dB
UE distribution	Uniform
UE speed	3, 30, 120 kmph
UE direction of movement	uniform randomly chosen within $[0°, 360°)$
Min. distance between UE and eNode-B	35 m
Power control frequency	20 kHz
Power control step size	± 1 dB
Resource allocation period	100 TTI
BLER target	10%
SINR target	6 dB
MCS	16QAM 1/2
Traffic model	Full buffer
Number of UEs	100 (fixed during simulation time)
Simulation time	50 s

user speeds. The fast fading is modeled using the Typical Urban (TU) power delay profile with 20 paths [92].

Since the successive shadow fading samples are spatially correlated the L3 filtering period is influenced by the degree of correlation present in the signal. Therefore accurate modeling of spatial correlation is important for handover studies. In this study, the successive shadow fading samples are spatially correlated by using a negative exponential function (Gudmundson's model) [93]. The model for the spatial correlation, $R(k)$, is as

Table 6.3: Handover Specific Parameters

Parameter	Assumptions
Measurement bandwidth (BW_m)	1.25, 2.5, 5, 10 MHz
Hysteresis margin (H_m)	2, 4, 6 dB
Handover measurement period (T_m)	150 ms
Handover update period (T_u)	300, 3000 ms
Handover avoidance timer	1 s
Downlink measurement error	ON

defined in (6.6) where v represents UE speed, T is time sample, D is correlation distance and k is an integer [93].

$$R(k) = e^{\frac{-vT}{D}|k|} \tag{6.6}$$

In this study a handover avoidance timer of 1 s is used in the analysis. Since shadow fading samples are completely uncorrelated between sites, hence the ping-pong handovers can also be eliminated almost completely by L3 filtering if done over the sufficient filtering period depending on the user speed.

For the RSS and CIR measurements, the reference symbols are not explicitly modeled. The measurement at the reference symbol in a TTI is assumed to be highly correlated in both time and frequency domain and represented by a single measurement per PRB.

In LTE the intra-cell interference is principally zero. The interference on the PRBs a user is transmitting in a cell is generated by the users transmitting on the same PRBs in other cells. The received uplink Signal-to-Interference-plus-Noise Ratio (SINR) of a user at the serving eNode-B is calculated as a fraction of signal power received at the eNode-B over the total interference power plus thermal noise.

The closed loop power control adjusts the transmit power of the user depending on the received uplink SINR in order to match the SINR target. If the received uplink SINR at eNode-B is less than the SINR target, a power-up command is given to user. However, if the received uplink SINR at eNode-B is greater than the SINR target, a power-down command is given to user. The power control step-size is set to 1 dB, and the SINR target is set to 6 dB corresponding to 10% BLock Error Rate (BLER) for 16QAM modulation and coding rate of 1/2. In this study only the fixed Modulation and Coding Scheme (MCS) of 16QAM 1/2 is used. The power control used here represents a special case of standardized Fractional Power Control (FPC) for LTE as discussed in Section 2.7.1. The SINR target for all the users is fixed in the handover study, compared to the SINR targets for each user depending on the path loss compensation factor [38]. The power control up and down commands is similar to the power control methodology used for WCDMA system [79].

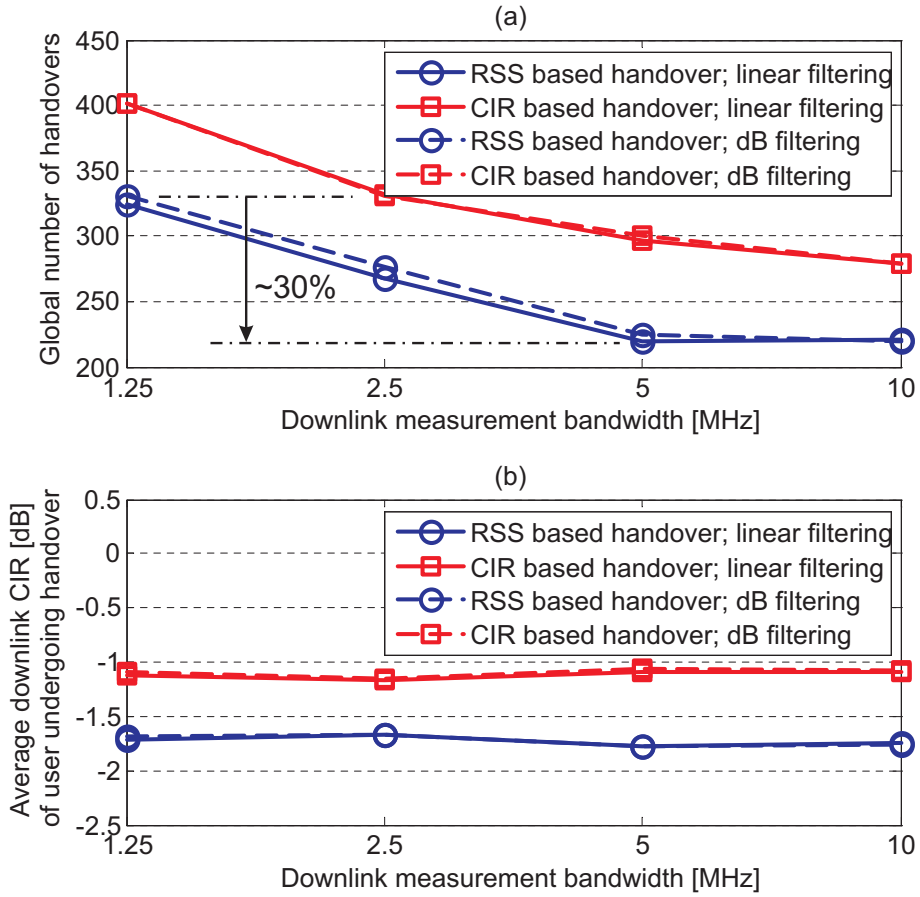

Figure 6.7: Handover performance based on RSS and CIR measurements, and linear and dB domain filtering for different measurement bandwidths. User speed = 3 kmph, $H_m = 2$ dB, $T_m = 150$ ms and $T_u = 300$ ms.

In this study the packet scheduling algorithm in ELIISE equally distributes the available PRBs among the users associated with the same sector [29]. The number of allocated PRBs per user changes only when the number of users in the cell changes due to handover. General simulation parameters listed in Table 6.2 are chosen according to the specifications and assumptions given in [14].

6.5 Performance Evaluation

The system performance evaluation is carried out in terms of number of handovers and average downlink CIR for the users undergoing handover for the parameters given in Table 6.3 [84]. All the results presented in this chapter take into account the effect of measurement error as described in Section 6.3.3.

Figure 6.7 and Figure 6.8 show the effect of handover based on RSS and CIR measurements, and linear and dB domain L3 filtering at 3 kmph and 120 kmph respectively.

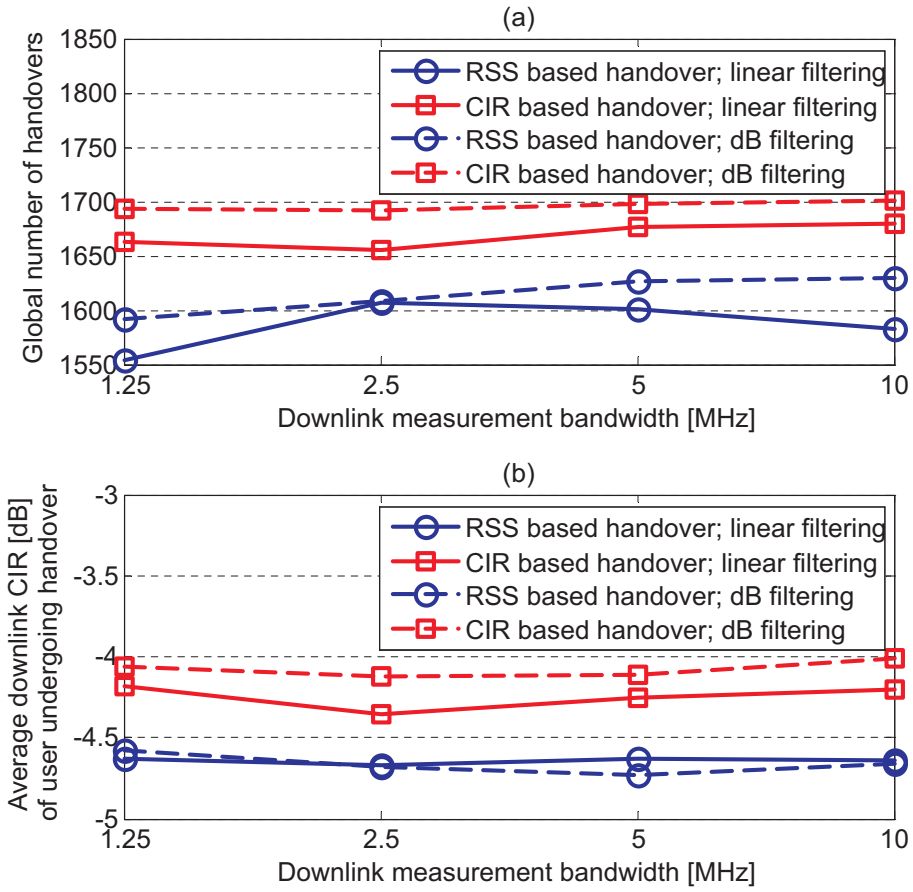

Figure 6.8: Handover performance based on RSS and CIR measurements, and linear and dB domain filtering for different measurement bandwidths. User speed = 120 kmph, $H_m = 2$ dB, $T_m = 150$ ms and $T_u = 300$ ms.

Since LTE supports scalable transmission bandwidth, the comparison is shown for the measurement bandwidth of 1.25, 2.5, 5, 10 MHz. The results show for both investigated user speeds that handover based on RSS measurement performs much better as compared to handover based on CIR measurement in terms of reduced number of handovers. At the same time the downlink CIR is higher for handover based on CIR measurement. The decrease in downlink CIR for RSS based handover is due to the delayed handover reporting and hence on average lower downlink CIR compared to CIR based handover. Moreover, for CIR based handover increase in number of handover will increase the signaling overhead and delay involved in handover execution. Hence, RSS is a better measurement quantity for handover in terms of number of handovers, and CIR is a better measurement in terms of the downlink CIR (signal quality) for the same values of H_m and T_u. Larger value of H_m and longer T_u can be used to decrease the number of handovers, but this would at the same time reduce the average downlink CIR and add to the delay in handover.

At low speed of 3 kmph, by increasing the downlink measurement bandwidth from 1.25 to 5 MHz around 30% decrease in average number of handover is noticed in Figure 6.7. This is due to the improved L1 filtering (frequency domain averaging) at higher

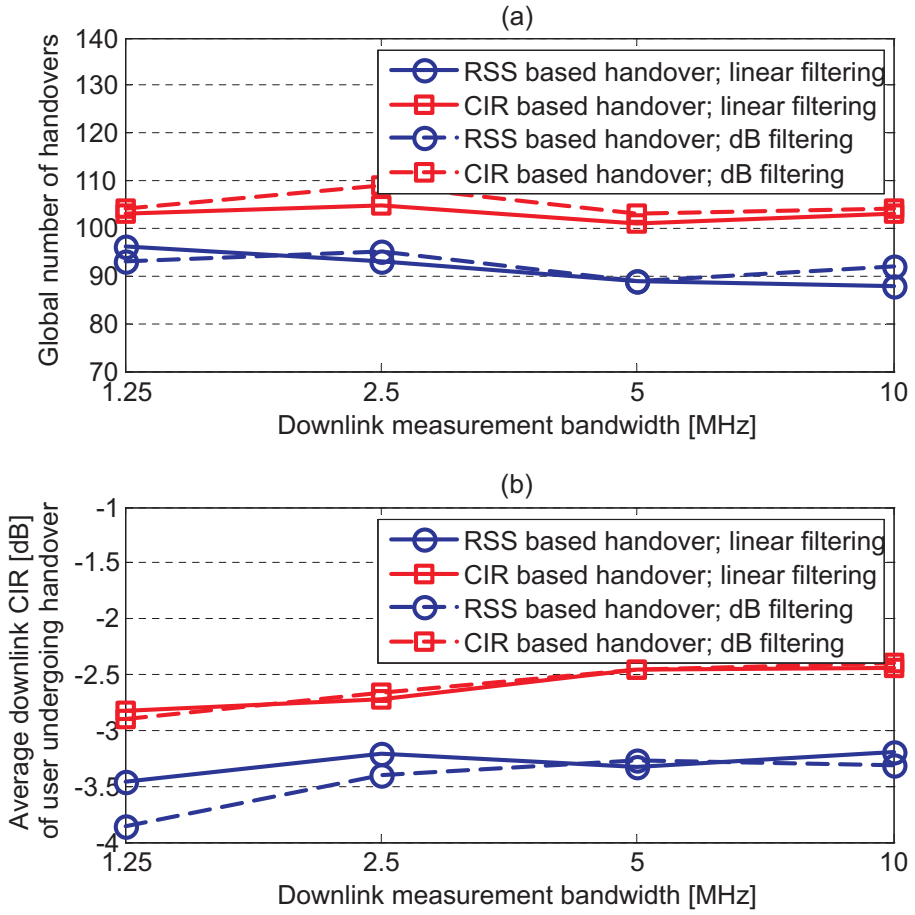

Figure 6.9: Handover performance based on RSS and CIR measurements, and linear and dB domain filtering for different measurement bandwidths. User speed = 3 kmph, $H_m = 2$ dB, $T_m = 150$ ms and $T_u = 3000$ ms.

bandwidth. While at high speed of 120 kmph there is a negligible change in number of handovers by increasing downlink measurement bandwidth as shown in Figure 6.8.

Figure 6.9 shows the effect of handover based on RSS and CIR measurements, and linear and dB domain L3 filtering for user speed of 3 kmph and $T_u = 3000$ ms. It shows that the gain in terms of lower number of handovers due to the use of larger measurement bandwidth at 3 kmph can also be achieved by using longer L3 filtering period as compared to Figure 6.7. This is due to the fact that log-normal shadowing samples are not highly correlated at high speed and hence require shorter filtering period as compared to the slow speed users which require longer filtering period. For longer filtering period of 3000 ms the number of handovers is halved for a penalty of around 2 dB on the downlink CIR. Hence for a proper choice of filtering period, depending on the user speed, the gain for using larger measurement bandwidth can be made negligible for a penalty on downlink CIR.

For CIR based handover at 3 kmph linear and dB domain filtering perform almost exactly the same in Figure 6.7. While for RSS based handover at 3 kmph and 1.25 MHz

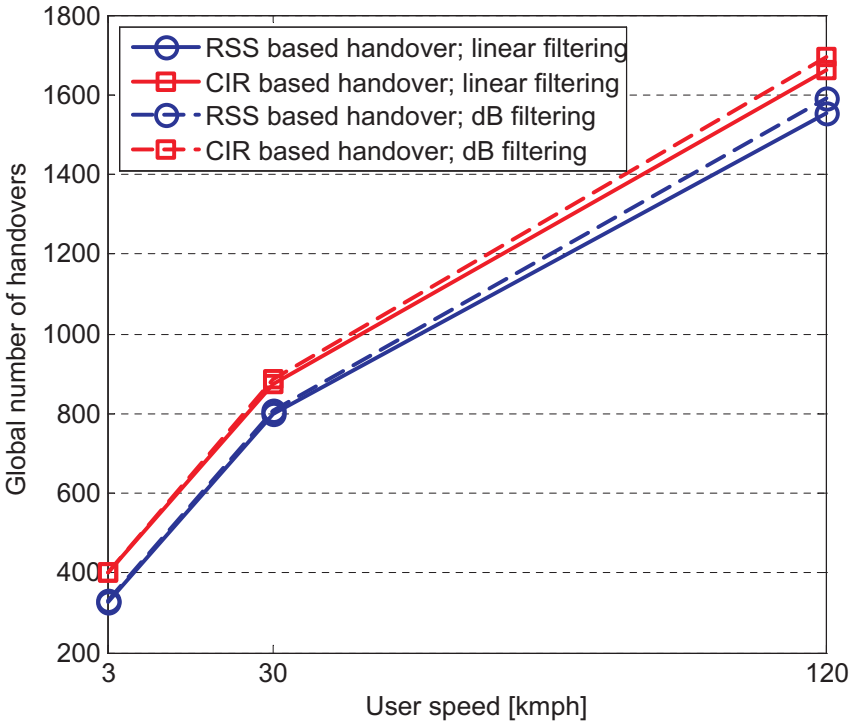

Figure 6.10: Handover based on RSS and CIR measurements vs. user speed at 1.25 MHz measurement bandwidth for $H_m = 2$ dB and $T_u = 300$ ms.

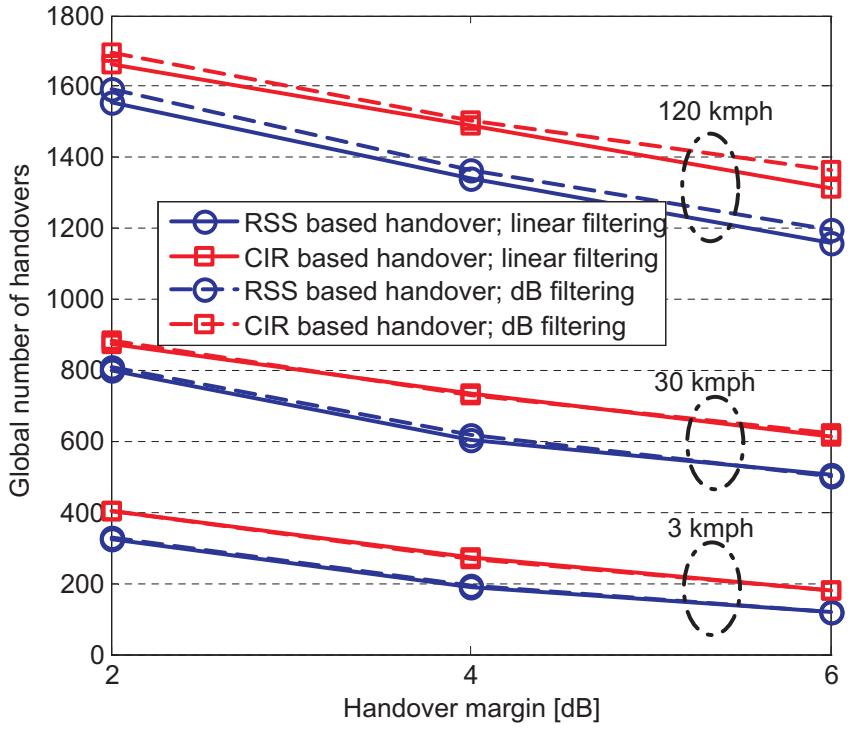

Figure 6.11: Handover based on RSS and CIR measurements vs. handover margin for different user speeds at 1.25 MHz measurement bandwidth for $H_m = 2$ dB and $T_u = 300$ ms.

measurement bandwidth, linear filtering gives a small reduction in number of handovers for a negligible change in downlink CIR. The benefit of using linear filtering becomes more prominent at a speed of 120 kmph in terms of number of handovers and a small penalty in downlink CIR as seen in Figure 6.8.

Figure 6.10 shows the number of handovers for RSS and CIR measurement based handover and linear and dB domain L3 filtering for different user speeds. It is noticed that both the linear and dB domain L3 filtering perform rather closely in terms of number of handovers, and the performance of linear domain filtering in terms of number of handovers is a little bit better at higher speeds.

Figure 6.11 shows the effect of different handover margins on the linear and dB domain L3 filtering for handover based on RSS and CIR measurements. It is noticed that linear and dB domain L3 filtering gives almost no difference in the performance in terms of the number of handovers at different handover margins. Hence, the performance difference in the scale of L3 filtering used is only due to the increasing UE speed, and it is not sensitive to the handover margin.

6.6 Conclusions

A handover algorithm based on the downlink RSS and CIR measurements, along with linear and dB domain L3 filtering has been studied. The handover measurement error is modeled and is added to the frequency averaged RSS and CIR measurements before L3 filtering. The results suggest that handover based on RSS measurement performs better than handover based on CIR measurement in terms of reduced number of handovers and around 0.5 dB penalty on the downlink CIR. Moreover, linear and dB domain L3 filtering is shown to perform closely in terms of number of handovers and average downlink CIR. Furthermore, L3 filtering is standardized to be performed in the same domain as measurement or reporting is done i.e. dB domain filtering for measurements in dB [94].

The effect of measurement bandwidth on the handover performance has been evaluated. The results show that the use of larger measurement bandwidth makes significant improvement in the performance in terms of number of handovers in the low Doppler environments e.g. 30% less number of handovers for user speed of 3 kmph. However, with the high Doppler shift, larger measurement bandwidth does not provide any significant performance gain in terms of number of handovers. Further, it is noticed that for an adaptive choice of filtering period, depending on the user speed, the gain for using larger measurement bandwidth can be made negligible for a penalty on signal quality. Hence, it is recommended to use 1.25 MHz of measurement bandwidth for a good choice of L3 filtering period. The scalable bandwidth of 1.25, 2.5, 5, 10 MHz signifying 6, 12, 25, 50 PRBs respectively [14] is assumed, which fit rather well to the finally agreed 3GPP LTE bandwidth of 1.4, 3, 5, 10 MHz signifying 6, 15, 25, 50 PRBs respectively [11]. Hence, the conclusions will remain the same for the latest bandwidth recommendation since the number of PRBs used for 1.4 MHz is same as for 1.25 MHz. The findings of this study have been published in [59].

Chapter 7

Evaluation of Hard Handover Based on RSRP Measurement

7.1 Introduction

The Reference Signal Received Power (RSRP) is standardized as a downlink handover measurement for LTE [18]. RSRP is defined for a considered cell as the linear average over the power contributions of the resource elements that carry the cell-specific reference signals within the considered measurement frequency bandwidth [95]. If receiver diversity is in use by the User Equipment (UE), the RSRP will be equal to the linear average of the power values of all diversity branches. The analogous handover measurement for RSRP in GSM and UMTS are Received Signal Strength Indicator (RSSI) and Received Signal Code Power (RSCP) respectively [96][79]. Among these technologies GSM uses hard handover while UMTS uses soft handover. In [97] performance of handover parameters such as margin and averaging window for the Received Signal Strength (RSS) based hard handover for GSM network is studied. In [98] an adaptive RSS based handover algorithm to adaptively control the averaging interval based on the user speed is studied.

To the best of our knowledge, effect of handover parameters on different Key Performance Indicators (KPIs) in LTE for a realistic scenario has no extensive studies in the open literature. Hence, the target of this chapter is to evaluate the performance of a RSRP based hard handover algorithm for parameters such as measurement bandwidth, handover margin and measurement period at different users speeds based on the parameters described in [14]. The KPIs chosen to evaluate this study are number of handovers, time between two consecutive handovers and uplink Signal-to-Interference-plus-Noise Ratio (SINR) for users about to experience the handover.

This chapter is organized as follows: In Section 7.2, a realistic intra-LTE hard handover algorithm based on RSRP measurement is analyzed and a modification is proposed. Another algorithm based on Average Path Gain (APG) is used as a baseline reference. The APG is calculated assuming no fast fading effect while RSRP measurement includes

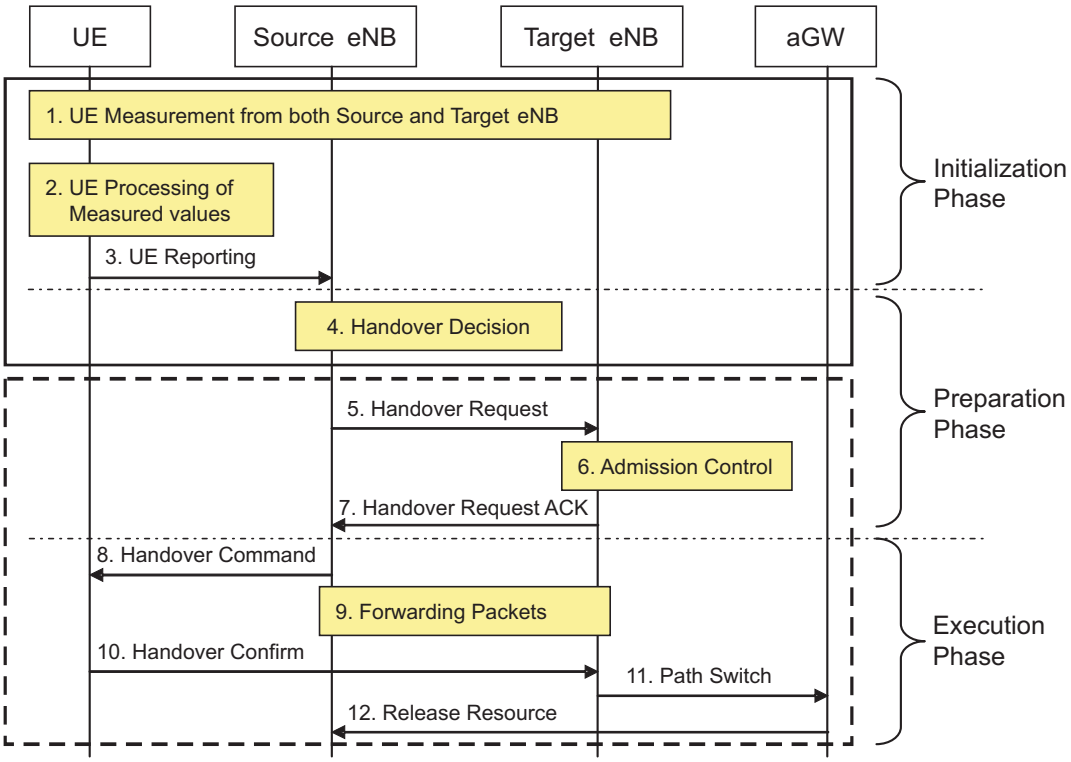

Figure 7.1: The different phases of an intra-LTE hard handover process

the fast fading effect. For algorithm based on RSRP measurement, a realistic estimate of measurement imperfection due to the limited number of reference symbols is modeled and added to the RSRP measurements before the processing. These algorithms are verified and evaluated using Efficient Layer II Simulator for E-UTRAN (ELIISE). In Section 7.3, simulation results are discussed and Section 7.4 contains the concluding remarks.

7.2 Handover in LTE

Figure 7.1 illustrates the different phases of an intra-LTE hard handover process. The enclosures within the solid box including handover measurement, processing and decision are the focus of this chapter. Handover measurements are channel measurements usually in downlink, which are processed in the UE. Processing is done to filter out the effect of fast-fading and Layer 1 (physical layer) (L1) measurement/estimation imperfections. These processed measurements are reported back to the eNode-B in a periodic or event based manner. Hence a handover is initiated based on the processed handover measurements and if certain decision criteria are met then the target cell becomes the serving cell performing the network procedures with the assistance of the UE [73]. The enclosures within the dashed box including signaling, Admission Control (AC), packet forwarding, and path switching in Figure 7.1 are out of the scope of this chapter.

In the following section a Average Path Gain (APG) based handover as a baseline reference, followed by the analysis of a realistic handover algorithm based on RSRP measurement. Further, a modification to RSRP based handover to further reduce the number of handovers is proposed.

7.2.1 APG Based Handover

In this algorithm the UE is assumed to have the APG from each cell[1] which includes path loss, antenna gain, and log-normal shadowing. This algorithm excludes fast fading effect which mean it assumes ideal fast fading filtering. If condition given in (7.1) is true, where H_m is handover margin (in dB), handover is executed and the target cell becomes the serving cell. The target cell (TC) is defined as the cell in the network from which the UE experiences maximum APG, excluding the serving cell (SC).

$$APG_{TC} \geq APG_{SC} + H_m \text{ [dB]} \tag{7.1}$$

7.2.2 RSRP Based Handover

In this algorithm the UE measures the $RSRP$ which includes path loss, antenna gain, log-normal shadowing and fast fading averaged over all the reference symbols (pilot) within measurement bandwidth BW_m. The filtered RSRP, $\overline{RSRP}$, is measured every handover measurement period (T_m) at the UE as the output of a first order Infinite Impulse Response (IIR) filter as defined in (7.2). The relative influence on $\overline{RSRP}$ of the recent measurement and older measurements is controlled by the forgetting factor β. In this study β is chosen depending on the handover decision update period (T_u) and T_m as $\beta = T_m/T_u$, where T_u is an integer multiple of T_m. The L3 filtering is done in linear domain, hence the RSRP measurement is also taken in linear domain. The RSRP measurement on downlink reference signal structure and its processing for LTE is schematically shown in Figure 7.2.

$$\overline{RSRP}[nT_m] = \beta \cdot RSRP[nT_m] + (1-\beta) \cdot \overline{RSRP}\,[(n-1)\,T_m] \tag{7.2}$$

The limited number of reference symbols available in a handover measurement bandwidth for $RSRP$ measurement introduces measurement error. This error is modeled as normally distributed in dB (log-normal) with mean zero and standard deviation σ dB as defined in (7.3) [89]. This measurement error in linear domain is multiplied to each $RSRP$ measurement before the filtering in (7.2). For smaller measurement bandwidth (i.e. lower number of reference symbols) larger error level are expected, as compared to the larger measurement bandwidth (i.e. higher number of reference symbols) as shown in Section 6.3.3.

$$\Delta RSRP \sim 10^{N(0,\sigma^2)} \tag{7.3}$$

[1]Terms cell and sector are used interchangeably with the same meaning.

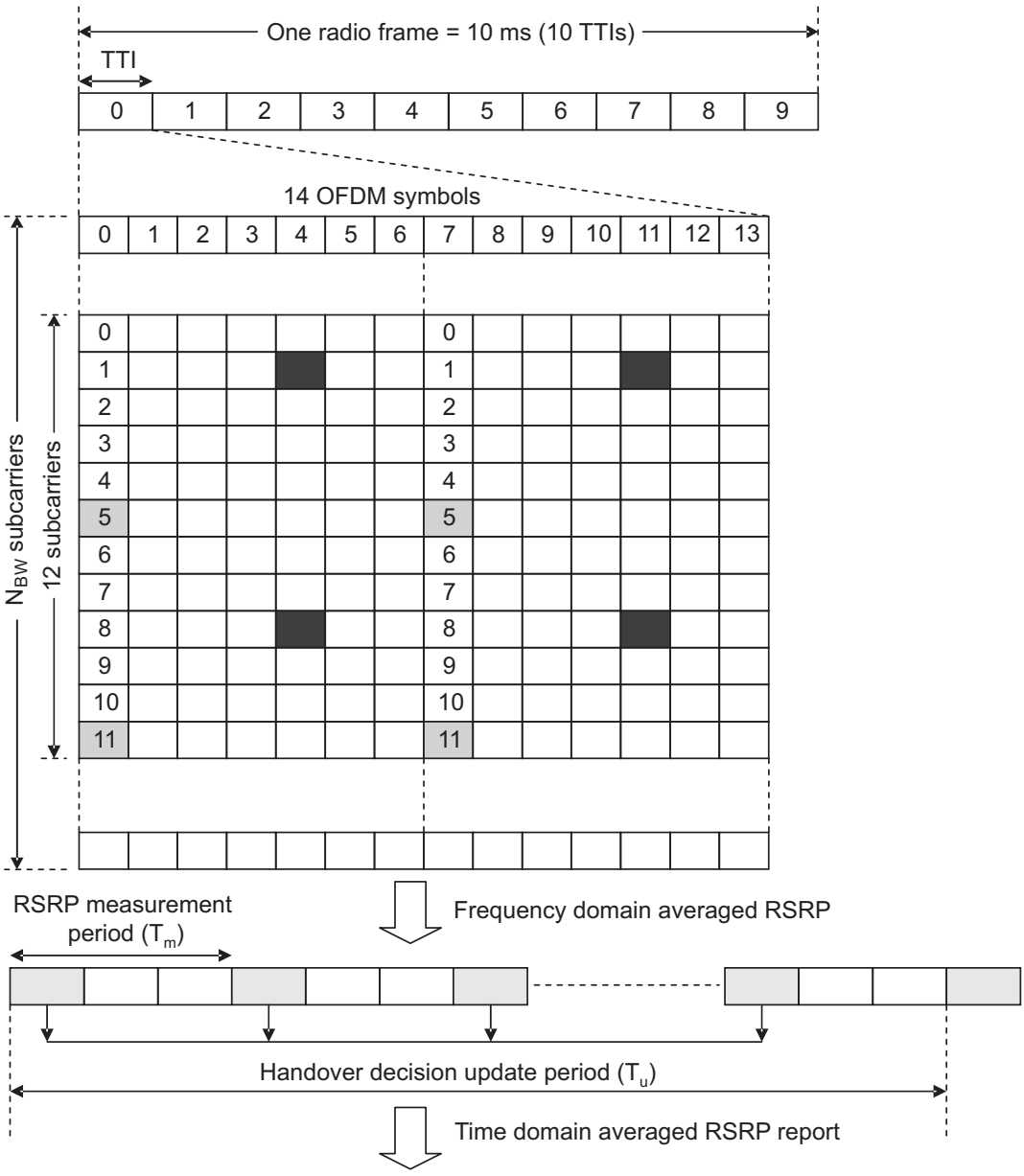

Figure 7.2: Summary of RSRP measurement at reference symbols, and frequency and time domain averaging

The handover decision is based on the $\overline{RSRP}$ and is executed if the condition in (7.4) is satisfied. The RSRP based handover process is summarized in Figure 7.3.

$$\overline{RSRP}_{TC}[nT_u] \geq \overline{RSRP}_{SC}[nT_u] + H_m \text{ [dB]} \tag{7.4}$$

7.2.3 RSRP Based Handover with Time-to-Trigger Window

This algorithm is similar to the RSRP based handover algorithm except that the handover is initiated if the same cell remains the potential target cell for a certain number of time

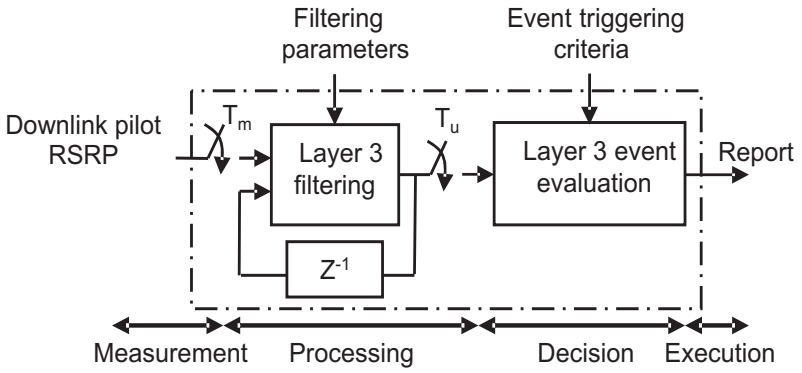

Figure 7.3: L3 filtering of frequency averaged RSRP measurement [79]

windows. The handover trigger is defined in terms of Time-to-Trigger (TTT) window size. Each TTT window is equivalent to T_u. Let us assume that the Id_{TC} and Id_{SC} are the memory queues of target and serving cell identifications respectively, each of TTT window size, while id_{TC} and id_{SC} are the target and serving cell identities. The pseudo code of the proposed algorithm using stack push operation is as follows:

1. INITIALIZE Id_{TC}, Id_{SC}

2. IF (7.4) is true

   Id_{TC}.push(id_{TC})

   ELSE

   Id_{SC}.push(id_{SC})

3. IF $Id_{TC}[i] \neq Id_{SC}[i]$ and $Id_{TC}[i]$ = $Id_{TC}[j]$

   for all i, $j \in$ TTT window size, $j \neq i$

   EXECUTE handover

RSRP based handover algorithm with n TTT window size will be represented as RSRP$_n$ based handover, with a subscript n. RSRP based handover in Section 7.2.2 is a special case of this algorithm with TTT window size of 1 i.e. RSRP$_1$ based handover.

Introducing TTT window is one way to suppress the number of unnecessary handovers called ping-pong handovers. The ping-pong handover is defined as a handover to one of the neighboring cell that returns to the original cell after a short time. Each handover requires network resources to re-route the call to the new eNode-B. Thus, minimizing the expected number of handovers minimizes the signaling overhead. Another solution to reduce the number of handovers is to introduce a handover avoidance timer which allows handover only after the timer expires. The trade off between number of handovers and

Table 7.1: Handover Specific Parameters

Parameter	Assumptions
Measurement bandwidth (BW_m)	1.25, 2.5, 5, 10 MHz
Hysteresis margin (H_m)	0, 2, 4, 6, 8, 10 dB
Handover measurement period (T_m)	3, 50, 150, 300 ms
Handover update period (T_u)	300 ms
Handover avoidance timer	1 s

signaling overhead is out of scope of this study.

7.3 Performance Evaluation

ELIISE – a multi-cell, multi-user, dynamic system level simulation described in Section 6.4 is used to evaluate the performance of hard handover based on RSRP measurement for the handover simulation parameters listed in Table 7.1. The system performance is measured using the following KPIs: number of handovers per UE per second, time between two consecutive handovers and uplink SINR of UEs having a potential target sector. For UEs having a potential target sector means the UEs which will make a handover within next one TTT window (T_u).

Figure 7.4 (a) shows the effect of varying downlink measurement bandwidth for the RSRP based handover at user speed of 3 kmph on average number of handovers and average uplink SINR with measurement error. Increasing the measurement bandwidth from 1.25 to 10 MHz a decrease in average number of handovers for a negligible change in average uplink SINR of the UEs with a potential target sector is noticed. This is because larger measurement bandwidth means improved frequency domain averaging of fast fading.

Figure 7.4 (b) shows the effect of varying downlink measurement bandwidth for the RSRP based handover at user speed of 3 kmph on average number of handovers and average uplink SINR without measurement error. Comparing Figure 7.4 (a) and (b), it is noticed that in the case with RSRP measurement error, the increase in average number of handovers is relatively larger at 1.25 MHz compared to at 10 MHz. This is because of the reduced error standard deviation for increased measurement bandwidth. The increased number of handovers would lead to an increased average uplink SINR. This is due to the fact that increased number of handovers lead a user to be connected to a better cell with higher probability, which in turn increases the signaling between the serving and target cell due to negotiation and data forwarding. Hence the average number of handovers and average uplink SINR are sensitive to the RSRP measurement error at 3 kmph. The sensitivity decreases in terms of number of handovers and uplink SINR with increasing measurement bandwidth. We expect that at higher speeds the chosen KPIs will be lesser

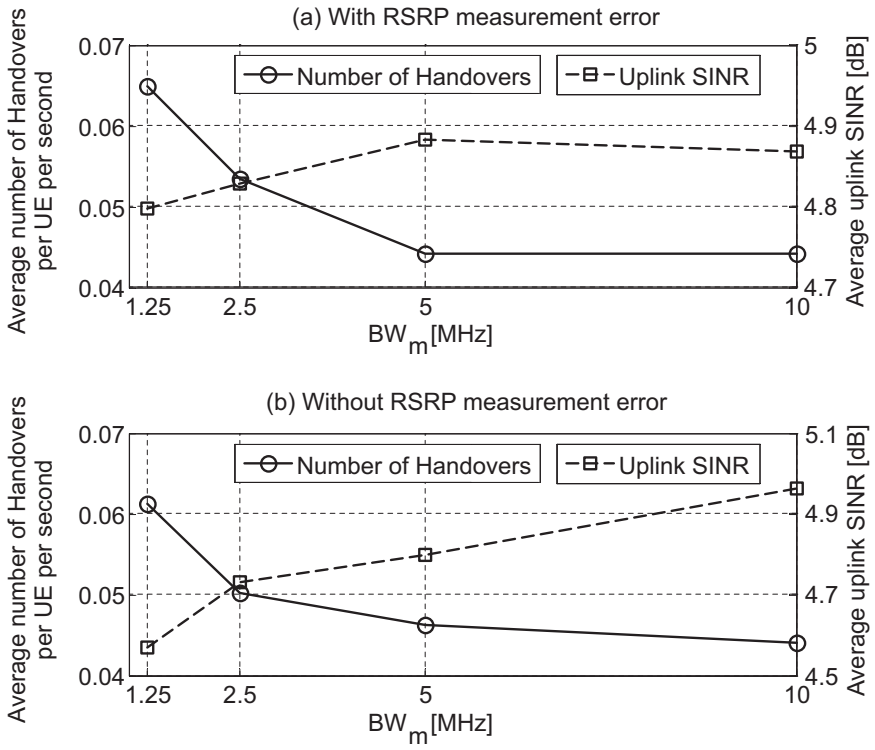

Figure 7.4: Effect of varying measurement bandwidth (BW_m) for the RSRP based handover at user speed of 3 kmph on average number of handovers per UE per second and average uplink SINR. $H_m = 2$ dB and $T_m = 150$ ms.

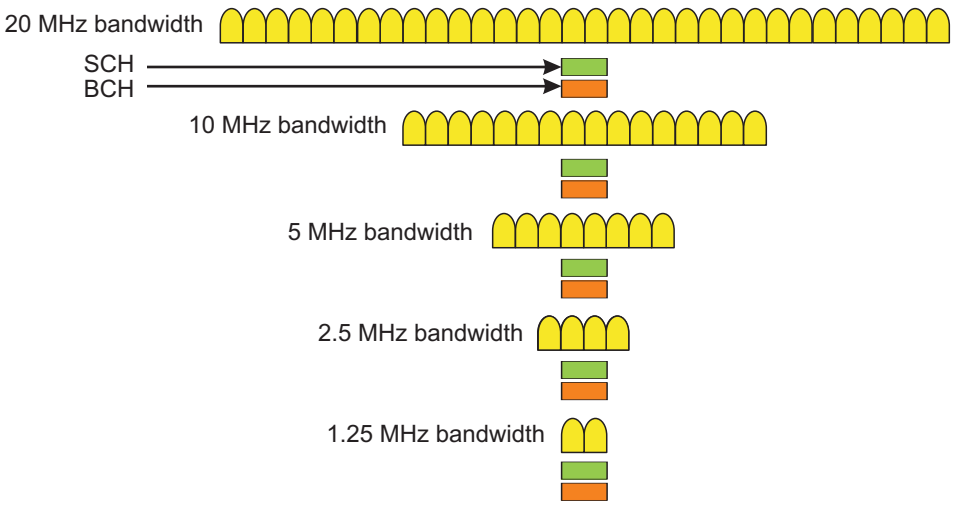

Figure 7.5: Frequency allocation of the downlink SCH and BCH. Independent of the overall transmission bandwidth, the SCH and BCH are defined for 1.25 MHz and centered in the middle of the overall transmission bandwidth [14].

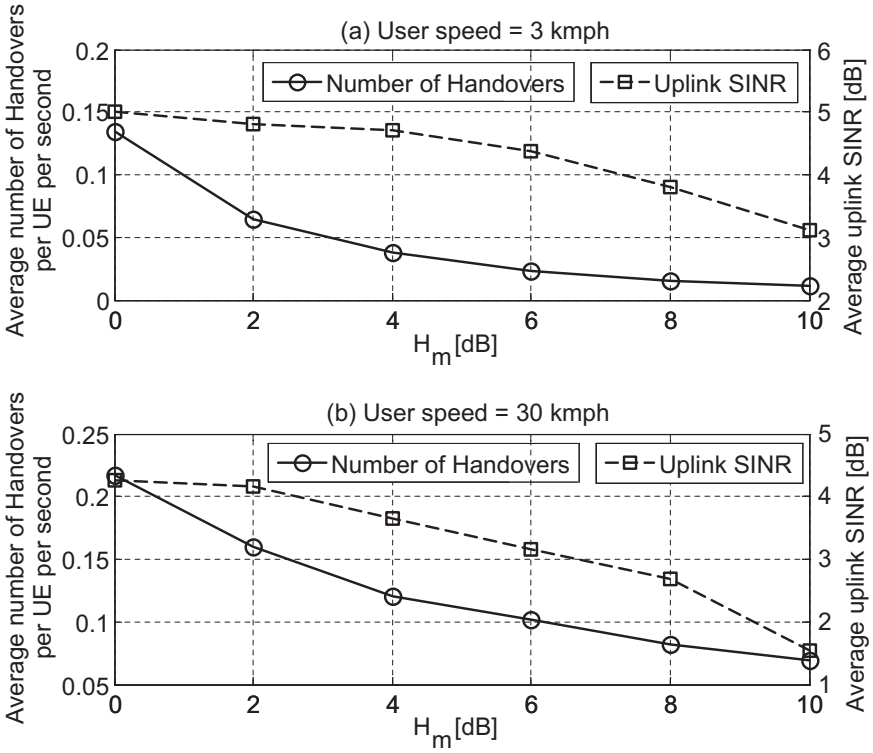

Figure 7.6: Effect of varying H_m for the RSRP based handover on average number of handovers and average uplink SINR at the user speeds of 3 and 30 kmph. $BW_m = 1.25$ MHz and $T_m = 150$ ms.

sensitive to measurement error because of larger variations in channel condition. The sensitivity due to measurement error can be reduced by reducing the forgetting factor of L3 filter. Rest of the simulations in this study are run with RSRP measurement error.

Although there is a performance gain in using 10 MHz of measurement bandwidth similar average uplink SINR performance is seen to be attained using 1.25 MHz as in Figure 7.4. Moreover, in situations when different cells are operating at different transmission bandwidths, one possibility is to limit the measurement bandwidth to some well defined fixed value. One suggestion is to limit to the constant bandwidth of 1.25 MHz i.e., center 72 subcarriers, that is occupied by the control channels, Synchronization Channel (SCH) and Broadcast Channel (BCH), used for handover procedures in LTE regardless of the scalable overall transmission bandwidth of 1.25 MHz to 20 MHz as illustrated in Figure 7.5. This will speed up the measurement process in a sense that UE does not need to know the actual bandwidth of the cell. Hence, rest of the simulations in this study assume $BW_m = 1.25$ MHz. The measurement bandwidth can also be set by the network over which UE should measure the neighbor cells assuming network is aware of the deployment scenario. For example the network can signal the measurement bandwidth as the minimum of the cells' bandwidth deployed in a coverage area. The measurement bandwidth can vary from one coverage area to another depending on the cell transmission bandwidth used in an area [99].

Figure 7.6 shows the effect of varying H_m for the RSRP based handover at user speeds

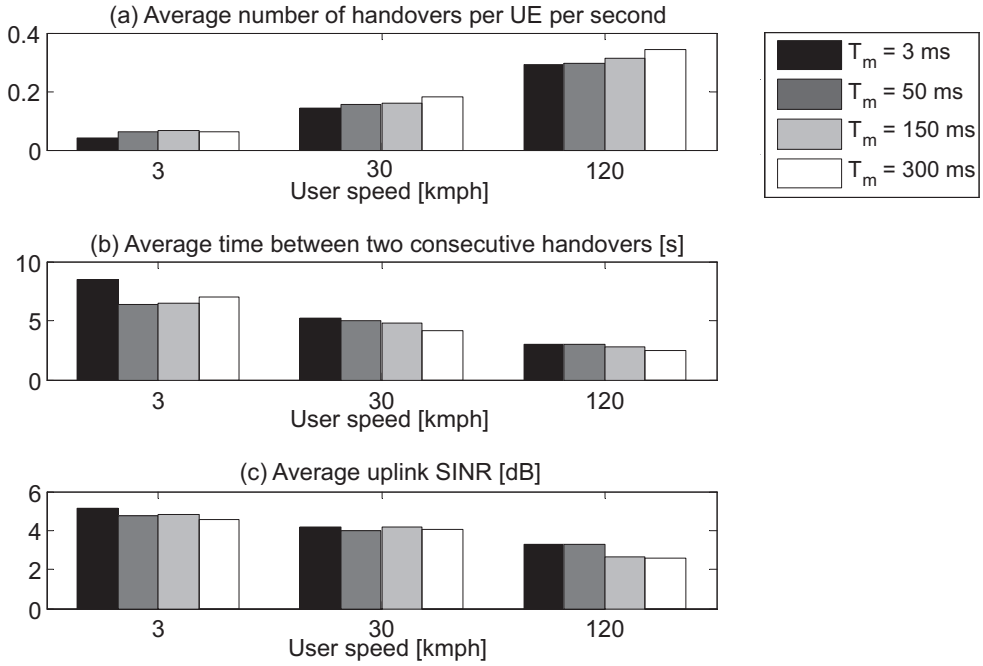

Figure 7.7: Effect of varying T_m and user speeds for the RSRP based handover on different KPIs: (a) Average number of handovers per UE per second, (b) Average time between two consecutive handovers, (c) Average uplink SINR. $H_m = 2$ dB and $BW_m = 1.25$ MHz.

of 3 kmph and 30 kmph. We notice that at 3 kmph, going from H_m of 0 to 2 dB, leads to a significant decrease in average number of handovers per UE per second while there is a negligible decrease in average uplink SINR; from 2 to 6 dB there is a large decrease in average number of handovers per UE per second for about 0.5 dB decrease in average uplink SINR; from 6 to 10 dB there is a small decrease in average number of handovers per UE per second for about 1.3 dB decrease in average uplink SINR. We notice similar trends at 30 kmph in Figure 7.6 (b). Gain in reduction of the average number of handovers will decrease at higher speeds since log-normal shadowing samples are not highly correlated at higher speeds over the handover decision update period. On an average, uplink SINR is lower at higher speeds since power control is slow and it is unable to track the changing channel conditions. The reduction in number of handovers per UE per second is one of the desired criteria but at the same time it also leads to the reduction of average uplink SINR, which is not desired. For these reasons we choose to use the range of H_m for which there is a penalty on uplink SINR within 0.5 dB. Hence we recommend H_m of 2 to 6 dB at 3 kmph and 2 to 4 dB at 30 kmph depending on the design tradeoff required between number of handovers and average uplink SINR of the UEs with a potential target sector.

Figure 7.7 shows the effect of varying measurement update period and user speed for the RSRP based handover on different KPIs. Increasing the measurement update period we notice, that average number of handovers per UE per second increases, which results in a decrease of average time between two consecutive handovers for a negligible penalty on average uplink SINR. Though there is a benefit in using shorter measurement update period, it will lead to increase in signaling overhead and processing at the UE as compared to larger update periods. Hence even a single measurement that is $T_m = T_u = 300$ ms

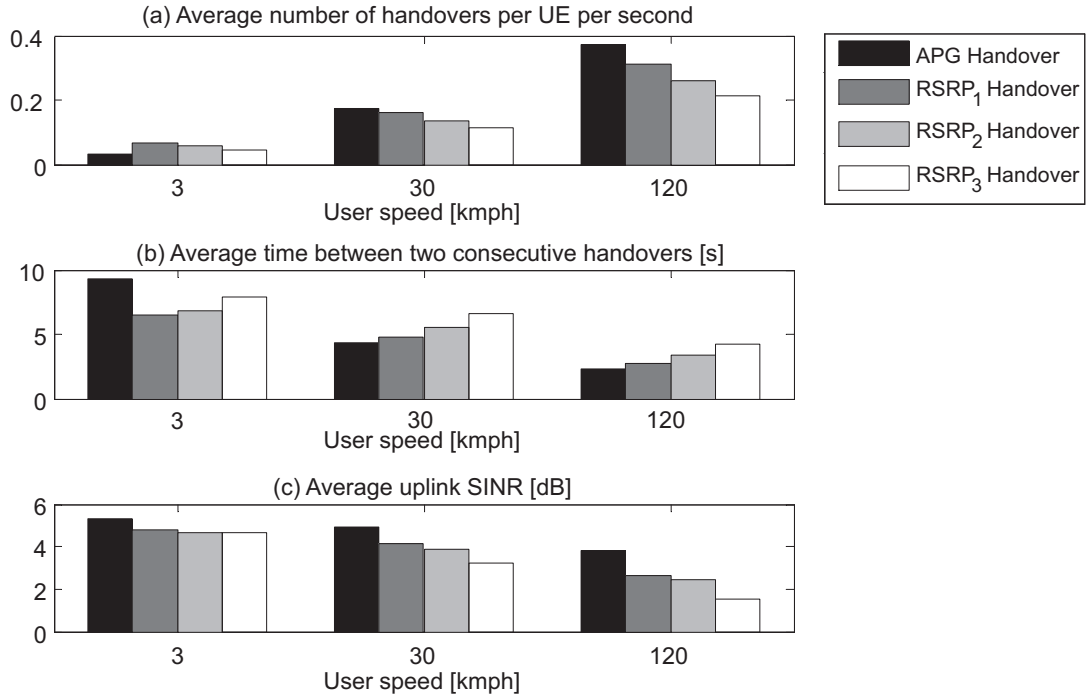

Figure 7.8: Effect of different handover algorithms and user speeds on different KPIs: (a) Average number of handovers per UE per second, (b) Average time between two consecutive handovers, (c) Average uplink SINR. $H_m = 2$ dB, $BW_m = 1.25$ MHz and $T_m = 150$ ms.

should be enough to take the handover decision without any noticeable impact on the performance of UEs experiencing handover. This is because of the diversity gain from the dual antenna MRC at the UE receiver.

Figure 7.8 shows the effect of different handover algorithms and user speeds on different KPIs. It is observed that increasing the TTT window size for RSRP based handover, average number of handovers per UE per second decreases while average time between two consecutive handovers increases. At the same time we notice a penalty in the form of reduced average uplink SINR. Increasing TTT window is a way to reduce the number of ping-pong handovers. At higher speeds there are higher number of ping-pong handovers due to lower correlation in log-normal shadowing samples over the handover decision update period. Hence, the reduction in number of handovers is more pronounced at higher speeds.

7.4 Conclusions

In this chapter, a hard handover algorithm based on the downlink RSRP measurement for LTE is studied. The handover measurement error model is multiplied to the frequency averaged RSRP measurement before L3 filtering in linear domain. Further, a modification in RSRP based algorithm with TTT window is proposed. The RSRP based handover algorithm with TTT window is shown to reduce the average number of handovers with

increasing TTT window size while decreasing the average uplink SINR. Moreover, effect due to handover measurement bandwidth, margin and measurement update period is analyzed for different KPIs and user speeds. For the parameter set studied, use of 1.25 MHz of measurement bandwidth, a 2 to 4 dB of handover margin and 300 ms of measurement update period is recommended for user speeds of 3 to 120 kmph. The findings of this study have been published in [84].

Chapter 8

Overall Conclusions and Recommendations

The goal of this thesis has been to study the uplink Radio Resource Management (RRM) issues for QoS provisioning in Long Term Evolution (LTE). The thesis is divided into two parts. In the first part the problem of QoS provisioning in uplink using Admission Control (AC) and Packet Scheduler (PS) is studied and new algorithms have been derived. The proposed AC and PS algorithms are analyzed at the system level taking into account the realistic model of fast Link Adaptation (LA) by means of Adaptive Modulation and Coding (AMC) and Fractional Power Control (FPC), Hybrid Automatic Repeat reQuest (HARQ), Adaptive Transmission Bandwidth (ATB), and Outer Loop Link Adaptation (OLLA). The performance analysis is done using a semi-static system level simulator. The analytical modeling, implementation, and testing of proposed AC, Poisson arrival, QoS aware PS metrics, Constant Bit Rate (CBR) streaming traffic etc. in the semi-static simulator is carried out as part of the PhD study. In the second part performance evaluation of intra-frequency hard handover is analyzed. The performance results are generated using a dynamic system level simulator – Efficient Layer II Simulator for E-UTRAN (ELIISE) which is co-developed to study the mobility issues.

In the following sections, a summary of the whole thesis is given, drawing the main findings from the most relevant topics investigated. Finally, some outlook regarding the future work is given.

8.1 Admission Control and Packet Scheduler design

One of the main contributions of this thesis is the derivation of a closed-form solution of an uplink AC algorithm utilizing the FPC formula agreed in 3GPP for LTE. The FPC based AC determines if a user requesting admission can be accepted based on the average path gain so as to fulfill the QoS of the new and existing users. To compare the performance of the FPC based AC, a capacity based reference AC algorithm with R_{max}

parameter is proposed. In this study Guaranteed Bit Rate (GBR) is considered as the main QoS parameter. The admitted users in a cell uses a decoupled Time-Domain (TD) and Frequency-Domain (FD) PS. In Chapter 3, the FPC based AC algorithm is analyzed with a GBR aware TDPS and PF-scheduled FDPS metrics allocating fixed transmission bandwidth to users in a single GBR scenario. The results show that FPC based AC performs best in terms of outage probability and unsatisfied user probability among the studied algorithms. At 10% of unsatisfied user probability, the FPC based AC can support 5.5% more carried traffic, and 7.5% more offered traffic over the reference AC - 5 Mbps for Macro Case 1. Moreover, the average number of users for the FPC based AC is close to reference AC - 5 Mbps for Macro Case 1, while it is close to reference AC - 2 Mbps for Macro Case 3. Moreover, the R_{max} value for reference AC is sensitive to the propagation scenario and hence need to be tuned. In contrast the FPC based AC algorithm is robust as it tunes itself inherently to the load conditions and is recommended as a practical QoS-aware AC algorithm for LTE uplink.

In Chapter 4, the TDPS and FDPS metrics are proposed to fulfill the respective QoS requirements of different user classes in a mixed traffic scenario of admitted users. In this chapter users are scheduled using a ATB based PS according to the proposed FDPS metric. It is shown that FPC based AC along with proposed GBR aware TDPS and GBR weighted FDPS are able to effectively differentiate especially in the case of a mixed traffic scenario with relatively high difference in the GBR requirements for example in a mixed GBR scenario of 64 kbps and 1000 kbps. Additionally, in a mixed GBR scenario the FPC based AC is shown to block the users with a very low path gain, and fulfill the required GBR of admitted users with a near 0% outage probability. The reference AC, unlike FPC based AC, admits a user irrespective of its channel condition and very low path gain bearers are eventually served with a significantly higher outage probability. Further, FPC based AC is shown to automatically adjusts to the traffic mixes, cell load, and user channel conditions. Hence, the proposed combined AC and PS framework is necessary for effective QoS provisioning and differentiation in a mixed GBR scenario.

In Chapter 5, the FPC based AC algorithm is generalized to take into account the source activity factor for a realistic ON/OFF traffic. The proposed AC algorithm is analyzed for CBR streaming traffic for single and mixed GBR settings, as well as for an ON/OFF traffic with single GBR setting and deterministic ON and OFF durations. The modified AC algorithm is shown to perform best in terms of outage probability and unsatisfied user probability as well as carried traffic in terms of average number of users per cell.

8.2 Handover design

In the second part of the thesis, an intra-frequency hard handover based on downlink channel measurements for LTE has been studied. The proper choice of channel measurement quantity for handover has an important impact on the performance of users undergoing handover. The handover measurements studied in Chapter 6 are the downlink Received

Signal Strength (RSS) and Carrier to Interference Ratio (CIR) measurements. These measurements are linearly averaged in frequency domain and then averaged in time domain using a L3 filter in linear or logarithmic domain. The handover measurement error is modeled and is added to the frequency averaged RSS and CIR measurements before L3 filtering. The results suggest that handover based on RSS measurement reduces the number of handovers by around 17% compared to the handover based on CIR measurement for around 0.5 dB penalty on the downlink CIR. Moreover, linear and dB domain L3 filtering is shown to perform closely in terms of number of handovers and average downlink CIR. In LTE, RSS measurement at reference symbols is standardized as Reference Signal Received Power (RSRP) [18].

In addition, the effect of measurement bandwidth on the handover performance is evaluated. It is shown that the use of larger measurement bandwidth makes significant improvement in the performance in terms of number of handovers in the low Doppler environments. For example at 3 kmph by increasing the measurement bandwidth from 1.25 to 5 MHz a decrease of 30% in average number of handovers is noticed. Although higher measurement bandwidth provide performance gain but in situations when different cells are operating at different transmission bandwidth an idea is to limit the measurement bandwidth to a well defined fixed value. Additionally, with the high Doppler shift, larger measurement bandwidth does not provide any significant performance gain in terms of number of handovers. Further, it is noticed that for an adaptive choice of filtering period, depending on the user speed, the gain for using larger measurement bandwidth can be made negligible for a penalty on signal quality. Hence, it is recommended to use 1.25 MHz of measurement bandwidth for a good choice of L3 filtering period.

In Chapter 7, the hard handover algorithm based on the downlink RSRP measurement for LTE is analyzed. The measurement error is modeled and is taken into account for the RSRP based handover. In addition, a modification in RSRP based algorithm with Time-to-Trigger (TTT) window is proposed. This algorithm is shown to reduce the average number of handovers with increasing TTT window size while decreasing the average uplink SINR. Moreover, effect due to handover measurement bandwidth, margin and measurement update period is analyzed for different KPIs and user speeds. It is recommended that handover margin between 2 to 4 dB and measurement update period of 300 ms gives best trade off between the number of handovers and signal quality for user speeds of 3 to 120 kmph.

8.3 Topics for Future Research

This study is done for delay tolerable data traffic, and the FPC based AC should be studied for delay sensitive ON/OFF traffic for example Voice over Internet Protocol (VoIP), which is one of the main interests to operators. In order to compensate for the delay budget requirement for the delay sensitive traffic some capacity (or bandwidth) need to be reserved. This is to accommodate for a situation when more than the average number of ON periods become active at the same time. In the case of FPC based AC the load safety parameter

can be used to control the number of unsatisfied delay sensitive users. This is especially the case when there is a very high percentage of delay sensitive traffic in the system. In the case of mixed delay sensitive GBR bearers and Non-GBR bearers, Non-GBR bearers can be delayed (or even dropped) to meet the QoS requirements of delay sensitive GBR bearers without the need of load safety parameter. Additionally, scheduling metrics should be modified to take into account the delay budget to prioritize the users to be allocated in time and frequency domain. Furthermore, the proposed AC framework to differentiate between mixed GBR and Non-GBR bearers need to be evaluated using scheduling which prioritizes GBR bearer over Non-GBR bearers.

Moreover, this study has assumed that the activity factor of the traffic source is fixed and is available during the QoS parameter setting by the Quality Class Identifier (QCI) table based on the service type. The procedure to set the activity factor using QCI table is not standardized. The use of fixed activity factor using QCI table may also not represent the real source activity factor since ON and OFF durations are usually randomly distributed. Therefore, it is important to investigate realistic methods to estimate the source activity factor.

In this thesis AC and handover is studied separately using semi-static and dynamic system simulators respectively. Since the proposed AC algorithm is useful for both new users and handover users, it would be quite interesting to study the proposed AC to study the performance of handover users. In a mobility scenario with both new and handover users requesting admission it is important to design a strategy such that handover users are blocked with negligible probability, and outage probability is negligible for all the admitted users. Further, load control issues for example if a user with high GBR requirement is accepted and it started moving towards the cell edge, it is possible that due to the user mobility more stationary low GBR requirement users are not accepted because of the increased resource requirements. Hence, it is important to study and design load control algorithms to maintain low unsatisfied user probability and high carried traffic.

Appendix A

Semi-Static System Level Simulator Description

This appendix describes the models used in the semi-static simulator used for performance assessment of the uplink framework combining AC and PS for QoS provisioning in Chapter 3, Chapter 4, and Chapter 5. This chapter is organized as follows: In Section A.1 the general description of the simulator including the network layout is presented. In Section A.2 and Section A.3 the Channel State Information (CSI) and OLLA is modeled respectively. In Section A.4 HARQ model used is presented. In Section A.5 the link-to-system performance mapping is detailed, while in Section A.6 the traffic model used are described. Finally, the Key Performance Indicators (KPIs) used to compare the performance are defined.

A.1 Semi-Static System Simulator

The semi-static system simulator consists of a detailed multi-cell deployment, based on the latest LTE guidelines [14]. The framework consists of a hexagonal regular grid cellular setup, where the center three cells are surrounded by the two tiers of cells, as shown in Figure A.1. There are nineteen cell sites in the simulation area, each consisting of three sectors per site, giving a total of fifty seven sectors. The orientation of the main lobes of directional sector antenna elements is indicated by arrows in Figure A.1. In order to avoid the drawback of limited network layout the wrap around techniques is employed.

A 3-sector network topology with 70 degrees half power beam width eNode-B is assumed for the Macro cell deployment. The propagation modeling consists of the path loss, shadowing and fast fading. The path loss model for the Macro cell case includes a 20 dB outdoor-to-indoor penetration loss. Fast fading is simulated according to the Typical Urban (TU) power delay profile for user speed of 3 kmph[92], which is a tapped delay line implementation with uncorrelated Rayleigh fading paths [100]. The users are created in the system according to a Poisson call arrival process. If the proposed AC decision

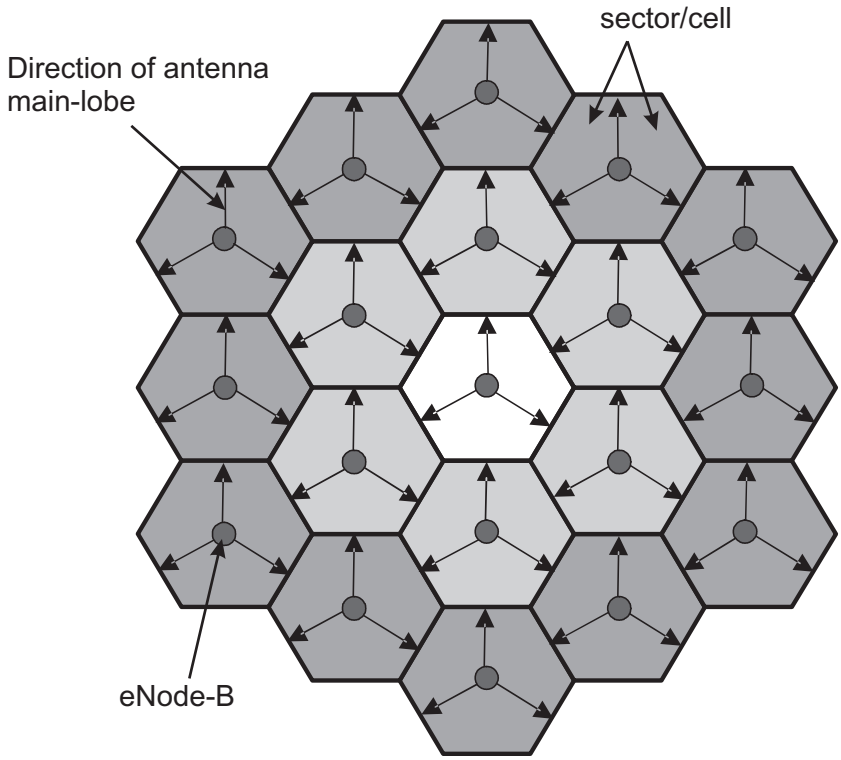

Figure A.1: The hexagonal regular grid cellular setup used in the system simulator according to the LTE guidelines [14][101].

criterion is fulfilled, the user is admitted otherwise the user is rejected or blocked. During a packet call the path loss and shadowing components are assumed to be constant for each user, while the fast fading is time-varying. Shadowing is fully correlated between cells of the same site, while the correlation is 0.5 between sites. The serving cell for a new user is selected according to the lowest total path loss including distance dependent path loss, shadowing, and effective antenna gains.

The RRM functionalities such as LA, PS, and HARQ are accurately modeled for all the sectors. The LA is modeled as fast AMC based on CSI. To maintain the BLER target in the first transmission OLLA offset is used to bias the CSI before using it for Modulation and Coding Scheme (MCS) selection. The PS is modeled as decoupled TD and FD scheduler as shown in Figure 2.7 including HARQ. The total number of PRBs used for the data transmission is 48, while 2 PRBs are reserved for control signaling transmission. The default simulation assumptions and parameters are listed in Table A.1.

A.2 Channel State Information Model

The LA selects the most suitable MCS based on Signal-to-Interference-plus-Noise Ratio (SINR) estimations over the allocated bandwidth [41]. Such estimations are obtained from the Sounding Reference Signal (SRS) transmitted by the user and used at the Evolved

Node B (eNode-B) to extract near-instantaneous frequency selective CSI. It is assumed that the CSI is available at the eNode-B every Transmission Time Interval (TTI) over the entire system bandwidth for all the active users with a given bandwidth resolution. The reference symbols are not explicitly modeled. The CSI of a user i on PRB k at time instant t is modeled as [41]:

$$CSI_{i,k}(t) = \sum_{r=1}^{M} \left(\frac{\sum_{j \in K} S^r_{j,i}(t)}{\sum_{j \in K} \bar{I}^r_{j,b(i)}(t)} \right) \cdot 10^{\frac{\epsilon(t)}{10}} \tag{A.1}$$

where M is the number of receiving antennas at the eNode-B, $S^r_{j,i}$ is the desired SRS power received on PRB j from user i at antenna r, $I^r_{j,b(i)}$ is the interference signal power received on PRB j at antenna r on eNode-B $b(i)$, $b(i)$ is the serving eNode-B of user i, K is the set of simultaneously sounded PRBs that PRB k belongs to, ϵ is a zero mean Gaussian distributed random variable with standard deviation σ_{CSI}. The random variable $\epsilon(t)$ and $\epsilon(t+m)$ are uncorrelated for $m \neq 0$.

In uplink the interference is characterized by higher variability in a PRB compared to downlink. Therefore, an average measurement of the interference is used for the CSI estimation. Hence the interference component in (A.1) is calculated as:

$$\bar{I}^r_{j,b(i)}(t) = \eta \cdot I^r_{j,b(i)}(t) + (1-\eta) \cdot \bar{I}^r_{j,b(i)}(t-1) \tag{A.2}$$

where η is forgetting factor which controls the relative influence on the average interference of the recent measurement on the older measurements.

A.3 Outer Loop Link Adaptation Model

The OLLA algorithm is modeled such that it only controls the BLER target for the first transmission of the users. The OLLA algorithm is used to offset the CSI reports (expressed in decibels) received from the UE by using a offset parameter (A_{CSI}):

$$CSI_{i,eff} = CSI_i - A_{CSI} \text{ [dB]}. \tag{A.3}$$

The offset A_{CSI} is adjusted following the rules of outer loop power control as in WCDMA [102]:

1. If the first transmission is correctly received decrease the A_{CSI} by $A_{StepUp} = S \cdot BLER_T$

2. If the first transmission is not correctly received increase the A_{CSI} by $A_{StepDown} = S \cdot (1 - BLER_T)$

where S represents the step size and $BLER_T$ is the BLER which the algorithm will converge to if the offset A_{CSI} remains within a specified range $A_{CSI,min} \leq A_{CSI} \leq$

$A_{CSI,max}$. The BLER target can be expressed as follows:

$$BLER_T = \frac{A_{StepDown}}{A_{StepDown} + A_{StepUp}} \tag{A.4}$$

In this study, the OLLA step size is equal to 0.5 dB for all the users. The OLLA offset range is assumed to be [-4.0, 4.0] dB.

A.4 HARQ Model

The explicit scheduling of HARQ processes is implemented in the system model. The combining gain is modeled using a simple HARQ process model, taken from [103]. Only Chase Combining (CC) is considered, where the SINR after HARQ combining is given by:

$$\left(\overline{SINR}\right)_{C,n} = \sum_{k=1}^{n} \left(\overline{SINR}\right)_k \quad , \tag{A.5}$$

where $\left(\overline{SINR}\right)_{C,n}$ represents the combined SINR after n transmissions, and $\left(\overline{SINR}\right)_k$ denotes the SINR of the transmission k. In this study the HARQ process allows a maximum of three retransmissions before discarding a block, i.e., $n = 4$.

A.5 Link-to-System Performance Mapping

In order to estimate the performance at the system-level with reasonable accuracy, an evaluation based on extensive simulations under a variety of scenarios is crucial. A single simulator approach would be preferable, but the complexity of such a simulator including everything from link-level processing to multi-cell network is too high for the required simulation resolution [79]. Therefore, separate link-level and system-level simulators are needed. The link and system levels are connected through a link-to-system performance mapping function, which is used to predict the instantaneous BLER at system-level without performing detailed link-level processing steps. This function is estimated using link-level simulations, and it takes into account factors such as MCS format, receiver type, and channel state [104]. The desired characteristics of the link-to-system mapping function are that it should be general enough to cover different multiple access strategies and transceiver types, including different antenna techniques. Further, it should be possible to derive the parameters of the model from a limited number of link-level evaluations. In this study, the Actual Value Interface (AVI) method is used for the link-to-system mapping [105][90]. The AVI tables constructed from an extensive link-level simulations are used to map the average received SINR to the corresponding BLock Error Probability (BLEP). The target BLER ($BLER_{target}$) corresponds to the value used as input to the OLLA algorithm.

A.6 Traffic Model

In this study finite buffer traffic model is used to abstract the behavior of Best Effort (BE) services. The finite buffer model allows each user to download the same amount of data. Once the download is finished the session is terminated. The session time is proportional to the experienced data rates. Thus users located at the cell edge are expected to stay longer in the system in comparison to the users located close to the cell center. Hence the data rates delivered to the cell edge users will dominate the average cell throughput.

The CBR streaming traffic model is used for a realistic GBR service. For each CBR user a fixed amount of data packets are generated at the user with a constant packet size and constant inter-arrival time. In case the system is able to fulfill the GBR requirement of CBR services, the session time of each CBR user will be same as the streaming duration irrespective of the user location. Hence, if the AC and scheduling framework is working effectively the CBR users will fulfill their GBR requirements.

A.7 Key Performance Indicators

The KPIs used in this system-level study to evaluate the performance of AC and scheduling are as follows:

- The average cell throughput ($\overline{TP}_{cell}$) is defined as:

$$\overline{TP}_{cell} = \frac{\text{total correctly received bits per cell}}{\text{simulation time}} \tag{A.6}$$

- The average user throughput ($\overline{TP}_i$) for user i is defined:

$$\overline{TP}_i = \frac{\text{correctly received bits from user } i}{\text{session time}} \tag{A.7}$$

- The blocking probability (P_b) is defined as the ratio of the number of blocked users to the number of new users requesting admission.
- The outage probability (P_o) is defined as the ratio of the number of users not fulfilling their GBR requirements to the total number of users admitted.
- The unsatisfied user probability (P_u) is defined as:

$$P_u = 1 - (1 - P_b)(1 - P_o) \tag{A.8}$$

A.8 Acknowledgment

The system simulator was developed in collaboration with other colleagues in research group as well as in partnership with Nokia Siemens Networks.

Table A.1: System model assumptions based on the 3GPP Macro cell outdoor-to-indoor deployment, and default simulation parameters setting [14][19].

Parameter	**Setting**
Cellular Layout	Hexagonal grid, 19 cell sites, 3 cells/sectors per site
Inter-site distance	500 m (Macro case 1) 1732 m (Macro case 3)
System bandwidth	10 MHz
Number of sub-carriers per PRB	12
Number of PRBs	50 (180 kHz per PRB)
Sub-frame/TTI duration	1 ms
Maximum User transmit power	24 dBm (250 mW)
Distance dependent path loss	$128.1 + 37.6 \log_{10}(\text{distance in km})$
Penetration loss	20 dB
Log-normal shadowing	standard deviation = 8 dB correlation distance = 50 m correlation between sectors = 1.0 correlation between sites = 0.5
Minimum distance between UE and cell	35 m
Power delay profile	TU3, 20 taps [92]
CSI log-normal error standard deviation	1 dB
CSI resolution	2 dB
OLLA step size	0.5 dB
OLLA offset range	[-4.0, 4.0] dB
Control channel overhead	14% (2/14 symbols)
Link adaptation	Fast AMC
Modulation/code rate settings	QPSK [R = 1/10, 1/6, 1/4, 1/3, 1/2, 2/3, 3/4], 16QAM [R=1/2, 2/3, 3/4, 5/6]
HARQ model	Ideal chase combining
Max. No. of HARQ transmission attempts	4
Ack/Nack delay	2 ms
Channel estimation	Ideal
Carrier frequency	2 GHz
eNode-B antenna gain	14 dBi
UE antenna gain	0 dBi
UE noise figure	9 dB (-124 dBm/sub-carrier)
UE speed	3 kmph
UE receiver	2-Rx Maximal Ratio Combining (MRC)
Frequency re-use factor	1

Appendix B

Statistical Significance Assessment

B.1 Introduction

This chapter assesses the statistical significance of the KPIs obtained from the semi-static simulator described in Appendix A by using standard statistical methods. The chapter is organized as follows: The modeling assumptions including the list of selected simulation scenarios is outlined in Section B.2. The results and discussion are presented in Section B.3.

B.2 Modeling Assumptions

The statistical significance analysis is performed by running large number of simulations (fifty) with identical parameter setup, but with different seed for random number generator. The variation in the KPIs is investigated by means of the box and whiskers diagram (or box plot) [106]. The following most relevant KPIs have been considered which have been defined in Section A.7.

- Average cell throughput
- Average user throughput
- Average 95% coverage throughput
- Blocking probability
- Outage probability
- Average number of users per cell

The statistical significance investigation is carried out for FPC based AC and reference AC ($R_{max} = 5$ Mbps) using fixed PRB allocation to users in Macro case 1 (interference-limited) and Macro case 3 (noise-limited)scenarios studied in Chapter 3. The idea is to provide an indication of the stability of the KPIs for studied AC algorithms and propogation scenarios. The selected cases for the statistical assessment are as follows:

1. Verification of the FPC based AC and reference AC with single GBR of 256 kbps and user arrival rate of 8 users/cell/s for Macro case 1 in Section 3.5.1.
2. Verification of the FPC based AC with single GBR of 256 kbps and user arrival rate of 6 users/cell/s for Macro case 3 in Section 3.5.2.

B.3 Results and Discussions

Figure B.1 shows the box and whiskers diagrams for the average cell throughput, average user throughput, and average 95% coverage throughput for FPC based AC and Macro case 1 and the simulation scenario in Section 3.5.1. The KPIs are normalized to the sample mean i.e. the mean value obtained from all the simulations. In the box and whiskers diagram the box is drawn from the lower hinge defined as the 25% percentile, to the upper hinge corresponding to the 75% percentile. The median value is shown as a line across the box. The legth of the box gives the inter-quartile range, while the whiskers on each side of the box is extended to the most extreme data value within 1.5 times of the inter-quartile range. Data values lying beyond the ends of the whiskers are marked as outliers.

We notice that in Figure B.1 the deviation in average cell throughput from its corresponding sample mean is within $\pm$1.5%, while the deviation in user throughput and coverage throughput from their sample mean is within $\pm$5% and $\pm$3% respectively for FPC based AC and Macro case 1.

Figure B.2 shows the box plot for the blocking probability, outage probability, and number of users per cell for FPC based AC and Macro case 1. The deviation in blocking probability from its corresponding sample mean is within $\pm$12%. The range of outage probability for the ran simulations is between 0.06% – 0.36%, but the deviation from its sample mean (0.2%) is within $\pm$80%. This is because negligible percentage of users are in outage with FPC based AC, hence to precisely predict the outage probability significantly higher number of completed calls need to be simulated. The deviation of the average number of users per cell from its sample mean is within $\pm$5%.

Figure B.3 shows the box plot for the average cell throughput, average user throughput, and average 95% coverage throughput for reference AC and Macro case 1. It is seen that the deviation in average cell throughput from its sample mean is within $\pm$2.5%. Similarly, the deviation in user throughput and coverage throughput from their sample mean is within $\pm$8% and $\pm$2.5% respectively.

Figure B.4 shows the box plot for the blocking probability, outage probability, and

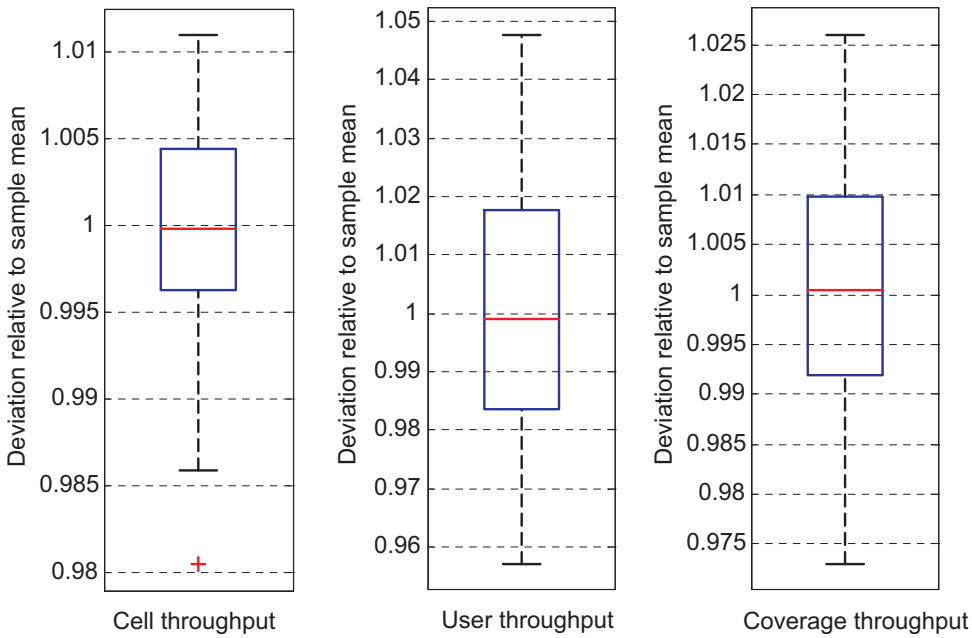

Figure B.1: Box plots of the KPIs obtained for the FPC based AC with single GBR of 256 kbps and user arrival rate of 8 users/cell/s for Macro case 1 in Section 3.5.1.

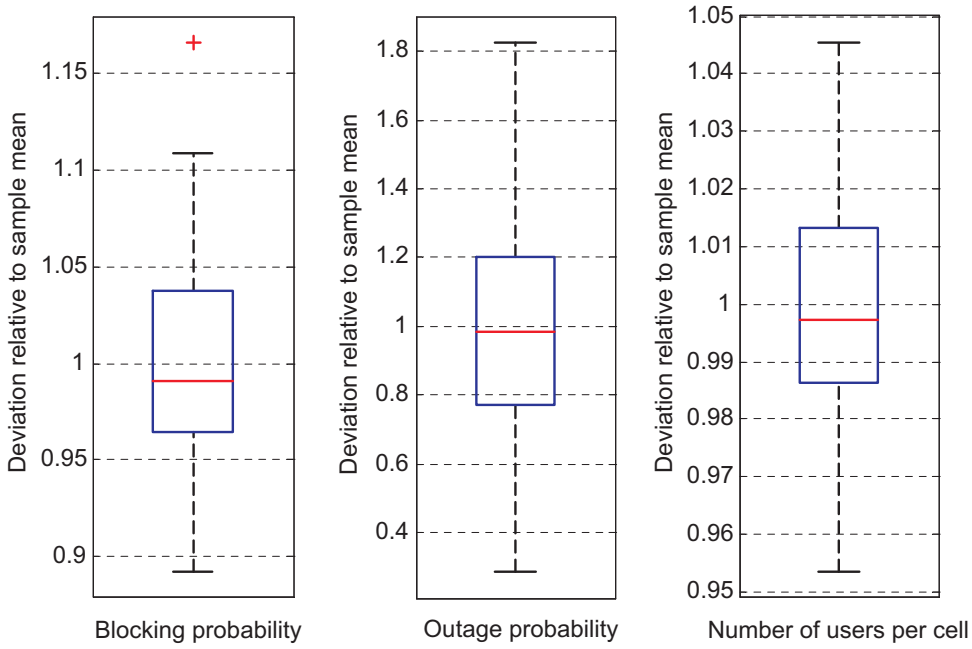

Figure B.2: Box plots of the KPIs obtained for the FPC based AC with single GBR of 256 kbps and user arrival rate of 8 users/cell/s for Macro case 1 in Section 3.5.1.

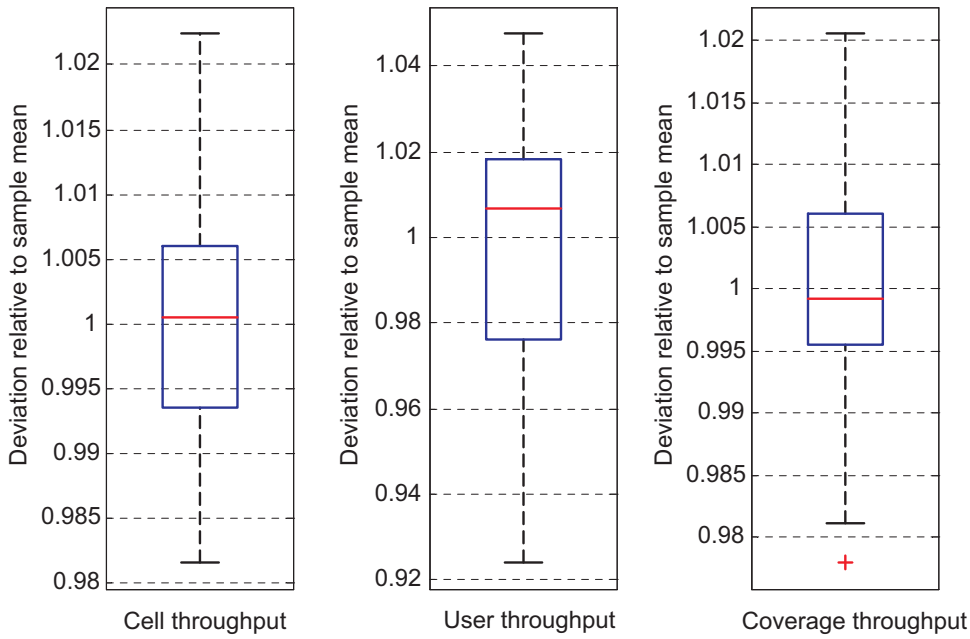

Figure B.3: Box plots of the KPIs obtained for the reference AC with single GBR of 256 kbps and user arrival rate of 8 users/cell/s for Macro case 1 in Section 3.5.1.

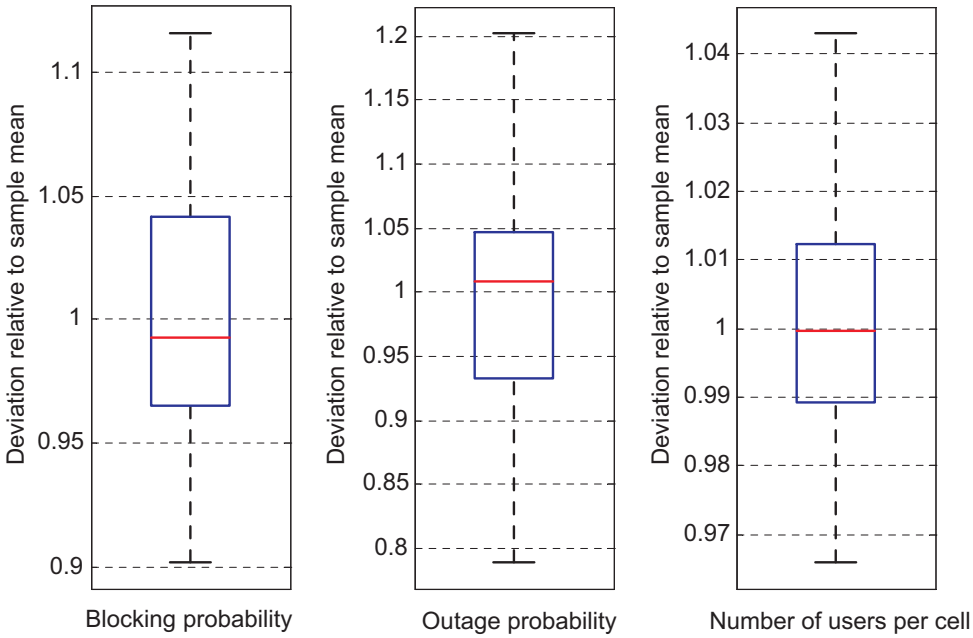

Figure B.4: Box plots of the KPIs obtained for the reference AC with single GBR of 256 kbps and user arrival rate of 8 users/cell/s for Macro case 1 in Section 3.5.1.

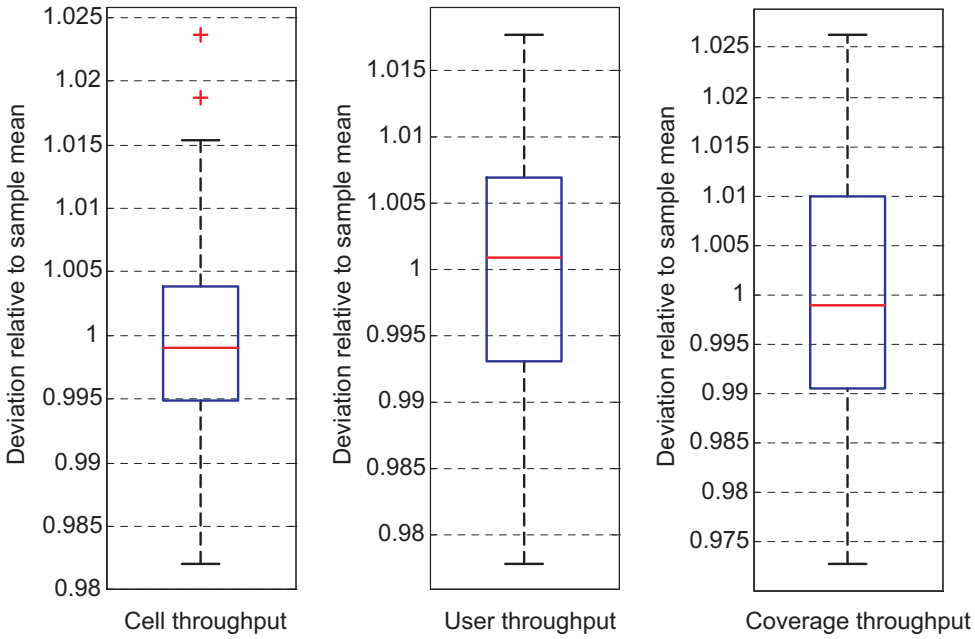

Figure B.5: Box plots of the KPIs obtained for the FPC based AC with single GBR of 256 kbps and user arrival rate of 6 users/cell/s for Macro case 3 in Section 3.5.2.

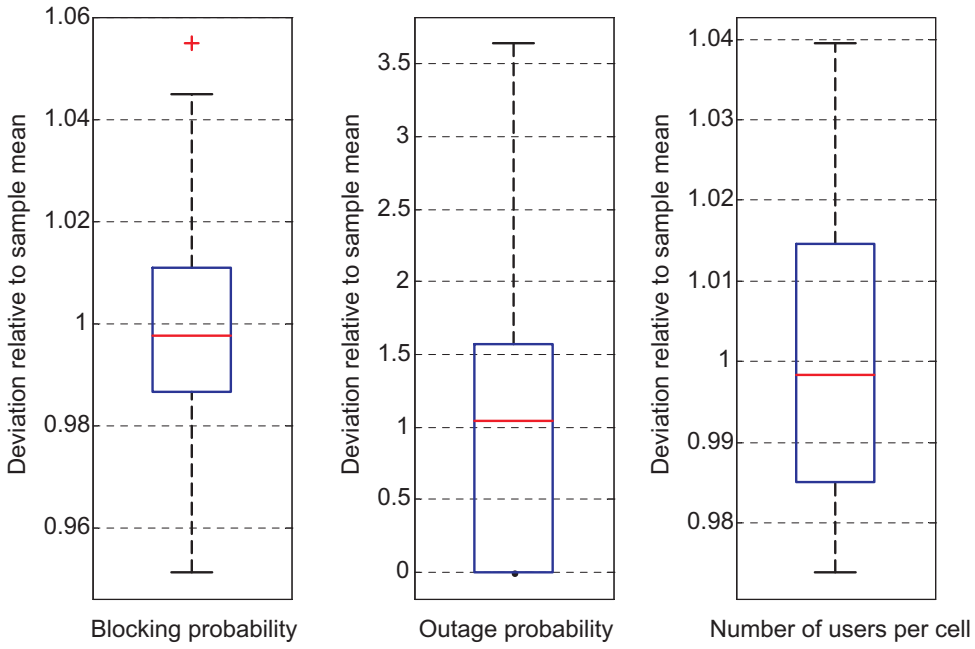

Figure B.6: Box plots of the KPIs obtained for the FPC based AC with single GBR of 256 kbps and user arrival rate of 6 users/cell/s for Macro case 3 in Section 3.5.2.

number of users per cell for reference AC and Macro case 1. The deviation in blocking probability and outage probability from their corresponding sample mean is within $\pm 13\%$ and $\pm 22\%$ respectively. The outage probability in the case with reference AC is more accurate compared to FPC based AC because higher number of users are in outage with reference AC. The deviation of the average number of users per cell from its sample mean is within $\pm 5\%$. Similar results are presented for Macro case 3 in Figure B.5 and Figure B.6.

We notice that the deviation in the average cell throughput, average user throughput, and average 95% coverage throughput from their corresponding sample means is within $\pm 2.5\%$, $\pm 8\%$, and $\pm 3\%$ respectively, which are sufficiently accurate. The deviation in blocking probability from its corresponding sample means is within $\pm 12\%$. However, the inter-quartile range is within $\pm 5\%$, i.e. in 50% of cases the error in blocking probability is smaller than 5%. The deviation in outage probability from its corresponding sample means is within $\pm 80\%$ for Macro case 1, while it is $+350\%$ for Macro case 3. This is because outage probability tends toward zero with FPC based AC, and hence very small variation leads to a high percentage of error and hence reduced statistical accuracy.

Bibliography

[1] H. Holma and A. Toskala, Eds., *WCDMA for UMTS – HSPA Evolution and LTE*. John Wiley & Sons Ltd, 2007.

[2] ——, *HSDPA/HSUPA for UMTS – High Speed Radio Access for Mobile Communications*. John Wiley & Sons Ltd, 2006.

[3] ——, *WCDMA for UMTS – Radio Access for Third Generation Mobile Communications*, 3rd ed. John Wiley & Sons Ltd, 2004.

[4] 3GPP Technical Specification 25.211, version 5.8.0, *Physical channels and mapping of transport channels onto physical channels (FDD) (Release 5)*, December 2005.

[5] 3GPP RP-080228, *Feasibility Study on Dual-Cell HSDPA operation*, March 2008.

[6] 3GPP TSG-RAN, RP040461, *Proposed Study Item on Evolved UTRA and UTRAN*, December 2004.

[7] A. Toskala and P. E. Mogensen, "UTRAN Long Term Evolution in 3GPP," in *Proceedings of the International Symposium on Wireless Personal Multimedia Communications (WPMC)*, Aalborg, Denmark, 2005.

[8] E. Dahlman, H. Ekström, A. Furuskär, Y. Jading, J. Karlsson, M. Lundevall, and S. Parkvall, "The 3G Long-Term Evolution - Radio Interface Concepts and Performance Evaluation," in *Proceedings of the IEEE Vehicular Technology Conference (VTC)*, vol. 1, Melbourne, Australia, May 2006, pp. 137–141.

[9] 3GPP Technical Report 25.913, version 7.3.0, *Requirements for Evolved UTRA (E-UTRA) and Evolved UTRAN (E-UTRAN)*, March 2006.

[10] B. Classon, K. Baum, V. Nangia, R. Love, Y. Sun, R. Nory, K. Stewart, A. Ghosh, R. Ratasuk, W. Xiao, and J. Tan, "Overview of UMTS Air-Interface Evolution," in *Proceedings of the the IEEE Vehicular Technology Conference (VTC)*, Montreal, Canada, October 2006.

[11] 3GPP Technical Specifications 36.101, version 8.2.0, *Evolved Universal Terrestrial Radio Access (E-UTRA); User Equipment (UE) Radio Transmission and Reception (Release 8)*, May 2008.

[12] 3GPP Technical Specifications 36.104, version 8.2.0, *Evolved Universal Terrestrial Radio Access (E-UTRA); Base Station (BS) Radio Transmission and Reception (Release 8)*, May 2008.

[13] A. Toskala, H. Holma, K. Pajukoski, and E. Tiirola, "UTRAN Long Term Evolution in 3GPP," in *Proceedings of the IEEE International Symposium on Personal, Indoor and Mobile Radio Communications (PIMRC)*, Helsinki, Finland, 2006.

[14] 3GPP Technical Report 25.814, version 7.1.0, *Physical Layer Aspect for Evolved Universal Terrestrial Radio Access (UTRA)*, September 2006.

[15] H. G. Myung, J. Lim, and D. J. Goodman, "Single Carrier FDMA for Uplink Wireless Transmission," *IEEE Vehicular Technology Magazine*, pp. 30–38, September 2006.

[16] H. Ekström, A. Furuskär, J. Karlsson, M. Meyer, S. Parkvall, J. Torsner, and M. Wahlqvist, "Technical Solutions for the 3G Long-Term Evolution," *IEEE Communications Magazine*, pp. 38–45, March 2006.

[17] 3GPP Technical Specification 36.300, version 8.3.0, *Evolved Universal Terrestrial Radio Access (E-UTRA) and Evolved Universal Terrestrial Radio Access (E-UTRAN); Overall Description; Stage 2*, January 2008.

[18] 3GPP Technical Specification 36.133, version 8.2.0, *Evolved Universal Terrestrial Radio Access (E-UTRA); Requirements for Support of Radio Resource Management (Release 8)*, May 2008.

[19] Orange, China Mobile, KPN, NTT DoCoMo, Sprint, T-Mobile, Vodafone, Telecom Italia, "LTE physical layer framework for performance verification," *3GPP TSG-RAN1, R1-070674*, February 2007.

[20] 3GPP Technical Specification 36.213, version 8.1.0, *Evolved Universal Terrestrial Radio Access (E-UTRA); Physical Layer Procedures*, November 2007.

[21] B. Stroustrup, *The C++ Programming Language - Third Edition*. Addison Wesley.

[22] 3GPP Technical Specification 23.401, version 8.0.0, *General Packet Radio Service (GPRS) Enhancements for Evolved Universal Terrestrial Radio Access Network (E-UTRAN) Access*, December 2007.

[23] P. Hosein, "A Class-Based Admission Control Algorithm for Shared Wireless Channels Supporting QoS Services," in *Proceedings of the 5^{th} IFIP TC6 International Conference on Mobile and Wireless Communications Networks (MWCN)*, October 2003.

[24] B. Eklundh, "Channel Utilization and Blocking Probability in a Cellular Mobile Telephone System with Directed Retry," *IEEE Transactions on Communicaitons*, vol. 34, no. 4, pp. 329–337, April 1986.

[25] G. Song and Y. Li, "Cross-layer optimization for OFDM wireless networks-part I: theoretical framework," *IEEE Transactions on Wireless Communications*, vol. 4, no. 2, pp. 614–624, March 2005.

[26] ——, "Cross-layer optimization for OFDM wireless networks-part II: algorithm development," *IEEE Transactions on Wireless Communications*, vol. 4, no. 2, pp. 625–634, March 2005.

[27] 3GPP Technical Specification 36.211, version 8.3.0, *Evolved Universal Terrestrial Radio Access (E-UTRA); Physical Channels and Modulation*, May 2008.

[28] J. Lim, H. G. Myung, K. Oh, and D. J. Goodman, "Proportional Fair Scheduling of Uplink Single Carrier FDMA Systems," in *Proceedings of the 17^{th} IEEE International Symposium on Personal, Indoor and Mobile Radio Communications (PIMRC)*, Helsinki, Finland, September 2006, pp. 1–6.

[29] F. D. Calabrese, M. Anas, C. Rosa, P. E. Mogensen, and K. I. Pedersen, "Performance of a Radio Resource Allocation Algorithm for UTRAN LTE Uplink," in *Proceedings of the 65^{th} IEEE Vehicular Technology Conference (VTC)*, Dublin, Ireland, April 2007, pp. 2895–2899.

[30] A. Pokhariyal, "Downlink Frequency-Domain Adaptation and Scheduling – A Case Study Based on the UTRA Long Term Evolution," Ph.D. dissertation, Radio Access Technology Section, Institute of Electronic Systems, Aalborg University, Aalborg, Denmark, August 2007.

[31] G. Monghal, K. I. Pedersen, I. Z. Kovacs, and P. E. Mogensen, "QoS Oriented Time and Frequency Domain Packet Schedulers for the UTRAN Long Term Evolution," in *Proceedings of the 67^{th} IEEE Vehicular Technology Conference (VTC)*, Singapore, May 2008, pp. 2532–2536.

[32] A. Pokhariyal, K. I. Pedersen, G. Monghal, I. Z. Kovacs, C. Rosa, T. E. Kolding, and P. E. Mogensen, "HARQ Aware Frequency Domain Packet Scheduler with Different Degrees of Fairness for the UTRAN Long Term Evolution," in *Proceedings of the 65^{th} IEEE Vehicular Technology Conference (VTC)*, Dublin, Ireland, April 2007, pp. 2761–2765.

[33] 3GPP Technical Specification 36.321, version 8.3.0, *Evolved Universal Terrestrial Radio Access (E-UTRA) Medium Access Control (MAC) protocol specification (Release 8)*, September 2008.

[34] F. D. Calabrese, P. H. Michaelsen, C. Rosa, M. Anas, C. U. Castellanos, D. L. Villa, K. I. Pedersen, and P. E. Mogensen, "Search-Tree based Uplink Channel Aware Packet Scheduling for UTRAN LTE," in *Proceedings of the 67^{th} IEEE Vehicular Technology Conference (VTC)*, Singapore, May 2008, pp. 1949–1953.

[35] F. D. Calabrese, C. Rosa, M. Anas, P. H. Michaelsen, K. I. Pedersen, and P. E. Mogensen, "Adaptive Transmission Bandwidth Based Packet Scheduling for LTE Uplink," in *Proceedings of the 68th IEEE Vehicular Technology Conference (VTC)*, Calgary, Canada, September 2008, pp. 1–5.

[36] Nokia, "Frequency-Domain User Multiplexing for the E-UTRAN Downlink," *3GPP TSG-RAN1, R1-060188*, January 2006.

[37] K. B. Letaief and Y. J. Zhang, "Dynamic Multiuser Resource Allocation and Adaptation for Wireless Systems," *IEEE Wireless Communications*, vol. 13, no. 4, pp. 38–47, August 2006.

[38] C. U. Castellanos, D. L. Villa, C. Rosa, K. I. Pedersen, F. D. Calabrese, P. H. Michaelsen, and M. Jurgen, "Performance of Uplink Fractional Power Control in UTRAN LTE," in *Proceedings of the 67th IEEE Vehicular Technology Conference (VTC)*, Singapore, May 2008, pp. 2517–2521.

[39] A. J. Goldsmith and S.-G. Chua, "Adaptive Coded Modulation for Fading Channels," *IEEE Transactions on Communications*, vol. 46, no. 5, pp. 595–602, May 1998.

[40] *Mobile WiMAX - Part I: A Technical Overview and Performance Evaluation*, WiMAX Forum, www.wimaxforum.org/home, August 2006.

[41] C. Rosa, D. L. Villa, C. U. Castellanos, F. D. Calabrese, P. H. Michaelsen, K. I. Pedersen, and P. Skov, "Performance of Fast AMC in E-UTRAN Uplink," in *Proceedings of the IEEE International Conference on Communications (ICC)*, Beijing, China, May 2008, pp. 4973–4977.

[42] B. E. Priyanto, H. Codina, S. Rene, T. B. Sorensen, and P. E. Mogensen, "Initial Performance Evaluation of DFT-Spread OFDM Based SC-FDMA for UTRA LTE Uplink," in *Proceedings of the 65th IEEE Vehicular Technology Conference (VTC)*, Dublin, Ireland, April 2007, pp. 3175–3179.

[43] Y. Ofuji, Y. Kishiyama, K. Higuchi, and M. Sawahashi, "Group-Wised Reference Signal Allocation for Single-Carrier FDMA Radio Access in Evolved UTRA Uplink," in *Proceedings of the 65th IEEE Vehicular Technology Conference (VTC)*, Dublin, Ireland, April 2007, pp. 1871–1875.

[44] K. I. Pedersen, F. Frederiksen, T. E. Kolding, T. F. Lootsma, and P. E. Mogensen, "Performance of High-Speed Downlink Packet Access in Coexistance With Dedicated Channels," *IEEE Transactions on Vehicular Technology*, vol. 56, no. 3, pp. 1262–1271, May 2007.

[45] 3GPP Technical Report 25.813, version 7.0.0, *E-UTRA and E-UTRAN; Radio Interface Protocol Aspects*, June 2006.

[46] H. Holma and J. Laakso, "Uplink Admission Control and Soft Capacity with MUD in CDMA," in *Proceedings of the 50th IEEE Vehicular Technology Conference (VTC)*, September 1999.

[47] J. O. Carnero, "Uplink Capacity Enhancement in WCDMA – Multi Cell Admission Control, Synchronized Schemes and Fast Packet Scheduling," Ph.D. dissertation, Department of Communication Technology, Aalborg University, Aalborg, Denmark, March 2004.

[48] S. S. Jeong, J. A. Han, and W. S. Jeon, "Adaptive Connection Admission Control Scheme for High Data Rate Mobile Networks," in *Proceedings of the 62nd IEEE Vehicular Technology Conference (VTC)*, September 2005.

[49] D. Niyato and E. Hossain, "Connection Admission Control Algorithms for OFDM Wireless Networks," in *Proceedings of the IEEE Global Telecommunications Conference (GLOBECOM)*, December 2005.

[50] C. F. Ball, E. Humburg, K. Ivanov, and F. Treml, "Performance Analysis of IEEE802.16 Based Cellular MAN with OFDM-256 in Mobile Scenarios," in *Proceedings of the 61th IEEE Vehicular Technology Conference (VTC)*, May 2005.

[51] B. Rong, Y. Qian, and H. H. Chen, "Adaptive Power Allocation and Call Admission Control in Multiservice WiMAX Access Networks," *IEEE Wireless Communications*, pp. 14–19, February 2007.

[52] D. Hong and S. S. Rappaport, "Traffic Model and Performance Analysis of Cellular Radio Telephone Systems with Prioritized and Nonprioritized Handoff Procedures," *IEEE Transactions on Vehicular Technology*, vol. 35, pp. 77–92, August 1986.

[53] J. Y. Lee, J. G. Choi, K. Park, and S. Bahk, "Realistic Cell-Oriented Adaptive Admission Control for QoS Support in Wireless Multimedia Networks," *IEEE Transactions on Vehicular Technology*, vol. 52, pp. 512–524, May 2003.

[54] K. I. Pedersen, P. E. Mogensen, and T. E. Kolding, "Overview of QoS Options for HSDPA," *IEEE Communications Magazine*, vol. 44, no. 7, pp. 100–105, July 2006.

[55] P. E. Mogensen, W. Na, I. Z. Kovacs, F. Frederiksen, A. Pokhariyal, K. I. Pedersen, K. Hugl, and M. Kuusela, "LTE Capacity versus Shannon," in *Proceedings of the 65th IEEE Vehicular Technology Conference (VTC)*, Dublin, Ireland, April 2007, pp. 1234–1238.

[56] CATT, Ericsson, LGE, Motorola, Nokia, Nokia-Siemens, Nortel, NTT DoCoMo, Orange, Panasonic, Philips, Qualcomm, Samsung, Sharp, TI and Vodafone, "Way Forward on Power Control of PUSCH," *3GPP TSG-RAN WG1, R1-073224*, June 2007.

[57] A. M. Rao, "Reverse Link Power Control for Managing Inter-Cell Interference in Orthogonal Multiple Access Systems," in *Proceedings of the 66th IEEE Vehicular Technology Conference (VTC)*, October 2007.

[58] T. E. Kolding, "Link and System Performance Aspects of Proportinal Fair Packet Scheduling in WCDMA/HSDPA," in *Proceedings of 58th IEEE Vehicular Technology Conference (VTC)*, vol. 3, Orlando, Florida, USA, October 2003, pp. 1717–1722.

[59] M. Anas, F. D. Calabrese, P. E. Östling, K. I. Pedersen, and P. E. Mogensen, "Performance Analysis of Handover Measurements and Layer 3 Filtering for UTRAN LTE," in *Proceedings of the IEEE International Symposium on Personal, Indoor and Mobile Radio Communications (PIMRC)*, Athens, Greece, September 2007, pp. 1–5.

[60] T. E. Kolding, "QoS-Aware Proportional Fair Packet Scheduling with Required Activity Detection," in *Proceedings of IEEE Vehicular Technology Conference (VTC)*, Montreal, Canada, September 2006, pp. 1–5.

[61] M. Anas, C. Rosa, F. D. Calabrese, P. H. Michaelsen, K. I. Pedersen, and P. E. Mogensen, "QoS-Aware Single Cell Admission Control for UTRAN LTE Uplink," in *Proceedings of the 67th IEEE Vehicular Technology Conference (VTC)*, Singapore, May 2008, pp. 2487–2491.

[62] D. Niyato and E. Hossain, "Service Differentiation in Broadband Wireless Access Networks with Scheduling and Connection Admission Control: A Unified Analysis," *IEEE Transactions on Wireless Communications*, vol. 6, pp. 293–301, January 2007.

[63] H. W. Lee and S. Chong, "Combined Packet Scheduling and Call Admission Control with Minimum Throughput Guarantee in Wireless Networks," *IEEE Transactions on Wireless Communications*, vol. 6, pp. 3080–3089, August 2007.

[64] J. S. Gomes, M. Yun, H. A. Choi, J. H. Kim, J. Sohn, and H. I. Choi, "Scheduling Algorithms for Policy Driven QoS Support in HSDPA Networks," in *Proceedings of the 65th IEEE Vehicular Technology Conference (VTC)*, Dublin, Ireland, April 2007, pp. 799–803.

[65] K. B. Johnsson and D. C. Cox, "An Adaptive Cross-Layer Scheduler for Improved QoS Support of Multiclass Data Services of Wireless Systems," *IEEE Journal on Selected Areas in Communications*, vol. 23, pp. 334–343, February 2005.

[66] W. S. Jeon and D. G. Jeong, "Combined Connection Admission Control and Packet Transmission Scheduling for Mobile Internet Services," *IEEE Transactions on Vehicular Technology*, vol. 55, pp. 1582–1593, September 2006.

[67] D. Laselva, J. Steiner, F. Khokhar, T. E. Kolding, and J. Wigard, "Optimization of QoS-Aware Packet Schedulers in Multi-Service Scenarios over HSDPA," in *Proceedings of IEEE International Symposium of Wireless Communication Systems (ISWCS)*, Trondheim, Norway, October 2007, pp. 123–127.

[68] M. Anas, C. Rosa, F. D. Calabrese, K. I. Pedersen, and P. E. Mogensen, "Combined Admission Control and Scheduling for QoS Differentiation in LTE Uplink," in *Proceedings of the 68th IEEE Vehicular Technology Conference (VTC)*, Calgary, Canada, September 2008, pp. 1–5.

[69] K. Gopalan, L. Huang, G. Peng, and T.-C. Chiueh, "Statistical Admission Control Using Delay Distribution Measurements," *ACM Transactions on Multimedia Computing, Communicaitons and Applications*, vol. 2, no. 4, pp. 258–281, November 2006.

[70] A. Leon-Garcia, *Probability and Random Processes for Electrical Engineering*. Addison Wesley Publishing Company, 1994.

[71] L. Nielsen, "Power Based Resource Allocation Algorithm for WCDMA Using Probabilistic Overbooking of Bursty Packet Traffic," in *Proceedings of the International Symposium on Wireless Personal Multimedia Communications (WPMC)*, Aalborg, Denmark, September 2001.

[72] 3GPP Technical Specifications 22.105, version 8.4.0, *Technical Specification Group Services and System Aspects Service Aspects; Service and Service Capabilities*, June 2007.

[73] G. P. Pollini, "Trends in Handover Design," *IEEE Communications magazine*, 1996.

[74] Y. Chen, "Soft Handover Issues in Radio Resource Management for 3G WCDMA Networks," Ph.D. dissertation, Department of Electronics Engineering, Queen Mary, University of London, London, UK, September 2003.

[75] K. Sipilä, M. Jäsberg, J. Laiho-Steffens, and A. Wacker, "Soft Handover Gains in a Fast Power Controlled WCDMA Uplink," in *Proceedings of the 49^{th} IEEE Vehicular Technology Conference (VTC)*, Houston, Texas, USA, May 1999, pp. 1594–1598.

[76] S. Akhtar and D. Zeghlache, "CIR Based Soft Handover for UTRA FDD Uplink," in *Proceedings of the 11^{th} IEEE International Symposium on Personal, Indoor and Mobile Radio Communications (PIMRC)*, London, UK, September 2000.

[77] R. Vijayan and J. M. Holtzman, "A Model for Analyzing Handoff Algorithms," *IEEE Transactions on Vehicular Technology*, pp. 351–356, August 1993.

[78] S. Kim, C. Kang, and K. Kim, "An Adaptive Handover Decision Algorithm Based on the Estimating Mobility for Signal Strength Measurements," in *Proceedings of the 60^{th} IEEE Vehicular Technology Conference (VTC)*, Los Angeles, California, USA, September 2004, pp. 1004–1008.

[79] H. Holma and A. Toskala, *WCDMA for UMTS – Radio Access for Third Generation Mobile Communications*, 2nd ed. ISBN 0-470-84467-1: John Wiley & Sons Inc, 2002.

[80] P. E. Östling, "Performance of RSS-, SIR-based Handoff and Soft Handoff in Microcellular Environments," *Wireless Personal Communications, Kluwer Academic Publishers*, 1996.

[81] 3GPP Technical Specifications 25.331, version 7.3.0, *Radio Resource Control (RRC); Protocol Specifications*, December 2006.

[82] Nokia, "Background Information of L3 Filtering Simulation Results," *3GPP RP-030172*, March 2003.

[83] Motorola, "Unit of Layer 3 Filtering," *3GPP RP-020635*, September 2002.

[84] M. Anas, F. D. Calabrese, P. E. Mogensen, C. Rosa, and K. I. Pedersen, "Performance Evaluation of Received Signal Strength based Hard Handover for UTRAN LTE," in *Proceedings of the 65^{th} IEEE Vehicular Technology Conference (VTC)*, Dublin, Ireland, April 2007, pp. 1046–1050.

[85] K. D. Dimou and A. Furuskär, "On the Use of Uplink Received Signal Strength Measurements for Handover," in *Proceedings of the 67^{th} IEEE Vehicular Technology Conference (VTC)*, Singapore, May 2008, pp. 2567–2571.

[86] P. Dassanayake, "Spatial Correlation of Shadow Fading and its Impact on Handover Algorithm Parameter Settings," in *Proceedings of IEEE Networks Conference*, 1995.

[87] T. E. Kolding, F. Frederiksen, and A. Pokhariyal, "Low Bandwidth Channel Quality Indication for OFDMA Frequency Domain Packet Scheduling," in *Proceedings of the IEEE International Symposium on Wireless Communication Systems (ISWCS)*, 2006.

[88] Nokia, "Evaluation Method for Benchmarking CQI Schemes for LTE," *3GPP TSG-RAN, WG1 R1-063383*, November 2006.

[89] K. Hiltunen, N. Binucci, and J. Bergström, "Comparison Between the Periodic and Event-Triggered Intra-Frequency Handover Measurement Reporting in WCDMA," in *Proceedings of IEEE Wireless Communications and Networking Conference (WCNC)*, 2000.

[90] C. Rosa, "Enhanced Uplink Packet Access in WCDMA," Ph.D. dissertation, Department of Communication Technology, Aalborg University, Aalborg, Denmark, December 2004.

[91] T. Hytönen, "Optimal Wrap Around Network Simulation," *Helsinki University of Technology Report, A432*, 2001.

[92] 3GPP Technical Report 25.943, version 7.0.0, *Deployment Aspects (Release 7)*, June 2007.

[93] M. Gudmundson, "Correlation Model for Shadow Fading in Mobile Radio Systems," *Electronic Letters*, November 1991.

[94] 3GPP Technical Specifications 36.331, version 8.2.0, *Evolved Universal Terrestrial Radio Access (E-UTRA); Radio Resource Control (RRC); Protocol Specifications (Release 8)*, May 2008.

[95] 3GPP Technical Specification 36.214, version 8.2.0, *Evolved Universal Terrestrial Radio Access (E-UTRA); Physical Layer - Measurements (Release 8)*, May 2008.

[96] T. S. Rappaport, *Wireless Communications — Principles and Practice, second edition*. ISBN 0-13-042232-0: Prentice Hall, 2002.

[97] S. Kourtis and R. Tafazolli, "Evaluation of Handover Related Statistics and the Applicability of Mobility Modelling in Their Prediction," in *Proceedings of the IEEE International Symposium on Personal, Indoor and Mobile Radio Communications (PIMRC)*, 2000.

[98] J. M. Holtzman and A. Sampath, "Adaptive Averaging Methodology for Handoffs in Cellular Systems," *IEEE Transactions on Vehicular Technology*, February 1995.

[99] Ericsson, "Bandwidth of Mobility Related Measurements in E-UTRAN," *3GPP TSG-RAN WG4, R4-070192*, February 2007.

[100] T. B. Sørensen, P. E. Mogensen, and F. Frederiksen, "Extension of the ITU Channel Models for Wideband (OFDM) Systems," in *Proceedings of the IEEE Vehicular Technology Conference (VTC)*, vol. 1, Dallas, Texas, USA, September 2005, pp. 392–396.

[101] 3GPP Technical Report 25.892, version 0.5.2, *Feasibility Study for OFDM for UTRAN enhancement*, December 2003.

[102] A. Sampath, P. S. Kumar, and J. M. Holtzman, "On Setting Reverse Link Target SIR in a CDMA System," in *Proceedings of the 47^{th} IEEE Vehicular Technology Conference (VTC)*, Phoenix, USA, May 1997, pp. 929–933.

[103] F. Frederiksen and T. E. Kolding, "Performance and Modeling of WCDMA/HSDPA Transmission/H-ARQ Schemes," in *Proceedings of 56th IEEE Vehicular Technology Conference (VTC)*, vol. 1, Vancouver, British Columbia, Canada, September 2002, pp. 472–476.

[104] K. Brueninghaus, D. Astley, T. Salzer, S. Visuri, A. Alexiou, S. Karger, and G.-A. Seraji, "Link Performance Models for System Level Simulations of Broadband Radio Access Systems," in *Proceedings of the IEEE Personal Indoor and Mobile Radio Communications Conference (PIMRC)*, vol. 4, Berlin, Germany, September 2005, pp. 2306–2311.

[105] S. Hämäläinen, P. Slanina, M. Hartman, A. Lappeteläinen, H. Holma, and O. Salonaho, "A Novel Interface between Link and System Level Simulations," in *Proceedings of ACTS Summit*, Aalborg, Denmark, October 1997, pp. 599–604.

[106] R. L. Mason, R. F. Gunst, and J. L. Hess, *Statistical Design and Analysis of Experiments – With Applications to Engineering and Science*. John Wiley & Sons, 2003.

Paper Reprints

Annex I

Search-Tree Based Uplink Channel Aware Packet Scheduling

F. D. Calabrese, P. H. Michaelsen, C. Rosa, M. Anas, C. Úbeda Castellanos, D. López Villa, K. I. Pedersen, and P. E. Mogensen, "Search-Tree Based Uplink Channel Aware Packet Scheduling for UTRAN LTE", in *Proceedings of IEEE Vehicular Technology Conference VTC2008-Spring*, pp. 699-703, Singapore, May, 2008.

Search-Tree Based Uplink Channel Aware Packet Scheduling for UTRAN LTE

F. D. Calabrese[†], P. H. Michaelsen[‡], C. Rosa[‡], M. Anas[†], C. Úbeda Castellanos[†], D. López Villa[†], K. I. Pedersen[‡] and P. E. Mogensen[‡]
[†]Department of Electronic Systems, Aalborg University, Denmark
[‡]Nokia Siemens Networks, Denmark

***Abstract*— UTRAN Long Term Evolution is currently under standardization within 3GPP with the aim of providing a spectral efficiency 2 to 4 times higher than its predecessor HSUPA/HSDPA Release 6. Single Carrier FDMA has been selected as multiple access for the uplink. This technology requires the subcarriers allocated to a single user to be adjacent. The consequence is a reduced allocation flexibility which makes it challenging to design effective packet scheduling algorithms. This paper provides a search-tree based channel aware packet scheduling algorithm and evaluates its performance in terms of throughput and noise rise distributions. It is shown that, despite measurement errors and high inter-cell interference variability, the proposed algorithm can increase the uplink capacity by 24% for the Macro 1 scenario and 19% for the Macro 3 scenario.**

I. Introduction

UTRAN Long Term Evolution (LTE) is a system currently under standardization within 3GPP. One of the targets of such a system is to improve the spectral efficiency by a factor of 2 to 3 for the uplink (UL) and 3 to 4 for the downlink (DL) compared to HSUPA/HSDPA Release 6. In order to achieve this goal new functionalities are introduced and different access schemes are selected. Orthogonal Frequency Division Multiplexing (OFDM), in particular, is regarded as a key technology given its high immunity to multipath, spectral efficiency and bandwidth scalability. Orthogonal Frequency Division Multiple Access (OFDMA), a OFDM based multiple access scheme, has been selected for downlink (DL). OFDMA provides high flexibility and relatively low complexity, but suffers from high Pick to Average Power Ratio (PAPR) which makes it a difficult candidate for UL given the power limitations in the mobile handset. For this reason a modified form of OFDMA, namely SC-FDMA (also known as DFT-spread OFDMA), is selected for the UL. While retaining most of the advantages of OFDMA, it also exhibits significantly lower PAPR resulting in reduced power consumption and improved coverage.

While providing some benefits, SC-FDMA requires the subcarriers, and therefore the Physical Resource Blocks (PRBs)[1], allocated to a single terminal to be adjacent. This has proven to be a challenging constraint to cope with, when it comes to designing packet scheduling algorithms. Like in every multi-user system the Packet Scheduler (PS) plays the fundamental role of multiplexing User Equipments (UEs) in time and frequency domain based on some optimization criterion. If the system is affected by time and frequency selective fading the PS can exploit the multi-user diversity by assigning each UE to the portion of the bandwidth which exhibits favorable conditions for that UE. This mechanism, also known as Channel Dependent Scheduling (CDS), requires the system to monitor the channel ideally for every UE and over all the frequency band and adapt the allocation based on changes to the channel conditions.

For this reason 3GPP has introduced in the standard the channel sounding concept [2]. Channel sounding consists in the terminal transmitting a Sounding Reference Signal (SRS). This signal is processed at the eNode-B to extract near-instantaneous frequency selective Channel State Information (CSI) which is then used for channel dependent functionalities like fast Link Adaptation (LA) and frequency domain packet scheduling.

The performance of channel aware packet scheduling algorithms has already been investigated for UTRA LTE downlink [3] but differences with the UL scenario exist and their impact on performance is remarkable. Apart from the difference on access technology highlighted above, another difference relevant to this work pertains the interference variations. The source of interference

[1]The basic time-frequency resource available for data transmission consisting of adjacent OFDM subcarriers [1]. It is also known as Resource Unit. Its size is equal to 180 KHz.

for a given UE can change from Transmission Time Interval (TTI) to TTI, and has a different interfering effect depending on its location and its transmitting power. This leads to a highly uncorrelated interference pattern for a given frequency, with variations which are larger and occur at a faster pace than in full load conditions in DL [4].

Previous work regarding the topic of UL PS have either assumed the channel knowledge to be available at the eNode-B [5] or have based channel knowledge acquisition on a different and less reliable mechanism than CSI [6]. The current work focuses on the performance evaluation of a search-tree based PS algorithm in UTRAN LTE UL which relies on CSI acquired via SRS. The search-tree is built by selecting a restricted set of allocations for each UE. The allocation is performed by searching and choosing the path, within the tree, with the highest global metric.

The paper is organized as follows. The PS functionality is described in general terms in Section II-A, while Section II-B describes in detail the algorithm deployed. Section III gives an overview of the simulator together with general parameters and assumptions. Section IV provides an analysis of the simulation results for the different parameter settings while Section V draws conclusions and offers hints for further studies.

II. Packet Scheduling Functionality

Radio Resource Management (RRM) for UTRAN LTE UL represents a complex problem given the number of parameters and constraints involved. Within the RRM functionalities, PS plays a central role. It interacts with the LA unit and the Hybrid ARQ (HARQ) manager to produce an allocation table which tries to maximize some utility function while exploiting channel knowledge.

A. General framework

CDS can be seen as a search algorithm which traverses the solution space to find an optimum solution defined according to a utility function. The utility function is designed as a trade off between overall spectral efficiency and fairness among UEs and it defines how different quantities (channel gain, traffic, QoS requirements) have to be taken into account. The problem is very complex because of the high number of parameters involved and the huge number of resulting combinations. Different decisions are therefore taken in order to reduce the search space. The basic inter-working of PS with other RRM functionalities is shown in Fig.1.

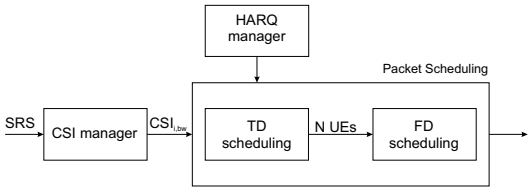

Fig. 1. Basic inter-working between PS and other RRM functionalities.

In order to perform frequency domain channel-aware PS, Channel State Information (CSI) is needed, ideally for all the UEs and over all the frequency band. Such information is provided by the CSI manager which extracts it from the SRSs. It is assumed that CSIs are available at the eNode-B every TTI over the entire system bandwidth, for every UE and with given bandwidth resolution. Such assumptions are ideal but the CSI mechanism is realistic, i.e. the CSIs are derived considering the real channel gain and interference conditions and model also SINR estimation errors.

The HARQ manager provides the set of UEs that have to undergo a retransmission. It is supposed to be synchronous and adaptive, which means that retransmissions can take place anywhere in the bandwidth but in a specific TTI.

The PS is divided in two units: Time Domain Packet Scheduler (TDPS) and Frequency Domain Packet Scheduler (FDPS). The TDPS, based on information from the HARQ manager, identifies the scheduling candidates, i.e., the UEs that are capable of transmitting in the next TTI. The TDPS also sorts the UEs according to a certain metric and then passes the first N to the FDPS. The sorting in time domain can either take place based on a frequency blind metric (e.g. Round Robin (RR)), or based on a metric that pertains the whole frequency band (as the position that the UEs will be occupying within the frequency band is not known at this stage). The UEs are then handed over to the FDPS which further exploits the channel knowledge and performs the most computationally intense operation trying to determine the best allocation table based on a channel aware metric. In this work the focus is on FDPS, therefore no action is performed by the TDPS which simply passes all the UEs on to the FDPS.

B. Algorithm description

In the following the bandwidth is assumed to be fixed and equal for all the UEs. It is indicated as resource chunk (RC) and is constituted by a set of consecutive

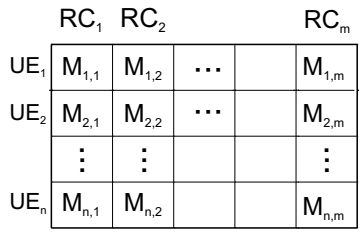

Fig. 2. Metric values for each UE and each RC.

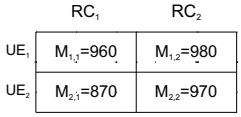

Fig. 3. Simple scenario with two UEs and two RCs: the algorithm fails to identify the optimum.

PRBs. The size of the RC is chosen to be a sub-multiple of the system bandwidth so that an integer number of UEs can be accommodated without creating bandwidth fragmentation.

Assuming a fixed bandwidth size we can define our goal as to maximize the utility function:

$$M_{sum} = \sum M_{n,k} A_{n,k} \quad (1)$$

where $M_{n,k}$ is the metric for UE n and RC k, $n \in \{UEs\}$, $k \in \{RCs\}$ and $A_{n,k} = \{0, 1\}$ with 1 for UE n allocated to RC k, 0 otherwise.

A simple optimization mechanism is based on arranging UEs and bandwidth chunks in a matrix containing the metric value for each UE and each RC, as shown in Fig.2.

The matrix is then fed as input to the FDPS which performs the following algorithm:

1) Find the UE and RC with the highest metric
2) Allocate the RC to the UE
3) Delete corresponding row (UE) and column (RC)
4) Repeat from 1 with the resulting sub-matrix

This approach provides a significant gain over a static scheduling (like a random allocation), but does not achieve the global optimum. As an example let's consider a case with two UEs and two RCs with the metrics given in Fig.3.

If we apply the algorithm just described, we would end up with RC_2 allocated to UE_1 and RC_1 allocated to UE_2. The resulting global metric (which we assume to be the sum of the metrics) would be $M_{sum} = 1850$. Performing the opposite allocation (RC_1 to UE_1 and RC_2 to UE_2) it would provide the maximal global metric $M_{sum} = 1930$. This offers a hint on how the algorithm could be improved to perform a more exhaustive search. Rather than considering only the best RC, we also consider what is, globally, the second best RC. For every RC considered we derive a sub-matrix from which we consider again the two best RCs. In this way we derive a binary search tree where the best allocation corresponds to the path with the highest sum of metrics.

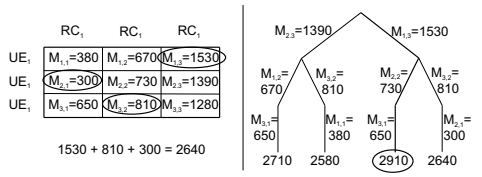

Fig. 4. Scheduling example with three UEs and three RCs. To the left the circles indicate the allocation performed using the matrix algorithm. To the right the thick line indicates the allocation performed using the tree algorithm with $N_{out} = 2$.

Fig.4 provides an example with three UEs and three RCs. The matrix algorithm, which is equivalent to the tree algorithm with an out-degree of 1 ($N_{out} = 1$) is shown to the left. The tree built for $N_{out} = 2$ (binary tree) is shown to the right. For the metric values considered, the tree algorithm is able to provide two allocations whose global metric is higher than the one provided by the matrix algorithm. N_{out} can of course be increased (by including for example third and fourth best choices), but the number of combinations increases dramatically for a reasonable number of UEs (about 10). This is a serious limitation considering the real time constraints. Moreover, as shown afterwards, the gain provided from increasing such a parameter fairly soon saturates. For all these reasons N_{out} should probably not be higher than 2. When the retransmissions are also included, the allocation is split in two phases. In the first phase only the first transmission UEs are considered and their allocation is optimized considering the entire system bandwidth. The rationale behind this is to optimize their gain in order to reduce the chances of retransmission. In the second phase the retransmission UEs, which can benefit from Chase Combining (CC), are considered and their allocation is optimized within the remaining bandwidth [7].

III. Simulator description and assumptions

The performance evaluation is based on a detailed multi-cell system level simulator which follows the guidelines in [2]. The system bandwidth is fixed to

10 MHz with settings according to the LTE working assumptions. The full (infinite) buffer traffic model proposed for LTE benchmarking evaluation in [8] is assumed. In the beginning of a simulation run the location of the UEs is randomly assigned with a uniform distribution within each cell. UEs never leave the system until the end of the simulation run. One simulation consists of several simulation runs. The network layout is a regular grid comprising 57 cells and includes the wrap-around technique [9]. The link-to-system level mapping is based on the actual value interface (AVI) method [10]. It is assumed that distance-dependent path loss and shadowing are maintained constant for each UE. On the other hand, fast fading is updated every TTI based on the ITU Typical Urban (TU) power delay profile and depending on the UE speed. Further, shadowing is fully correlated between cells of the same site, while the correlation is 0.5 between sites. The system model includes synchronous adaptive HARQ with Chase Combining. The power control (PC) is implemented according to the formula standardized in [11]. The optional close-loop adjustments are not considered, thus the power is set as:

$$P = \min\{P_{\max}, P_0 + 10 \cdot \log_{10} M + \alpha \cdot L\} \quad (2)$$

where P_{max} is the maximum UE transmit power, P_0 is a cell-specific parameter, M is the number of PRBs allocated to the UE, α is a cell-specific path-loss compensation factor and L is the path-loss measured at the UE.

The TDPS works according to the RR metric while two metrics are considered for the FDPS: a metric which is defined as random (RAN) and the well known PF metric which has been widely investigated in [3] for the downlink. The RAN metric simply consists in assigning a random positive value (in a certain range) to each UE and each RC for every TTI. This results in a dynamic allocation which is blind to the channel conditions.

TABLE I

MAIN SIMULATION PARAMETERS.

Parameter	**Value**
Simulation Time	10s/run - 2s/run warm-up - 8 runs
Layout	19 sites - 3 sectors/site
Propagation Scenario	Macro 1 [ISD 500m]
	Macro 3 [ISD 1732m]
Thermal Noise per RU	-116 dBm
Penetration Loss	20dB
System Bandwidth	10MHz
	[50 PRBs, 2 used for control]
UEs per Sector	10, 30
UE Bandwidth	1080KHz, 360KHz [6, 2 PRBs]
eNode-B Receiver	2-Rx MRC
Channel Estimation	Real (included in AVI model)
Max UE Tx Power	250mW [∼24dBm]
UE Speed	3Kmph
TD Scheduling	Round Robin
FD Scheduling	Random, Proportional Fair
Forgetting Factor (for PF)	0.002
HARQ	Synchronous Adaptive
HARQ Delay - # Channels	4ms - 4
Traffic Model	Full Buffer [8] with balanced load
BLER Target	20%
Link Adaptation	Fast AMC
Shadowing Correlation	1.0 for intra-site, 0.5 for inter-site
Shadowing Statistics	μ = 0dB and σ = 8dB
Available MCSs	BPSK [R = 1/5, 1/3]
	QPSK [R = 1/4, 1/3, 1/2, 2/3, 3/4]
	16QAM [R = 2/3, 3/4, 5/6]
α (for PC)	0.6
P_0 (for PC)	-59dBm
σ_{CSI}	1 dB
CSI Resolution	2 RUs

TABLE II

SYSTEM PERFORMANCE FOR RAN AND PF METRICS (SAME NR DISTRIBUTIONS).

	RAN	**PF**	**Gain**
M1: Average Cell Thr.	7.5 Mbps	9.3 Mbps	24.0%
M1: UE Thr. @95% Coverage	249 kbps	343 kbps	37.2%
M3: Average Cell Thr.	6.3 Mbps	7.5 Mbps	19.0%
M3: UE Thr. @95% Coverage	53 kbps	59 kbps	11.3%

IV. SIMULATION RESULTS

First the effect of the PF metric on throughput and noise rise (NR) is investigated assuming $N_{out} = 1$. Fig.5 (b) shows that, regardless of the metric utilized, the instantaneous NR distribution does not change given the use of OLPC. The effect of the different metrics can be seen on the scheduled SINR distribution given in Fig.5 (a), which shows, for PF, a median value 1.5 dB higher than for RAN.

Similarly the average throughput per UE is increased for all UEs (Fig.5 (c)) leading to the performance numbers summarized in Table II for both the Macro 1 (M1) and Macro 3 (M3) cases.

Another interesting result can be seen in Fig.5 (c). The gain numbers expressed in Table II are actually the result of two mechanisms. One is the well known effect of the PF metric which tries to allocate an equal amount of resources, over time, to the different UEs while also exploiting the multi-user diversity. The other effect is that the PF metric produces an allocation in frequency which is less dynamic than the one obtained with the RAN metric. This reduces the interference fluctuations and therefore has a positive effect on SINR estimation

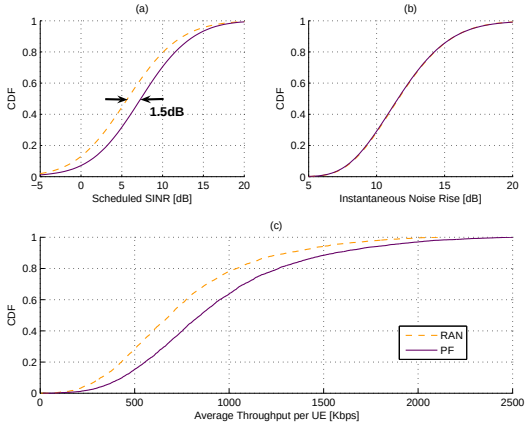

Fig. 5. Scheduled SINR, instantaneous NR and time averaged throughput per UE using RAN and PF metrics for 10 UEs per sector.

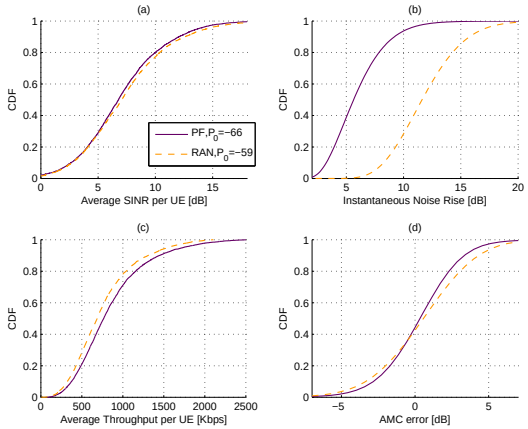

Fig. 6. Average SINR, instantaneous NR, average user throughput and AMC error distributions for RAN and PF metrics under similar average SINR distributions. The PF shows a closer match between the SINR in input to the AMC and the experienced SINR.

TABLE III

SYSTEM PERFORMANCE FOR RAN AND PF METRICS (MACRO 1, 10 UES, 6 PRBS PER UE).

	RAN	**PF**	**Gain**
Average Cell Thr.	7.54 Mbps	8.48 Mbps	12.5%
UE Thr. @95% Coverage	249 kbps	291 kbps	16.9%

and fast AMC performance. To evaluate the contribution of this effect to the overall gain we can reduce the parameter P_0 for the PF case until the distributions of the average SINR per UE are approximately the same (see Fig.6 (a)). At this point the NR distribution for the PF is shifted to the left by approximately 6 dB, Fig.6 (b), as consequence of the power reduction. Our expectation is confirmed as shown in Fig.6 (c). The distribution of the average throughput per UE shows that the PF metric still performs better than the RAN metric. For completeness Fig.6 (d) shows how the AMC error, defined as the difference between the SINR given in input to the AMC and the SINR experienced during the transmission, is reduced for PF compared to RAN. Throughput numbers are shown in Table III. The numbers are just used to highlight a trend and are subject to change in different load scenarios or with the introduction of TDPS.

Next, the effect of multi-user diversity has been investigated. As expected, a smaller bandwidth and, consequently, a larger number of users, increases the gain provided by the PF metric. In the Macro 1 case this produces an overall increase of the scheduled SINR and specifically a median value 0.7 dB higher (see Fig.7 (a)). The gain is larger in the Macro 3 case especially

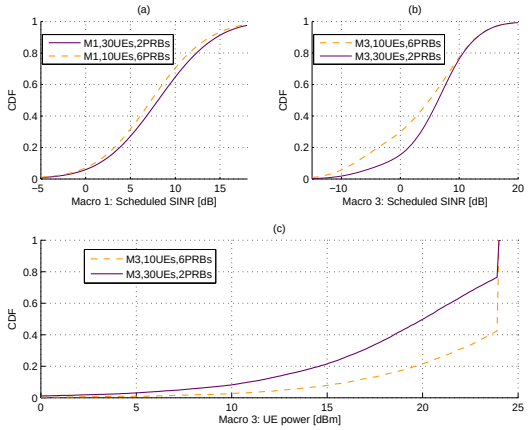

Fig. 7. Scheduled SINR and UE power for different number of users and PRBs and different scenarios.

in the lower range of the SINR as shown in Fig.7 (b). This is due to the power limitations experienced by cell edge users. Fig.7 (c) shows that reducing the bandwidth allocated to power limited users significantly reduces the percentage of users transmitting at maximum power. This, in turn, increases their chances of meeting the SINR target and therefore their throughput. Throughput numbers are shown in Table IV.

Finally, the effect of different N_{out} values is analyzed. Increasing N_{out} to 2 gives a gain of just 1% for both cases of 6 and 4 PRBs in average cell throughput (see Fig.8). The UE throughput at 95% coverage is increased

TABLE IV

SYSTEM PERFORMANCE FOR PF METRIC FOR DIFFERENT NUMBER OF USERS AND BANDWIDTH SETTINGS (MACRO 1 AND MACRO 3 CASES).

	10UEs, 6PRBs	**30UEs, 2PRBs**	**Gain**
M1: Average Cell Thr.	9.3 Mbps	10.0 Mbps	7.5%
M1: UE Outage Thr.×#UE	3430 kbps	3430 kbps	0%
M3: Average Cell Thr.	7.54 Mbps	8.64 Mbps	14.6%
M3: UE Outage Thr.×#UE	590 kbps	960 kbps	62.7%

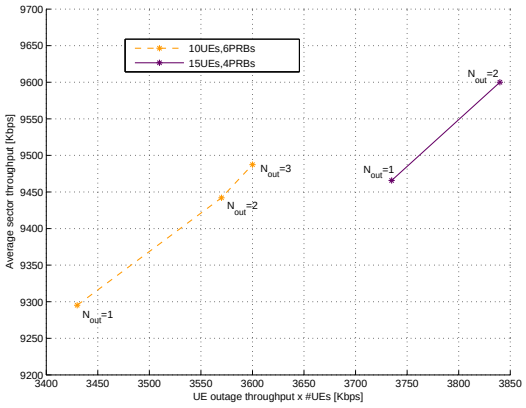

Fig. 8. Average cell throughput and UE throughput at 95% coverage for different out-degrees values and different number of users.

by just 3 or 4%. The gain deriving from $N_{out} = 3$ (possible only for 6 PRBs given the computational complexity) doesn't provide almost any additional gain. $N_{out} = 1$ seems therefore the most reasonable choice as it achieves most of the gain with a very limited computational complexity compared to higher values of N_{out}.

V. CONCLUSIONS AND FUTURE WORK

This paper addresses the performance a search-tree based PS algorithm in UTRAN LTE UL. It is shown that a PF metric, compared to a frequency blind scheduler, can provide a cell throughput gain of about 24% and a UE throughput at 95% coverage of more than 37% for the Macro 1 scenario compared to RAN. The gain is the result of two main factors: the exploitation of the multi-user diversity in a system under frequency selective fading as well as the improvement of fast AMC performance. It has also been shown that increasing the UE diversity order and decreasing the frequency bandwidth brings a benefit which becomes especially significant when considering the Macro 3 scenario. Finally, the effect of a higher N_{out} degree is analyzed. The results show that for bandwidths of 6 and 4 PRBs the gain achieved by increasing N_{out} is quite limited, therefore the greedy approach with $N_{out} = 1$ is preferable given the computational complexity.

Future studies will address the topic of adaptive transmission bandwidth in connection with PS together with more realistic sounding schemes.

REFERENCES

[1] A. Pokhariyal, G. Monghal, K. I. Pedersen, P. E. Mogensen, I. Z. Kovács, C. Rosa, and T. E. Kolding. Frequency Domain Packet Scheduling Under Fractional Load for the UTRAN LTE Downlink. *Proceedings of IEEE Vehicular Technology Conference (VTC) 2007 Spring*, April 2007.

[2] 3GPP TR 25.814 V7.1.0. Physical Layer Aspects For Evolved UTRA. September 2006.

[3] A. Pokhariyal, T.E. Kolding, and P.E. Mogensen. Performance of Frequency Domain Packet Scheduling for the UTRAN Long Term Evolution. *Proceedings of IEEE PIMRC*, September 2006.

[4] I. Viering, A. Klein, M. Ivrlac, M. Castaneda, and J.A. Nossek. On Uplink Intercell Interference in a Cellular System. *Proceedings of IEEE Interenational Conference on Communications (ICC)*, June 2006.

[5] J. Lim, H.G. Myung, and D.J.Goodman. Proportional Fair Scheduling of Uplink Single Carrier FDMA Systems. *Proceedings of IEEE Personal Indoor and Mobile Radio Communication Conference (PIMRC)*, September 2006.

[6] F.D. Calabrese, M. Anas, C. Rosa, P.E. Mogensen, and K.I. Pedersen. Performance of a Radio Resource Allocation Algorithm for UTRAN LTE Uplink. *Proceedings of IEEE Vehicular Technology Conference (VTC) 2007 Spring*, April 2007.

[7] A. Pokhariyal, K.I. Pedersen, G.Monghal, I.Z. Kovacs, C.Rosa, T.E. Kolding, and P.E. Mogensen. HARQ Aware Frequency Domain Packet Scheduler with Different Degrees of Fairness for the UTRAN LTE Donwlink. *Proceedings of the IEEE Vehicular Technology Conference (VTC)*, April 2007.

[8] 3GPP TSG-RAN WG1. R1-070674, LTE physical layer framework for performance verification. February 2007.

[9] T. Hytönen. Optimal Wrap-Around Network Simulation. *Helsinki University of Technology, Report A432*, 2001.

[10] S. Hämäläinen, P. Slanina, M. Hartman, A. Lappeteläinen, and H. Holma. A Novel Interface Between Link and System Level Simulations. *Proceedings of the ACTS Mobile Telecommunications Summit*, October 1997.

[11] R1-073224. Way Forward on Power Control of PUSCH. *3GPP TSG-RAN WG1 49-bis*, June 2007.

Annex II

Adaptive Transmission Bandwidth Based Packet Scheduling

F. D. Calabrese, C. Rosa, M. Anas, P. H. Michaelsen, K. I. Pedersen, and P. E. Mogensen, “Adaptive Transmission Bandwidth Based Packet Scheduling for LTE Uplink”, in *Proceedings of IEEE Vehicular Technology Conference VTC2008-Fall*, Calgary, Canada, September, 2008.

Adaptive Transmission Bandwidth Based Packet Scheduling for LTE Uplink

F. D. Calabrese[†], C. Rosa[‡], M. Anas[†], P. H. Michaelsen[‡], K. I. Pedersen[‡], P. E. Mogensen[‡]
[†]Department of Electronic Systems, Aalborg University, Denmark
[‡]Nokia Siemens Networks, Denmark

***Abstract*—UTRAN Long Term Evolution is currently under standardization within 3GPP with the aim of providing a spectral efficiency 2 to 4 times higher than its predecessor HSUPA/HSDPA Release 6. Single Carrier FDMA has been selected as multiple access for the uplink. This technology requires the subcarriers allocated to a single user to be adjacent. The consequence is a reduced allocation flexibility which makes it challenging to design effective packet scheduling algorithms. This paper proposes a channel aware packet scheduling algorithm which exploits the bandwidth flexibility offered by the system to perform an allocation which closely resembles the frequency domain envelope of the metric to be optimized. Compared to a fixed bandwidth approach, the proposed algorithm provides a greater flexibility given the inbuilt adaptation to different scenarios and loads, as well as an improvement in term of performance for the Macro 3 case. In this case the uplink capacity is increased by approximately 20% in average cell throughput and 10% in UE outage compared to a fixed bandwidth channel aware approach.**

I. Introduction

UTRAN Long Term Evolution (LTE) is a system currently under standardization within 3GPP. One of the targets of such a system is to improve the spectral efficiency by a factor of 2 to 3 for the uplink (UL) and 3 to 4 for the downlink (DL) compared to HSUPA/HSDPA Rel. 6. In order to achieve this goal new functionalities are introduced and different access schemes are selected. Orthogonal Frequency Division Multiplexing (OFDM), in particular, is regarded as a key technology given its high immunity to multipath, spectral efficiency and bandwidth scalability.

Single Carrier Frequency Domain Multiple Access (SC-FDMA), an OFDM based multiple access scheme, has been selected for UL. SC-FDMA requires the subcarriers, and therefore the Physical Resource Blocks (PRBs)[1] allocated to a single terminal, to be adjacent. This has proven to be a challenging constraint to cope with, when it comes to designing packet scheduling algorithms. Like in every multi-user system the Packet Scheduler (PS) plays the fundamental role of multiplexing User Equipments (UEs) in time and frequency domain based on some optimization criterion. If the system is affected by time and frequency selective fading the PS can exploit the multi-user diversity by assigning each UE to the portion of the bandwidth which exhibits favorable conditions for that UE. This mechanism is also known as Channel Dependent Scheduling (CDS).

Previous works regarding the topic of UL PS have limited the problem complexity by either removing the constraint on the contiguity of PRBs as required by the single carrier technology [2] or by assuming a fixed size for the bandwidth allocable to each UE [3]. This paper, taking inspiration from the algorithm used in [4] for DL, proposes an incremental algorithm which exploits the bandwidth flexibility to produce an allocation which closely resembles the optimum (defined according to a specific criterion) while satisfying the single carrier constraint. The size of the bandwidth is thus decided as part of the allocation algorithm performed by the scheduler rather than by another functionality.

The paper is organized as follows. Section II-A describes in general terms the PS functionality and the algorithm used as reference. Section II-B describes in detail the proposed algorithm. Section III gives an overview of the simulator together with general parameters and assumptions. Section IV provides an analysis of the simulation results for the different parameter settings and Section V draws conclusions and offers hints for further studies.

[1]The basic time-frequency resource available for data transmission consisting of adjacent OFDM subcarriers [1]. It is also known as Resource Unit. Its size is equal to 180 KHz.

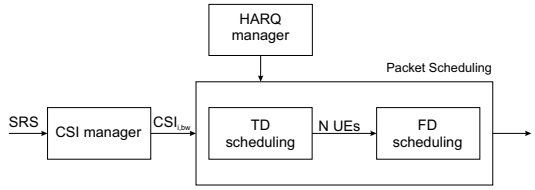

Figure 1. Basic inter-working between PS and other RRM functionalities.

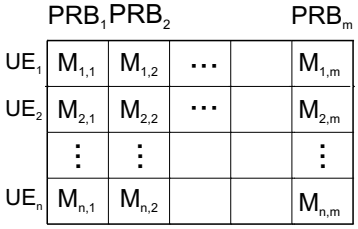

Figure 2. Metric values for each UE and each PRB.

II. Packet Scheduling Functionality

Radio Resource Management (RRM) for UTRAN LTE UL represents a complex problem given the number of parameters and constraints involved. Within the RRM functionalities, PS plays a central role. It interacts with the Link Adaptation (LA) unit and the Hybrid ARQ (HARQ) manager to produce an allocation table which tries to maximize some utility function by exploiting channel knowledge.

A. General framework

CDS can be seen as a search algorithm which traverses the solution space to find an optimum solution defined according to a utility function. The utility function is designed as a trade off between overall spectral efficiency and fairness among UEs and it defines how different quantities (channel gain, traffic, QoS requirements) have to be taken into account. The problem is complex because of the high number of parameters involved and the huge number of resulting combinations. Different decisions are therefore taken in order to reduce the search space. The basic inter-working of PS with other RRM functionalities is shown in Fig. 1.

In order to perform frequency domain channel-aware PS, Channel State Information (CSI) is needed, ideally for all the UEs and over all the frequency band. It is assumed that CSIs are available at the eNode-B every TTI over the entire system bandwidth, for every UE and with a given bandwidth resolution. Such assumptions are ideal but the CSI mechanism is realistic, i.e. the CSIs are derived considering the real channel gain and interference conditions and model also SINR estimation errors.

The HARQ manager provides the set of UEs that have to undergo a retransmission. It is supposed to be synchronous and adaptive, which means that retransmissions can take place anywhere in the bandwidth but in a specific TTI.

The PS is divided in two units: Time Domain Packet Scheduler (TDPS) and Frequency Domain Packet Scheduler (FDPS). The TDPS, based on information from the HARQ manager, identifies the scheduling candidates, i.e., the UEs that are capable of transmitting in the next TTI and hands them over to the FDPS. The FDPS performs the most computationally intense operations trying to determine the best allocation table based on a channel aware metric. Assuming that a metric value is available for each UE and each PRB, we can define our goal as to maximize, under the single-carrier constraint, the utility function:

$$M_{sum} = \sum M_{i,j} A_{i,j} \; with \; i \in \Omega_i, j \in \Omega_j \qquad (1)$$

where $M_{i,j}$ is the metric for UE i and PRB j, $\Omega_i$is the set of UEs, $\Omega_j$is the set of PRBs, and $A_{i,j} = \{0, 1\}$ with 1 for UE i allocated to PRB j, 0 otherwise. For convenience of representation, the metric values per each UE and each PRB are arranged in a $n \times m$ matrix as shown in Fig. 2.

As a reference case, a simple yet effective algorithm based on Fixed Transmission Bandwidth (FTB) is used [3]. This algorithm relies on the input matrix shown in Fig. 2 where the PRB is replaced with the resource chunk (RC), that is, a set of consecutive PRBs. The size of the RC is chosen so that a fixed number of UEs can fit within the system bandwidth. The algorithm is then performed as follows:

1) Find the UE and the RC with the highest metric
2) Allocate the RC to the UE
3) Delete corresponding row (UE) and column (RC)
4) Repeat from 1. using the resulting sub-matrix

B. Adaptive Transmission Bandwidth (ATB) PS algorithm description

The main motivation for integrating the ATB into the PS functionality is not only the semplification of the RRM functionalities but mostly the need of providing a more flexible algorithm which can accommodate for different traffic types - e.g. VOIP, which requires a limited bandwidth - as well as UEs with different power

capabilities. The advantage of this approach is that no additional functionality is required to tune the bandwidth, that is, the capability of coping with varying traffic loads and power limitations[2] is inbuilt in the algorithm.

The idea behind the algorithm is to produce an allocation table which closely follows the envelope of the UEs metrics by first picking the user with the highest metric and then expanding its bandwidth as long as its metric is highest.

The steps of the algorithm, exemplified in Fig. 3, are as follows:

1) Find, within the matrix of metric values, the UE i and the PRB j with the highest metric value[3] and allocate PRB j to UE i.
2) Expand the bandwidth of UE i until one of the following conditions is met:
   a) another user has a higher metric on the adjacent PRB (Fig. 3(a));
   b) the expansion has reached physical constraints on one side (a bandwidth edge or another user already allocated) and condition (a) on the other side;
   c) the expansion has reached physical constraints on both sides;
   d) the estimated transmit power is above the maximum.
3) Temporarily exclude UE i and its metric values if conditions 2(a) or 2(b) are verified, otherwise permanently exclude the user.
4) Repeat steps 1, 2 and 3 considering the reduced set of users and metrics (Fig. 3(b)).
5) If any, readmit temporarily excluded users as further expansion may be possible because of the exclusion of other users and relative metrics (Fig. 3(c)).
6) Repeat the steps from 1 to 5 until all the users have reached a permanent stopping condition (Fig. 3(d)).

The retransmissions, when they occur, are placed in the initial part of the bandwidth. This is possible because of the adaptive HARQ and is done to avoid bandwidth fragmentation. In this way the algorithm can be applied to first transmission users within the remaining portion of the bandwidth.

[2]Situation where UEs with high path-loss hit the maximum transmit power.

[3]For a user partially allocated only the adjacent PRBs are considered

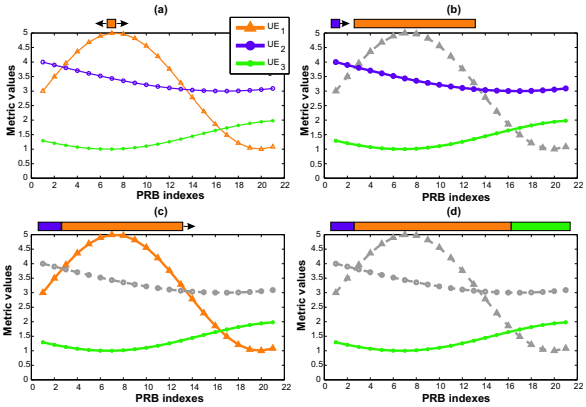

Figure 3. Algorithm description with 3 UEs and 21 PRBs. The grey dashed curves indicate UE (and associated metrics) which have temporarily or permanently been excluded.

III. Simulator description and assumptions

The performance evaluation is based on a detailed multi-cell system level simulator which follows the guidelines in [5]. The system bandwidth is fixed to 10 MHz with settings according to the LTE working assumptions. The full (infinite) buffer traffic model proposed for LTE benchmarking evaluation in [6] is assumed. In the beginning of a simulation run the UEs are dropped in the system. The distribution of the users depends on whether the load is balanced or unbalanced. In case of balanced load an equal number of UEs is distributed uniformly within each cell area. In case of unbalanced load the UEs are distributed still uniformly but over the whole network area leading to a different number of UEs per cell. UEs never leave the system until the end of the simulation run. One simulation consists of several simulation runs. The network layout is a regular grid comprising 57 cells and includes the wrap-around technique. The link-to-system level mapping is based on the actual value interface (AVI) method [7]. It is assumed that distance-dependent path loss and shadowing are maintained constant for each UE. On the other hand, fast fading is updated every TTI based on the ITU Typical Urban (TU) power delay profile and depending on the UE speed. Further, shadowing is fully correlated between cells of the same site, while the correlation is 0.5 between sites. The system model includes synchronous adaptive HARQ with Chase Combining. The power control (PC) is implemented according to the formula standardized in [8]. The optional closed-loop adjustments are not

Table I
MAIN SIMULATION PARAMETERS.

Parameter	Value
Simulation Time	10s/run - 2s/run warm-up - 10 runs
Layout	19 sites - 3 sectors/site
Propagation Scenario	Macro 1 [ISD 500m] Macro 3 [ISD 1732m]
Thermal Noise per PRB	-116 dBm
Penetration Loss	20dB
System Bandwidth	10 MHz [50 PRBs, 2 used for control]
UEs per Sector	6, 8, 10, 12
UE Bandwidth	FTB: 6, 4 PRBs ATB: [1, 24] PRBs, [2, 24] PRBs
eNode-B Receiver	2-Rx MRC
Channel Estimation	Real (included in AVI model)
Max UE Tx Power	250 mW [∼24 dBm]
UE Speed	3Kmph
TD Scheduling	Round Robin
FD Scheduling	Random, Proportional Fair
Forgetting Factor (for PF)	0.002
HARQ	Synchronous Adaptive
HARQ Delay - # Channels	4ms - 4
Traffic Model	Full Buffer [6], balanced and unbalanced
BLER Target	30%
Link Adaptation	Fast AMC
Shadowing Correlation	1.0 for intra-site, 0.5 for inter-site
Shadowing Statistics	μ = 0 dB and σ = 8 dB
Available MCSs	QPSK; R = 1/10, 1/6, 1/4, 1/3, 1/2, 2/3, 3/4 16QAM; R = 2/3, 3/4, 5/6
[α, P_0] (for PC)	Macro 1: [0.6, -58 dBm] Macro 3: [0.6, -64 dBm], [0.6, -62 dBm]
σ_{CSI}	1 dB
CSI Resolution	2 PRBs

considered, thus the power is set as:

$$P = \min\{P_{\max}, P_0 + 10 \cdot \log_{10} M + \alpha \cdot L\} \quad (2)$$

where P_{max} is the maximum UE transmit power, P_0 is a cell-specific parameter, M is the number of PRBs allocated to the UE, α is a cell-specific path-loss compensation factor and L is the path-loss measured at the UE.

IV. SIMULATION RESULTS

In the following we are going to show the performance of ATB-PS in different scenarios compared to the FTB-PS. In both cases the well known PF metric, which has been widely investigated in [9] for DL, is used. The analysis is limited to a full infinite buffer traffic scenario with 8 UEs and 6 PRBs or 12 UEs and 4 PRBs.

First the performance is evaluated in a balanced load Macro 1 scenario where power limitation is not an issue.

Fig. 4 (b) shows that, regardless of the algorithm utilized, the instantaneous Noise Rise (NR)[4] distribution does not change significantly given the use of (2) which

[4]The NR is defined as $(I + N)/N$

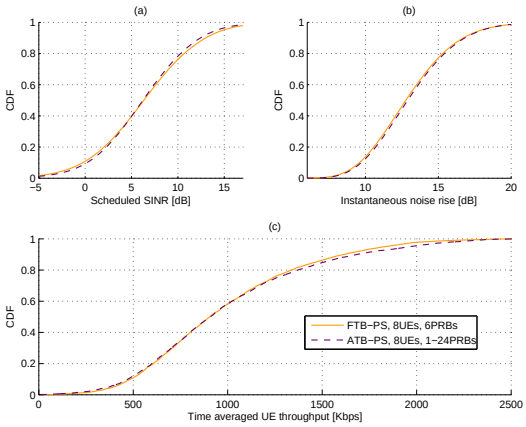

Figure 4. Macro 1 case. Scheduled SINR, instantaneous NR and time averaged UE throughput using PF metric.

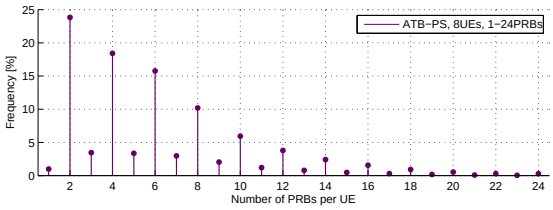

Figure 5. Macro 1 case. Bandwidth allocation per UE. The higher frequency of allocation for the even number of PRBs is due to the CSI granularity of 2 PRBs.

results in the same power spectral density for both cases. Fig. 4 (a) shows an improvement in the scheduled SINR in the lower SINR range. This does not result in a higher average throughput for the UEs at the cell edge due to the fact that such users in average transmit using a lower bandwidth. Such behaviour could be modified by adding constraints on the minimum number of PRBs per UE. Fig. 5 shows the distribution of the allocated number of PRBs. In general the allocation of an even numbers of PRBs is preferred given the CSI granularity of 2 PRBs. The gain numbers are summarized in Table II.

Next the performance of the ATB-PS is analyzed in a Macro 3 scenario where the performance of part of the users is penalized due to power limitations. The P_0 parameter of (2) is chosen to maximize the cell edge performance. Simulation results show that this is achieved at -62 dBm for the ATB-PS and -64dBm for the FTB-PS. The transmission bandwidth in the ATB-PS is allowed to vary from 2 to 24 PRBs. Fig. 6 (a) shows a considerable increase of the SINR especially in the lower

Table II
MACRO 1 CASE. SYSTEM PERFORMANCE FOR FTB-PS AND ATB-PS.

	FTB-PS	ATB-PS	Gain
8 UEs: average cell thr.	7.86 Mbps	7.97 Mbps	1.4%
8 UEs: UE thr. @5% outage	396 kbps	373 kbps	-5.8%
12 UEs: average cell thr.	8.0 Mbps	8.22 Mbps	2.75%
12 UEs: UE thr. @5% outage	276 kbps	264 kbps	-4.5%

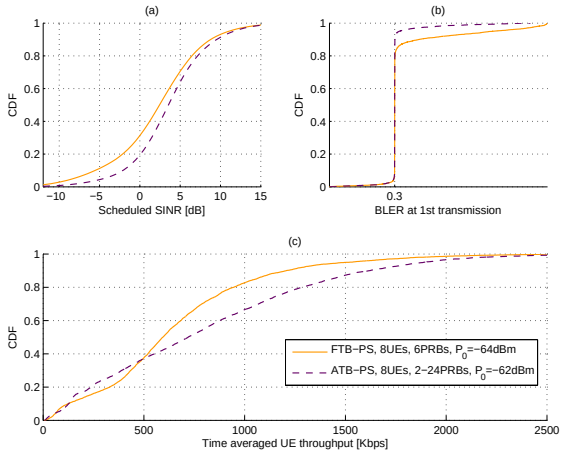

Figure 6. Macro 3 case. Scheduled SINR, BLER at 1st transmission and time averaged UE throughput.

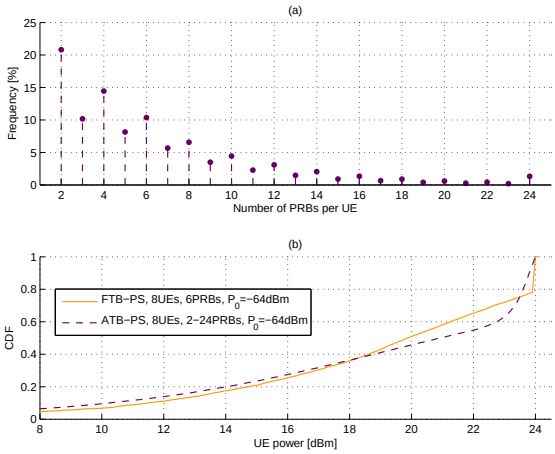

Figure 7. Macro 3 case. Bandwidth allocation per UE and UE power.

Table III
MACRO 3 CASE. SYSTEM PERFORMANCE FOR FTB-PS AND ATB-PS.

	FTB-PS	ATB-PS	Gain
8UEs: average cell thr.	5.29 Mbps	6.41 Mbps	21.2%
8UEs: UE thr. @5% outage	68 kbps	73 kbps	7.3%
12UEs: average cell thr.	5.51 Mbps	6.54 Mbps	18.7%
12UEs: UE thr. @5% outage	56 kbps	63 kbps	12.5%

range of the CDF. This results in a higher percentage of 1st transmissions matching the BLER target (see Fig. 6 (b)) and therefore in a lower number of retransmissions. Moreover the throughput of the UEs below 10% outage is not reduced while the throughput in the upper CDF range is considerably increased as shown in Fig. 6 (c). The statistics in Fig. 7 help clarifying such behaviour. Fig. 7 (a) shows the distribution of the allocated number of PRBs per user. The lowest number of PRBs (2 in this case) is the most frequent allocation and the UEs which are close to the maximum power are most likely to be given such allocation. This strategy reduces the number of users hitting the maximum power (from 23% to 5% as in Fig. 7 (b)) with the benefit in SINR and BLER distribution just shown. Moreover the allocation of a narrower bandwidth to some of the users leaves a larger bandwidth to users in better conditions thus resulting in a notable improvement of the average cell throughput. Table III summarizes the absolute numbers and the relative gains.

Finally the perfomance of ATB-PS is compared to FTB-PS in an unbalanced load scenario. In this case there are two main factors contributing in opposite directions to the system performance. On one side there is the bandwidth utilization, expected to be higher with ATB-PS, which contributes to a higher throughput. On the other side there is the interference level, expressed in terms of NR, also expected to be higher for the ATB-PS because of the higher bandwidth utilization, which leads to a lower throughput. The interaction of these two different effects is going to determine the final system performance.

Fig. 8 shows the cell and outage throughputs as well as the bandwidth utilization and the noise rise for different load scenarios.

It is worth highlighting that for a very low number of users (6 UEs in the figure) the average cell throughput increases for the ATB-PS as consequence of the higher bandwidth utilization but the outage performance is considerably lower as a consequence of the higher noise rise compared to FTB-PS. For a higher number of UEs (e.g. 10 UEs) both the gain in average cell throughput and the loss in outage of ATB compared to FTB are reduced as the bandwidth utilization and NR become similar. The ATB-PS algorithm anyway is flexible enough that a similar behaviour, where part of the cell throughput gain is traded for a better outage performance, could

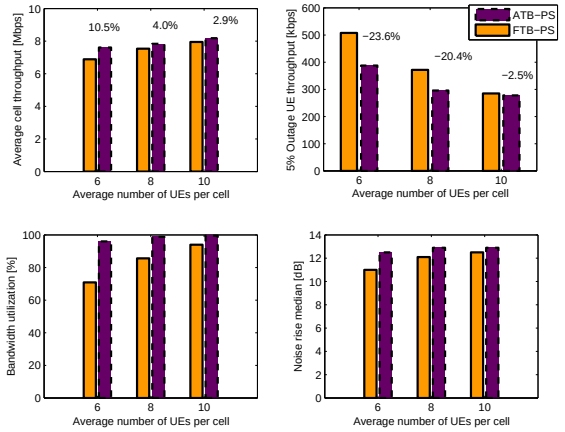

Figure 8. Macro 1 case. Average cell throughput, 5% outage UE throughput, bandwidth utilization and noise rise median for different load scenarios (6 PRBs in case of FTB-PS; 1-24 PRBs in case of ATB-PS).

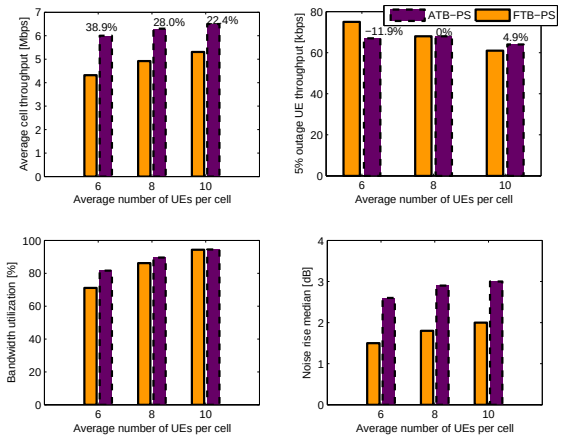

Figure 9. Macro 3 case. Average cell throughput, 5% outage UE throughput, bandwidth utilization and noise rise median for different load scenarios (6 PRBs, P_0=-64dBm in case of FTB-PS; 2-24 PRBs, P_0=-62dBm in case of ATB-PS).

be obtained by reducing the maximum bandwidth per user. The influence of NR is considerably reduced in a noise limited scenario (e.g. the Macro 3 case) where the interference has a much lower impact. Fig. 9 shows that for lower loads the gain in average cell throughput of ATB-PS over the FTB-PS is accompanied by a smaller loss in outage while for higher loads a gain is visible in both average cell throughput and outage UE throughput.

V. Conclusions and Future Work

This paper addresses the performance of an ATB-PS algorithm in UTRAN LTE UL. The algorithm is shown to exhibit a greater flexibility in terms of adaptation to different scenarios as well as a higher gain in a power limited scenario. The cases analyzed show a cell throughput gain of more than 24% for the Macro 3 case. In an unbalanced load and interference limited scenario the gain in cell throughput comes at a cost of a reduced cell edge performance. In an unbalanced and noise limited scenario a loss is present in outage only for very low load while the average cell throughput gain is considerable in all considered loads. Future studies will address the topic of ATB-PS under time-varying sector load conditions as well as QoS based ATB-PS.

References

[1] A. Pokhariyal, G. Monghal, K. I. Pedersen, P. E. Mogensen, I. Z. Kovács, C. Rosa, and T. E. Kolding. Frequency Domain Packet Scheduling Under Fractional Load for the UTRAN LTE Downlink. *Proceedings of IEEE Vehicular Technology Conference (VTC) 2007 Spring*, April 2007.

[2] J. Lim, H.G. Myung, and D.J.Goodman. Proportional Fair Scheduling of Uplink Single Carrier FDMA Systems. *Proceedings of IEEE Personal Indoor and Mobile Radio Communication Conference (PIMRC)*, September 2006.

[3] F.D. Calabrese, P.H.Michaelsen, C. Rosa, M. Anas, C. Úbeda Castellanos, D. Lopez Villa, K.I. Pedersen, and P.E. Mogensen. Search Tree Based Uplink Channel Aware Packet Scheduling for UTRAN LTE. *Proceedings of IEEE Vehicular Technology Conference (VTC) 2008 Spring*, May 2008.

[4] 3GPP TSG-RAN WG1 LTE. R1-060188, Frequency-domain user multiplexing for the E-UTRAN downlink. January 2006.

[5] 3GPP TR 25.814 V7.1.0. Physical Layer Aspects For Evolved UTRA. September 2006.

[6] 3GPP TSG-RAN WG1. R1-070674, LTE physical layer framework for performance verification. February 2007.

[7] S. Hämäläinen, P. Slanina, M. Hartman, A. Lappeteläinen, and H. Holma. A Novel Interface Between Link and System Level Simulations. *Proceedings of the ACTS Mobile Telecommunications Summit*, October 1997.

[8] 3GPP TS 36.213 V8.1.0. Evolved Universal Terrestrial Radio Access E-UTRA. *Physical Layer Procedures (Release 8)*, November 2007.

[9] A. Pokhariyal, T.E. Kolding, and P.E. Mogensen. Performance of Frequency Domain Packet Scheduling for the UTRAN Long Term Evolution. *Proceedings of IEEE PIMRC*, September 2006.